Syntheses of 8-(phenoxymethyl)caffeine analogues and their evaluation as inhibitors of monoamine oxidase and as antagonists of the adenosine A_{2A} receptor.

Rozanne Harmse

B.Pharm

Dissertation submitted in partial fulfilment of the requirements for the degree *Magister Scientiae*, in Pharmaceutical Chemistry at the North-West University, Potchefstroom Campus.

Supervisor: Prof. G. Terre'Blanche

Co-Supervisor: Dr. A. Petzer

2013

Potchefstroom

TABLE OF CONTENTS

ABSTRACT ..... **IV**

UITTREKSEL ..... **VII**

ACKNOWLEDGEMENTS ..... **X**

CHAPTER 1 ..... **1**

INTRODUCTION AND OBJECTIVES 1

1.1 INTRODUCTION 1

1.2 RATIONALE 4

1.3 HYPOTHESIS 6

1.4 OBJECTIVES 7

CHAPTER 2 ..... **8**

PARKINSON'S DISEASE, MONOAMINE OXIDASE AND THE ADENOSINE A_{2A} RECEPTOR 8

2.1 PARKINSON'S DISEASE 8

2.1.1 General background *8*

2.1.2 Pathophysiology – neurochemical and neuropathological features *9*

2.1.3 Etiology *12*

2.1.3.1 Environmental factors 12

2.1.3.2 Genetic factors 14

2.1.4 Pathogenesis *14*

2.1.4.1 Oxidative stress and mitochondrial dysfunction 14

2.1.4.2 Protein aggregation and misfolding 16

2.1.5 Clinical features, symptoms and diagnosis *17*

2.1.6 Treatment *18*

2.1.6.1 Levodopa (L-dopa) 18

2.1.6.2 Dopamine receptor agonists 20

2.1.6.3 Catechol-O-methyltransferase (COMT) inhibitors 21

2.1.6.4 Selective MAO-B inhibitors 21

2.1.6.5 Muscarinic receptor antagonists 22

2.1.7 Neuroprotection *22*

2.1.7.1 Dopamine receptor agonists 23

2.1.7.2 Adenosine receptor antagonists 23

2.1.8 Conclusion *23*

2.2 MONOAMINE OXIDASE 25

2.2.1 Introduction *25*

2.2.2 Classification and Characteristics *25*

2.2.2.1 Classification 25

2.2.2.2 Characteristics 26

2.2.3 Localization and tissue distribution *27*

2.2.4 Physiological functions *27*

2.2.5 Molecular structure and characteristics of MAO *28*

2.2.6 The catalytic cycle of MAO-B *31*

2.2.7 Parkinson's disease and MAO inhibitors *33*

2.2.8 Adverse effects of MAO inhibitors *34*

2.2.9 Pharmacology of MAO-B inhibitors *36*

2.2.9.1 Deprenyl 36

2.2.9.2 Rasagiline 36

2.2.9.3 Lazabemide 37

2.2.9.4 Ladostigil 37
2.2.10 Conclusion *38*
2.3 THE ADENOSINE A_{2A} RECEPTOR 39
2.3.1 Introduction *39*
2.3.2 Adenosine Receptors *39*
2.3.3 Basal ganglia organization and adenosine A_{2A} receptors *41*
2.3.4 Interactions with other neurotransmitter receptors *43*
2.3.4.1 Dopamine D_2 receptor 43
2.3.4.2 Glutamate mGlu5 receptor 44
2.3.4.3 Adenosine A_1 receptor 45
2.3.5 Adenosine antagonists and Parkinson's disease *45*
2.3.6 Classification of Adenosine A_{2A} Antagonists *46*
2.3.6.1 Xanthines 46
2.3.6.2 Aminouracil Derivatives 48
2.3.7 Neuroprotection of A_{2A} antagonists in Parkinson's disease *48*
2.3.8 Conclusion *49*

CHAPTER 3: **50**

SYNTHESES OF 8-(PHENOXYMETHYL)CAFFEINE ANALOGUES 50
3.1 INTRODUCTION 50
3.2 MATERIALS AND INSTRUMENTATION 52
3.3 GENERAL SYNTHETIC PROCEDURES 53
3.3.1 Synthesis of 1,3-dimethyl-5,6-diaminouracil and 1,3-diethyl-5,6-diaminouracil *53*
3.3.2 Synthesis of phenoxyacetic acids *54*
3.3.3 Synthesis of 1,3-dimethyl-8-phenoxymethyl-7H-xanthinyl and 1,3-diethyl-8-phenoxymethyl-7H-xanthinyl analogues *56*
3.3.4 Synthesis of the 8-(phenoxymethyl)caffeines (series 1) and 1,3-diethyl-7-methyl-8-(phenoxymethyl)xanthines *56*
3.4 PHYSICAL CHARACTERIZATION 56
3.4.1 8-(4-Methylphenoxymethyl)caffeine (11) *57*
3.4.2 8-(4-Methoxyphenoxymethyl)caffeine (12): *58*
3.4.3 8-(4-Iodophenoxymethyl)caffeine (13): *59*
3.4.4 8-(3,4-Dimethylphenoxymethyl)caffeine (14): *60*
3.4.5 1,3-Diethyl-7-methyl-8-(4-chlorophenoxymethyl)xanthine (16) *61*
3.4.6 1,3-Diethyl-7-methyl-8-(4-bromophenoxymethyl)xanthine (17) *62*
3.4.7 1,3-Diethyl-7-methyl-8-(4-fluorophenoxymethyl)xanthine (18) *63*
3.4.8 1,3-Diethyl-7-methyl-8-(4-methylphenoxymethyl)xanthine (19) *64*
3.4.9 1,3-Diethyl-7-methyl-8-(4-methoxyphenoxymethyl)xanthine (20) *65*
3.4.10 1,3-Diethyl-7-methyl-8-(4-iodophenoxymethyl)xanthine (21) *66*
3.4.11 1,3-Diethyl-7-methyl-8-(3,4-dimethylphenoxymethyl)xanthine (22) *67*
3.5 INTERPRETATION OF MASS SPECTRA 68
3.6 INTERPRETATION OF HPLC-TRACES 68
3.7 CONCLUSION: 69

CHAPTER 4: **70**

ENZYMOLOGY 70
4.1 GENERAL BACKGROUND ON ENZYME KINETICS 70
4.2 ENZYME KINETICS: K_M DETERMINATION 70
4.3 MAO-B INHIBITION STUDIES 72
4.3.1 Introduction *72*
4.3.2 Chemicals and Instrumentation *73*
4.3.3 Method *73*

4.3.4 Results *76*
4.3.4.1 Series 1 77
4.3.4.2 Series 2 80
4.3.5 Comparison of the MAO-B inhibitory activities of series 1 and series 2 ..... *81*
4.3.6 Comparison of the MAO-B inhibitory activities of the C3- and C4-substituted 8-(phenoxymethyl)caffeine analogues *82*
4.3.7 Conclusion *84*

CHAPTER 5 ..... **85**

ADENOSINE A_{2A} RECEPTOR BINDING STUDIES 85
5.1 INTRODUCTION 85
5.2 PRINCIPLES OF THE ADENOSINE A_{2A} RECEPTOR BINDING ASSAY 87
5.3 EXPERIMENTAL PROCEDURE 87
5.3.1 Materials and Instrumentation *88*
5.3.2 Tissue Preparations *88*
5.3.3 Preparation of stock solutions and buffers *89*
5.3.4 Binding affinity assay *89*
5.3.5 IC_{50} and K_i Determinations *91*
5.3.6 Results *92*
5.3.7 Conclusion *95*

CHAPTER 6: **97**

SUMMARY 97

BIBLIOGRAPHY: **103**

APPENDIX A **123**

LIST OF SYMBOLS AND ABBREVIATIONS 123

APPENDIX B **126**

LIST OF FIGURES 126

APPENDIX C **129**

LIST OF TABLES 129

APPENDIX D **131**

LIST OF EQUATIONS 131

APPENDIX E **132**

^{1}H-NMR AND ^{13}C-NMR 132

APPENDIX F **144**

HPLC DATA 144

APPENDIX G **149**

MASS SPECTRAL DATA 149

ABSTRACT

Background and rationale: Parkinson's disease (PD) is a progressive, degenerative disorder of the central nervous system and is characterized by the loss of dopaminergic neurons in the substantia nigra pars compacta. The loss of functional dopamine in the striatum is thought to be responsible for the typical symptoms of PD. Cardinal features of PD include bradykinesia, muscular rigidity, resting tremor and impairment of postural balance. This study focuses on the inhibition of monoamine oxidase B (MAO-B) and antagonism of A_{2A} receptors as therapeutic strategies for PD.

Monoamine oxidase (MAO) is a flavin adenine dinucleotide (FAD)-containing mitochondrial bound isoenzyme which consists of two isoforms namely MAO-A and MAO-B. The primary function of MAO is to catalyze the oxidative deamination of dietary amines, monoamine neurotransmitters and hormones. MAO-A is responsible for the oxidative deamination of serotonin (5-HT) and norepinephrine (NE), while MAO-B is responsible for the oxidative deamination of dopamine (DA). The formation of DA takes place in the presynaptic neuron where it is stored in vesicles and released into the presynaptic cleft. The released DA then either binds to D_1 and D_2 receptors which results in an effector response. The excess DA in the presynaptic cleft is metabolized by MAO-B which may result in the formation of free radicals and a decrease in DA concentrations. Under normal physiological conditions free radicals are removed from the body via normal physiological processes, but in PD these normal physiological processes are thought to be unable to remove the radicals and this may lead to oxidative stress. Oxidative stress is believed to be one of the leading causes of neurodegeneration in PD. The rationale for the use of MAO-B inhibitors in PD would be to increase the natural DA levels in the brain and also diminish the likelihood of free radicals to be formed.

Adenosine is an endogenous purine nucleoside and yields a variety of physiological effects. Four adenosine receptor subtypes have been characterized: A_1, A_{2A}, A_{2B} and A_3. They are all part of the G-protein-coupled receptor family and have seven transmembrane domains. The A_{2A} receptor is highly concentrated in the striatum. There are two important pathways in the basal ganglia (BG) through which striatal information reaches the globus pallidus, namely the direct pathway containing A_1 and D_1 receptors and the indirect pathway containing A_{2A} and D_2 receptors. The direct pathway facilitates willed movement and the indirect pathway inhibits willed movement. A balance of the two pathways is necessary for normal movement. In PD, there is a decrease in DA in the striatum, thus leading to unopposed A_{2A} receptor signaling and ultimately resulting in overactivity of the indirect pathway. Overactivity of the indirect pathway results in the locomotor symptoms associated with PD. Treatment with an

A_{2A} antagonist will block the A_{2A} receptor, resulting in the restoration of balance between the indirect and direct pathways, thus leading to a decrease in locomotor symptoms.

Aim: In this study, caffeine served as a lead compound for the design of dual-targeted drugs that are selective, reversible MAO-B inhibitors as well as A_{2A} antagonists. Caffeine is a very weak MAO-B inhibitor and a moderately potent A_{2A} antagonist. Substitution on the C8 position of caffeine yields compounds with good MAO-B inhibition activities and A_{2A} receptor affinities. An example of this behaviour is found with (E)-8-(3-chlorostyryl)caffeine (CSC), which is not only a potent A_{2A} antagonist but also a potent MAO-B inhibitor. The goal of this study was to identify and synthesize dual-targeted xanthine compounds. Recently Swanepoel and co-workers (2012) found that 8-phenoxymethyl substituted caffeines are potent reversible inhibitors of MAO-B. Therefore, this study focused on expanding the 8-(phenoxymethyl)caffeine series and evaluating the resulting compounds as both MAO-A and -B inhibitors as well as A_{2A} antagonists.

Synthesis: Two series were synthesized namely the 8-(phenoxymethyl)caffeines and 1,3-diethyl-7-methyl-8-(phenoxymethyl)xanthines. The analogues were synthesized according to the literature procedure. 1,3-Dimethyl-5,6-diaminouracil or 1,3-diethyl-5,6-diaminouracil were used as starting materials and were acylated with a suitable substituted phenoxyacetic acid in the presence of N-(3-dimethylaminopropyl)-N'-ethylcarbodiimide hydrochloride (EDAC) as an activating reagent. The intermediary amide was treated with sodium hydroxide, which resulted in ring closure to yield the corresponding 1,3-dimethyl-8-phenoxymethyl-7H-xanthinyl or 1,3-diethyl-8-phenoxymethyl-7H-xanthinyl analogues. These xanthines were 7-N-methylated in the presence of an excess of potassium carbonate and iodomethane to yield the target compounds.

In vitro evaluation: A radioligand binding assay was performed to determine the affinities of the synthesized compounds for the A_{2A} receptor. The MAO-B inhibition studies were carried out via a fluorometric assay where the MAO-catalyzed formation of H_2O_2 was measured.

Results: Both series showed good to moderate MAO-B inhibition activities, while none of the compounds had activity towards MAO-A. Results were comparable to that of a known MAO-B inhibitor lazabemide. For example, lazabemide (IC_{50} = 0.091 µM) was twice as potent as the most potent compound identified in this study, 8-(3-chlorophenoxymethyl)caffeine (compound **3**; IC_{50} = 0.189 µM). Two additional compounds, 8-(4-iodophenoxymethyl)caffeine and 8-(3,4-dimethylphenoxymethyl)caffeine, also exhibited submicromolar IC_{50} values for the inhibition of MAO-B. The structure-activity relationships (SARs) indicated that 1,3-diethyl substitution resulted in decreased inhibition potency

towards MAO-B and that 1,3-dimethyl substitution was a more suitable substitution pattern, leading to better inhibition potencies towards MAO-B.

The compounds were also evaluated for A_{2A} binding affinity, and relatively weak affinities were recorded with the most potent compound, 1,3-diethyl-7-methyl-8-[4-chlorophenoxymethyl]xanthine (compound **16**), exhibiting a K_i value of 0.923 µM. Compared to KW-6002 (K_i = 7.94 nM), a potent reference A_{2A} antagonist, compound **16** was 35-fold less potent. Comparing compound **16** to CSC [$K_i(A_{2A})$ = 22.6 nM; IC_{50}(MAO-B) = 0.146 nM], it was found that compound **16** is 31-fold less potent as an A_{2A} antagonist and 21-fold less potent as a MAO-B inhibitor. Loss of MAO-B inhibition potency may be attributed to 1,3-diethyl substitution which correlates with similar conclusions reached in earlier studies. In addition, the replacement of the styryl functional group (as found with CSC and KW-6002) with the phenoxymethyl functional group (as found with the present series) may explain the general reduction in affinity for the A_{2A} receptor. This suggests that the styryl side chain is more appropriate for A_{2A} antagonism than the phenoxymethyl functional group.

Conclusion: In this study two series of xanthine derivatives were successfully synthesized, namely the 8-(phenoxymethyl)caffeines and 1,3-diethyl-7-methyl-8-(phenoxymethyl)xanthines (11 compounds in total). Three of the newly synthesized compounds were found to act as potent inhibitors of MAO-B, with IC_{50} values in the submicromolar range. None of the compounds were however noteworthy MAO-A inhibitors. The most potent A_{2A} antagonist among the examined compounds, compound **16**, proved to be moderately potent compared to the reference antagonists, CSC and KW-6002. It may be concluded that the styryl functional group (as found with CSC and KW-6002) is more optimal than the phenoxymethyl functional group (as found with the present series) for A_{2A} antagonism. 1,3-Diethyl substitution of the xanthine ring was found to be less optimal for MAO-B inhibition compared to 1,3-dimethyl substitution. These results together with known SARs provide valuable insight into the design of 8-(phenoxymethyl)caffeines as selective and potent MAO-B inhibitors. Such drugs may find application in the therapy of PD.

Keywords: Parkinson's disease, monoamine oxidase inhibitors, adenosine A_{2A} antagonists, 8-(phenoxymethyl)caffeine, dual-targeted compounds.

UITTREKSEL

Agtergrond en rasionaal: Parkinson se siekte (PS) is 'n progressiewe, degeneratiewe siekte van die sentrale senuweestelsel, wat gekenmerk word deur die verlies van dopaminergiese neurone in die substantia nigra pars compacta. Die verlies van funksionele dopamien (DA) in die striatum is moontlik verantwoordelik vir die tipiese simptome wat geassosieer word met PS. Die vernaamste kenmerke van PS sluit die volgende in: bradikinesie, rigiditeit, tremore gedurende rus en verswakking in posturale balans. Hierdie studie fokus op die remming van monoamienoksidase-B (MAO-B) en die antagonisme van A_{2A}-reseptore as behandeling vir PS.

Monoamienoksidase (MAO) is 'n flavienadeniendinukleotied- (FAD)-bevattende, mitochondriale gebonde ensiem, wat as twee isovorme, naamlik MAO-A en MAO-B voorkom. Die primêre funksie van MAO is die oksidatiewe deaminering van amiene, monoamien neuro-oordragstowwe en hormone. MAO-A is verantwoordelik vir die oksidatiewe deaminering van serotonien (5-HT) en norepinefrien (NE), terwyl MAO-B verantwoordelik is vir die oksidatiewe deaminering van DA. Die vorming van DA vind in die presinaptiese neuron plaas waar dit in vesikels gestoor word en daarna in die presinaptiese spleet vrygestel word. Die vrygestelde DA bind aan D_1- en D_2-reseptore, wat dan 'n effektor respons ontlok. Die oortollige DA in die presinaptiese spleet word deur MAO-B gemetaboliseer, wat lei tot die vorming van vry radikale en 'n afname in die DA-konsentrasie. Onder normale toestande word vry radikale uit die liggaam verwyder deur middel van normale fisiologiese prosesse, maar in die geval van PS is hierdie fisiologiese prosesse nie in staat om die radikale te verwyder nie. Hierdie proses mag tot oksidatiewe stres lei. Daar word beweer dat oksidatiewe stres een van die grootste oorsake van neurodegenerasie in die senuweestelsel van pasiënte met PS is. Die rasionaal vir die gebruik van MAO-B-remmers in PS is dus om die natuurlike DA-vlakke in die brein te verhoog, asook om die waarskynlike vorming van vry radikale te verminder.

Adenosien is 'n endogene puriennukleosied en is betrokke by verskeie fisiologiese funksies. Vier adenosienreseptor-subtipes is geïdentifiseer en soos volg geklassifiseer: A_1, A_{2A}, A_{2B} en A_3. Hulle is almal deel van die G-proteïengekoppelde reseptorfamilie en het sewe transmembraanhelikse. A_{2A}-reseptore is hoogs gekonsentreerd in die striatum. Daar is twee belangrike senuweebane in die basale ganglia waardeur striatale inligting die globus pallidus bereik, naamlik die direkte baan, wat A_1 en D_1 reseptore bevat, en die indirekte baan wat A_{2A} en D_2 reseptore bevat. Die direkte baan fasiliteer beheerde beweging en die indirekte baan rem beheerde beweging. 'n Balans tussen die twee bane is belangrik vir normale beweging. In PS is daar 'n afname in striatale DA, wat dus lei tot ongeopponeerde A_{2A}-

reseptorstimulering en die uiteindelike ooraktivering van die indirekte baan. Ooraktivering van die indirekte baan lei tot die lokomotor-simptome wat geassosieer word met PS. Behandeling met 'n A_{2A}-antagonis sal dus die A_{2A}-reseptor blokkeer, wat sal lei tot ’n herstel van die balans tussen die indirekte en direkte bane en uiteindelik tot 'n afname in lokomotor-simptome.

Doel: In hierdie studie is kafeïen as 'n leidraadverbinding gebruik vir die ontwerp van geneesmiddels wat as selektiewe omkeerbare MAO-B-remmers sowel as A_{2A}-antagoniste optree. Kafeïen, as sulks, is 'n swak MAO-B-remmer en 'n matig potente A_{2A}-antagonis. Substitusie op die C8-posisie van kaffeïen lewer verbindings wat beide potente MAO-B-remmers en goeie A_{2A}-reseptorantagoniste is. 'n Voorbeeld hiervan is (E)-8-(3-chlorostiriel)kafeïen (CSC), 'n verbinding wat nie net 'n goeie A_{2A}-antagonis is nie, maar ook 'n goeie MAO-B-remmer. Die doel van hierdie studie was om xantienverbindings te sintetiseer, wat beide A_{2A}-antagoniste en MAO-B-remmers is. Swanepoel en medewerkers (2012) het onlangs gevind dat 8-fenoksiemetielkafeïene potente omkeerbare remmers van MAO-B is. Daarom het hierdie studie gefokus op die uitbreiding van die 8-(fenoksiemetiel)kafeïen-reeks. Die verbindings wat in dié studie gesintetiseer is, is geëvalueer vir aktiwiteit as beide MAO-A- en MAO-B-remmers sowel as vir A_{2A}-antagonisme.

Sintese: Twee reekse verbindings is gesintetiseer, naamlik die 8-(fenoksiemetiel)kafeïene en die 1,3-diëtiel-7-metiel-8-(fenoksiemetiel)xantiene. Die analoë is volgens die literatuurprosedure gesintetiseer. 1,3-Dimetiel-5,6-diaminourasiel of 1,3-diëtiel-5,6-diaminourasiel is as uitgangstowwe gebruik en is met 'n gesubstitueerde fenoksie-asynsuur geasetileer in die teenwoordigheid van N-(3-dimetielaminopropiel)-*N*’- etielkarbodiïmied (EDAC), wat as aktiveringsreagens optree. Die intermediêre amied is met natriumhidroksied behandel, wat ringsluiting bewerkstellig het, om die 1,3-dimetiel-8-fenoksimetiel-7H-xantien- of 1,3-diëtiel-8-fenoksimetiel-7H-xantien-analoë te lewer. Die xantiene is op die N7-posisie, in die teenwoordigheid van 'n oormaat kaliumkarbonaat en jodometaan, gemetileer om die teikenverbindings te lewer.

In vitro evaluering: `n Radioligandbindingstudie is uitgevoer om die affiniteit van die gesintetiseerde verbindings vir die $A_{2A}$-reseptor te bepaal. MAO-B-remming-studies is uitgevoer met behulp van `n fluorometriese toets waar die MAO-gekataliseerde vorming van H_2O_2 gemeet is.

Resultate: Beide reekse het goeie tot matige MAO-B-remming getoon, terwyl geen van die verbindings aktiwiteit teenoor MAO-A getoon het nie. Die resultate was vergelykbaar met dié

van 'n bekende MAO-B-remmer, lasabemied. Lasabemied (IC_{50} = 0,091 µM) is twee keer meer potent as die mees potente verbinding wat in hierdie studie geïdentifiseer is, naamlik 8-(3-chlorofenoksiemetiel)kafeïen, (verbinding **3**, IC_{50} = 0,189 µM). Twee ander verbindings, 8-(4-jodofenoksiemetiel)kafeïen en 8-(3,4-dimetielfenoksiemetiel)kafeïen, het submikromolêre IC_{50}-waardes getoon vir MAO-B-remming. Die struktuuraktiwiteitsverwantskappe (SAV) het getoon dat 1,3-diëtiel substitusie gelei het tot 'n verlaagde potensie teenoor MAO-B en dat 1,3-dimetiel substitusie meer geskik is vir potente remming van MAO-B.

Die verbindings is ook as A_{2A}-antagoniste geëvalueer maar het redelike swak affiniteite getoon vir die A_{2A}-reseptor. Die mees potente verbinding was 1,3-diëtiel-7-metiel-8-[4-chlorofenoksiemetiel]xantien (verbinding **16**), met 'n K_i-waarde van 0.923 µM. Verbinding **16** is dus 35 keer minder potent as KW-6002 (K_i = 7.94 nM), 'n potente A_{2A}-antagonis. Indien verbinding **16** met CSC [$K_i(A_{2A})$ = 26.2 nM; IC_{50}(MAO-B) = 0.146 nM], vergelyk word, is dit 31 keer swakker as 'n A_{2A}-antagonis en 21 keer swakker as MAO-B-remmer. Verlies in MAO-B-remming kan toegeskryf word aan 1,3-diëtielsubstitusie, 'n bevinding wat met gevolgtrekkings van vorige studies korreleer. Verder kan die vervanging van die stiriel funksionele groep (wat voorkom by CSC en KW-6002) met die fenoksiemetiel funksionele groep (soos in die huidige reeks) die verlaging van affiniteit teenoor die A_{2A}-reseptor verduidelik. Hieruit kan afgelei word dat die stirielsyketting meer geskik is vir A_{2A}-antagonisme as die fenoksiemetiel funksionele groep.

Gevolgtrekking: In hierdie studie is twee reekse xantienderivate, naamlik die 8-(fenoksiemetiel)kafeïene en 1,3-diëtiel-7-metiel-8-(fenoksiemetiel)xantiene ('n totaal van 11 verbindingsl) suksesvol gesintetiseer. Drie van die nuutgesintetiseerde verbindings was potente MAO-B-remmers met submikromolêre IC_{50}-waardes. Geen van die 11 verbindings was noemenswaardige MAO-A remmers nie. Die mees potente A_{2A}-antagonis, verbinding **16**, het matige potente affiniteit getoon vir die A_{2A}-reseptor in vergelyking met CSC en KW-6002. Die gevolgtrekking kan dus gemaak word dat die stiriel funksionele groep (soos gevind by CSC en KW-6002) meer optimaal is vir A_{2A}-antagonisme as die fenoksiemetiel funksionele groep (soos gevind in die huidige reeks). 1,3-Diëtielsubstitusie op die xantienring is minder optimaal vir MAO-B-remming as 1,3-dimetiel substitusie. Hierdie resultate saam met reeds bekende SAV's, voorsien waardevolle insig ten opsigte van die ontwerp van 8-(fenoksiemetiel)kafeïene as selektiewe en potente MAO-B-remmers. Sulke verbindings kan moontlik gebruik word vir die behandeling van PS.

Kernwoorde: Parkinson se siekte, monoamienoksidaseremmers, adenosien-A_{2A}-antagoniste, 8-(fenoksiemetiel)kafeïen, dubbelwerkende geneesmiddels

ACKNOWLEDGEMENTS

I would like to thank the following people and affiliations that played a role in helping me complete my Master's study:

- Firstly to my Lord and Saviour for His grace, guidance and patience
- My supervisor, Prof. G. Terre'blanche for her support, wisdom and always being there when needed most
- My co-supervisor, Dr. A. Petzer for all her help and understanding my frustration of the MAO assays
- Prof. J.P. Petzer for all his help and intelligent insights about the synthesis of compounds and finalizing remarks
- Prof. Bergh for his wisdom and guidance
- My family and friends for their love and support
- The NRF and NWU for funding
- The NWU for the laboratories and assay facilities provided
- Johan Jordaan and Andrè Joubert for the MS and NMR data
- Esjee Robinson, Madelein Geldenhuys and Sharlene Lowe with the help received with the A_{2A} assays

CHAPTER 1

INTRODUCTION AND OBJECTIVES

1.1 **Introduction**

Parkinson's disease

Parkinson's disease (PD) is currently regarded as one of the most common neurodegenerative disorders (Bovè *et al.,* 2005), where the incidence increases dramatically with age. The median age of onset is 60 years, with a lifetime risk of developing the disease of 1.5% (Katzenschlager *et al.,* 2008). The mean duration of the disease is 15 years, which includes diagnosis to death (Bower *et al.,* 1999).

PD results primarily from the death of dopaminergic neurons in the substantia nigra (SN, Dauer & Przedborski, 2003). It is a progressive disorder of the central nervous system (CNS), and is characterized by the loss of dopamine (DA) neurons in areas in the brain that are important for motor function, mood and cognition. Although the primary symptom of PD is motor dysfunction, the disease also has co-morbidities associated with it, including anxiety, depression and cognitive impairment (Lees *et al*., 2009).

The loss of DA via neurodegeneration results in the deficit of motor function. The cardinal clinical features of the disease include bradykinesia (slowness and poverty of movement), muscular rigidity, resting tremor and gait impairment.

Currently the therapy of PD is largely focused on DA replacement strategies such as the DA precursor, levodopa, and DA agonist drugs (Allain *et al*., 2008). Although these strategies are highly effective in controlling the early stages of the disease, long-term treatment is associated with drug-related complications such as a loss of drug efficacy, the onset of dyskinesias and the occurrence of psychosis and depression (Schwarzschild *et al.*, 2006; Dauer & Przedborski, 2003). The inadequacies of DA replacement therapy have prompted the search for alternative drug targets (Pretorius *et al.,* 2008). The adenosine A_{2A} receptor has emerged as one such target and antagonists of this receptor (A_{2A} antagonists) are considered promising agents for the symptomatic treatment of PD (Xu *et al.,* 2005). Another target is monoamine oxidase B (MAO-B), since inhibition of this enzyme may prevent the breakdown of DA.

Monoamine oxidase

Monoamine oxidase A and B (MAO-A and -B) are flavin adenine dinucleotide (FAD) containing enzymes which catalyze the oxidation of a variety of endogenous and xenobiotic amines in the brain and peripheral tissues (Youdim & Bakhle, 2006). In addition to the oxidation of amines such as DA and serotonin (5HT), these enzymes also function to oxidize ingested amines such as phenethylamine and tyramine to prevent their functioning as false neurotransmitters (Edmonson *et al.,* 2007).

A renewed interest in the inhibition of MAO-B has resulted from the observed age-related increase of MAO-B levels in humans (Kumar *et al.,* 2003) and possible connection to neurodegenerative diseases of the elderly such as PD (Edmondson *et al.,* 2007). The rationale behind the usage of MAO-B inhibitors in PD was originally based on the concept that DA is preferentially deaminated by this isoenzyme in the human nigrostriatal dopaminergic system. Thus, the increase in DA levels caused by MAO-B inhibitors should compensate for the nigrostriatal deficits in this neurotransmitter (Knoll, 2000).

The oxidation of biogenic amines by MAO results in the production of potentially toxic hydrogen peroxide, ammonia, and aldehydes that represent a risk factor for cell oxidative injury (Hauptmann *et al.,* 1996; Vindis *et al.,* 2000). MAO-B also metabolizes xenobiotic amines such as MPTP (1-methyl-4-phenyl-1,2,3,6-tetrahydropyridine), to the toxic metabolite, MPP^+ (1-methyl-4-phenylpyridine), which causes effects similar to those observed in PD (Langston *et al.,* 1984). Protection against MPTP-induced parkinsonism by MAO-B inhibitors could therefore be the result of reduced toxin activation as well as reduced production of hydrogen peroxide, ammonia and aldehyde species (Cohen *et al.,* 1997). These biological actions of MAO inhibition are of pharmacological interest, making MAO-B inhibitors an option either as monotherapy in early PD or as adjunctive therapy in patients treated with levodopa that are experiencing motor complications (Herraiz & Chaparro, 2005).

The adenosine receptor and A_{2A} antagonists

Adenosine is a neuromodulator that coordinates responses to DA and other neurotransmitters in areas of the brain that are important for motor function, learning and memory (Muller *et al.,* 1998). Adenosine acts on four G-protein coupled receptors: A_1, A_{2A}, A_{2B} and A_3 (Fredholm *et al.,* 2001). The A_{2A} receptor, which is highly expressed in the striatum (Dunwiddie & Masino, 2001), is a much sought after target in the pharmaceutical industry because of its potential to treat PD and other neurodegenerative disorders (Klaasse *et al*., 2008). A balance between the direct (striatonigral) and indirect (striatopallidal) pathways in the BG is required for normal movement. Impaired movement in PD is the result

of an imbalance in the activity of these two pathways due to DA deficiency in the striatum, which leads to an increased function of the indirect pathway (Morelli *et al*., 2007).

Adenosine A_{2A} receptors and dopaminergic D_2 receptors are co-localized in the striatopallidal neurons of the indirect pathway and have an antagonistic interaction. Depletion of DA in PD leads to an increased inhibition of the striatopallidal pathway due to unopposed A_{2A} receptors and disinhibition can be achieved by an A_{2A} antagonist (Müller & Ferre, 2006). A_{2A} antagonists may thereby provide relief of the symptoms of PD.

Evidence has suggested that A_{2A} antagonists may also slow the course of PD by protecting against the underlying neurodegenerative processes (Chen *et al.,* 2001). It may also prevent the development of dyskinesias that are normally associated with levodopa and DA agonist treatment (Bibbiani *et al.,* 2003). It is noteworthy that the symptomatic relief conferred by A_{2A} antagonists are additive to the effect produced by DA replacement therapy. It may therefore be possible to reduce the dose of dopaminergic drugs and the occurrence of side effects (Schwarzschild *et al.,* 2006; Bara-Jimenez *et al.,* 2003). A_{2A} antagonists are therefore a promising adjunctive to DA replacement therapy (Kase *et al.,* 2004).

Caffeine

Caffeine is arguably the world's most widely consumed psychoactive compound (Fredholm, *et al.,* 1999). Caffeine is a xanthine derived compound and a non-selective adenosine A_{2A} receptor antagonist. Interestingly, men and postmenopausal women who take no or very low quantities of daily caffeine, seem to be at an increased risk (25%) of developing PD (Lees *et al.,* 2009). This finding suggests that caffeine may possess neuroprotective properties in PD. In addition, caffeine increases the striatal DA release via blockade of the adenosine A_{2A} receptor, a finding that further supports a role for caffeine in PD (Dauer & Przedborski, 2003). In this study caffeine will be used as scaffold for the design of new derivatives with potential A_{2A} receptor antagonistic properties. The caffeine moiety has previously been shown to be suitable as a scaffold for the design of A_{2A} antagonists. (E)-8-(3-Chlorostyryl)caffeine (CSC) and KW-6002, two reference A_{2A} antagonists, are examples of such compounds (Figure 1.1) (Pretorius *et al.,* 2008; Müller *et al.,* 1997). In addition, the caffeine moiety is also used in the design of MAO-B inhibitors (Swanepoel, 2010; Pretorius *et al.,* 2008). Therefore these findings open the possibility of designing dual-targeted xanthine drugs that may have enhanced therapeutic potential as antiparkinsonian drugs.

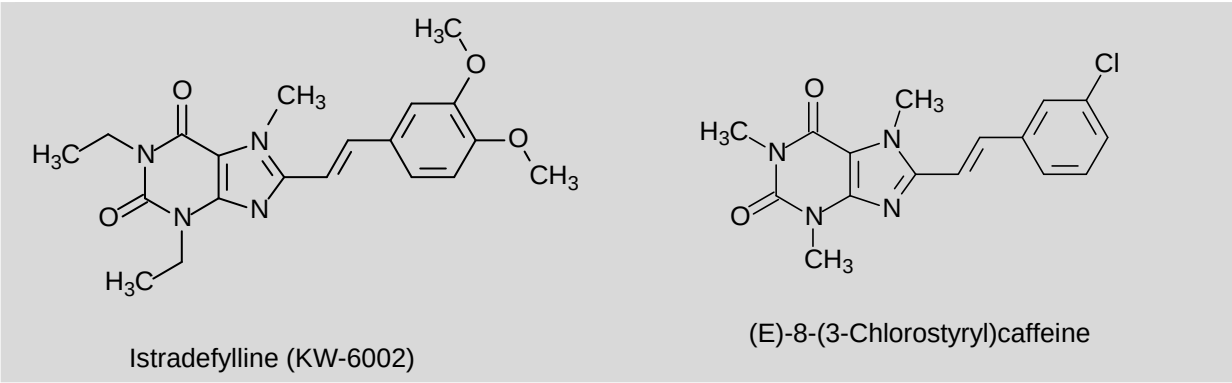

Figure 1.1 **The structures of CSC and KW-6002.**

1.2 **Rationale**

Caffeine (Figure 1.2) is reported to be a weak inhibitor of MAO-B and a moderately potent adenosine A_{2A} antagonist (Petzer *et al.,* 2009). Substitution on the C8 position of the caffeine ring, however, yields compounds with good affinities for the A_{2A} receptor and the MAO-B enzyme (Petzer *et al*., 2003). An example of a C8 substuituent which dramatically enhances MAO-B inhibition potency of caffeine is the phenoxymethyl side chain (Swanepoel, 2010; Pretorius *et al.,* 2008). Recently it was shown that a series of 8-(phenoxymethyl)caffeine analogues (Figure 1.2) are exceptionally potent reversible inhibitors of MAO-B (Swanepoel, 2010). These compounds were relatively weak inhibitors of MAO-A, and may therefore be classified as selective MAO-B inhibitors. The inhibition potencies of these compounds towards MAO-B ranged from 0.148 to 5.78 µM with the homologues containing halogens on the phenyl ring being the most potent inhibitors.

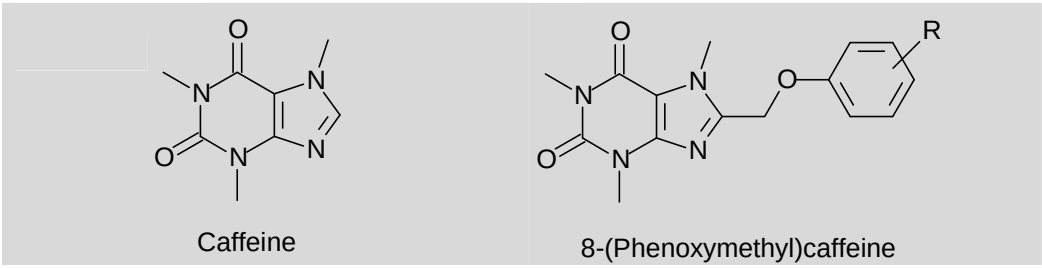

Figure 1.2: **Molecular structures of caffeine and 8-phenoxymethylcaffeine**

The main objective of this study is the design and synthesis of caffeine derivatives as dual-targeted drugs, compounds that are selective and reversible MAO-B inhibitors as well as potent adenosine A_{2A} antagonists.

Based on the previous finding by our research group that 8-(phenoxymethyl)caffeine analogues are potent reversible inhibitors of MAO-B (Swanepoel, 2010), in the present study we propose to prepare a series of new 8-(phenoxymethyl)caffeine analogues. These newly synthesized compounds will expand on the earlier series by including additional substituents of the C3 and C4 positions of the phenoxymethyl ring. The previously synthesized series examined the MAO inhibitory properties of 8-(phenoxymethyl)caffeine analogues containing C3 substituents (Cl, Br, F, CF_3, CH_3, OCH_3) and C4 substituents (Cl, Br, F) on the phenoxymethyl ring. This study will examine 8-(phenoxymethyl)caffeine analogues containing additional C4 substituents (I, CH_3, OCH_3) and the 3,4-dimethyl substituent on the phenoxymethyl ring. In addition a second series of 1,3-diethyl-7-methyl-8-(phenoxymethyl)xanthines will be synthesized. These homologues will also contain various substituents on the phenoxymethyl ring (4-Cl, 4-Br, 4-F, 4-CH_3, 4-OCH_3, 4-I, 3,4-diCH_3). The selection of the structures of series two is based on the observation that the structures of the analogues of series two are similar to the structure of KW-6002 with respect to the 1,3-diethyl substitution of the xanthine ring. Since KW-6002 is a potent A_{2A} antagonist, these compounds, therefore, may act as A_{2A} receptor antagonists. The 8-(phenoxymethyl)caffeine analogues synthesized in this study will therefore be examined as potential A_{2A} receptor antagonists. In addition selected members of the previously synthesized 8-(phenoxymethyl)caffeine analogues (Swanepoel, 2010) will also be examined as, for the first time, potential A_{2A} receptor antagonists

Previous Study (Swanepoel, 2010):

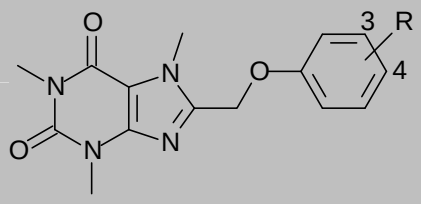

(a)

Compound no:	R:	Compound no:	R:
1	H	**8**	4-Cl
2	3-Cl	**9**	4-Br
3	3-Br	**10**	4-F
4	3-F		
5	3-CF_3		
6	3-CH_3		
7	3-OCH_3		

Series 1:

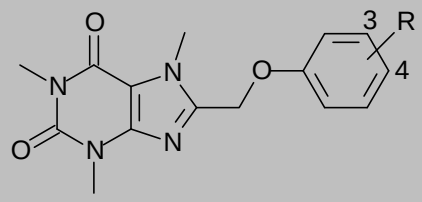

(b)

Compound no:	R:
11	4-CH_3
12	4-OCH_3
13	4-I
14	3,4-CH_3

Series 2:

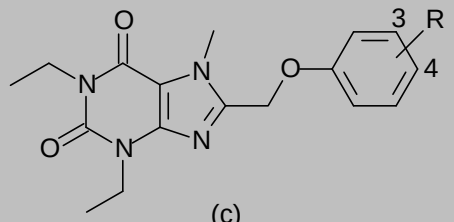

(c)

Compound no:	R:
15[#]	H
16	4-Cl
17	4-Br
18	4-F
19	4-CH_3
20	4-OCH_3
21	4-I
22	3,4-CH_3

[#] **Compound previously synthesized by Van der Walt (2012)**

Figure 1.3: **(a) 8-(Phenoxymethyl)caffeine analogues synthesized in a previous study (Swanepoel, 2010).**
(b) 8-(Phenoxymethyl)caffeine analogues of series 1 of the current study.
(c) 1,3-Diethyl-7-methyl-8-(phenoxymethyl)xanthines of series 2 of the current study.

1.3 **Hypothesis**

Based on the finding that 8-(phenoxymethyl)caffeines are potent MAO-B inhibitors, it is postulated that this class of compounds is a promising lead for the design of potent MAO-B inhibitors, and that the appropriate alkyl (CH_3 and OCH_3) or halogen (F, Cl, Br, I) substituents on the C3 and C4 positions of the phenoxy ring will further enhance the inhibition potencies of the existing members of this class (Swanepoel, 2010). It is further postulated that, since these compounds are structurally similar to the known A_{2A} antagonists, CSC and KW-6002, the 8-(phenoxymethyl)caffeines may also possess affinities for the A_{2A} receptor. In this respect, 1,3-diethyl-7-methyl-8-(phenoxymethyl)xanthines are particularly promising since 1,3-diethyl substitution pattern on the xanthine ring is also found in the structure of KW-6002.

1.4 **Objectives**

Based on the discussion above the objectives of this study are:

- Series of 8-(phenoxymethyl)caffeines (4 compounds) and 1,3-diethyl-7-methyl-8-(phenoxymethyl)xanthines (7 compounds) will be synthesized. For this purpose 1,3-dimethyl- or 1,3-diethyl-5,6-diaminouracil will be reacted with the appropriate substituted phenoxyacetic acid. In certain instances, the required phenoxyacetic acids are not commercially available and will be prepared from the corresponding phenols.

- The 8-(phenoxymethyl)caffeines and 1,3-diethyl-7-methyl-8-(phenoxymethyl)-xanthines will be evaluated as inhibitors of human MAO-A and MAO-B and the inhibition potencies will be expressed as the IC_{50} values (concentration of the inhibitor that produces 50% inhibition). The inhibition potencies will be compared to those obtained for a related series of 8-(phenoxymethyl)caffeines in a previous study (Swanepoel, 2010).

- The 8-(phenoxymethyl)caffeines and 1,3-diethyl-7-methyl-8-(phenoxymethyl)-xanthines will be evaluated as antagonists of the adenosine A_{2A} receptor and the potencies will be expressed as the K_i values (the receptor-ligand dissociation constant).

CHAPTER 2

PARKINSON'S DISEASE, MONOAMINE OXIDASE AND THE ADENOSINE A_{2A} RECEPTOR

2.1 PARKINSON'S DISEASE

2.1.1 General background

PD is a neurodegenerative disease that appears essentially as a sporadic condition (Bovè *et al.,* 2005). The pathological hallmark of PD is a loss of pigmented, dopaminergic neurons of the substantia nigra pars compacta (SNpc), with the appearance of intracellular inclusions known as Lewy bodies (LBs) (Gibb, 1992; Fearnley & Less, 1994). The loss of SNpc neurons from the nigrostriatal dopaminergic pathway leads to striatal DA deficiency. Replenishment of striatial DA through the oral administration of the DA precursor, levodopa (L-dopa), alleviates most of these symptoms. Although the discovery of L-dopa revolutionized the treatment of PD, it was soon noticed that after several years of treatment most patients developed involuntary movements, termed dyskinesia, which are difficult to control and significantly impair the quality of life (Dauer & Przedborski, 2003).

Progressive loss of DA containing neurons is a feature of normal aging, however, most people do not lose the 70% to 80% of dopaminergic neurons required to cause symptomatic PD. Without treatment, PD progresses over 5 to 10 years to a rigid, akinetic state in which patients are incapable of caring for themselves. Death frequently results from complications of immobility, including aspiration pneumonia or pulmonary embolism. The availability of effective pharmacological treatment has radically altered the prognosis of PD. In most cases, good functional mobility can be maintained for many years, and the life expectancy of adequately treated patients increase substantially (Standaert & Young, 2006).

Current research is directed toward prevention of dopaminergic neurodegeneration. Nevertheless, despite advances toward this goal, all current treatments are symptomatic and none halt or retard dopaminergic neuron degeneration. The main obstacle in the development of neuroprotective drugs is a lack of information on specific molecular events that provoke neurodegeneration in PD. Prior to the last 5 years, most of the current hypotheses about the etiology and pathogenesis of PD, were derived from post mortem tissue or neurotoxic animal models using MPTP to induce dopaminergic neurodegeneration. Exposure of humans to MPTP causes a syndrome that mimics the core neurological

symptoms and relatively selective dopaminergic neurodegeneration of PD. These studies have focused on three types of cellular dysfunction that may be important in the pathogenesis of PD: oxidative stress, defective mitochondrial respiration, and abnormal protein aggregation (Dauer & Przedborski, 2003).

2.1.2 **Pathophysiology – neurochemical and neuropathological features**

Symptoms of PD result from degeneration of the dopaminergic pathway from the substantia nigra (SN) to the corpus striatum. Voluntary movement is controlled by the BG (Figure 2.1), which is a group of subcortical nuclei consisting of the striatum (caudate and putamen), globus pallidus (externa and interna), SN (pars compacta and reticularis) and the subthalamic nucleus (Tugwell, 2008).

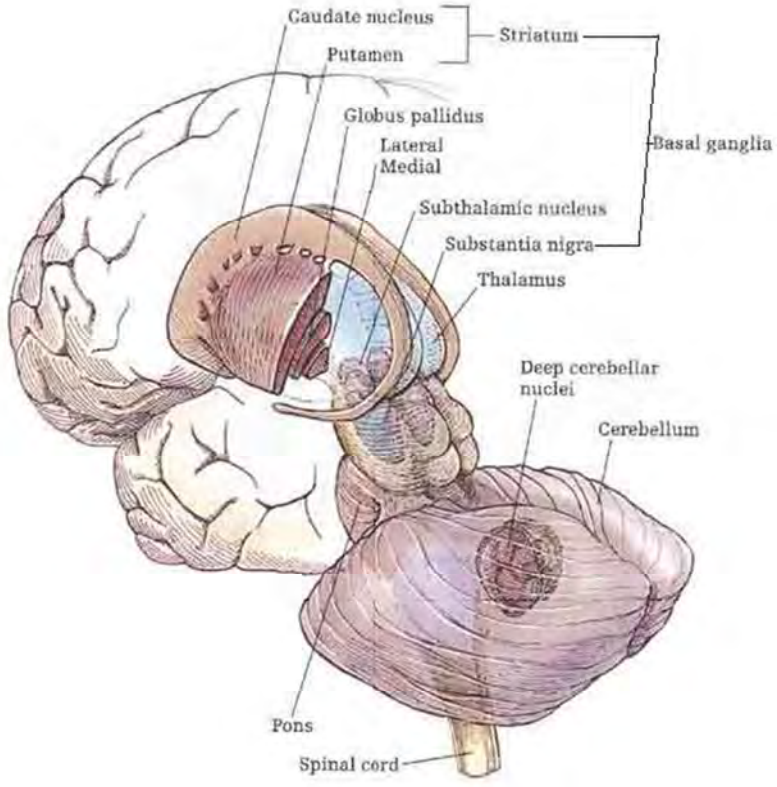

Figure 2.1: Breakdown of the BG (St. Clair *et al.*, 2005)

One of the pathological hallmarks of PD is the loss of the nigrostriatal dopaminergic neurons (Dauer & Przedborski, 2003). The normal nigrostriatal pathway is composed of dopaminergic neurons whose cell bodies are located in the SNpc. These neurons project to the BG and synapse in the striatum (putamen and caudate nucleus, Figure 2.2a). In PD (Figure 2.2b),

the nigrostriatal pathway degenerates. There is a marked loss of dopaminergic neurons that project to the putamen and a much more modest loss of those that project to the caudate. The normal pigmentation of the SNpc is due to the presence of neuromelanin within the dopaminergic neurons (Figure 2.2a). The loss of the dopaminergic neurons thus produces the classical gross neuropathological finding of SNpc depigmentation (Figure 2.2b) (Dauer & Przedborski, 2003).

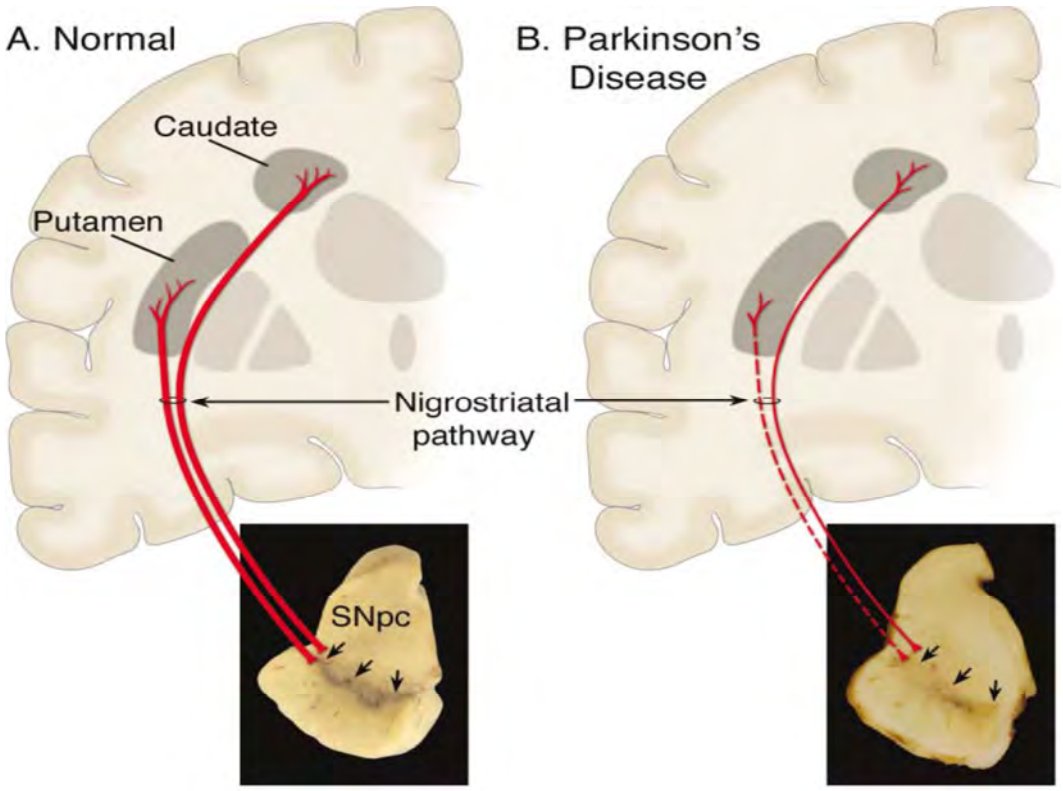

Figure 2.2: **(a) Represents the normal nigrostriatal pathway, whose cell bodies are located in the SNpc and projects (thick solid red lines) to the putamen and caudate nucleus in the striatum. The black arrows indicate normal pigmentation of the SNpc produced by neuromelanin in the DA neurons.**
(b) Represents a diseased nigrostriatal pathway. In PD, the nigrostriatal pathway degenerates and there is a marked loss of dopaminergic neurons that project to the putamen (dashed line) and a modest loss of those that project to the caudate (thin red solid line). Due to the marked loss of dopaminergic neurons, the loss of dark-brown pigmentation in the SNpc can be seen (black arrows) (Dauer & Przedborski, 2003).

Another pathological hallmark of PD is the presence of intraneuronal proteinacious cytoplasmic inclusions, termed LBs (Grefferd *et al.,* 2008). LBs (Figure 2.3) are intracytoplasmic eosinophilic inclusions that are found in damaged neurons (Tugwell, 2008). These protein aggregates are composed of numerous proteins including α-synuclein, parkin,

ubiquitin, and neurofilaments, and they are found in all affected brain regions (Forno, 1996; Spillantini *et al.,* 1998). Their presence within the pigmented brainstem nuclei is a feature of PD, although it remains unclear whether they are a result of the disease, or in some way involved in the cause of the pathology resulting in PD. With PD, LBs are predominantly present in the brainstem and their presence in peripheral autonomic nuclei may be associated with some of the autonomic features of the disease (Tugwell, 2008).

Figure 2.3: **Immunohistochemical labeling of LBs in a SNpc dopaminergic neuron. On the left immunostaining was done with an antibody against α-synuclein and on the right with an antibody against ubiquitin (Dauer & Przedborski, 2003).**

Although it is commonly thought that the neuropathology of PD is characterized solely by dopaminergic neuron loss, the neurodegeneration extends well beyond dopaminergic neurons (Hornykiewicz & Kish, 1987). Neurondegeneration and LB formation are found in noradrenergic, serotonergic, and cholinergic systems as well as in the cerebral cortex, olfactory bulb, and autonomic nervous system. Degeneration of hippocampal structures and cholinergic cortical inputs contribute to the high rate of dementia that accompanies PD, particularly in older patients. Thus, while involvement of these neurochemical systems is generally thought to occur in more severe or late-state disease, the temporal relationship of damage to specific neurochemical systems is not well established. For example, some patients develop depression months or years prior to the onset of PD motor symptoms, which could be due to early involvement of nondopaminergic pathways (Dauer & Przedborski, 2003).

2.1.3 **Etiology**

Although PD is a sporadic disorder and its cause is not known, several genetic forms of parkinsonism have been identified but, these are rare. Some PD cases are thought to be due to environmental causes (Taylor *et al.,* 2005; Dick *et al.,* 2007). Environmental and genetic factors have been widely studied (Tugwell, 2008).

2.1.3.1 *Environmental factors*

An environmental hypothesis assumes that PD-related neurodegeneration results from exposure to a dopaminergic neurotoxin. In theory, progressive neurodegeneration of PD could be produced via chronic exposure of a neurotoxin which initiates a cascade of deleterious events (Dauer & Przedborski, 2003).

Although unrelated to any pesticide, MPTP (Figure 2.4) has clearly been shown to cause symptoms of PD. Following the intravenous injection of 1-methyl-4-phenyl-4-propionoxypiperidine (MPPP, Figure 2.4), a 'designer drug', several abusers began exhibiting symptoms of PD. It was found that MPTP, which was inadvertently produced during the illicit synthesis of MPPP, was the culprit behind this picture (Bovè *et al.,* 2005).

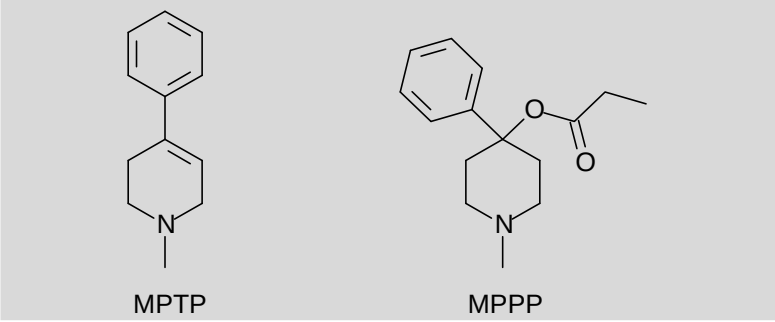

Figure 2.4: Molecular structures of MPTP and MPPP

Neuronal loss in the SN was present in the postmortem tissues of those people exposed to MPTP, which fits the current understanding of the pathophysiology of the disease. By inducing symptoms of PD with MPTP, a laboratory animal model could be created for researching new drugs to treat PD (Bovè *et al.,* 2005).

It is well established that MPTP produces an irreversible severe pakinsonian syndrome, characterized by all of the cardinal features of PD, including tremor, rigidity, slowness of movement, postural instability and freezing (Bovè *et al.,* 2005).

Other toxins that may induce PD include rotenone and paraquat (Figure 2.5).

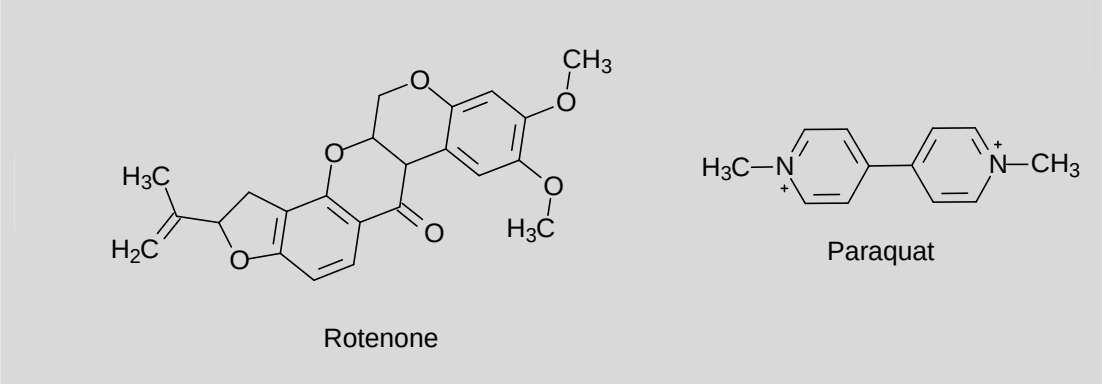

Figure 2.5: Molecular structures of rotenone and paraquat

Rotenone is widely used as insecticide and fish poison (Hisata, 2002). Like MPTP, rotenone is highly lipophilic and thus readily gains access to all organs including the brain (Talpade *et al.,* 2000). Rotenone exerts its toxic action by inhibiting mitochondrial respiration, which leads to neuronal death.

Paraquat, which is used as an herbicide, is a prototypic toxin known to exert deleterious effects through oxidative stress yielding reactive oxygenated species (ROS) (Bovè *et al.,* 2005). Epidemiological studies have suggested an increased risk for PD due to paraquat exposure (Liou *et al.,* 1997). This raised the possibility that paraquat could be an environmental parkinsonian toxin. In keeping with this, it is relevant to point out that paraquat exhibits a striking structural similarity to MPTPs toxic metabolite MPP^+ (Figure 2.6) (Bovè *et al.,* 2005).

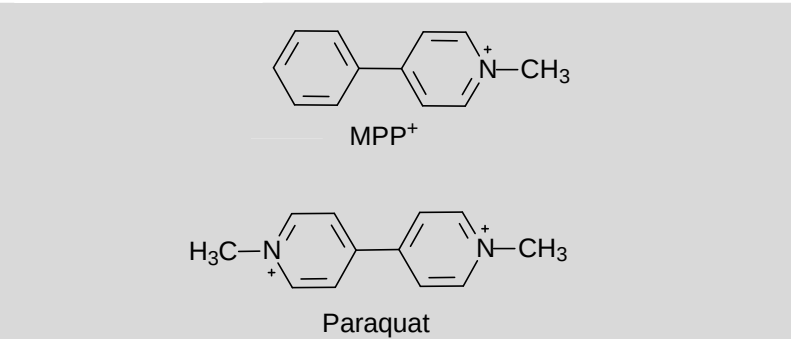

Figure 2.6: Comparison of chemical structures of MPP^+ and paraquat (Przedborski *et al.,* 1992)

2.1.3.2 Genetic factors

In recent years, geneticists have accumulated increasing evidence of genetic defects associated with the development of PD. Such monogenetic links have been found in very few families, and in the majority of cases PD is not thought to be directly inherited. It has been estimated that having a parent with PD increases the lifetime risk of developing PD from 2% to 6%. Most patients have no genetic cause for their PD. It is currently believed that only 5% of all PD cases have a genetic cause (Tugwell, 2008).

Genetic studies have shown that several mutations in seven genes are linked with L-dopa-responsive parkinsonism. One of these is the gene for α-synuclein (Healy *et al.,* 2008). Loss-of-function mutations in four genes namely: parkin, DJ-1, PINK1 and ATP13A2 can cause recessive early onset parkinsonism (Olanow & McNaught, 2006).

2.1.4 **Pathogenesis**

An understanding of the mechanisms underlying the development and progression of PD pathology is critical for the development of neuroprotective therapies (Yacoubain & Standaert, 2009). Similar to other neurodegenerative diseases, aging is a major risk factor (Lees *et al.,* 2009). Several mechanisms have been implicated as crucial to PD pathogenesis with oxidative stress and protein aggregation and misfolding as the most important mechanisms. Other mechanisms include: inflammation, excitotoxicity, apoptosis and other cell death pathways, and loss of trophic support. No one mechanism appears to be primary in all cases of PD, and these pathogenic mechanisms likely act synergistically through complex interactions to promote neurodegeneration (Yacoubain & Standaert, 2009).

2.1.4.1 Oxidative stress and mitochondrial dysfunction

Oxidative stress results from an overabundance of reactive free radicals secondary to either an overproduction of reactive species or a failure of cell buffering mechanisms that normally limit their accumulation. Excess reactive species can react with cellular macromolecules and thereby disrupt their normal functions. Oxidative damage to proteins, lipids, and nucleic acids has been found in the SN of patients with PD (Alam *et al.,* 1997; Dexter *et al.,* 1994). Both overproduction of reactive species and failure of cellular protective mechanisms appear to be operative in PD.

DA metabolism (Figure 2.7) promotes oxidative stress through the production of quinones, peroxides, and other ROS (Hastings *et al.,* 1996).

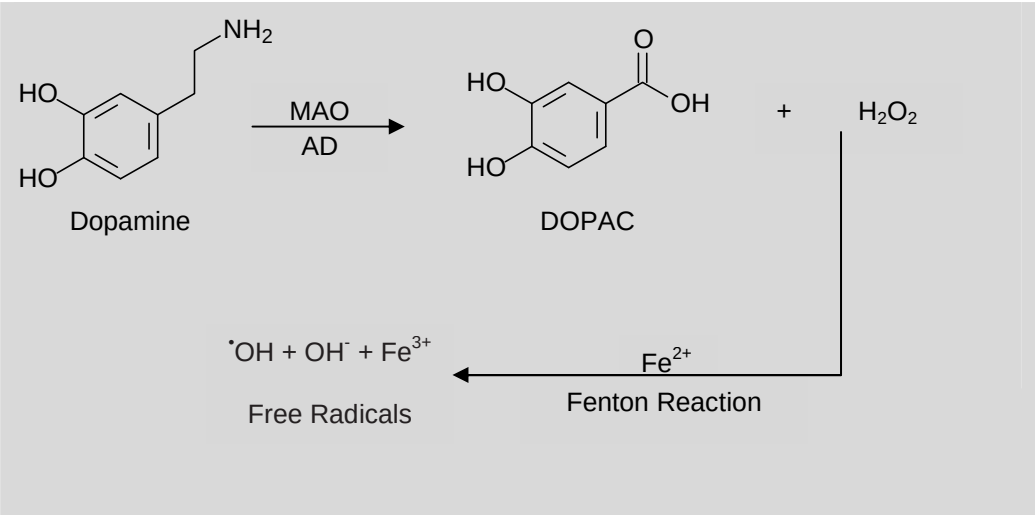

Figure 2.7: **DA Metabolism – DA is metabolised via MAO and aldehyde dehydrogenase (AD) to yield dihydroxyphenylacetic acid (DOPAC) and hydrogen peroxide (H_2O_2). H_2O_2 reacts with excess iron which, via the Fenton Reaction produces free hydroxyl radicals (adapted from Youdim & Bahkle, 2006)**

Mitochondrial dysfunction is another source for the production of ROS, which can then further damage mitochondria (Yacoubain & Standaert, 2009). Nearly 100% of molecular oxygen is consumed by mitochondrial respiration, and powerful oxidants are normally produced as by-products, including hydrogen peroxide and superoxide radicals. These molecules may cause cellular damage by reacting with nucleic acids, proteins and lipids. One target of these reactive species may be the electron transport chain (Cohen, 2000), leading to mitochondria damage and further production of ROS (Dauer & Przedborski, 2003).

Increased iron levels have also been seen in the SN of PD patients (Dexter et *al.,* 1989; Riederer *et al.,* 1989) and could promote free radical damage, particularly in the presence of neuromelanin (Yacoubian & Standaert, 2009). Whether iron has a primary or a secondary role in neurodegeneration it is still unknown (Youdim & Buccafusco, 2005).

An increase in oxidative stress is the link between neuronal damage, iron and MAO. Hydrogen peroxide (H_2O_2) is a normal product of MAO metabolism (Figure 2.7). Under normal circumstances, H_2O_2 is inactivated in the brain via glutathione peroxidase (GPO), an enzyme which uses glutathione (GSH) as a cofactor. But, H_2O_2 may also be chemically converted by Fe^{2+} ions, via the Fenton reaction (Figure 2.7), to yield highly active hydroxyl radicals. Hydroxyl radicals can cause neuronal damage and cell death. In PD it has been found that there are decreased levels of GSH and increased levels of iron and MAO. The decreased level of GSH leads to the accumulation of H_2O_2 which is then in turn available for

the Fenton reaction, resulting in the increase of oxidative damage to neurons (Youdim & Bahkle, 2006).

Several different strategies have been proposed to limit oxidative stress in PD. These strategies include inhibitors of MAO, a key enzyme involved in DA catabolism; enhancers of mitochondrial electron transport, such as Coenzyme Q10; compounds that can directly quench free radicals, such as vitamin E; and molecules that can promote endogenous mechanisms to buffer free radicals, such as selenium. The advantage of many of these agents is that they are well tolerated with few adverse effects, although convincing clinical evidence for the effectiveness of this approach is still lacking (Yacoubian & Standaert, 2009).

2.1.4.2 Protein aggregation and misfolding

Protein aggregation and misfolding have emerged as important mechanisms in many neurodegenerative disorders, including PD and Alzheimer's disease. While the proteins involved in these disorders are different, each is associated with characteristic aggregates of misfolded protein, and these abnormal aggregates appear to acquire toxic properties (Yacoubian & Standaert, 2009). Aggregated or soluble misfolded proteins could be neurotoxic through a variety of mechanisms. Protein aggregates could directly cause damage, perhaps by deforming the cell or interfering with intracellular trafficking of neurons. Protein inclusions may also seize proteins that are important for cell survival (Dauer & Przedborski, 2003).

The primary aggregating protein in PD is α-synuclein (Yacoubian & Standaert, 2009). Oxidative modified α-synuclein resides inside LBs. Modified α-synuclein exhibits a greater tendency to aggregate than unmodified α-synuclein (Giasson *et al.,* 2000). Several herbicides and pesticides provoke aggregation of α-synuclein (Uversky *et al.,* 2001). Also, there appears to be an age-related decline in the ability of cells to handle misfolded proteins (Sherman & Goldberg, 2001).

Together, these observations suggest that overproduction or impaired clearance of α-synuclein, resulting in aggregation thereof, may be a central mechanism in PD. Therefore, therapeutic strategies to prevent protein aggregation or to enhance the clearance of misfolded proteins are the subject of intensive study at present. Inhibitors of α-synuclein aggregation could serve as potential neuroprotective therapies, although a clearer understanding of the toxic form of α-synuclein is important. Molecules that promote protein clearance could also have therapeutic potential (Yacoubian & Standaert, 2009).

2.1.5 **Clinical features, symptoms and diagnosis**

PD commonly presents with impairment of dexterity or, less commonly, with a slight dragging of one foot. The onset is gradual and the earliest symptoms might be unnoticed and misinterpreted for a long time (Lees *et al.,* 2009). Over time, symptoms worsen, and prior to the introduction of L-dopa, the mortality rate among PD patients was three times that of the normal age-matched subjects (Dauer & Przedborski, 2003).

Clinically, any disease that includes striatal DA deficiency or direct striatal damage may lead to parkinsonism (Dauer & Przedborski, 2003), a clinical syndrome consisting of four cardinal features: bradykinesia (slowness and poverty of movement), muscular rigidity, resting tremor and impairment of postural balance (Standaert & Young, 2006).

PD tremor occurs at rest but decreases with voluntary movement, and thus typically does not impair activities of daily living. Rigidity refers to the increased resistance or stiffness to passive movements of a patient's limbs. Bradykinesia, hypokinesia (reduction in movement) and akinesia (absence of normal unconscious movements) manifest as a variety of symptoms that include the following:

- Hypomimia - lack of normal facial expression
- Hypophonia – decreased voice volume
- Drooling – failing to swallow without thinking about it
- Micrographia – decreased size and speed of writing
- Decreased stride length during walking

Bradykinesia significantly impairs the quality of life because it takes much longer to perform everyday tasks such as dressing or eating. PD patients also typically develop a stooped posture and may lose normal postural reflexes, leading to falls. Other common symptoms of parkinsonism include freezing (the inability to begin voluntary movement) and abnormalities of affect and cognition (patients become passive or withdrawn). Depression is common, and dementia is significantly more frequent in PD, especially in older patients (Dauer & Przedborski, 2003).

There are many means and methods to diagnose PD (Table 2.1), but the diagnosis cannot be made without the detection of bradykinesia. Bradykinesia is confirmed with the demonstration of slowness, and a progressive reduction of speed and amplitude on chronological motor tasks (Lees *et al.,* 2009). Although the presence of rest tremor is helpful

for the diagnosis of PD, a similar tremor can occur in some cases of dystonic and atypical tremor syndromes (Cortès *et al.,* 1998).

Table 2.1: Diagnostic criteria for PD (Katzenschlager *et al.,* 2003).

QUEEN SQUARE BRAIN BANK CLINICAL DIAGNOSTIC CRITERIA		
STEP 1: **Diagnosis of parkinsonian Syndrome**	**STEP 2:** **Exclusion criteria for Parkinson's Disease**	**STEP 3:** **Supportive prospective criteria of Parkinson's Disease**
➢ Bradykinesia ➢ And at least one of the following: - Muscular rigidity - 4-6 Hz rest tremor - Postural instability not caused by primary visual, vestibular, cerebellar, or proprioceptive dysfunction	➢ History of repeated strokes with stepwise progression of parkinsonian features ➢ History of repeated head injury ➢ History of definite encephalitis ➢ Oculogyric crisis ➢ Neuroleptic treatment at onset of symptoms ➢ More than one affected relative ➢ Sustained remission ➢ Strictly unilateral features after 3 years ➢ Supranuclear gaze palsy ➢ Cerebellar signs ➢ Early severe autonomic involvement ➢ Early severe dementia with disturbances of memory, language and praxis ➢ Babinski signs ➢ Presence of a cerebral tumor or communicating hydrocephalus on a CT scan ➢ Negative response to large doses of L-dopa and MPTP exposure	Three or more required for diagnosis of definite Parkinson's Disease: ➢ Unilateral onset ➢ Rest tremor present ➢ Progressive disorder ➢ Persistent asymmetry affecting the side onset most ➢ Excellent response (70-100%) to L-dopa ➢ L-dopa response for 5 years or more ➢ Severe L-dopa-induced chorea ➢ Clinical course of 10 years or more ➢ Hyposmia ➢ Visual hallucination

2.1.6 **Treatment**

PD is still an incurable progressive disease, but treatment substantially improves quality of life and functional capacity (Lees *et al.,* 2009).

2.1.6.1 Levodopa (L-dopa)

Levodopa (L-dopa), the metabolic precursor of DA, is the single most effective agent in the treatment of PD. L-dopa is itself largely inert and both its therapeutic and adverse effects result from the decarboxylation of L-dopa to DA. In the brain, L-dopa is converted to DA by

decarboxylation primarily within the presynaptic terminals of dopaminergic neurons in the striatum. The DA produced is responsible for the therapeutic effectiveness of the drug in PD. After release, it is either transported back into dopaminergic terminals by the presynaptic uptake mechanism or metabolized by the actions of MAO and catechol-*O*-methyltransferase (COMT) (Figure 2.8).

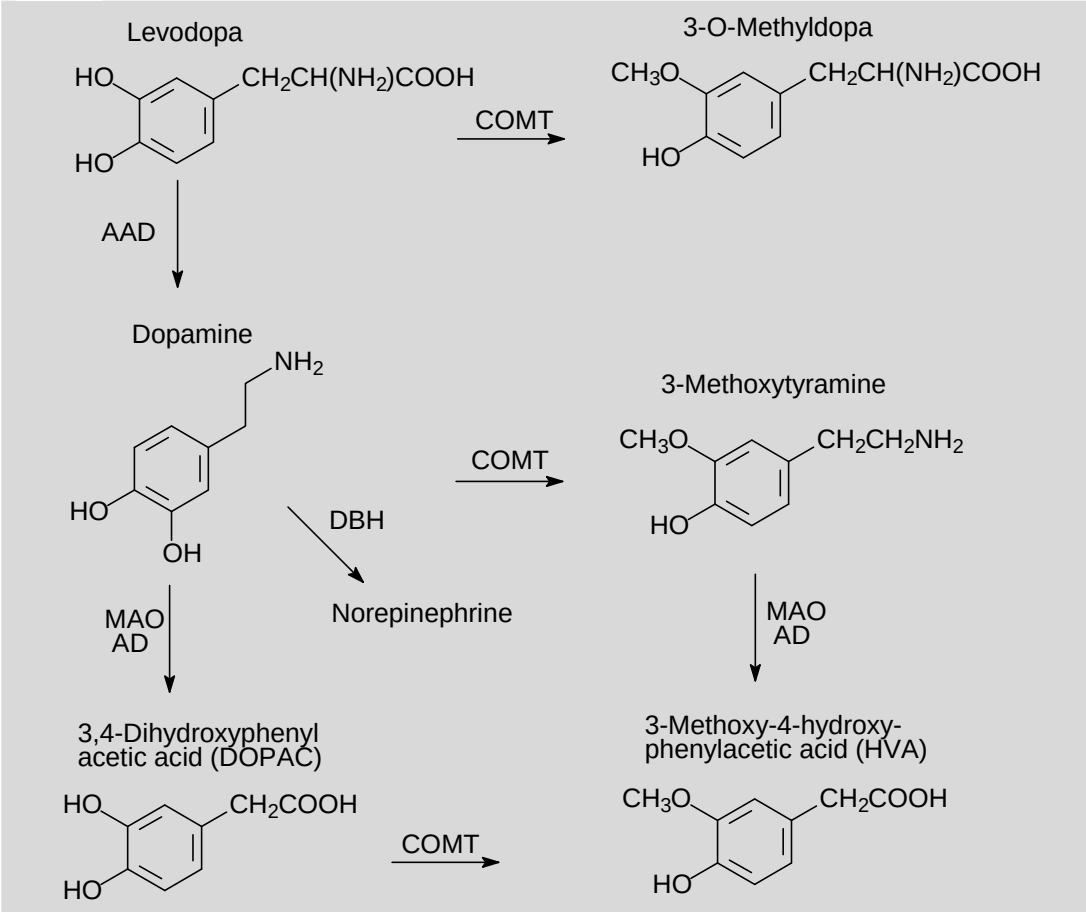

Figure 2.8: **Metabolism of levodopa (L-dopa). AD, aldehyde dehydrogenase; COMT, catechol-*O*-methyltransferase; DβH, DA β-hydroxylase; AAD, aromatic L-amino acid decarboxylase; MAO, monoamine oxidase (Standaert & Young, 2006).**

In practice, L-dopa is almost always administered in combination with a peripherally acting inhibitor of aromatic L-amino acid decarboxylase, such as carbidopa or benserazide that do not penetrate well into the CNS. If L-dopa is administered alone, the drug is largely decarboxylated by enzymes in the intestinal mucosa and other peripheral sites so that relatively little unchanged drug reaches the cerebral circulation and probably less than 1% penetrates the CNS.

L-dopa therapy can have a dramatic effect on all the signs and symptoms of PD. Early in the course of the disease, the degree of improvement in tremor, rigidity, and bradykinesia may be nearly complete. A principal limitation of the long-term use of L-dopa therapy is that with time this apparent "buffering" capacity is lost, and the patient's motor state may fluctuate dramatically with each dose of L-dopa. A common problem is the development of the "wearing off" phenomenon: each dose of L-dopa effectively improves mobility for a period of time, perhaps 1 to 2 hours, but rigidity and akinesia return rapidly at the end of the dosing interval. Increasing the dose and frequency of administration can improve this situation, but this often is limited by the development of dyskinesias and excessive and abnormal involuntary movements (Standaert & Young, 2006).

2.1.6.2 Dopamine receptor agonists

An alternative to L-dopa is the use of drugs that are direct agonists of striatal DA receptors, an approach that offers several potential advantages. Most DA receptor agonists in clinical use have durations of action substantially longer than that of L-dopa and often are useful in the management of dose-related fluctuations in motor state (Standaert & Young, 2006).

The non-ergoline DA antagonists (pramipexole and ropinirole, Figure 2.9) are efficacious drugs that, in contrast to L-dopa, when used in monotherapy do not provoke dyskinesias. They are a popular first-line treatment in patients under 55 years of age, however, treatment with L-dopa is usually necessary within 3 years of diagnosis (Lees *et al.,* 2009). L-dopa is used as initial treatment in older patients who may be more vulnerable to the cognitive effects of the DA agonists (Standaert & Young, 2006).

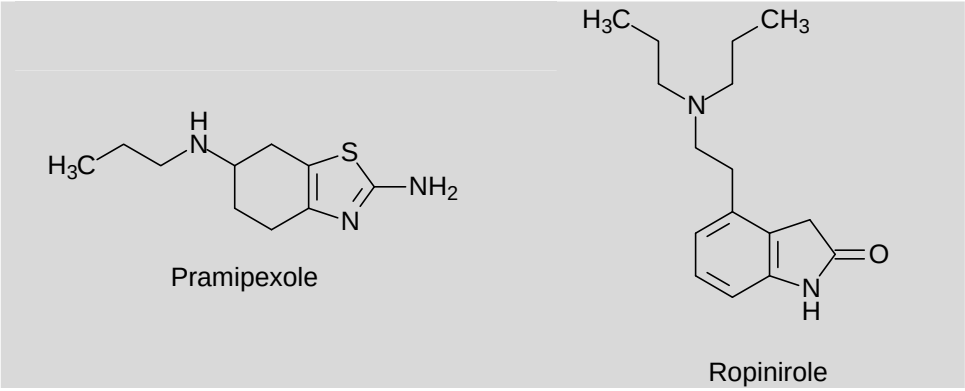

Figure 2.9: Molecular structure of pramipexole and ropinirole

2.1.6.3 Catechol-O-methyltransferase (COMT) inhibitors

A recently developed class of drugs for the treatment of PD consists of inhibitors of COMT (Figure 2.10). COMT and MAO are responsible for the catabolism of L-dopa as well as DA. When L-dopa is administered orally, nearly 99% of the drug is catabolized and does not reach the brain. The principal therapeutic action of the COMT inhibitors is to block this peripheral conversion of L-dopa to 3-*O*-methyldopa, increasing both the plasma half-life of L-dopa as well as the fraction of each dose that reaches the CNS (Standaert & Young, 2006).

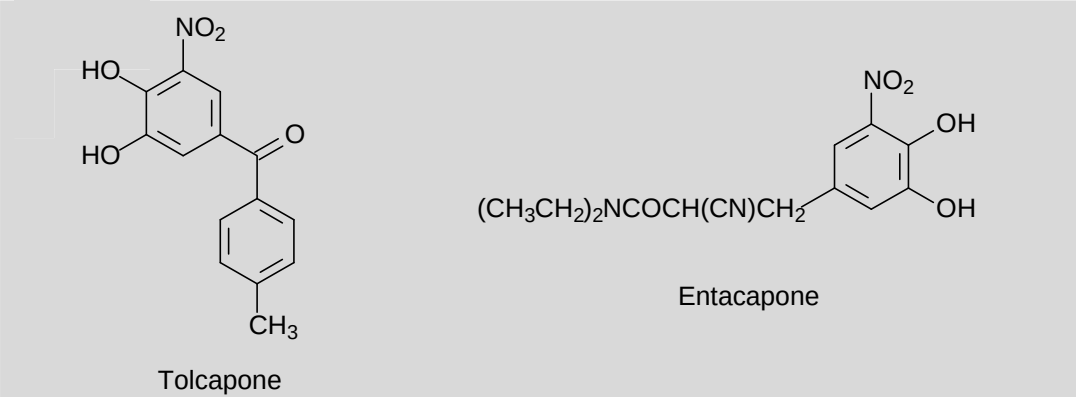

Figure 2.10: Molecular structures of the COMT inhibitors, tolcapone and entacapone

2.1.6.4 Selective MAO-B inhibitors

While both MAO isoenzymes (MAO-A and MAO-B) are present in the periphery and inactivate monoamines of intestinal origin, the isoenzyme MAO-B is the predominant form in the striatum and is responsible for most of the oxidative metabolism of DA in this brain region. At low to moderate doses (10 mg/day or less), deprenyl (Figure 2.11), is a selective inhibitor of MAO-B, leading to irreversible inhibition of the enzyme (Olanow, 1993). Unlike nonspecific inhibitors of MAO (such as phenelzine, tranylcypromine, and isocarboxazid), deprenyl does not inhibit peripheral metabolism of catecholamines. It may thus be taken safely with L-dopa (Standaert & Young, 2006).

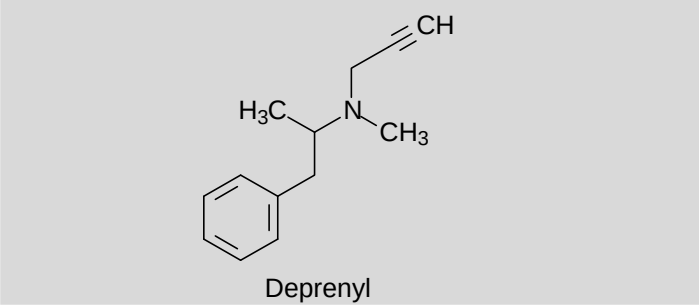

Figure 2.11: Molecular structure of a selective MAO-B inhibitor, deprenyl

2.1.6.5 Muscarinic receptor antagonists

Antagonists of muscarinic acetylcholine receptors were used widely for the treatment of PD before the discovery of L-dopa. Several drugs with anticholinergic properties are currently used in the treatment of PD, including trihexyphenidyl and diphenhydramine (Figure 2.12). The adverse effects of these drugs are a result of their anticholinergic properties. Most troublesome are sedation and mental confusion (Standaert & Young, 2006).

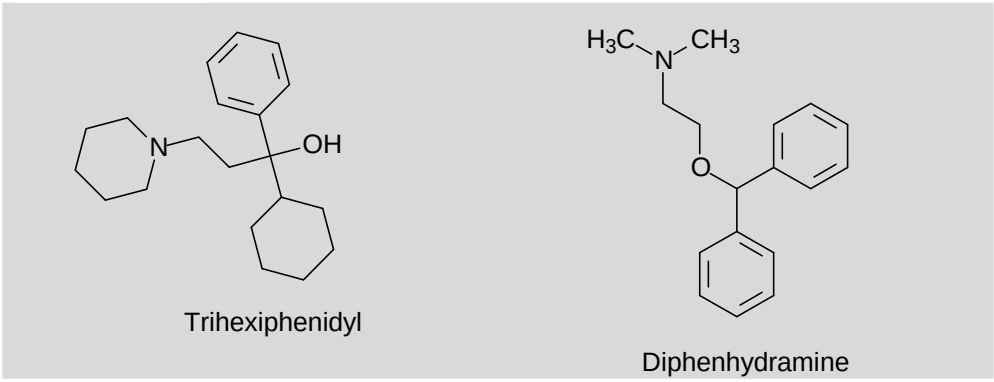

Figure 2.12: Molecular structures of muscarinic receptor antagonists.

2.1.7 **Neuroprotection**

It would be desirable to identify a treatment that modifies the progressive degeneration that underlies PD rather than simply controlling the symptoms. Current research strategies are based on the mechanistic approaches described earlier (oxidative stress, environmental triggers and protein aggregation and misfolding) and on discoveries related to the genetics of PD (Cantuti-Castelvetri *et al.,* 2005).

2.1.7.1 Dopamine receptor agonists

Some of the strongest evidence for a neuroprotective action has emerged from the long-term studies of the effects of the DA agonists, pramipexole and ropinirole (Standaert & Young, 2006). They are potentially neuroprotective by acting at D_2 autoreceptors found on dopaminergic SN terminals (Yacoubian & Standaert, 2009). By stimulating presynaptic receptors, pramipexole and ropinirole may reduce endogenous DA production and release, thereby diminishing oxidative stress (Standaert & Young, 2006).

2.1.7.2 Adenosine receptor antagonists

Epidemiological studies have indicated that caffeine may reduce the incidence of PD, at least in men (Ross *et al.,* 2000; Ascherio *et al.,* 2001). As caffeine mediates its action by antagonizing adenosine receptors, this finding has led to the interest in evaluating adenosine receptor antagonists as potential neuroprotective agents (Schwarzchild *et al.,* 2006). In the striatum, the stimulation of the A_{2A} receptor may lead to the heterodimerization of A_{2A} receptors and D_2 receptors to inhibit DA signaling (Ferrè & Fuxe, 1992; Ferrè *et al.,* 1993), while inhibition of the A_{2A} receptor can promote DA function. Two small clinical trials with the A_{2A} antagonist, istradefylline (KW-6002), have demonstrated potential symptomatic effects in advanced PD (Bara-Jimenez *et al.,* 2003; Chen *et al.,* 2001). More recent research has suggested that A_{2A} antagonists not only improve symptomatic function in PD but may also be neuroprotective. Caffeine and istradefylline are both neuroprotective in the MPTP model of PD (Chen *et al.,* 2001; Ikeda *et al.,* 2002), and caffeine (and related A_{2A} antagonists) has been identified as a priority agent to be evaluated for neuroprotection in clinical trials (Ravina *et al.,* 2003). A potential advantage of A_{2A} antagonists is that they have also been shown to be neuroprotective in non-dopaminergic brain areas in animal models (Monopoli *et al.,* 1998) so that they may protect against PD neurodegeneration found in regions besides the SN (Yacobain & Standaert, 2009).

2.1.8 **Conclusion**

PD is a common neurodegenerative movement disorder that is associated with significant medical disability and reduction in quality of life. The pharmacologic treatment of PD can be divided into neuroprotective and symptomatic therapy. However, nearly all of the available treatments are symptomatic in nature and do not appear to slow or reverse the natural course of the disease. Once identified and shown to be effective, neuroprotective drugs could be used in patients with early clinical signs of disease or potentially even prior to the appearance of disease in those shown to be at genetic risk.

Several potential neuroprotective agents for PD have shown some promise in animals and/or humans and are undergoing further investigation. These include MAO inhibitors, DA agonists, and adenosine A_{2A} antagonists such as KW-6002 and (E)-8-(3-chlorostyryl)caffeine (CSC) (Figure 2.13).

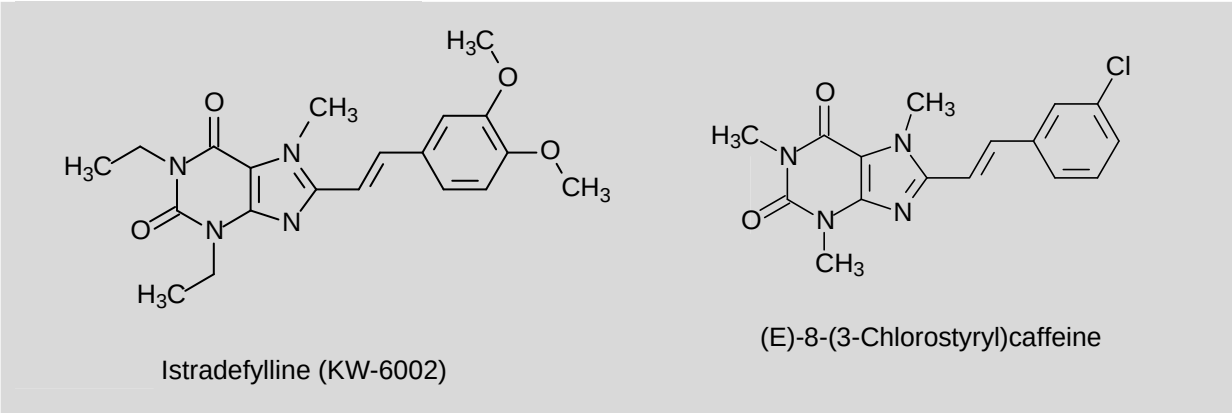

Figure 2.13: **Adenosine A_{2A} antagonists, istradefylline and (E)-8-(3-chlorostyryl)caffeine (CSC).**

2.2 **MONOAMINE OXIDASE**

2.2.1 **Introduction**

Enzymes have been traditionally thought to act as catalysts in complex biochemical pathways within a cell, and are classified according to the nature of the enzymatic reaction they catalyze (e.g. nucleotidases, oxidases, kinases). These molecules have the capacity to catalyze enzymatic reactions in the immediate vicinity of the cell surface, and thereby regulate the concentration and functions of their substrates and end-products, which are often biologically active (Jalkanen & Salmi, 2001).

The MAO's (MAO-A and –B) are mitochondrial bound isoenzymes which catalyze the oxidative deamination of dietary amines and monoamine neurotransmitters, such as serotonin, norepinephrine, DA and other trace amines. The rapid degradation of these molecules ensures the proper functioning of synaptic neurotransmission and is critically important for the regulation of emotional behaviors and other brain functions (Bortolato *et al.,* 2008).

Inhibitors of MAO with selectivity and specificity for MAO-B prolong the activity of both endogenously and exogenously derived DA, making them an option either as monotherapy in early PD or as adjunctive therapy in patients treated with L-dopa, which are experiencing motor complications. In addition to symptomatic benefits, experimental data suggest that MAO-B inhibitors may be neuroprotective through MAO-B inhibition and other mechanisms that have yet to be clearly defined (Herraiz & Chaparro, 2005).

MAO was first discovered as tyramine oxidase by Hare in 1928, since it catalyzed the oxidative deamination of tyramine. This enzyme was then found to oxidize various monoamines including catecholamines such as DA, noradrenaline, adrenaline and 5-HT (Nagatsu, 2004).

2.2.2 **Classification and Characteristics**

2.2.2.1 Classification

Amine oxidases (AO's) have been traditionally divided into two main groups, based on the chemical nature of the attached cofactor (Figure 2.14). The FAD containing enzymes are intracellular enzymes (Shih *et al.,* 1999) and consist of MAO and polyamine oxidase (PAO). The other class of AO's contain a cofactor possessing one or more carbonyl groups, which appears to be topa-quinone (TPQ). This class of AO's is also known as the copper-

containing semicarbazide-sensitive amine oxidases (SSAO) (Klinman & Mu, 1994; Lyles, 1996). These enzymes include diamine oxidases (DAO), lysyl oxidase, and plasma membrane and soluble MAO's. The FAD- and TPQ-containing AO's not only differ in their cofactors, but are also distinct in terms of their subcellular distribution, substrates, and inhibitors, and biological functions. MAO-A and -B are well known mitochondrial enzymes that have firmly established roles in the metabolism of neurotransmitters (e.g. noradrenaline) and other biogenic amines (e.g. tyramine, adrenaline) (Shih *et al.,* 1999). FAD-containing polyamine oxidases use secondary amines spermine and spermidine as their preferred substrates, and thereby possibly regulate cell growth (Seiler, 1990).

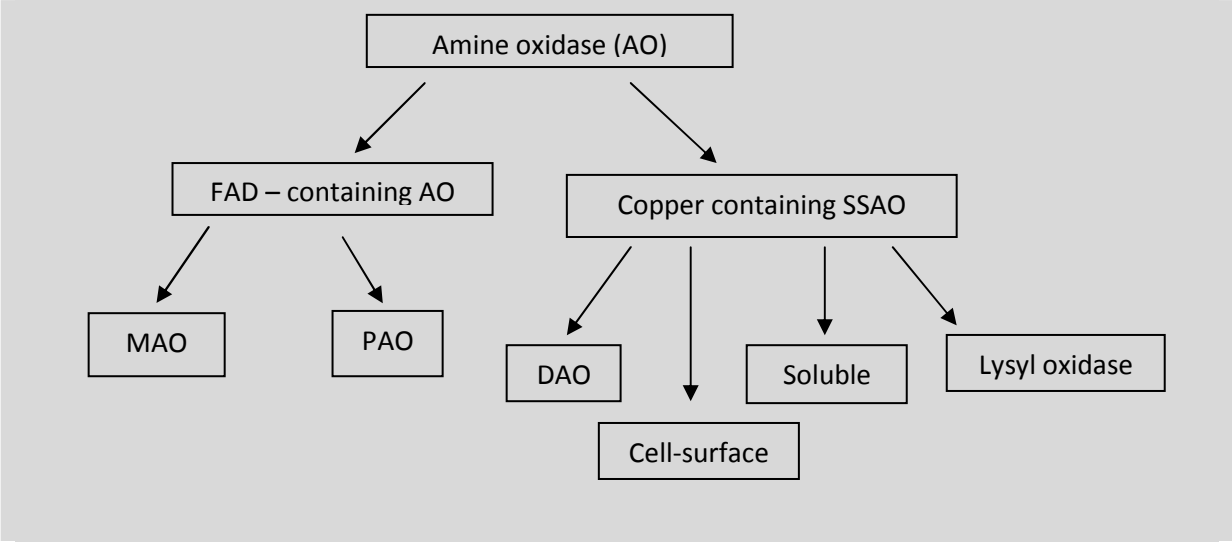

Figure 2.14: Classification of amine oxidases (Adapted from Jalkanen & Salmi, 2001)

2.2.2.2 Characteristics

The crystal structures of MAO-A and MAO-B have only recently been elucidated, necessitating a radical revision of some long-held ideas about how the enzyme interacts with substrates and inhibitors (Youdim *et al.,* 2006). The distinction between the two isoforms of MAO was first defined on the basis of substrate and inhibitor sensitivity, before their molecular characterization. The metabolism of DA and other monoamines (such as tryptamine and tyramine) is generally attributed by both isoforms (Figure 2.15). Notably, however, DA is mainly degraded by MAO-A in the rodent brain, while MAO-B predominantly metabolizes DA in the brains of humans and other primates. Both proteins are predominantly located in the outer membrane of mitochondria, to which they are anchored by the C-terminal domain (Rebrin *et al.,* 2001).

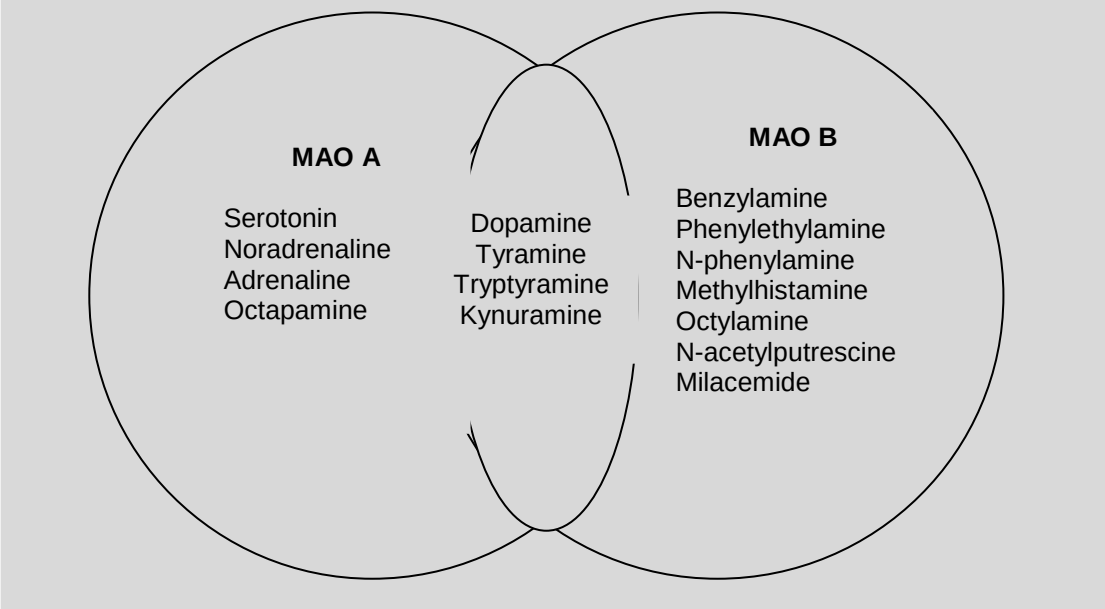

Figure 2.15: MAO-A and MAO-B substrate specificities

2.2.3 **Localization and tissue distribution**

MAO-A and MAO-B are tightly associated with the mitochondrial outer membrane, although a small proportion of each enzyme is associated with the microsomal fraction. MAO is present in most mammalian tissues, but the proportions of the two isoenzymes vary from tissue to tissue (Youdim *et al.,* 1988). In the rat peripheral nervous system (PNS), histochemical studies have shown that MAO is localized in the endothelial cells of the endoneurial vessels, in Schwann cells and in the unmyelinated axons of some neurons (Matsubayashi *et al.,* 1986). The two isoenzymes are not evenly distributed in the human brain, and the main form in the BG is MAO-B. Only MAO-A is involved in DA metabolism in the rat brain, whereas, despite earlier claims to the contrary, both MAO-A and MAO-B can contribute to DA metabolism in the human brain (Youdim *et al.,* 2006). In the brain, MAO-A is predominantly found in catecholaminergic neurons, whereas MAO-B is detected in serotonergic and histaminergic neurons and in glial cells (Jahung *et al.,* 1997; Saura *et al.,* 1994). MAO-B expression is higher in the adult human brain than in the foetal brain and MAO-B expression increases as the brain ages (Shih, 1979).

2.2.4 **Physiological functions**

MAO in peripheral tissues, such as the intestine, liver, lungs and placenta, seems to protect the body by oxidizing amines from the blood or by preventing their entry into the circulation. MAO-B in the micro-vessels of the blood–brain barrier presumably has a similar protective function, acting as a metabolic barrier. It has been suggested that in the PNS and CNS

intraneuronal MAO-A and MAO-B protect neurons from exogenous amines, terminate the actions of amine neurotransmitters and regulate the contents of intracellular amine stores. Noradrenergic neurons contain both MAO-A and MAO-B (O'Carroll *et al.,* 1983), and NA is a reasonably good substrate for both forms of the enzyme.

2.2.5 **Molecular structure and characteristics of MAO**

MAO is a FAD-containing enzyme located at the outer membranes of the mitochondria (Herraiz & Chaparro, 2005), to which they are anchored by the C-terminal domain (Rebrin *et al.,* 2001). The rest of the protein is exposed to the cytoplasm (Youdim *et al.,* 2006). MAO-A and MAO-B share a 70% sequence identity (Binda *et al.,* 2007) and are distinguished by their substrate and inhibitor selectivities (Kalgutkar *et al.,* 2001). Human MAO-B crystallizes as a dimer and laboratory evidence suggests that it may also occur as a dimer in its membrane environment (Binda *et al.,* 2002). The structure of a single monomer of the dimeric form is shown in Figure 2.16a. In contrast to human MAO-B, human MAO-A crystallizes as a monomer (Figure 2.16b, DeColibus *et al.,* 2005).

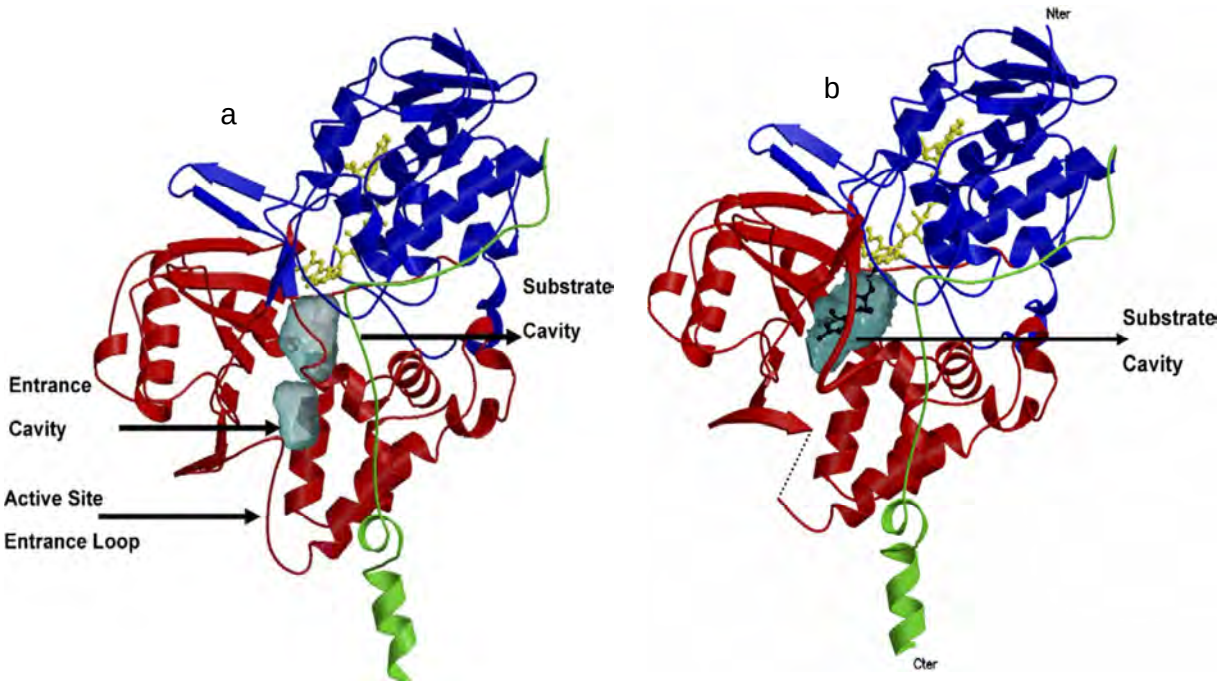

Figure 2.16: **(a) Ribbon diagram of the monomeric unit of the human MAO-B structure. The covalent flavin moiety is shown in a ball and stick model in yellow. The flavin binding domain is in blue, the substrate domain in red and the membrane binding domain in green.**

(b) Ribbon diagram of the human MAO-A structure. The colouring of the domains follows as for the structure of MAO-B (Edmonson *et al.,* 2007).

A prominent feature of MAO-B is the presence of two adjacent cavities in the interior of the protein (Figure 2.16a). For a substrate molecule to reach the flavin center, it must first negotiate a protein loop at the entrance to one of two cavities before reaching the flavin coenzyme. The first cavity is termed the “entrance cavity”, is very hydrophobic in nature and exhibits a volume of 290 $Å^3$. Separating the “entrance cavity” from the similarly hydrophobic substrate cavity (volume = 390 $Å^3$) is an isoleucine199 (Ile-199) side chain which serves as a “gate” between the two cavities. Depending on the substrate or bound inhibitor, it can exist in either an open or a closed form which has been shown to be important in defining the inhibitor specificity of harmine for MAO-B (Hubalek *et al.,* 2005). At the end of the substrate cavity is the FAD coenzyme which is covalently bound in an 8α-thioether linkage (Kearney *et al.,* 1971) to cysteine397 (Cys-397). Analysis of the active site cavities show them both to be very hydrophobic with sites for favorable amine binding to the flavin involving two nearly parallel tyrosyl (398 and 435) residues (Figure 2.17) which forms an “aromatic cage” (Edmonson *et al.,* 2007). This structure has potential functional significance, because inhibitors and substrates must pass between the two tyrosyl phenolic rings to reach the flavin ring (Youdim *et al.,* 2006).

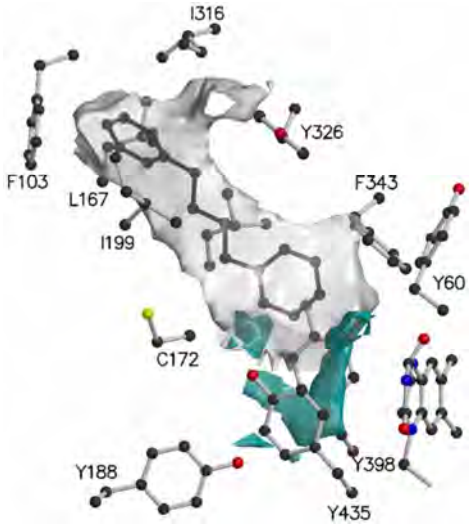

Figure 2.17 Aromatic cage of MOA-B (Edmonson *et al.,* 2007)

The structure of MAO-B bound to the acetylenic inhibitor rasagiline, a selective, irreversible MAO-B inhibitor, has led to several new insights into its structural properties. Rasagiline and pargyline, nonselective MAO inhibitors, both form covalent N(5)-flavocyanine adducts with MAO-B. Both the R and S isomers of rasagiline can covalently bind to MAO-B, although only the *R* isomer is pharmacologically active. The two isomers are covalently bound in the same manner; however, the aminoindan rings, which are partially extended into the entrance

cavity, are in opposite orientations in their bound forms (Figure 2.18). The side chain of Ile-199 is rotated to an 'open' conformation, which results in the fusing of the two cavities to a volume of ~700 Å^3. These observations have led to the hypothesis that Ile-199 serves as a 'gate' to separate the substrate and entrance cavities of MAO-B. Mutation of Ile-199 to phenyalanine, as is found in bovine MAO-B and in all known MAO-A sequences, results in an active enzyme that binds rasagiline and other irreversible inhibitors, but is unable to bind the reversible MAO-B-specific inhibitors namely 1,4-diphenyl-2- butene, CSC and farnesol (Hubalek *et al.,* 2005). Structural studies of two of these three reversible inhibitors show them to occupy both the entrance and substrate cavities when bound to human MAO-B. These insights provide a rationale for the development of MAO-B-specific neuro protectant inhibitors (Youdim *et al.,* 2006).

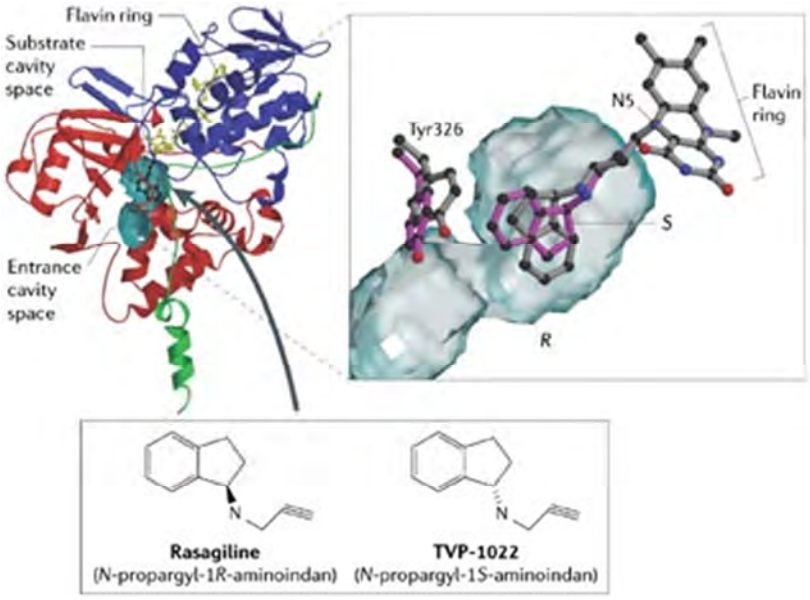

Figure 2.18: **The crystal structure of MAO-B and effect of stereochemistry on rasagiline binding to human MAO-B (Youdim *et al.*, 2006)**

A comparison of the active sites for human MAO-B and MAO-A are shown in Figure 2.19. MAO-B has a bipartite elongated cavity that occupies a combined volume close to 700 Å^3 when the side chain of Ile-199 is in the "open" conformation and consists of two smaller cavities. MAO-A has a single cavity that exhibits a "rounder" shape and is larger in volume than the "substrate" cavity of MAO-B. Analysis of residue side chains in either active site shows the substrate to have less freedom for rotation in the MAO-B site than in MAO-A. The structural basis for differences between the two cavities can be partially attributed to conformational differences of a six residue segment (residues 200-215) that constitutes what is termed a "cavity shaping loop" in MAO-A and MAO-B. This loop is in a more extended

conformation in MAO-A and is in a more compact conformation in MAO-B. Aside from this difference in structure, the Cα-chain trace comparison between the two enzymes (~70% amino acid sequence identity) is 0.7Å[3] (DeColibus *et al.,* 2005).

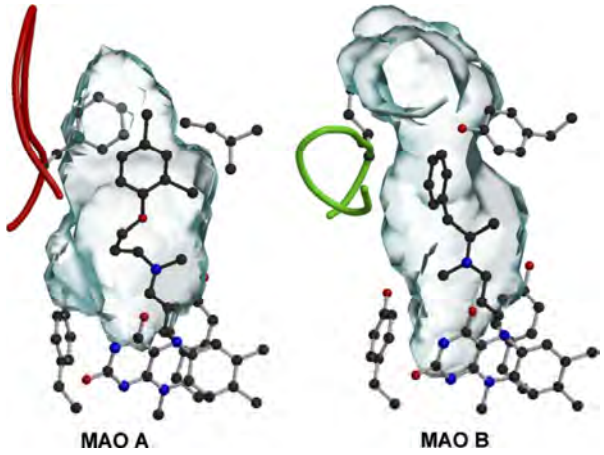

Figure 2.19: **Comparison of the active site cavities of human MAO-A (left) and human MAO-B (right). Clorgyline is in the active site of MAO A and deprenyl is in the active site of MAO B. Both of these inhibitors form covalent N(5) flavocyanine adducts with the respective flavin coenzymes. The active site ''shaping loop'' is shown in red for MAO A and green for MAO B (Edmonson *et al.,* 2007).**

2.2.6 **The catalytic cycle of MAO-B**

Monoamine oxidase (flavin-containing) catalyzes the following reaction:

$RCH_2NH_2 + H_2O + O_2 \rightarrow RCHO + NH_3 + H_2O_2$.

The catalytic site of MAO-B is situated in the substrate binding cavity and contains an FAD molecule that acts as a co-factor (Kearnly *et al.,* 1971).

A number of mechanisms have been proposed to describe the chemical events involved in flavin-dependant amine oxidations (Binda *et al.,* 2002). The single electron transfer mechanism (Silverman *et al.,* 1995) is one of the more popular mechanisms used to describe these oxidations (Figure 2.20). One of the key features of this mechanism is that the flavin serves as a one-electron oxidant of the amine to form the aminium cation radical as the first initial reversible step in the catalysis. This leaves the α-proton acidic enough to allow a basic amino acid residue at the active site to abstract the proton. After a second one electron transfer from the substrate to the flavin, and subsequent radical recombination, the imine product and reduced flavin are formed as products (Binda *et al.,* 2002).

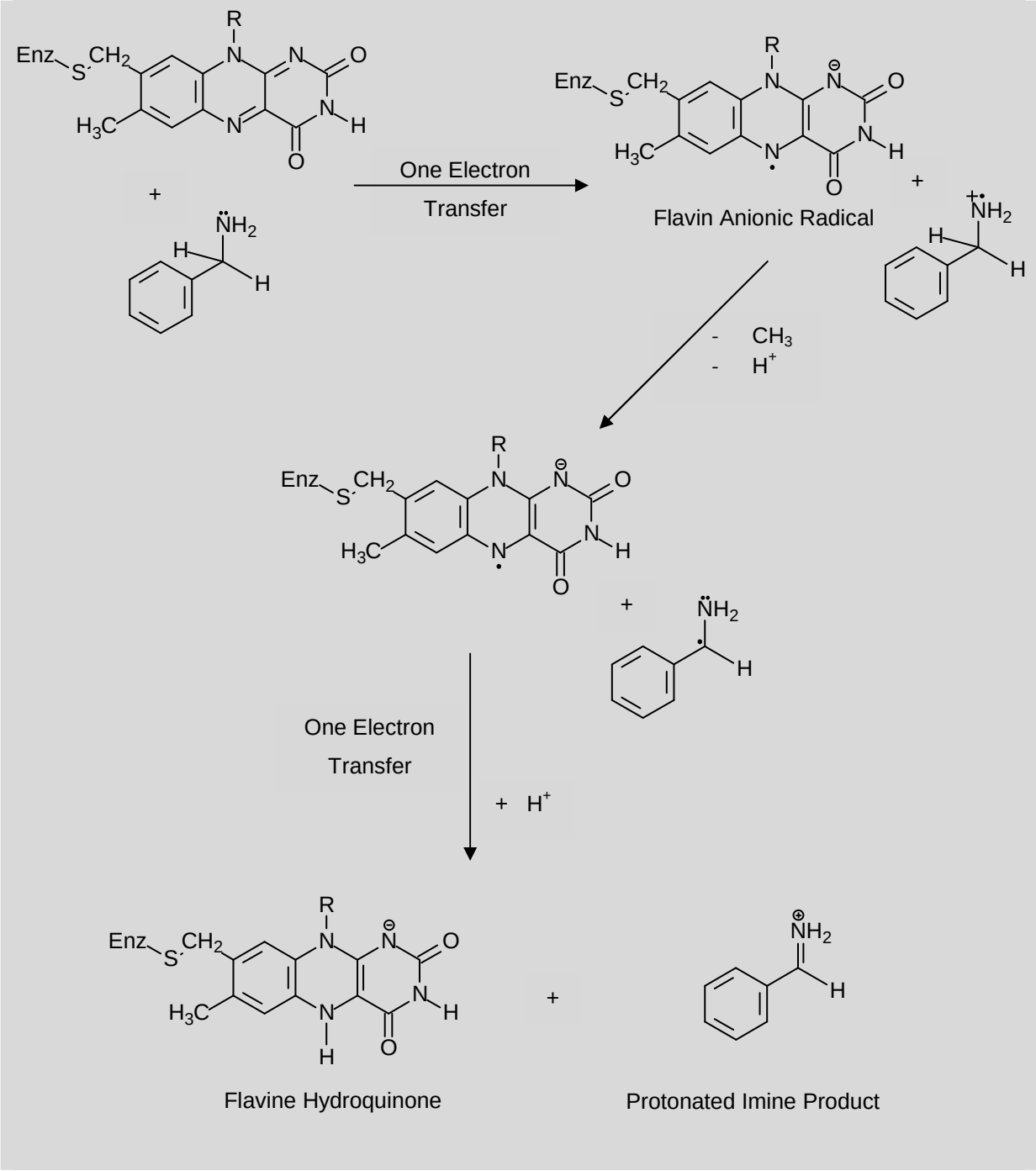

Figure 2.20 **Representation of the single electron transfer mechanism proposed for MAO catalysis (adapted from Binda *et al.,* 2002; Edmonson *et al.,* 2004).**

A second mechanism, the polar nucleophilic mechanism, suggests that the amine functionality adds to the C(4a)-position of the flavin in a nucleophilic manner (Figure 2.21). This leads to the activation of the N5-position to function as a strong active site base. After the α-proton has been transferred to N5, the imine product is released. (Binda *et al.,* 2002). The imine product is hydrolyzed to the corresponding aldehyde and ammonia (or amine if

the substrate is a secondary or tertiary amine). Molecular oxygen acts as an electron acceptor, which oxidizes the reduced flavin and forming H_2O_2. The catalytic cycle is thereby completed (Binda *et al.,* 2002).

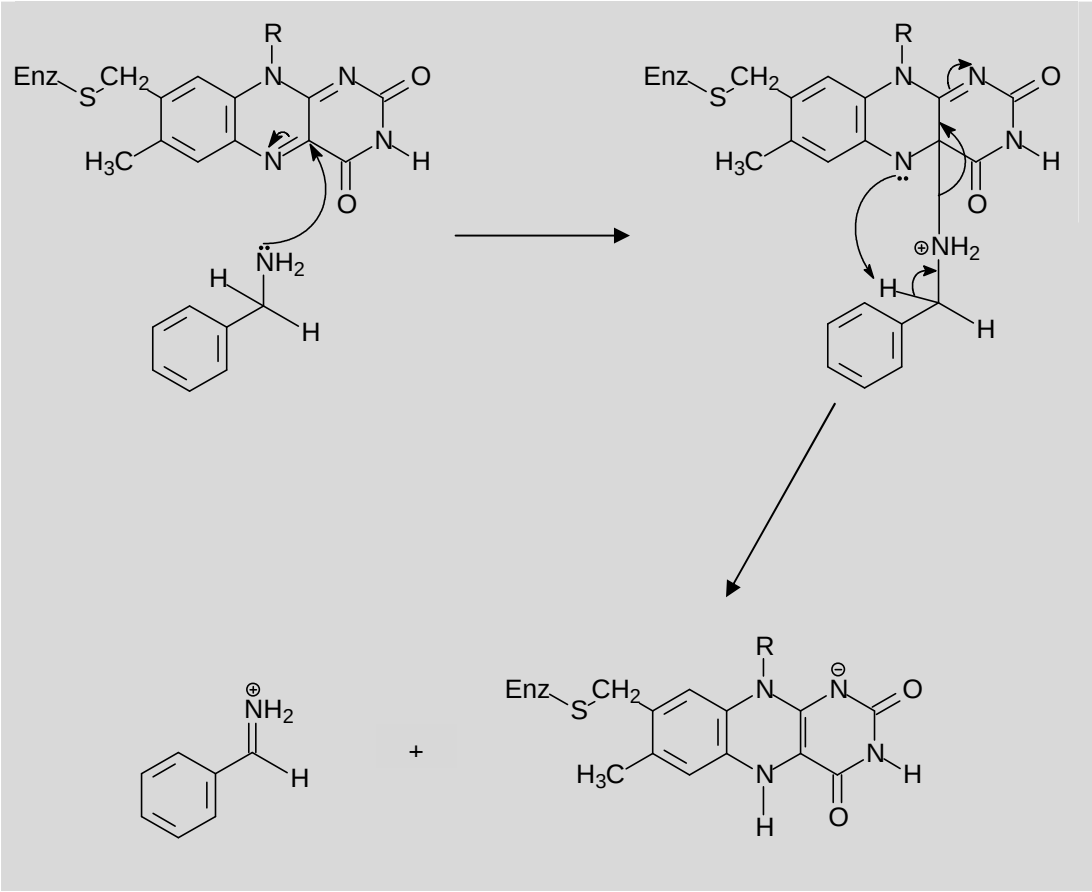

Figure 2.21: **Representation of the polar nucleophilic mechanism proposed for MAO catalysis (Binda *et al.,* 2002).**

2.2.7 **Parkinson's disease and MAO inhibitors**

As previously discussed, the central pathology of PD is the progressive deterioration of the melanin-containing dopaminergic neurons in the SNpc resulting in a depletion of DA along the nigrostriatal pathway. The primary rationale for using selective MAO-B inhibitors in PD is that it enhances striatal dopaminergic activity by inhibiting the metabolism of DA, thereby improving PD motor symptoms (Samii *et al.,* 2004; Riederer *et al.,* 1978).

Since MAO-B appears to be predominantly responsible for DA metabolism in the BG (Collins *et al.,* 1970), inhibition of this enzyme in the brain may conserve the depleted supply of DA (Figure 2.19). MAO-B inhibitors are used in combination with L-dopa as DA replacement therapy in patients diagnosed with early PD (Birkmayer *et al.,* 1975). MAO-B inhibitors have

been shown to elevate DA levels in the striatum of primates treated with L-dopa (Finberg *et al.,* 1998). Furthermore, for each mole of DA oxidized by MAO-B, one mole of H_2O_2 is produced (Barnham *et al*., 2004). Failure to remove excess H_2O_2 is thought to result in the generation of ROS, produced through the interaction of H_2O_2 with chelatable (free ionic) iron (Fenton chemistry, Figure 2.7) that would initiate oxidative stress (Youdim & Buccafusco, 2005). Inhibition of MAO-B, therefore, may also exert a protective effect by reducing H_2O_2 production in the brain (Youdim & Bahkle, 2006). These effects of MAO-B inhibitors are especially relevant when considering that the brain shows an age-related increase in MAO-B activity (Nicotra *et al.,* 2004; Fowler *et al.,* 1997). In the aged parkinsonian brain, inhibition of MAO-B may counter the effects of increased MAO-B activity and protect against further neurodegeneration (Nagatsu & Sawada, 2006).

As mentioned above, MAO-B inhibitors may possess neuroprotective properties by reducing the formation of H_2O_2 that is associated with the MAO catalytic cycle. A second, and to some extent theoretical, rationale for the use of selective MAO-B inhibitors as neuroprotective agents in PD, is based on the finding that MAO-B is responsible for the biotransformation of MPTP into MPP^+, a potent parkinsonism-inducing neurotoxin (Chiba *et al.,* 1984). The discovery that MAO-B inhibition attenuates MPP^+-induced toxicity helped generate the hypothesis that MAO-B inhibitors modify the underlying processes of PD. This hypothesis was first tested in the Deprenyl and Tocopherol Antioxidative Therapy of Parkinsonism (DATATOP) trial, a doubleblind, randomized, placebo-controlled study of deprenyl and tocopherol (vitamin E) in patients with early PD (Parkinson Study Group, 1993). The results suggested that deprenyl may slow the degenerative processes in PD, although this effect was relatively small.

2.2.8 **Adverse effects of MAO inhibitors**

Although MAO-B inhibitors are relatively free from adverse effects, MAO-A inhibitors may lead to serious unfavourable effects when combined with certain drugs and food:

(1) Most notably, when MAO-A inhibitors are used with indirectly acting sympathomimetic amines such as tyramine, which is present is certain foods, cardiovascular side effects may occur (Youdim & Bakhle, 2006; 1988; Brown *et al.,* 1989) (Figure 2.22). Tyramine is normally metabolized by MAO-A in the intestinal endothelial cells, which prevents excessive amounts of tyramine from entering the systemic circulation. Inhibition of MAO-A in the peripheral tissues prevents this normal degradation of tyramine and thus leads to increased systemic concentrations of tyramine. Tyramine initiates the release of noradrenaline from peripheral

adrenergic neurons and as a consequence a severe hypertensive response, which may be fatal, may occur.

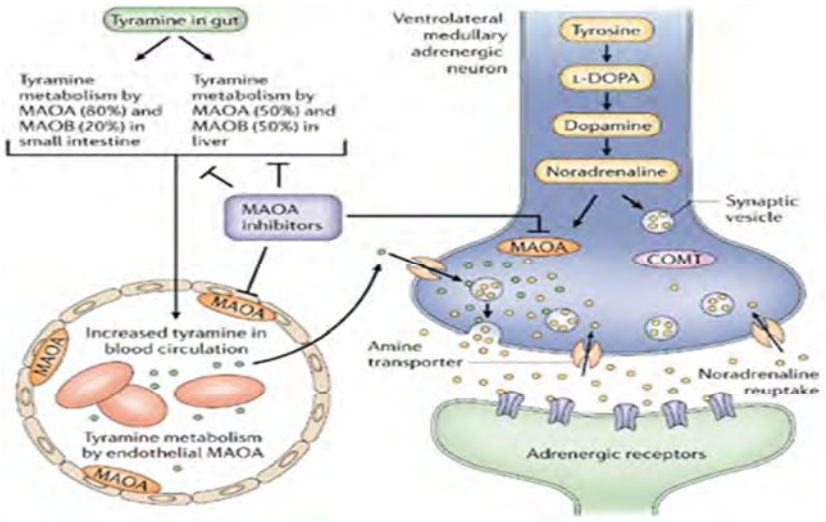

Figure 2.22: **The mechanism of potentiation of cardiovascular effects of tyramine: the 'cheese reaction' (Youdim *et al.,* 2006**

(2) In combination with 5-hydroxytryptaminergic agents, MAO-A inhibitors may cause serotonin toxicity (ST) (Ramsay *et al.,* 2007; Stanford *et al.,* 2009). ST is the result of excessive extracellular serotonin concentration in the central nervous system and is most often caused by a combination of MAO-A inhibitors, which result in the reduction of the MAO-A-catalyzed degradation of serotonin, with SSRIs and serotonin-releasing agents. ST is one of very few drug-to-drug interactions involving therapeutic doses of commonly used drugs which are capable of rapidly causing death (Stanford *et al.,* 2009).

(3) MAO-A inhibitors should also be used with caution in combination with L-dopa since this may lead to a hypertensive response (Zesiewicz & Hauser, 2002).

Because of these potential adverse effects, MAO-A inhibitors are used less frequently in the treatment of depression than the SSRIs and the tricyclic antidepressants, and are considered less suitable to enhance dopaminergic neurotransmission in the parkinsonian brain than MAO-B inhibitors. Recently developed reversible inhibitors of MAO-A, such as moclobemide, however are considered safer than the irreversible MAO-A type inhibitors (Bonnet, 2003). For example, moclobemide is essentially free form the tyramine reaction and ST occurs only when an excessive dose of the 5-hydroxytryptaminergic agent have been used (Wu *et al.,* 2003). In spite of its reversible mode of action, moclobemide retains an antidepressive effect.

2.2.9 **Pharmacology of MAO-B inhibitors**

2.2.9.1 Deprenyl

Deprenyl is an irreversible MAO-B selective inhibitor that prevents the metabolism of DA. As a result, when used in combination with L-dopa, deprenyl enhances the antiparkinsonian effects of L-dopa, thus allowing for a reduction in L-dopa dose. Consequently, the main indication for deprenyl is as adjunctive therapy with L-dopa in PD. Studies suggest that deprenyl also may retard disease progression (Cohen & Spina, 1989). In addition, patients treated with deprenyl are significantly less likely to experience the "on-off" phenomenon or freezing of gait, but significantly more likely to experience dyskinesia.

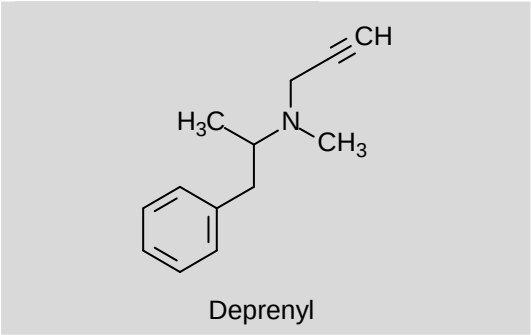

Figure 2.23: Molecular structure of deprenyl

2.2.9.2 Rasagiline

Rasagiline is an irreversible MAO-B inhibitor, which is currently recommended for adjunctive therapy in patients with PD to reduce "off" time associated with motor fluctuations (Pahwa, 2006). Rasagiline, in addition to its symptomatic benefits, has been shown to exert neuroprotective effects in several preclinical experiments (Chen & Swope, 2005; Kupsch *et al.,* 2001). The neuroprotective effects of rasagiline are dose dependent and are more pronounced than those of deprenyl (Goggi *et al.,* 2000; Maruyama *et al.,* 2000).

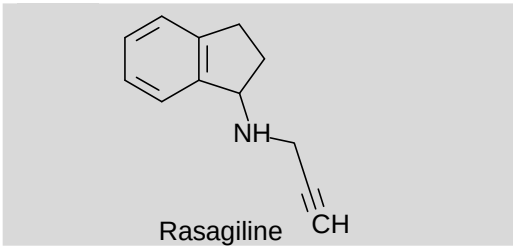

Figure 2.24: Molecular structure of rasagiline

2.2.9.3 Lazabemide

The initial results with deprenyl prompted consideration of additional MAO-B inhibitors as potential neuroprotective agents. Lazabemide (Figure 2.25) differs from selegiline in several properties: it is a reversible inhibitor of MAO that has greater selectivity for MAO-B than MAO-A and undergoes rapid clearance after discontinuation. Furthermore, lazabemide is not a propargylamine compound and is not metabolized to amphetamine as is deprenyl (LeWitt *et al.,* 1993; LeWitt & Taylor, 2008).

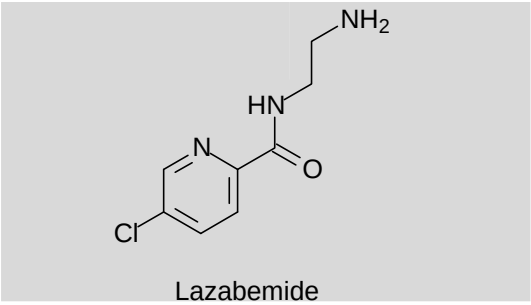

Figure 2.25: Molecular structure of lazabemide.

2.2.9.4 Ladostigil

Although ladostigil (Figure 2.26) is structurally related to rasagiline, it does not inhibit either MAO-A or -B *in vitro*. However, after chronic treatment for 1–8 weeks with ladostigil, both isoforms of MAO in brain are inhibited with very little inhibition of the enzyme in gut or liver. This unexpected, tissue-selective, action allows for the irreversible inhibition of all MAO activity in brain tissue, with no risk of precipitating the cheese reaction, reflecting the lack of inhibition of the enzyme in gut and liver (Sagi *et al.,* 2005). Furthermore, like other selective MAO-B inhibitors (deprenyl, rasagiline and lazabemide) ladostigil prevents the striatal neurodegeneration and DA depletion induced by the neurotoxin, MPTP, in the mouse model of PD (Sagi *et al.,* 2005). Because both isoforms of MAO are inhibited, ladostigil, unlike selegiline or rasagiline, markedly increases brain DA in MPTP-treated mice. In addition, ladostigil exhibited neuroprotective activities in cultures of neuronal cells.

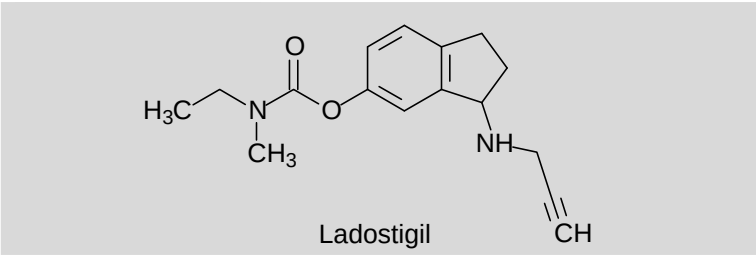

Figure 2.26: Molecular structure of ladostigil.

2.2.10 **Conclusion**

The mitochondrial outer membrane-anchored MAO's are important flavoenzymes that catalyzes the deamination of biogenic and xenobiotic amines. The two subtypes, MAO-A and MAO-B, are linked to several neurological disorders and are therefore interesting targets for drug design. Since MAO-B acts in the brain to degrade DA, inhibitors of MAO-B is considered to be useful therapeutic tools for the treatment of PD.

Knowledge of the three-dimensional crystal structures of MAO-A and MAO-B plays an important role in substrate and inhibitor recognition and to distinguish between A and B specificities. It also provides new insights into designing specific reversible MAO-B inhibitors for the treatment of PD.

2.3 THE ADENOSINE A_{2A} RECEPTOR

2.3.1 Introduction

Adenosine A_{2A} receptors have a unique cellular and regional distribution in the basal ganglia, being concentrated in areas richly innervated by DA such as the caudate-putamen (CPu) and the globus pallidus (GP) (Morelli *et al.,* 2007). They are predominantly expressed in enkephalin-expressing GABAergic striatopallidal neurons and therefore are highly relevant to the function of the indirect efferent pathway of the BG system. In these GABAergic enkephalinergic neurons, the A_{2A} receptor interacts structurally and functionally with the DA D_2 receptor. A_{2A} and D_2 receptors exhibit mutual antagonistic interactions that are central to the function of the indirect pathway and hence to BG control of movement, motor learning, motivation and reward. Consequently, this A_{2A}/D_2 receptors antagonistic interaction is also central to BG dysfunction in PD (Schiffmann *et al.,* 2007).

In the pursuit of improved treatments for PD, the adenosine A_{2A} receptor has emerged as an attractive non-dopaminergic target. Based on the compelling behavioural pharmacology and selective BG expression of this receptor, its antagonists are now crossing the threshold of clinical development as adjunctive symptomatic treatment for relatively advanced PD. The antiparkinsonian potential of A_{2A} antagonism has been boosted further by recent preclinical evidence that A_{2A} antagonists may favourably alter the course as well as the symptoms of the disease. Convergent epidemiological and laboratory data have suggested that A_{2A} blockade may offer neuroprotection against the underlying dopaminergic neuron degeneration. In addition, rodent and non-human primate studies have raised the possibility that A_{2A} receptor activation contributes to the pathophysiology of dyskinesias and that A_{2A} antagonism might help prevent them (Xu *et al.,* 2005).

2.3.2 Adenosine Receptors

Adenosine is a nucleoside composed of the purine base adenine and ribose. It is not a transmitter substance, but rather a normal metabolite that also serves a signalling function (Jenner *et al.,* 2009). Adenosine is not only an essential intracellular element of human biology but also a versatile extracellular signal under various physiological and pathological conditions. In the CNS, adenosine modulates sleep and arousal, locomotion, nociception, seizure susceptibility, neuroprotection, drug addiction, and other vitally important processes. To date, 4 adenosine receptor subtypes have been characterized namely A_1, A_{2A}, A_{2B} and A_3 (Xu *et al.,* 2005).

Like other adenosine receptors, the adenosine A_{2A} receptor has 7 transmembrane domains (Figure 2.27) and has the general structure that places it in the G-protein-coupled receptor (GPCR) superfamily. Like the A_1 receptor, the A_{2A} receptor binds adenosine with high affinity, whereas A_{2B} and A_3 receptors have considerably lower affinity for adenosine (Daly *et al.,* 1983).

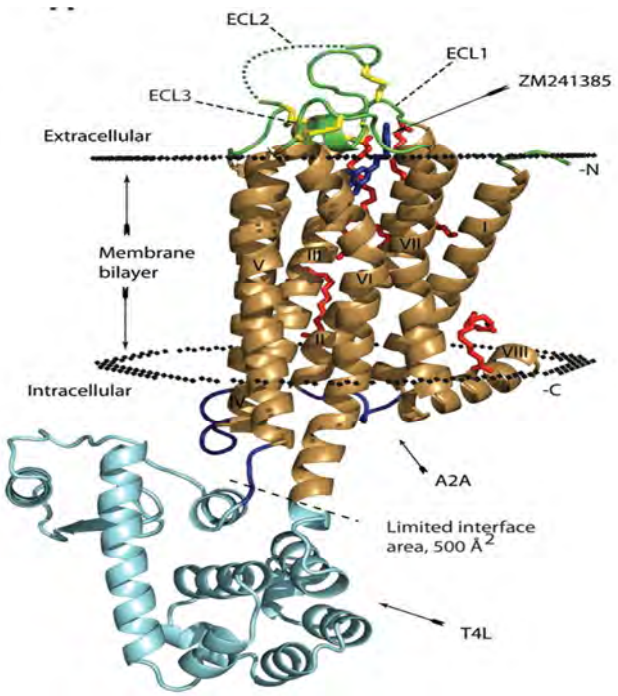

Figure 2.27: **Crystal structure of the A_{2A} receptor bound to ZM241385 (dark blue). The transmembrane helices is coloured in brown, the extracellular loops are green and the intracellular loops are coloured blue (Jaakola *et al.,* 2008).**

Adenosine A_{2A} receptors and their corresponding mRNAs are richly expressed in the striatum in both humans and rodents as shown in Figure 2.28. In the dorsal striatum of rodents and primates (including humans), A_{2A} receptor mRNA colocalizes with D_2 receptor mRNA (Fink *et al.,* 1992; Svenningsson *et al.,* 1998).

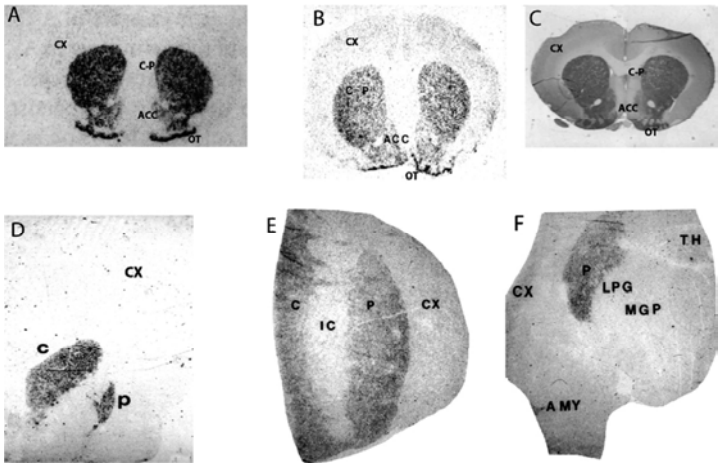

Figure 2.28: **Distribution of A_{2A} receptors in the BG of different mammalian species: *in situ* hybridization shows a very high level of A_{2A} receptor mRNA in the different sectors of the striatum including the caudate–putamen, the nucleus accumbens and the olfactory tubercle in mouse (A), rat (B), dog (D) and human (E, F) brain as compared to other brain areas. (C) Immunohistochemical detection of A_{2A} receptor confirms its high abundance in the rat striatum. Abbreviations: acc, accumbens; amy, amygdala; c, caudate; c–p, caudate–putamen; cx, cerebral cortex; ic, internal capsule; lgp, lateral globus pallidus; mgp, medial globus pallidus; p, putamen; ot, olfactory tubercle; th, thalamus. Modified from Schiffmann *et al.* (1991).**

2.3.3 **Basal ganglia organization and adenosine A_{2A} receptors**

The BG are a richly interconnected neural network involved in adaptive control of behaviour through interactions with sensorimotor, motivational and cognitive brain areas (Graybiel *et al.,* 1994). The striatum is the main input and information processing structure of the BG. The striatum is subdivided into the dorsal and ventral striatum. The dorsal striatum (mostly represented by the nucleus CPu) is involved in the performance and learning of complex motor acts. The dorsal striatum receives glutamatergic input from sensorimotor and association cortical areas and dopaminergic input from the SNpc (Gerfen, 2004).

Two pathways are present in the striata, namely the direct and indirect pathway (Figure 2.29). Stimulation of the direct pathway results in motor activation and stimulation of the indirect pathway produces motor inhibition (Müller & Ferrè, 2006). The direct pathway consists of the GABAergic dynorphinergic neurons and expresses the A_1 and D_1 receptor subtype, while the indirect pathway consists of GABAergic enkephalinergic neurons and expresses the A_{2A} and D_2 receptor subtypes. In normal conditions (Figure 2.29a) DA stimulates the striatonigral pathway via D_1 receptors and inhibits the striatopallidal route via D_2 receptors (the black arrows indicate inhibitory projections and grey arrows represent excitatory projection). In the parkinsonian state (Figure 29b) the lack of DA results in an imbalance between the indirect and direct output pathways. The result is inhibition of direct GABAergic striatonigral pathway and excessive activation of the indirect striatopallidal

pathway. These effects lead to an increased activity of the GABA nigrothalamic projection and a decreased Glu thalamocortical projection. Progressive degeneration of DA neurons and consequent loss of dopaminergic tone at different BG levels thus produce the bradykinesia, rigidity and tremor that characterize the disordered movement of PD (Obeso *et al.,* 2000).

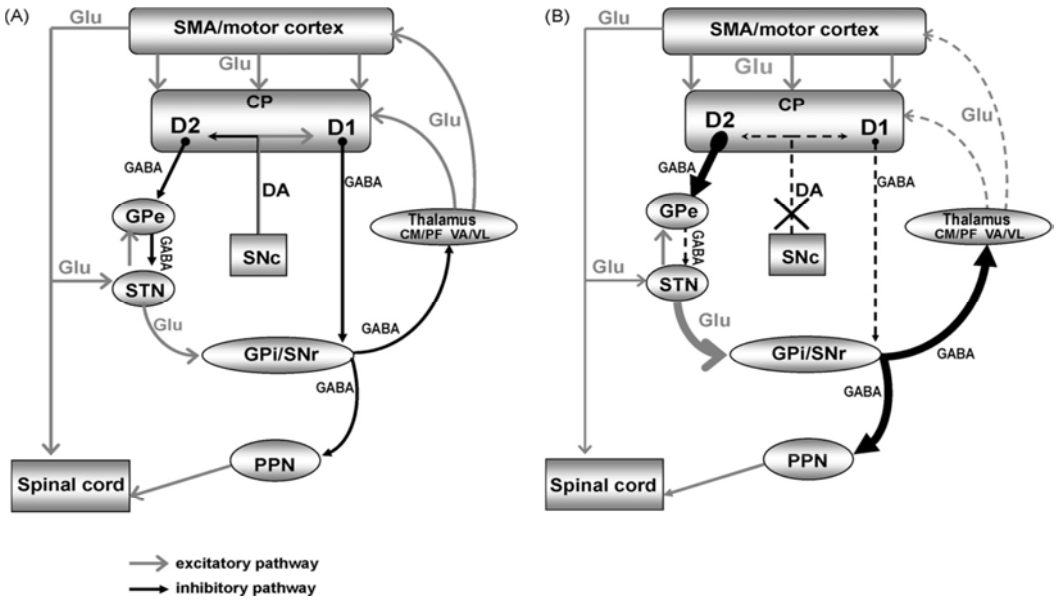

Figure 2.29: **Schematic diagram of the anatomical relationship between various BG nuclei, responsible for the motor dysfunction in PD. Thickness of arrows indicate the degree of activation of the pathway (Morelli *et al.,* 2007).**

It is particularly interesting to see that DA depletion leads to a partial loss of spines and glutamatergic synapses on the indirect striatopallidal pathway, but the direct pathway is unaffected (Day *et al.,* 2006). In addition, A_{2A} receptors in CPu are expressed by cholinergic nerve terminals, where A_{2A} antagonists can reduce the evoked release of acetylcholine (Kurokawa *et al.,* 1996).

It has been hypothesized that these interactions provide a mechanism of action for the depressant motor effects of adenosine agonists and for the motor stimulant effects of adenosine antagonists. Indeed, the adenosine system is the major target for methylxanthines, a class of substances that includes popular psychostimulants such as caffeine and theophylline. Caffeine is a competitive antagonist at both A_1 and A_{2A} receptors, which under normal conditions are activated by endogenous adenosine (Fredholm *et al.,* 1999).

2.3.4 **Interactions with other neurotransmitter receptors**

A receptor heteromer is defined as a macromolecular complex composed of at least two functional receptor units with biochemical properties that are noticeably different from those of its individual components (Ferrè *et al.,* 2009). The adenosine A_{2A} receptor has been found to interact with several neurotransmitter receptors in the brain (Figure 2.30), including the A_1, D_1, D_2, glutamatergic (both ionotropic and metabotropic), cholinergic (muscarinic and nicotinic), opioid, calcitonin gene-related peptide, and vasoactive intestinal peptide receptors. For example, there is co-localization as well as co-expression of mRNA for A_1 and A_{2A} receptors in the hippocampus (Cunha *et al.,* 1994).

Activation of A_{2A} receptors attenuates the ability of an A_1 agonist to inhibit hippocampal excitability (Cunha *et al.,* 1994; O'Kane & Stone, 1998). At the same time, A_1 receptor-mediated inhibition of A_{2A} actions has also been suggested (Abbracchio *et al.,* 1992). A_{2A} and D_1 receptors can also interact (Morelli *et al.,* 1994).

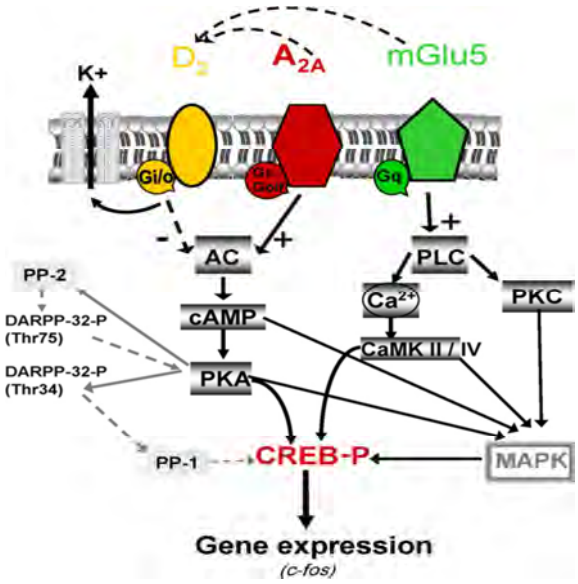

Figure 2.30: **Functional interactions between DA D_2, adenosine A_{2A} and metabotropic glutamate 5 receptors in striatopallidal neurons. Broken arrows, inhibitory effect; '+', stimulation; '-', inhibition; AC, adenylyl cyclase; Ca^{2+}, calcium ions (Morelli *et al.,* 2007).**

2.3.4.1 Dopamine D_2 receptor

The adenosine A_{2A}–D_2 receptor heteromer is one of the most studied receptor heteromers (Ferrè *et al.,* 2008). These heteromers constitutes almost half the populations of these receptors in the striatum and their malfunction plays a key role in the pathogenesis of BG disorders such as PD and Huntington's chorea (Fuxe *et al.,* 2007).

Neurochemical and behavioral research reveals that stimulation of pathways between striatum, GPe and SN leads to improved mobility. These results indicate a synergism between stimulation of D_2 receptors and inhibition of A_{2A} receptors (Fink *et al.,* 1992). Currently it is known that adenosine A_{2A} receptors participate in the antagonistic interaction between adenosine and DA, and could affect the mobility independent of D_2 receptors (Rosin *et al.,* 2003).

As mentioned, A_2 and D_2 receptors form heteromeric complexes with reciprocal antagonistic interactions which regulate the function of GABAergic enkephalinergic neurons (Agnati *et al.,* 2003). Stimulation of the A_{2A} receptors decreases the affinity of D_2 receptors for agonists by means of intermembrane interaction (Ferrè *et al.,* 1991), while stimulation of D_2 receptors inhibits A_{2A} receptor-induced activation of adenyl-cyclase (Ferrè *et al.,* 1997; Hillion *et al.,* 2002). For example, it was discovered that the activation of A_{2A} receptor in rat striatal membranes reduces the binding affinity of the D_2 receptor for its agonist (Ferre´ *et al.,* 1991). Moreover, an increase in antagonistic intramembrane A_{2A}-D_2 interaction was observed in the rat striatum after either striatal DA depletion or chronic D_2 antagonist treatment (Ferrè & Fuxe, 1992). Besides their physiological interactions, a close physical relationship between A_{2A} and D_2 receptors has also been shown in membranes from co-transfected cell lines (Hillion *et al.,* 2002) and as well as in living cells (Kamiya *et al.,* 2003). These data provide a molecular basis for an intramembrane A_{2A}-D_2 interaction. Since both A_{2A} and D_2 are coupled to adenylyl cyclase in addition to other signal transduction pathways, the antagonistic interaction between A_{2A} and D_2 receptors also takes place at the level of second messengers and beyond. The direct physical interactions between A_{2A} and D_2 receptors, and their antagonistic physiological actions, imply a functional interdependence. However, striatal A_{2A} function is not entirely dependent on the D_2 receptor (Aoyama *et al.,* 2000; Chen *et al.,* 2001), and data demonstrates that selective A_{2A} antagonists can exhibit their antiparkinsonian activities through D_2-independent as well as D_2-dependent mechanisms (Xu *et al.,* 2005).

2.3.4.2 Glutamate mGlu5 receptor

Glutamate, the main excitatory neurotransmitter in the brain, acts on two main categories of receptors: ionotropic receptors and G-protein-coupled metabotropic receptors (mGlu). Experimental findings strongly suggest that besides adenosine A_{2A} and DA D_2 receptors, the metabotropic glutamate 5 (mGlu5) receptors are colocalized postsynaptically in the striatopallidal GABAergic efferent neuron (Ferrè *et al.,* 2008). This co-localization provides a

structural framework for the existence of multiple functional interactions of A_{2A}, D_2 and mGlu5 receptors (Figure 2.30).

2.3.4.3 Adenosine A_1 receptor

Particularly surprising is the observation that there are functional antagonistic interactions between A_1 and A_{2A} receptors that modulate glutamate release in the striatum (Ciruela *et al.,* 2006; Quarta *et al.,* 2004). The existence of A_1-A_{2A} receptor heteromers in the cell surface of co-transfected cells has recently been demonstrated, by which stimulation of A_{2A} receptors decreases the affinity of A_1 receptors for their agonists (Ciruela *et al.,* 2006).

2.3.5 **Adenosine antagonists and Parkinson's disease**

Rigidity and rest tremor are features of PD and can be as disabling as akinesia or bradykinesia. A_{2A} blockade has been found to improve abnormalities of muscle tone and tremors in rodents, thus extending the suggestion of potential benefit of A_{2A} blockade for PD symptoms. In the light of recent clinical trials, A_{2A} receptor antagonists appear to be a promising non-dopaminergic therapy for PD (Feigin, 2003; Schwarzschild *et al.,* 2006). Interestingly, a recent report has shown that A_{2A} receptor antagonists counteract specific motor deficits even when administered without L-dopa (Pinna *et al.,* 2005).

In contrast to the non-specific adenosine antagonist caffeine, which can lose its motor stimulant effect with repeated exposure, A_{2A} selective antagonists did not produce tolerance effects after sub-chronic treatment in PD models (Pinna *et al.,* 2005). Like bradykinesia, muscle rigidity and parkinsonian rest tremor may also improve with A_{2A} blockade. Muscle rigidity can be reduced by an A_{2A} antagonist or eliminated by a synergistic combination of L-dopa plus A_{2A} antagonist (Wardas *et al.,* 2001). Parkinsonian rest tremor, which is relatively resistant to DA-replacement therapy, may also be targeted by A_{2A} antagonists (Simola *et al.,* 2004).

The mechanism by which A_{2A} antagonists improve parkinsonian motor dysfunction probably involves their direct inhibitory influence on striatopallidal neurons, which coexpress A_{2A} and D_2 receptors (Figure 2.31) (Schiffmann *et al.,* 1991; Fink *et al.,* 1992).

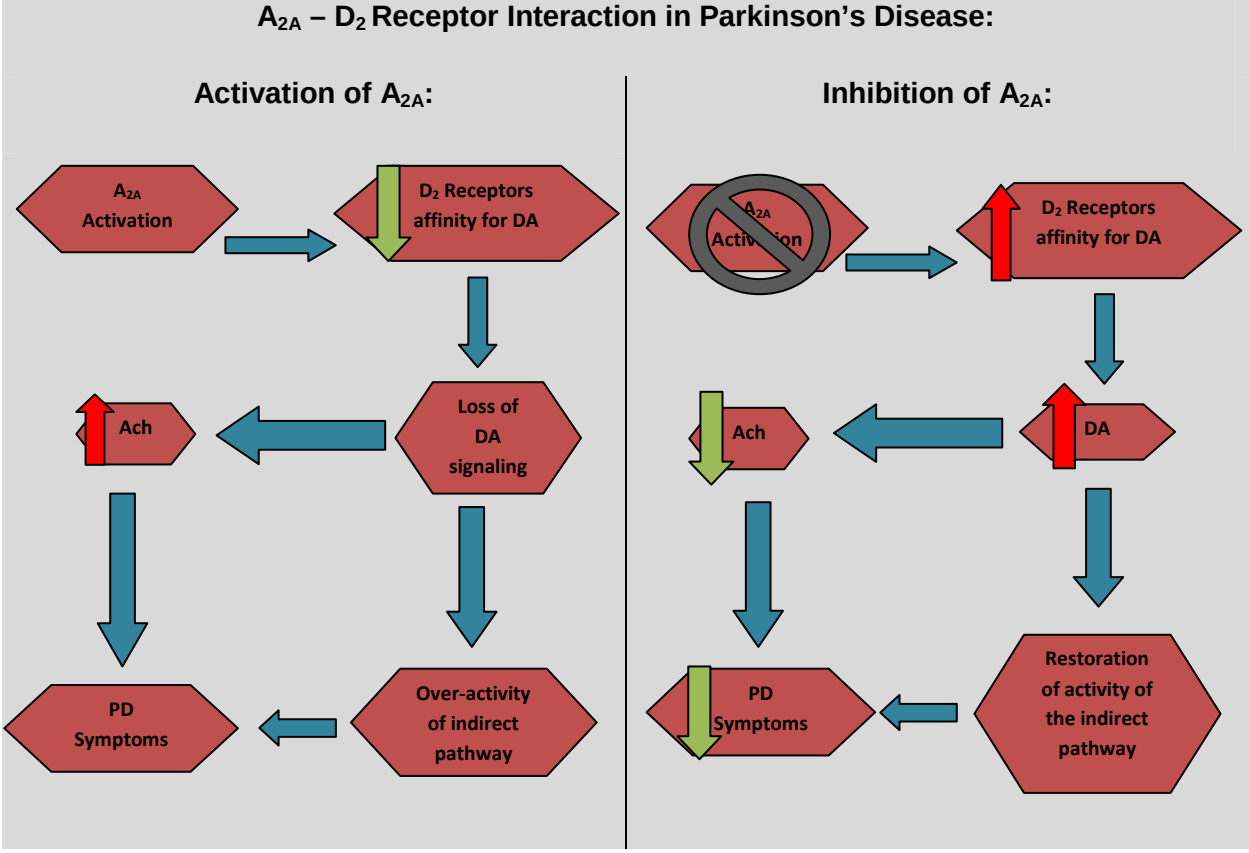

Figure 2.31: **(a) Activation of the A_{2A} receptor – A_{2A} stimulation decreases the affinity of the D_2 receptors which leads to the loss of DA signaling and unopposed adenosine signalling. This in turn leads to the over-activity of the stratiopallidal pathway. DA and Ach oppose one another, a decrease in the activity of one leads to an increase in the activity of the other, causing the symptoms of PD including bradykinesia, resting tremor, rigidity and impairment of gait. (b) Antagonism of the A_{2A} receptor - A_{2A} antagonism increases the affinity of the D_2 receptors, leading to an increase in DA signalling and decrease in Ach activity. This leads to the restoration of balance in the stratiopallidal pathway and normal controlled movements, without the symptoms of PD (Morelli *et al.*, 2007).**

2.3.6 **Classification of Adenosine A_{2A} Antagonists**

Most A_{2A} receptor antagonists belong to two different chemical classes, (i) xanthine derivatives and (ii) amino-substituted heterocyclic compounds, which are derived from adenine or structurally related to adenine (Müller & Ferrè, 2006).

2.3.6.1 Xanthines

The alkaloid caffeine, 1,3,7-trimethylxanthine, mediates its pharmacologic actions by a blockade of A_1, A_{2A}, and A_{2B} receptors. The observation that 8-substituted xanthine derivatives was better tolerated by the A_{2A} than the A_1 receptor (Shamim *et al.,* 1989), and that the 8-substituent had to be coplanar for achieving high A_{2A} receptor affinity (Erickson *et*

al., 1991; Müller *et al.,* 1997) led to the first highly potent and selective A_{2A} receptor antagonists, the xanthine derivatives CSC (Jacobson *et al.,* 1993), KW-6002 (istradefylline), and MSX-2 along with its water-soluble phosphate prodrug MSX-3 (Müller *et al.,* 1997).

(E)-8-(3-Chlorostyryl)caffeine (CSC)

In addition to its A_{2A} receptor blocking activity, CSC (Figure 2.32) has been reported to be a potent inhibitor of MAO-B (Chen *et al.,* 2002; Vlok *et al.,* 2006). This activity may contribute to the antiparkinsonian effects of CSC in animal models of PD, as well as its reported neuroprotective effects (Petzer *et al.,* 2003; Vlok *et al.,* 2006).

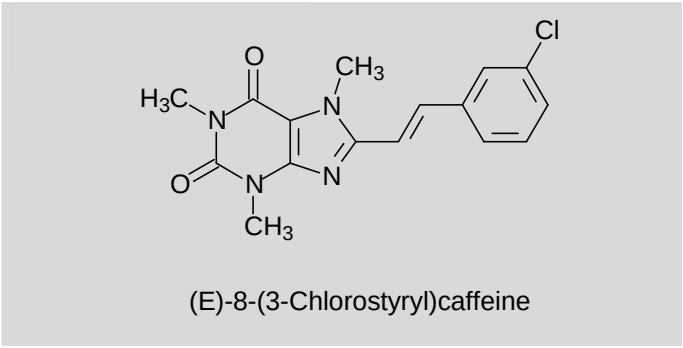

(E)-8-(3-Chlorostyryl)caffeine

Figure 2.32: Molecular structure of CSC

Istradefylline (KW-6002)

Istradefylline (Figure 2.33) is currently in Phase III clinical trials for PD therapy. In phase II clinical trials istradefylline was shown to reduce motoric dysfunction without producing dyskinesias (Müller & Fèrre, 2007). This xanthine derivative, which is an antagonist of the adenosine A_{2A} receptor in nanomolar concentrations, possesses selectivity towards A_{2A} receptors that is almost 70 times higher than for adenosine A_1 receptors. It was shown that selective adenosine A_{2A} antagonists such as KW-6002- decrease the symptoms of catalepsy caused by administration of haloperidol in animals. In addition KW-6002 reduces the symptoms of akinesia caused by reserpine (Jenner, 2003). Clinical trials showed that KW-6002 potentiates the motor benefits of a reduced dose of L-dopa and at the same time produced only approximately half the amount of dyskinesias (Bara-Jiminez *et al.,* 2003). The antidyskinetic effects of A_{2A} antagonists is especially relevant in the light of the observation that the therapeutic benefits of A_{2A} antagonists are additive to those of L-dopa and DA agonists, and it may therefore be possible to reduce the dose of the dopaminergic drugs and the severity of dyskinesias (Lundblad *et al.,* 2003).

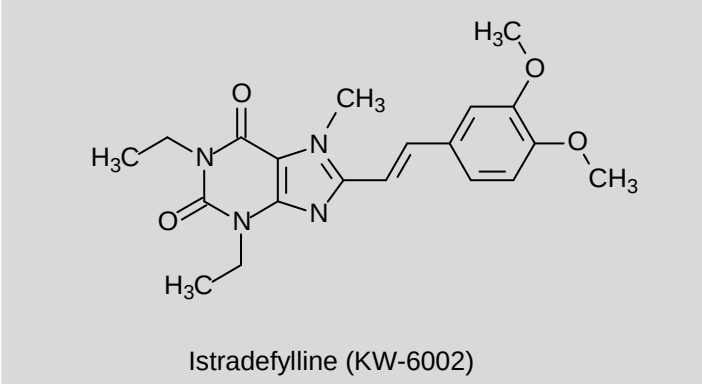

Figure 2.33: Molecular structure of KW-6002

2.3.6.2 Aminouracil Derivatives

SCH-420814

The potent and selective A_{2A} receptor antagonist, SCH- 420814 (Figure 2.34), is being developed for the treatment of PD and this compound has entered phase II clinical trials. Besides its anticataleptic activity, SCH-420814 also showed an antidepressant effect in rodent models of behavioural despair (Lachowicz *et al.,* 2006).

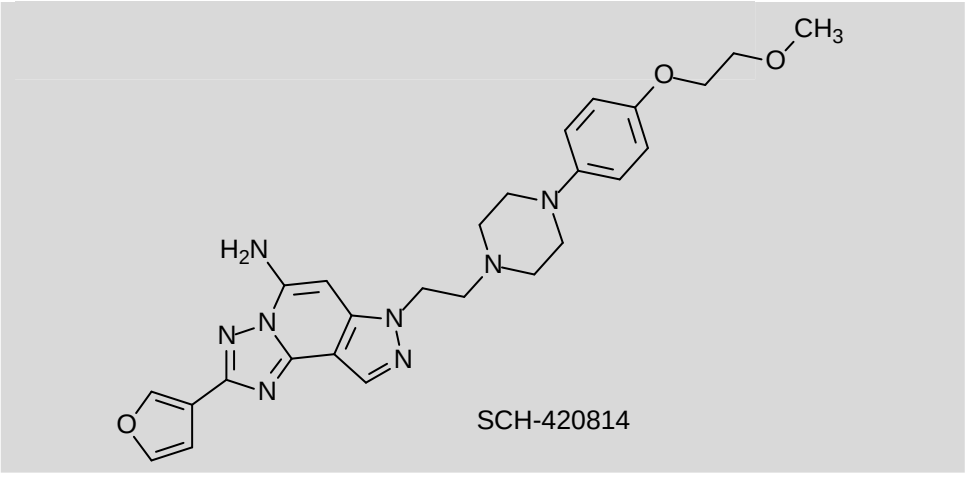

Figure 2.34: Molecular structure of SCH-42081

2.3.7 **Neuroprotection of A_{2A} antagonists in Parkinson's disease**

A_{2A} antagonism may also be associated with a neuroprotective effect in PD (Schwarzschild *et al.,* 2006; Bibbiani *et al.,* 2003). The evidence for this originated from the observation that caffeine consumption correlates with a reduced risk of developing PD (Ascherio *et al.,* 2001; Ross *et al.,* 2000). This effect of caffeine, a non-selective A_1/A_{2A} antagonist, has been linked

to its blockade of A_{2A} receptors since a number of selective A_{2A} antagonists, and not A_1 antagonists, protects against neurodegenerative processes in animal models (Chen *et al.,* 2001; Ikeda *et al.,* 2002). While the mechanism by which caffeine and A_{2A} antagonists protect against neurodegeneration is unclear, A_{2A} receptor antagonists are thought to exert this neuroprotective effect by inhibiting glutamate release (Blum *et al.,* 2003). It has also been suggested this neuroprotective effect may be extended to slow, progressive neurodegenerative disorders such as PD (Popoli *et al.,* 2004). Low concentrations of adenosine inhibit the release of glutamate, which is implicated in neurotoxicity, while high concentrations stimulate its release (Ciruela *et al.,* 2006).

2.3.8 **Conclusion**

The majority of PD treatment strategies aim at restoring DA function in the striatum, thereby reducing the severity of the motor symptoms. DA replacement therapy using L-dopa remains the standard treatment for PD. Other approaches include inhibition of DA metabolism using MAO-B inhibitors and COMT inhibitors, and treatment with DA agonist drugs. Although DA targeted therapies work well to relief PD related motor symptoms, they all produce undesirable side effects.

In the striatum adenosine A_{2A} receptors are co-localized with D_2 receptors. A_{2A} and DA receptors have opposing effects since the activation of A_{2A} receptors reduces D_2 receptor mediated signalling. The adenosine A_{2A} receptor has thus became a promising target for treating PD. Selective A_{2A} receptor antagonists was shown to be beneficial for not only enhancing the therapeutic effects of L-dopa but also reducing dyskinesia, a side effect of long-term L-dopa treatment (Dauer & Przedborski, 2003).

The finding that CSC possessed both A_{2A} antagonist and MAO-B inhibition properties, raised the possibility of designing dual-targeted-directed drugs that may provide enhanced symptomatic relief and also slow the progression of PD by protecting against further neurodegeneration (Petzer *et al*., 2009).

CHAPTER 3:

SYNTHESES OF 8-(PHENOXYMETHYL)CAFFEINE ANALOGUES

3.1 **Introduction**

As discussed in Chapter 1, the main objective of this study is the design of caffeine derivatives as dual-targeted drugs which are selective, reversible MAO-B inhibitors as well as potent A_{2A} antagonists. Such drugs may possess enhanced benefit in the treatment of PD.

Caffeine (Figure 3.1) is reported to be a weak MAO-B inhibitor and a moderate A_{2A} antagonist (Pretorius *et al.,* 2008), but substitution on the C8 position yields compounds with greatly enhanced MAO-B inhibitory activity. For example, the (E)-8-(3-chlorostyryl) substituent of CSC (Figure 3.1) enhances not only the MAO-B inhibition potency of caffeine, but the A_{2A} antagonistic activity as well. Recently it has been found that 8-phenoxymethyl substituted caffeines are exceptionally potent reversible inhibitors of MAO-B (Swanepoel, 2010) (Figure 3.1). Therefore, the current study will focus on expanding on the 8-(phenoxymethyl)caffeine series synthesizing additional homologues of this series and evaluating them as MAO inhibitors as well as A_{2A} antagonists. This study will also compare the various potencies of the newly synthesized 8-(phenoxymethyl)caffeine derivatives to that of the previous synthesized derivatives (Swanepoel, 2010).

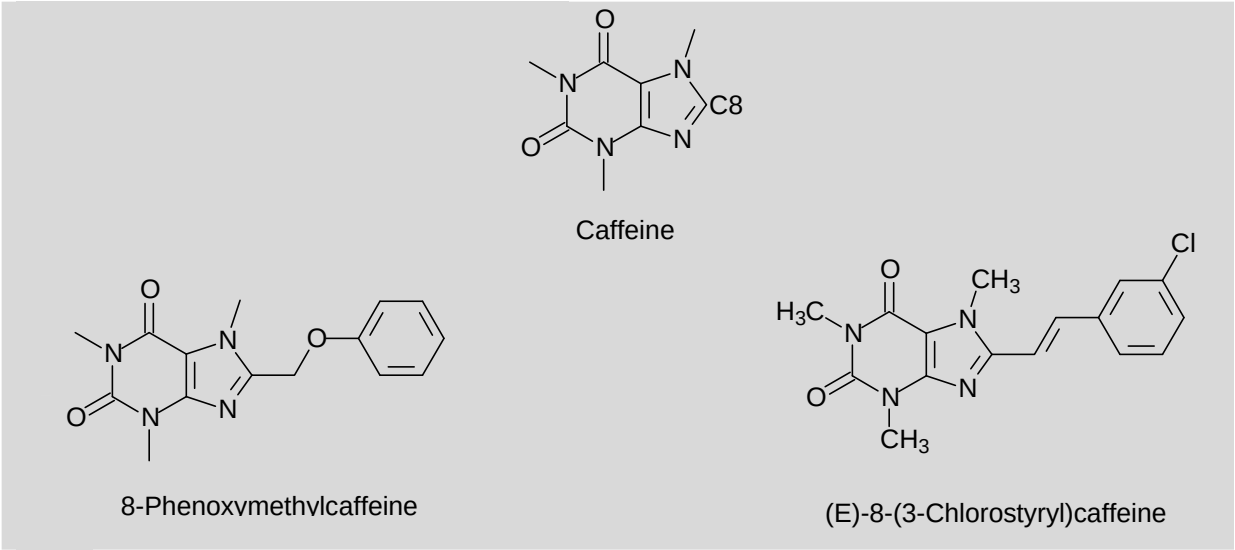

Figure 3.1: **Molecular structures of caffeine, CSC and 8-(phenoxymethyl)caffeine.**

Table 3.1 illustrates the 8-(phenoxymethyl)caffeine analogues that will be examined in this study. Compounds **1**, **8**-**10** and **15** have already been synthesized in previous studies (Swanepoel, 2010; Van der Walt, 2012) and were thus not synthesized in this study. As shown in Table 3.1, the compounds that will be examined in this study may be divided into two series. These are the 8-(phenoxymethyl)caffeines (series 1) and 1,3-diethyl-7-methyl-8-(phenoxymethyl)xanthines (series 2).

Table 3.1: Chemical structures of the 8-(phenoxymethyl)caffeine derivatives (Compounds **1**, **8**-**22**).

SERIES 1:

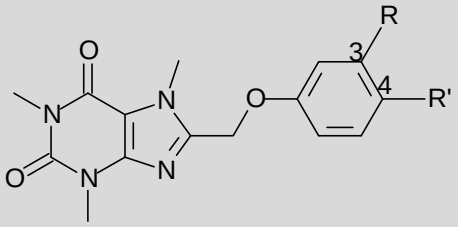

Compound:	R:	R':
1*	H	H
8*	H	Cl
9*	H	Br
10*	H	F
11	H	CH_3
12	H	OCH_3
13	H	I
14	CH_3	CH_3

SERIES 2:

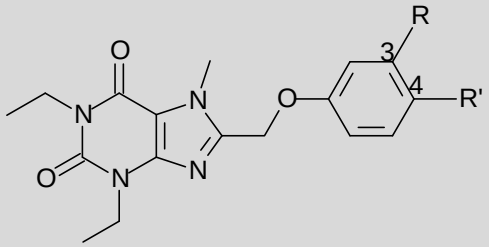

Compound:	R:	R':
15#	H	H
16	H	Cl
17	H	Br
18	H	F
19	H	CH_3
20	H	OCH_3
21	H	I
22	CH_3	CH_3

***Compounds synthesized by Swanepoel (2010) in a previous study**
 # Compound synthesized by Van der Walt (2012) in a previous study

For the synthesis of target compounds in Series 1 [8-(phenoxymethyl)caffeines] and Series 2 [1,3-diethyl-7-methyl-8-(phenoxymethyl)xanthines], the following synthetic route using, 1,3-dimethyl- or 1,3-diethyl-5,6-diaminouracil, as key reagents was used (Figure 3.2) (Shimada *et al.,* 1992; Suzuki *et al.,* 1993).

In the first step, 1,3-dimethyl- or 1,3-diethyl-5,6-diaminouracil (**i**) was acylated with an appropriately substituted phenoxyacetic acid (**ii**) (prepared from the corresponding phenol analogue). This was carried out in the presence of the dehydrating reagent, N-(3-dimethylaminopropyl)-N'-ethylcarbodiimide hydrochloride (EDAC). The intermediary amide obtained from this reaction was then treated with sodium hydroxide, which resulted in ring closure to yield the corresponding 1,3-dimethyl-8-phenoxymethyl-7H-xanthinyl or 1,3-diethyl-

8-phenoxymethyl-7H-xanthinyl analogues (**iii**) (Shimada *et al.,* 1992). These xanthinyl analogues were subsequently 7N-methylated in the presence of an excess of potassium carbonate and iodomethane to yield the target compounds (**iv**).

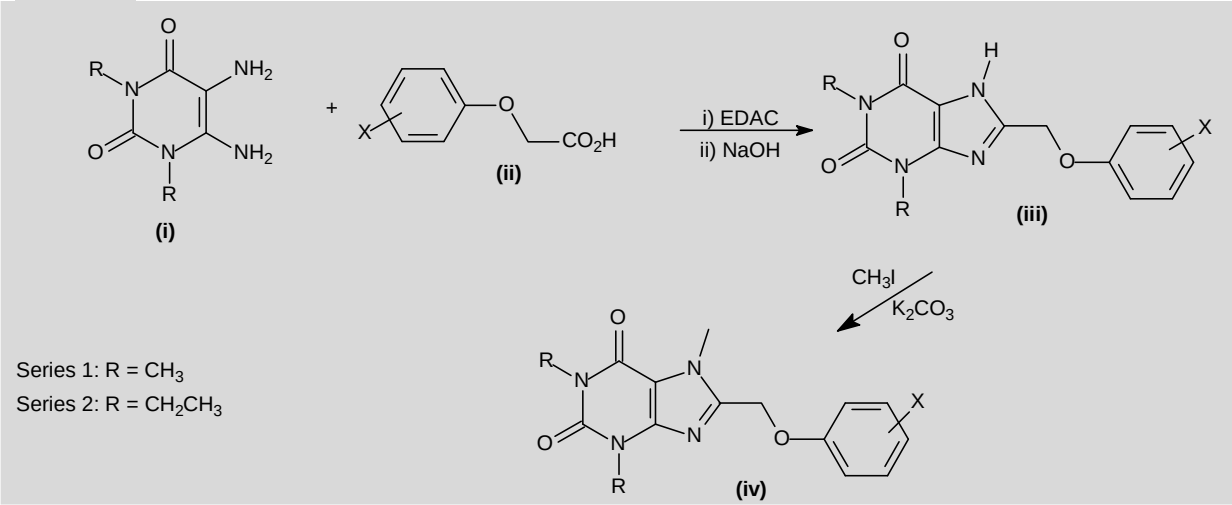

Figure 3.2: **Reaction scheme for the synthesis of 8-(phenoxymethyl)caffeines (series 1) and 1,3-diethyl-7-methyl-8-(phenoxymethyl)xanthines (series 2).**

3.2 **Materials and Instrumentation**

Materials: Starting materials that were not prepared were obtained from Sigma-Aldrich and used without further purification. All those starting materials that were prepared were purified by crystallization.

Thin layer chromatography (TLC): TLC was carried out to determine the completeness of the reaction. Silica gel 60 (Merck) containing UV_{254} fluorescent indicator were employed with a mobile phase consisting of 10 parts dioxane and 90 parts ethyl acetate. The developed TLC sheets were observed under an UV-lamp at a wavelength of 354nm.

Melting points (mp): A Büchi B-545 melting point apparatus was used to measure the mp of all of the synthesized compounds.

Mass spectra (MS): High resolution mass spectra (HRMS) and nominal mass spectra (MS) were obtained with a Bruker micrOTOF-Q II mass spectrometer in atmospheric-pressure chemical ionization (APCI) mode.

Nuclear magnetic resonance (NMR): A Bruker Avance III 600 spectrometer, at frequencies of 600 MHz and 150 MHz, were used to record proton (^{1}H) and carbon (^{13}C) NMR spectra, respectively. NMR measurements were conducted in $CDCl_3$ and the chemical shifts reported in parts per million (δ) downfield and were referenced to the residual solvent signal ($CDCl_3$

7.26 and 77.0 ppm for ^{1}H and ^{13}C respectively). Spin multiplicities are given as s (singlet), d (doublet), dd (doublet of doublets), t (triplet), q (quartet) or m (multiplet). The coupling constants (J) are given in Hz.

High performance liquid chromatography (HPLC): HPLC analyses were conducted with an Agilent 1100 HPLC system equipped with a quaternary pump and an Agilent 1100 series diode array detector (see supplementary material). The HPLC analyses were used to determine the purities of the synthesized compounds. HPLC grade acetonitrile (Merck) and Milli-Q water (Millipore) was used for the chromatography. A Venusil XBP C18 column (4.60 x 150 mm, 5 µm) was used for the separation and the mobile phase consisted at the start of each run of 30% acetonitrile and 70% Milli-Q water. The flow rate was set to 1 ml/min. At the start of each run a solvent gradient program was initiated. The composition of the acetonitrile in the mobile phase was increased linearly to 8% over a period of 5 min. Each HPLC run lasted 15 min and a time period of 5 min was allowed for equilibration between runs. A volume of 20 µl of solutions of the test compound (1 mM) was injected to the HPLC system and the eluent was monitored at a wavelength of 254 nm. The test compounds were dissolved in acetonitrile.

3.3 General Synthetic Procedures

3.3.1 Synthesis of 1,3-dimethyl-5,6-diaminouracil and 1,3-diethyl-5,6-diaminouracil

The synthesis of 1,3-dimethyl-5,6-diaminouracil and 1,3-diethyl-5,6-diaminouracil were carried out via a general procedure described by Traube (1900) (Figure 3.3).

N,N'dimethylurea or N,N'-diethylurea (**A**) (100 mmol) and cyanoacetic acid (**B**) (100 mmol) were placed in a 250 ml round bottom flask and acetic anhydride (12.5 ml) was added. The reaction was heated (60 ℃) for 3 h, with a $CaCl_2$ trap attached, to yield the corresponding cyanourea derivative (**C**) (a colorless to light yellow solution). The reaction was cooled on ice and 10% sodium hydroxide (100 ml) was added to obtain 1,3-dimethyl-6-aminouracil or 1,3-diethyl-6-aminouracil (**D**) after ring closure (Papesch & Schroeder, 1951). At this stage, the pH of the suspension was 12 and stirring was continued for a further 30 min at room temperature. A solution of sodium nitrate (120 mmol) and 12 ml of glacial acetic acid were added to the reaction over a period of 1 h. The reaction turned pink and then magenta, yielding the nitroso derivative (**E**). Stirring was continued for another 12 h at room temperature. The product was collected via filtration and washed with diethyl ether. The product was left to dry in the convection oven at 60 ℃.

The nitroso derivative (**E**) (50 mmol) was powdered and 50 ml ammonia water (32%) was added to yield an orange suspension. The suspension was heated to 40 ℃ and a fresh solution of sodium hydrosulfite (36 g in 100 ml water) was added over a period of 20 min. The suspension turned red and eventually light green in colour. Approximately 90 ml of sodium hydrosulfite was added and the reaction was cooled on ice for 2 h, yielding 1,3-dimethyl-5,6-diaminouracil or 1,3-dimethyl-5,6-diaminouracil (**F**) . The light yellow crystals were collected via filtration and washed with 20 ml water. The product was left to dry overnight in a fume hood at room temperature (Speer & Raymond, 1953).

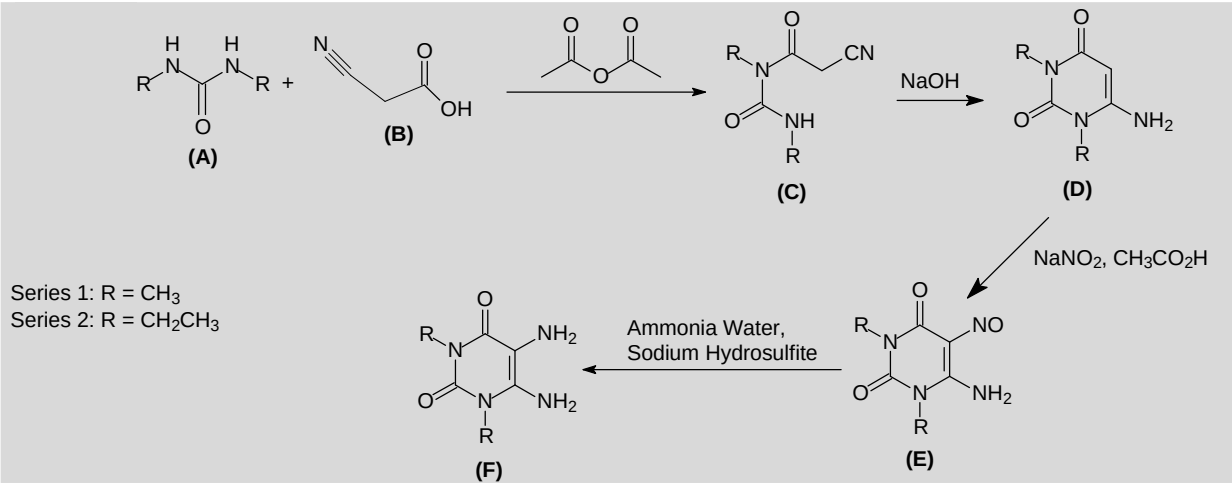

Figure 3.3: **Reaction scheme for the synthesis of 1,3-dimethyl-5,6-diaminouracil or 1,3-dimethyl-5,6-diaminouracil.**

3.3.2 **Synthesis of phenoxyacetic acids**

Among the phenoxyacetic acids that were required for this study, 6 were commercially available. The remaining 2 phenoxyacetic acids were synthesized via a general synthetic route illustrated in Figure 3.4 (Zhao *et al.,* 2005; Koelsch, 1931; Hayes & Branch, 1943). The appropriate substituted phenol (**G**) (20 mmol) was added to a solution of sodium hydroxide (10 ml) in water. Chloroacetic acid (34 mmol) was added and the reaction was heated (85–90 ºC) under reflux for 2 h and subsequently cooled to room temperature to yield a thick precipitation with a pH of 12. The reaction was acidified with concentrated hydrochloric acid to a pH of 2 and extracted to diethyl ether (100 ml). The ether phase was subsequently extracted thrice with 100 ml solution of sodium carbonate (5%). The pooled aqueous phases were acidified to a pH of 2 with hydrochloric acid to yield a precipitate. The desired phenoxy acetic acid (**H**) was collected by filtration and left to dry overnight in the fume hood. Analytical pure samples were obtained after recrystallization from methanol.

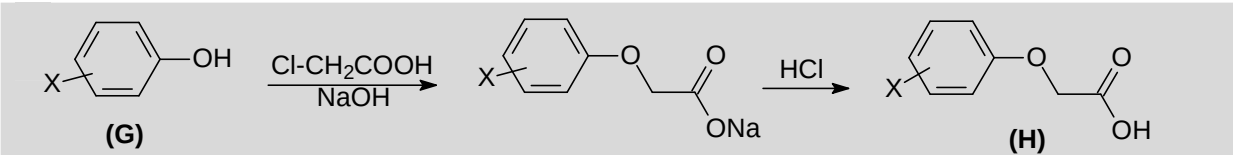

Figure 3.4: **Reaction scheme of the synthesis of the phenoxyacetic acids**

The structures of those phenoxyacetic acids that were commercially available and those that were synthesized are summerized in Table 3.2.

Table 3.2: The structures of the phenoxyacetic acids that were required for this study.

Phenoxyacetic acids:

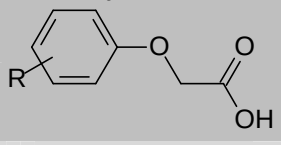

Acid R:	*Availibility:*	*Physical appearance:*	*Molecular weight (mw):*	*Melting point (ºC):*
H	Commercial	Off-white crystals	152.15	98-100
4-Cl	Commercial	White to light beige powder	186.59	157-159
4-Br	Commercial	White crystalline powder	231.04	149-153
4-F	Commercial	White crystalline powder	170.14	104-105
4-CH_3	Synthesized	Beige crystalline powder	166.17	140-142
4-OCH_3	Synthesized	Beige-brown crystalline solid	182.17	112-114
4-I	Commercial	White powder	278.04	154-157
3.4-diCH_3	Commercial	White crystalline powder	180.2	164-166

3.3.3 **Synthesis of 1,3-dimethyl-8-phenoxymethyl-7H-xanthinyl and 1,3-diethyl-8-phenoxymethyl-7H-xanthinyl analogues**

1,3-Dimethyl- or 1,3-diethyl-5,6-diaminouracil (5 mmol) and EDAC (6,7 mmol) were dissolved in 40 ml of dioxane/H_2O (1:1). The appropriate phenoxyacetic acid (5 mmol) was added and a thick suspension was obtained. The pH was adjusted to 3 with approximately 15 drops of 4 N aqueous hydrochloric acid and the reaction became light pink in color. Stirring was continued for 3 h at room temperature. The pH was adjusted to 7 with approximately 60 drops of 1 N NaOH. The suspension turned white and a thick precipitate formed. The precipitate was collected via filtration and suspended in 40 ml of dioxane. Addition of 40 ml NaOH (1 N) yielded a clear colorless solution. The solution was heated under reflux for 2 h at 110–120 °C and the solution became bright yellow. The reaction was cooled to room temperature and placed on ice for 15 min. At this point, the pH was 12 and was subsequently adjusted to 4 with 9 ml of hydrochloric acid (4 N) to yield a creamy precipitate. The corresponding 1,3-dimethyl-8-phenoxymethyl-7H-xanthinyl or 1,3-diethyl-8-phenoxymethyl-7H-xanthinyl analogue was collected via filtration and left to dry overnight in the fume hood.

3.3.4 **Synthesis of the 8-(phenoxymethyl)caffeines (series 1) and 1,3-diethyl-7-methyl-8-(phenoxymethyl)xanthines (series 2)**

The 1,3-dimethyl-8-phenoxymethyl-7H-xanthinyl or 1,3-diethyl-8-phenoxymethyl-7H-xanthinyl analogue (2 mmol) was dissolved in a minimum amount of DMF (approximately 12 ml) at 70–80 °C and an orange solution was obtained. Potassium carbonate (5 mmol) was added followed by iodomethane (4 mmol). The reaction was stirred at 70–80 °C for 3 h. When TLC indicated the completion of the reaction, the solution was filtered to remove insoluble materials. Water (150 ml) was added to the filtrate to yield a creamy precipitate, which was cooled on ice. The precipitate was collected via filtration and left to dry overnight at room temperature in the fume hood. The target products were recrystallized from an appropriate solvent as cited below.

3.4 **Physical Characterization**

^{1}H-NMR, ^{13}C-NMR and mass spectroscopy (nominal and high resolution) were used to verify the structures of the 8-(phenoxymethyl)caffeine and 1,3-diethyl-7-methyl-8-(phenoxymethyl)xanthene analogues. ^{1}H-NMR, ^{13}C-NMR spectra as well as HPLC and MS chromatograms are given in the appendixes. In the following tables and discussion the structures of the caffeine analogues are given and correlated with the ^{1}H-NMR, and ^{13}C-NMR data. All of the appropriate signals were observed for the synthesized compounds (**11**-

14 and **16**-**22**). These signals include the 3 singlets for the caffeine methyl groups of the 8-phenoxymethylcaffeine analogues. For the 1,3-diethyl-7-methylxanthine ring system of the 1,3-diethyl-7-methyl-8-(phenoxymethyl)xanthines a singlet (for the 7-CH_3) was observed as well as two triplets and two quartets (for the 1,3-diC_2H_5 groups). The CH_2 singlet in the C8 side chain and the signals for the aromatic protons on the phenyl ring were also present. In addition, the ^{13}C-NMR data also correlates with each of the target structures in terms of ^{13}C signals and their expected chemical shifts.

3.4.1 **8-(4-Methylphenoxymethyl)caffeine (11)**

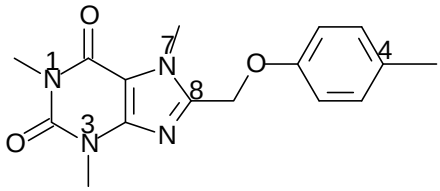

The title compound was prepared from 4-methylphenoxyacetic acid in a yield of 88%: mp 172.1 ºC (ethanol). **^{1}H-NMR** (Bruker Avance III 600, $CDCl_3$) δ 2.61 (s, 3H), 3.37 (s, 3H), 3.55 (s, 3H), 4.01 (s, 3H), 5.13 (s, 2H), 6.87 (d, 2H J = 8.3 Hz), 7.07 (d, 2H J = 8.6 Hz). **^{13}C-NMR** (Bruker Avance III 600, $CDCl_3$) δ 20.4, 27.9, 29.7, 32.4, 62.2, 108.7, 114.5, 130.1, 131.4, 147.4, 148.0, 151.5, 155.4. **Mass spectrometry**: EIMS 315; EI-HRMS *m*/*z*: calcd for **$C_{16}H_{18}N_4O_3$**, 315.1379, found 315.1461. **Purity** (HPLC): 99.0%.

^{1}H-NMR:	**^{13}C-NMR:**
• Methyl groups at N1, N3 and N7 correspond with the singlets at 3.37, 3.55 and 4.01 ppm (the signals integrate for 3 protons each). • CH_2 singlet corresponds with the signal at 5.13 ppm (the signal integrates for 2 protons). • The CH_3 singlet on position 4 of the phenyl ring corresponds with a singlet at 2.61 ppm (integrate for 3 protons). • Aromatic protons on the phenyl ring are represented by the doublets at 6.87 and 7.07 ppm (signals integrate for 2 protons each).	• Methyl groups at N1, N3, and N7 are represented by the signals at 27.9, 29.7 and 32.4 ppm. • CH_2 singlet corresponds with the signal at 62.2 ppm. • The CH_3 on position 4 of the phenyl ring corresponds with the signal at 20.4 ppm. • Aromatic carbons are represented by the signals at 108.7, 114.5, 130.1, 131.4, 147.4, 148.0, 151.5, and 155.4 ppm. • Only 8 signals are observed for the aromatic carbons as overlapping signals occur.

3.4.2 **8-(4-Methoxyphenoxymethyl)caffeine (12):**

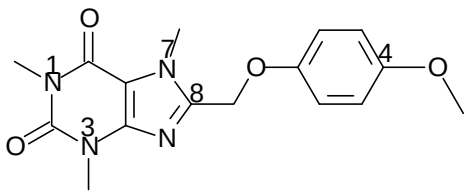

The title compound was prepared from 4-methoxyphenoxyacetic acid in a yield of 89%: mp 160.4 ºC (ethanol). **^{1}H-NMR** (Bruker Avance III 600, $CDCl_3$) δ 3.37 (s, 3H), 3.56 (s, 3H), 3.74 (s, 3H), 4.02 (s, 3H), 5.11 (s, 2H), 6.81 (d, 2H J = 9.1 Hz), 6.91 (d, 2H J = 9.4 Hz). **^{13}C-NMR** (Bruker Avance III 600, $CDCl_3$) δ 27.9, 29.7, 32.4, 55.7, 62.8, 108.7, 114.7, 115.8, 147.4, 148.1, 151.6, 154.7, 155.4. **Mass spectrometry**: EIMS 331; EI-HRMS *m*/*z*: calcd for **$C_{16}H_{18}N_4O_4$**, 331.1328, found 331.1404. **Purity** (HPLC): 97.3%.

^{1}H-NMR:	**^{13}C-NMR:**
• Methyl groups at N1, N3 and N7 correspond with the singlets at 3.37, 3.56 and 4.02 ppm (the signals integrate for 3 protons each). • CH_2 singlet corresponds with the signal at 5.11 ppm (the signal integrates for 2 protons). • The methoxy group on the phenyl ring corresponds to the singlet at 3.74 ppm (integrate for 3 protons). • Aromatic protons on the phenyl ring are represented by the doublets at 6.81 and 6.91 ppm (signals integrate for 2 protons each).	• Methyl groups at N1, N3, and N7 are represented by the signals at 27.9, 29.7 and 32.4 ppm. • CH_2 singlet corresponds with the signal at 62.8 ppm. • The methoxy group on the phenyl ring corresponds to the signal at 55.7 ppm. • Aromatic carbons are represented by the signals at 108.7, 114.7, 115.8, 147.4, 148.1, 151.6, 154.7 and 155.4 ppm. • Only 8 signals are observed for the aromatic carbons as overlapping signals occur.

3.4.3 **8-(4-Iodophenoxymethyl)caffeine (13):**

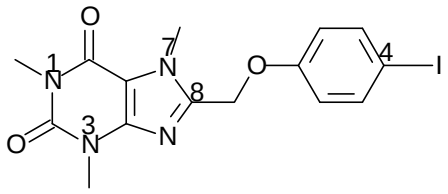

The title compound was prepared from 4-iodophenoxyacetic acid in a yield of 82%: mp 212.6 ºC (ethanol). **^{1}H-NMR** (Bruker Avance III 600, $CDCl_3$) *δ* 3.37 (s, 3H), 3.55 (s, 3H), 4.01 (s, 3H), 5.14 (s, 2H), 6.77 (d, 2H J = 9.0 Hz), 7.56 (d, 2H J = 9.0 Hz). **^{13}C-NMR** (Bruker Avance III 600, $CDCl_3$) *δ* 28.0, 29.7, 32.4, 62.0, 84.4, 108.8, 117.0, 138.5, 147.3, 151.5, 155.4, 157.4. **Mass spectrometry**: EIMS 427; EI-HRMS *m*/*z*: calcd for **$C_{15}H_{15}IN_4O_3$**, 427.0189, found 427.0268 **Purity** (HPLC): 99.4%.

^{1}H-NMR:	**^{13}C-NMR:**
• Methyl groups at N1, N3 and N7 correspond with the singlets at 3.37, 3.55 and 4.01 ppm (the signals integrate for 3 protons each). • CH_2 singlet corresponds with the signal at 5.14 ppm (the signal integrates for 2 protons). • Aromatic protons on the phenyl ring are represented by the doublets at 6.77 and 7.56 ppm (signals integrate for 2 protons each).	• Methyl groups at N1, N3, and N7 are represented by the signals at 28.0, 29.7 and 32.4 ppm. • CH_2 singlet corresponds with the signal at 62.0 ppm. • Aromatic carbons are represented by the signals at 84.4 108.8, 117.0, 138.5, 147.3, 151.5, 155.4 and 157.4 ppm. • Only 8 signals are observed for the aromatic carbons as overlapping signals occur.

3.4.4 **8-(3,4-Dimethylphenoxymethyl)caffeine (14):**

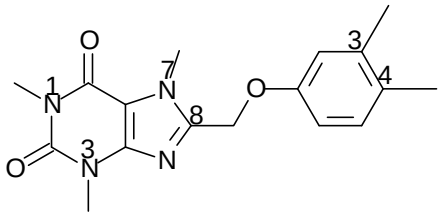

The title compound was prepared from 3,4-dimethylphenoxyacetic acid in a yield of 80%: mp 178.9 ºC (ethanol). **^{1}H-NMR** (Bruker Avance III 600, $CDCl_3$) δ 2.17 (s, 3H), 2.21 (s, 3H), 3.38 (s, 3H), 3.56 (s, 3H), 4.02 (s, 3H), 5.13 (s, 2H), 6.72 (dd, 1H, J = 2.3, 8.3 Hz), 6.78 (d, 1H J = 2.3 Hz) 7.02 (d, 1H, J = 8.3 Hz). **^{13}C-NMR** (Bruker Avance III 600, $CDCl_3$) δ 18.8, 20.0, 27.9, 29.7, 32.4, 62.1, 108.7, 111.4, 116.3, 130.1, 130.4, 138.1, 147.3, 148.1, 151.6, 155.4, 155.6. **Mass spectrometry**: EIMS 329; EI-HRMS *m*/*z*: calcd for **$C_{17}H_{20}N_4O_3$**, 329.1535, found 329.1615 **Purity** (HPLC): 98.9%.

^{1}H-NMR:	**^{13}C-NMR:**
• Methyl groups at N1, N3 and N7 correspond with the singlets at 3.38, 3.56 and 4.02 ppm (the signals integrate for 3 protons each). • CH_2 singlet corresponds with the signal at 5.13 ppm (the signal integrates for 2 protons). • The methyl groups on the phenyl ring correspond with the singlets at 2.17 and 2.21 ppm (the signals integrate for 3 protons each). • Aromatic protons on the phenyl ring are represented by the doublet of doublets at 6.72 ppm (integrate for 1 proton) and the doublets at 6.78 and 7.02 ppm (signals integrate for 1 proton each).	• Methyl groups at N1, N3, and N7 are represented by the signals at 27.9, 29.7 and 32.4 ppm. • CH_2 singlet corresponds with the signal at 62.1 ppm. • The methyl groups on the phenyl ring correspond to the signals at 18.8 and 20.0 ppm. • Aromatic carbons are represented by the signals at 108.7, 111.4, 116.3, 130.4, 138.1, 147.3, 148.1, 151.6, 155.4 and 155.6 ppm.

3.4.5 **1,3-Diethyl-7-methyl-8-(4-chlorophenoxymethyl)xanthine (16)**

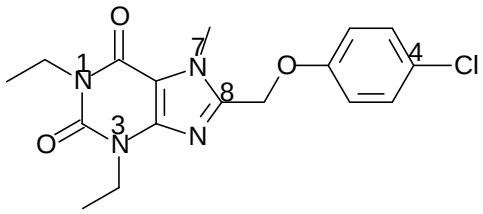

The title compound was prepared from 4-chlorophenoxyacetic acid in a yield of 87%: mp 109.7 ºC (ethanol). **^{1}H-NMR** (Bruker Avance III 600, $CDCl_3$) δ 1.22 (t, 3H J = 7.2 Hz), 1.32 (t, 3H J = 7.2 Hz), 4.02 (s, 3H), 4.05 (q, 2H J = 7.2 Hz), 4.13 (q, 2H J = 7.2 Hz), 5.15 (s, 2H), 6.88 (d, 2H J = 9.0 Hz), 7.37 (d, 2H J = 9.0 Hz). **^{13}C-NMR** (Bruker Avance III 600, $CDCl_3$) δ 13.2, 13.4, 32.4, 36.4, 38.5, 62.1, 109.0, 114.3, 116.5, 132.5, 146.8, 147.3, 150.6, 155.2, 156.6. **Mass spectrometry**: EIMS 363; EI-HRMS *m*/*z*: calcd for **$C_{17}H_{19}ClN_4O_3$**, 363.1146, found 363.1235 **Purity** (HPLC): 99.6%.

^{1}H-NMR:	**^{13}C-NMR:**
• Triplets at 1.22 and 1.32 ppm represent the CH_3 substituents on the ethyl side chain of N1 and N3 (signals integrate for 3 protons each). • Quartets at 4.05 and 4.13 ppm correspond with the CH_2 groups on position N1 and N3 (signals integrate for 2 protons each). • The methyl group at N7 corresponds with the singlet at 4.02, ppm (the signal integrates for 3 protons). • CH_2-O- singlet corresponds with the signal at 5.15 ppm (the signal integrates for 2 protons). • Aromatic protons on the phenyl ring are represented by the doublets at 6.88 and 7.37 ppm (signals integrate for 2 protons each).	• CH_3 substituents on the ethyl side chain of N1 and N3 are represented by the signals at 13.2 and 13.4 ppm. • CH_2 substituents on N1 and N3 correspond with the signals at 32.4 and 36.4 ppm. • The methyl group at N7 is represented by the signals at 38.5 ppm. • CH_2-O- singlet corresponds with the signal at 62.1 ppm. • Aromatic carbons are represented by the signals at 109.0, 114.3, 116.5, 132.5, 146.8, 147.3, 150.6, 155.2 and 156.6 ppm.

3.4.6 **1,3-Diethyl-7-methyl-8-(4-bromophenoxymethyl)xanthine (17)**

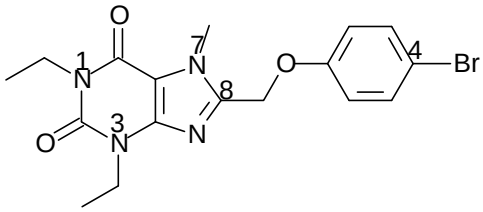

The title compound was prepared from 4-bromophenoxyacetic acid in a yield of 85%: mp 110.6 ºC (ethanol). **^{1}H-NMR** (Bruker Avance III 600, $CDCl_3$) δ 1.21 (t, 3H J = 7.2 Hz), 1.31 (t, 3H J = 7.2 Hz), 4.02 (s, 3H), 4.04 (q, 2H J = 7.2 Hz), 4.13 (q, 2H J = 7.2 Hz), 5.14 (s, 2H), 6.93 (d, 2H J = 9.0 Hz), 7.23 (d, 2H J = 9.0 Hz). **^{13}C-NMR** (Bruker Avance III 600, $CDCl_3$) δ 13.3, 13.4, 32.4, 36.4, 38.5, 62.2, 109.0, 116.0, 127.0, 129.6, 146.8, 147.3, 150.6, 155.2, 156.1. **Mass spectrometry**: EIMS 407; EI-HRMS *m*/*z*: calcd for **$C_{17}H_{19}BrN_4O_3$**, 407.0641, found 407.0735 **Purity** (HPLC): 99.4%.

^{1}H-NMR:	**^{13}C-NMR:**
• Triplets at 1.21 and 1.31 ppm represent the CH_3 substituents on the ethyl side chain of N1 and N3 (signals integrate for 3 protons each). • Quartets at 4.04 and 4.13 ppm correspond with the CH_2 groups on position N1 and N3 (signals integrate for 2 protons each). • The methyl group at N7 corresponds with the singlet at 4.02 ppm (the signal integrates for 3 protons). • O-CH_2 singlet corresponds with the signal at 5.14 ppm (the signal integrates for 2 protons). • Aromatic protons on the phenyl ring are represented by the doublets at 6.93 and 7.23 ppm (signals integrate for 2 protons each).	• CH_3 substituents on the ethyl side chain of N1 and N3 are represented by the signals at 13.3 and 13.4 ppm. • CH_2 substituents on N1 and N3 correspond with the signals at 32.4 and 36.4 ppm. • The methyl group at N7 is represented by the signal at 38.5 ppm. • CH_2-O- singlet corresponds with the signal at 62.2 ppm. • Aromatic carbons are represented by the signals at 109.0, 116.0, 127.0, 129.6, 146.8, 147.3, 150.6, 155.2 and 156.1 ppm.

3.4.7 **1,3-Diethyl-7-methyl-8-(4-fluorophenoxymethyl)xanthine (18)**

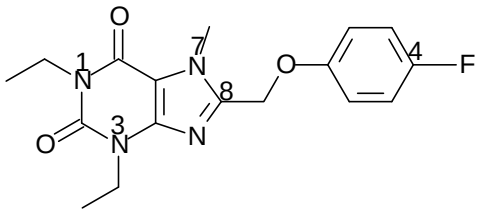

The title compound was prepared from 4-fluorophenoxyacetic acid in a yield of 81%: mp 122.7 ºC (ethanol). **^{1}H-NMR** (Bruker Avance III 600, $CDCl_3$) δ 1.22 (t, 3H J = 7.2 Hz), 1.32 (t, 3H J = 7.2 Hz), 4.03 s (3H); 4.05 (q, 2H J = 7.4 Hz), 4.14 (q, 2H J = 7.2 Hz), 5.13 (s, 2H), 6.94 (d, 2H J = 7.2 Hz), 6.96 (d, 2H J = 7.2 Hz). **^{13}C-NMR** (Bruker Avance III 600, $CDCl_3$) δ 13.2, 13.4, 32.4, 36.4, 38.5, 62.6, 109.0, 115.9, 116.2, 146.9, 147.6, 150.6, 153.6, 155.2, 158.7. **Mass spectrometry**: EIMS 347; EI-HRMS *m*/*z*: calcd for **$C_{17}H_{19}FN_4O_3$**, 347.1442, found 347.1527 **Purity** (HPLC): 99.0%.

^{1}H-NMR:	**^{13}C-NMR:**
• Triplets at 1.21 and 1.32 ppm represent the CH_3 substituents on the ethyl side chain of N1 and N3 (signals integrate for 3 protons each). • Quartets at 4.05 and 4.14 ppm correspond with the CH_2 groups on position N1 and N3 (signals integrate for 2 protons each). • The methyl group at N7 corresponds with the singlet at 4.03 ppm (the signal integrates for 3 protons). • CH_2-O- singlet corresponds with the signal at 5.13 ppm (the signal integrates for 2 protons). • Aromatic protons on the phenyl ring are represented by the doublets at 6.94 and 6.96 ppm (signals integrate for 2 protons each).	• CH_3 substituents on the ethyl side chain of N1 and N3 are represented by the signals at 13.2 and 13.4 ppm. • CH_2 substituents on N1 and N3 correspond with the signals at 32.4 and 36.4 ppm. • The methyl group at N7 is represented by the signal at 38.5 ppm. • CH_2-O- singlet corresponds with the signal at 62.6 ppm. • Aromatic carbons are represented by the signals at 109.0, 115.9, 116.2, 146.9, 147.6, 150.6, 153.6, 155.2 and 158.7 ppm.

3.4.8 **1,3-Diethyl-7-methyl-8-(4-methylphenoxymethyl)xanthine (19)**

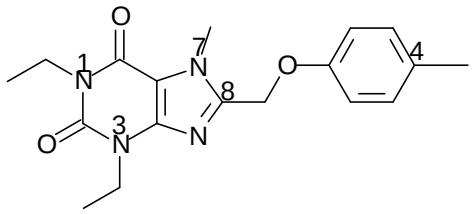

The title compound was prepared from 4-methylphenoxyacetic acid in a yield of 90%: mp 127.7 ºC (ethanol). **^{1}H-NMR** (Bruker Avance III 600, $CDCl_3$) δ 1.22 (t, 3H J = 7.2 Hz), 1.32 (t, 3H J = 7.2 Hz), 2.26 (s, 3H), 4.02 (s, 3H), 4.05 (q, 2H J = 7.2 Hz), 4.14 (q, 2H J = 7.2 Hz), 5.14 (s, 2H), 6.88 (d, 2H J = 8.7 Hz), 7.07 (d, 2H J = 8.3 Hz). **^{13}C-NMR** (Bruker Avance III 600, $CDCl_3$) δ 13.3, 13.4, 20.5, 32.4, 36.4, 38.5, 62.2, 109.9, 114.5, 130.1, 131.3, 146.9, 148.0, 150.6, 155.2, 155.4. **Mass spectrometry**: EIMS 343; EI-HRMS *m*/*z*: calcd for **$C_{18}H_{22}N_4O_3$**, 343.1692, found 343.1780 **Purity** (HPLC): 98.9%.

^{1}H-NMR:	**^{13}C-NMR:**
• Triplets at 1.2 and 1.32 ppm represent the CH_3 substituents on the ethyl side chain of N1 and N3 (signals integrate for 3 protons each). • Quartets at 4.05 and 4.14 ppm correspond with the CH_2 groups on position N1 and N3 (signals integrate for 2 protons each). • CH_3 substituent on position 4 if the phenl ring is represented by the singlet at 2.26 ppm (signal integrates for 3 protons). • The methyl group at N7 corresponds with the singlet at 4.02 ppm (the singnal intergrates for 3 protons). • CH_2-O- singlet corresponds with the signal at 5.14 ppm (the signal integrates for 2 protons). • Aromatic protons on the phenyl ring are represented by the doublets at 6.88 and 7.07 ppm (signals integrate for 2 protons each).	• CH_3 substituents on the ethyl side chain of N1 and N3 are represented by the signals at 13.3 and 13.4 ppm. • CH_3 substituent on position C4 of the phenyl ring is represented at 20.5 ppm. • CH_2 substituents on N1 and N3 correspond with the signals at 32.4 and 36.4 ppm. • The methyl group at N7 is represented by the signal at 38.5 ppm. • CH_2-O- singlet corresponds with the signal at 62.2 ppm. • Aromatic carbons are represented by the signals at 109.6, 114.5, 130.1, 131.3, 146.9, 148.0, 150.6, 155.2 and 155.4 ppm.

3.4.9 **1,3-Diethyl-7-methyl-8-(4-methoxyphenoxymethyl)xanthine (20)**

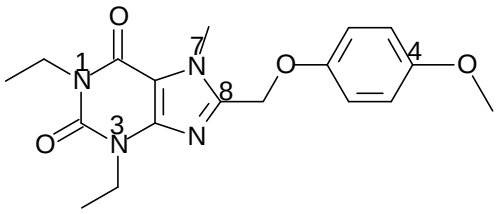

The title compound was prepared from 4-methoxyphenoxyacetic acid in a yield of 79%: mp 149.7 ºC (ethanol). **^{1}H-NMR** (Bruker Avance III 600, $CDCl_3$) δ 1.26 (t, 3H J = 7.2 Hz), 1.36 (t, 3H J = 7.2 Hz), 3.79 (s, 3H), 4.07 (s, 3H) 4.09 (q, 2H J = 7.2 Hz), 4.18 (q, 2H J = 7.2 Hz), 5.16 (s, 2H), 6.86 (d, 2H J = 9.0 Hz), 6.96 (d, 2H J = 9.0 Hz). **^{13}C-NMR** (Bruker Avance III 600, $CDCl_3$) δ 13.3, 13.4, 32.4, 36.4, 38.5, 55.7, 62.8, 109.0, 114.7, 115.8, 146.9, 148.0, 150.6, 151.6, 154.7, 155.2. **Mass spectrometry**: EIMS 359; EI-HRMS *m/z*: calcd for **$C_{18}H_{22}N_4O_4$**, 359.1641, found 359.1711 **Purity** (HPLC): 99.2%.

^{1}H-NMR:	**^{13}C-NMR:**
• Triplets at 1.26 and 1.36 ppm represent the CH_3 substituents on the ethyl side chain of N1 and N3 (signals integrate for 3 protons each). • Quartets at 4.09 and 4.18 ppm correspond with the CH_2 groups on position N1 and N3 (signals integrate for 2 protons each). • The methyl group at N7 correspond with the singlet at 4.07 ppm (the signal integrates for 3 protons). • The methoxy group on the phenyl ring corresponds to the singlet at 3.79 ppm (integrate for 3 protons). • CH_2-O- singlet corresponds with the signal at 5.16 ppm (the signal integrates for 2 protons). • Aromatic protons on the phenyl ring are represented by the doublets at 6.86 and 6.96 ppm (signals integrate for 2 protons each).	• CH_3 substituents on the ethyl side chain of N1 and N3 are represented by the signals at 13.3 and 13.4 ppm. • CH_2 substituents on N1 and N3 correspond with the signals at 32.4 and 36.4 ppm. • The methyl group at N7 is represented by the signal at 38.5 ppm. • The methoxy group on the phenyl ring corresponds to the signal at 55.7 ppm. • CH_2-O- singlet corresponds with the signal at 62.8 ppm. • Aromatic carbons are represented by the signals at 109.0, 114.7, 115.8, 146.9, 148.0, 150.6, 151.6, 154.7 and 155.2 ppm.

3.4.10 **1,3-Diethyl-7-methyl-8-(4-iodophenoxymethyl)xanthine (21)**

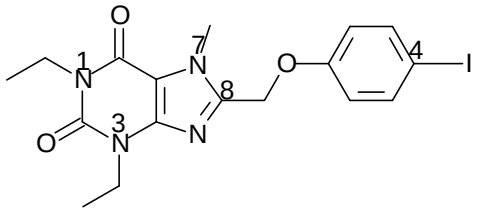

The title compound was prepared from 4-iodophenoxyacetic acid in a yield of 65%: mp 210.4 ºC (ethanol). **^{1}H-NMR** (Bruker Avance III 600, $CDCl_3$) δ 1.22 (t, 3H J = 7.2 Hz), 1.32 (t, 3H J = 7.2 Hz), 4.02 (s, 3H), 4.05 (q, 2H J = 7.2 Hz), 4.14 (q, 2H J = 7.2 Hz), 5.14 (s, 2H), 6.78 (d, 2H J = 9.0 Hz), 7.56 (d, 2H J = 9.0 Hz). **^{13}C-NMR** (Bruker Avance III 600, $CDCl_3$) δ 13.3, 13.4, 32.4, 36.4, 35.5, 62.0, 84.4, 109.0, 117.1, 138.5, 146.9, 147.3, 150.6, 155.2, 157.4. **Mass spectrometry**: EIMS 455; EI-HRMS *m*/*z*: calcd for **$C_{17}H_{19}IN_4O_3$**, 455.0502, found 455.0575 **Purity** (HPLC): 97.6%.

^{1}H-NMR:	**^{13}C-NMR:**
• Triplets at 1.22 and 1.32 ppm represent the CH_3 substituents on the ethyl side chain of N1 and N3 (signals integrate for 3 protons each). • Quartets at 4.05 and 4.14 ppm correspond with the CH_2 groups on position N1 and N3 (signals integrate for 2 protons each). • The methyl group at N7 corresponds with the singlet at 4.02 ppm (the signal integrates for 3 protons). • CH_2-O- singlet corresponds with the signal at 5.14 ppm (the signal integrates for 2 protons). • Aromatic protons on the phenyl ring are represented by the doublets at 6.78 and 7.56 ppm (signals integrate for 2 protons each).	• CH_3 substituents on the ethyl side chain of N1 and N3 are represented by the signals at 13.3 and 13.4 ppm. • CH_2 substituents on N1 and N3 correspond with the signals at 32.4 and 36.4 ppm. • The methyl group at N7 is represented by the signal at 35.5 ppm. • CH_2-O- singlet corresponds with the signal at 62.0 ppm. • Aromatic carbons are represented by the signals at 84.4, 109.0, 117.1, 138.5, 146.9, 147.3, 150.6, 155.2 and 157.4 ppm.

3.4.11 **1,3-Diethyl-7-methyl-8-(3,4-dimethylphenoxymethyl)xanthine (22)**

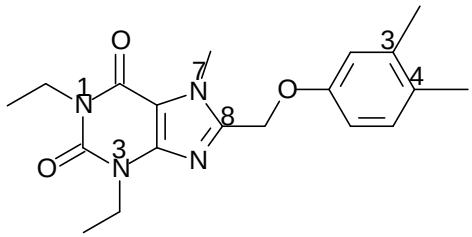

The title compound was prepared from 3,4-dimethylphenoxyacetic acid in a yield of 84%: mp 147.1 ºC (ethanol). **^{1}H-NMR** (Bruker Avance III 600, $CDCl_3$) δ 1.22 (t, 3H J = 7.2 Hz), 1.33 (t, 3H J = 7.2 Hz), 2.17 (s, 3H), 2.21 (s, 3H), 4.02 (s, 3H), 4.05 (q, 2H J = 7.2 Hz), 4.14 (q, 2H J = 7.2 Hz), 5.14 (s, 2H), 6.72 (dd, 1H J = 2.3, 8.3 Hz), 6.78 (d, 1H J = 2.6 Hz), 7.02 (d, 1H J = 8.3 Hz). **^{13}C-NMR** (Bruker Avance III 600, $CDCl_3$) δ 13.3, 13.4, 18.8, 20.0, 32.4, 36.4, 38.5, 62.1, 108.9, 111.6, 116.3, 130.1, 130.4, 138.1, 146.9, 148.1, 150.6, 155.2, 155.6. **Mass spectrometry**: EIMS 457; EI-HRMS *m*/*z*: calcd for **$C_{19}H_{24}N_4O_3$**, 457.1848, found 457.1921 **Purity** (HPLC): 97.6%.

^{1}H-NMR:	**^{13}C-NMR:**
• Triplets at 1.22 and 1.33 ppm represent the CH_3 substituents on the ethyl side chain of N1 and N3 (signals integrate for 3 protons each). • Quartets at 4.05 and 4.14 ppm correspond with the CH_2 groups on position N1 and N3 (signals integrate for 2 protons each). • The methyl group at N7 corresponds with the singlet at 4.02 ppm (the signal integrates for 3 protons). • CH_2-O- singlet corresponds with the signal at 5.14 ppm (the signal integrates for 2 protons). • Methyl groups on the phenyl ring are represented with the singlets at 2.17 and 2.21 ppm (signals integrate for 3 protons each). • Aromatic protons on the phenyl ring are represented by the doublet of	• CH_3 substituents on the ethyl side chain of N1 and N3 are represented by the signals at 13.3 and 13.4 ppm. • CH_2 substituents on N1 and N3 correspond with the signals at 32.4 and 36.4 ppm. • The methyl group at N7 is represented by the signal at 38.5 ppm. • Methyl groups on the phenyl ring (position C4) are represented by the signals at 18.8 and 20.0 ppm. • CH_2-O- singlet corresponds with the signal at 62.1 ppm. • Aromatic carbons are represented by the signals at 108.9, 116.6, 130.1, 130.4, 138.1, 146.9, 148.1, 150.6, 155.2 and 155.6 ppm.

	doublets at 6.72 ppm (signal integrates for 1 proton) and the doublets at 6.78 and 7.02 ppm (signals integrate for 2 protons each).	

3.5 **Interpretation of mass spectra**

The synthesized compounds were characterized by MS and the high resolution masses were calculated and experimentally determined (Table 3.3). The differences between the experimentally determined and calculated masses are indicative that the structures of the compounds correspond to those given in table 3.1.

Table 3.3: The calculated and experimentally high resolution masses of the synthesized compounds. All masses are given as M^+.

Mass Spectra:			
Compound:	**Formula:**	**Calculated:**	**Found:**
11	$C_{16}H_{18}N_4O_3$	315.1379	315.1461
12	$C_{16}H_{18}N_4O_4$	331.1328	331.1404
13	$C_{15}H_{15}IN_4O_3$	427.0189	427.0268
14	$C_{17}H_{20}N_4O_3$	329.1535	329.1615
16	$C_{17}H_{19}ClN_4O_3$	363.1146	363.1235
17	$C_{17}H_{19}BrN_4O_3$	407.0641	407.0735
18	$C_{17}H_{19}FN_4O_3$	347.1442	347.1527
19	$C_{18}H_{22}N_4O_3$	343.1692	343.1780
20	$C_{18}H_{22}N_4O_4$	359.1641	359.1711
21	$C_{17}H_{19}IN_4O_3$	455.0502	455.0575
22	$C_{17}H_{19}IN_4O_3$	457.1848	457.1921

3.6 **Interpretation of HPLC-traces**

HPLC analysis was used to determine the purities of the target compounds. Strong eluting conditions (up to 85% acetonitrile) were used in the HPLC analysis. The eluent was monitored at 210 nm, where most organic compounds absorb UV light. If any impurities are present, they are expected to elute and be detected under these HPLC-conditions. The chromatograms obtained for each compound are given in the addendum. As can be seen with the chromatograms, a single peak for each compound indicates a high degree of purity.

Where additional peaks occurred, the percentage purities were calculated. These calculations were based on the intergrated surface areas of the analyte and impurity peaks. Purities for the synthesized compounds are given in Table 3.4 and were estimated to be between 97.3-100%, which may be deemed acceptable.

Table 3.4: Purities of the synthesized compounds were determined using HPLC.

HPLC analysis:		
Compound:	**Purity determined (%):**	**Pure/Unpure:**
11	99.0	Pure
12	97.3	Pure
13	99.4	Pure
14	98.9	Pure
16	99.6	Pure
17	99.4	Pure
18	99.0	Pure
19	98.9	Pure
20	99.2	Pure
21	97.6	Pure
22	97.6	Pure

3.7 **Conclusion:**

All eleven of the target 8-(phenoxymethyl)caffeine analogues were synthesized successfully. The structures of the compounds were confirmed via ^{1}H-NMR, ^{13}C-NMR and mass spectroscopy. As shown by the analytical data, the structures of the target compounds exhibited the expected NMR spectra with respect to the amount of signals predicted, their chemical shifts and the multiplicities of the ^{1}H-NMR signals. The experimentally determined molecular masses also corresponded with those predicted. The purities of the compounds were determined with HPLC analysis. The HPLC analysis revealed a single predominant peak for each of the compounds that were analyzed and the purities were estimated at 97.3–100%.

CHAPTER 4:

ENZYMOLOGY

4.1 General background on enzyme kinetics

Enzymes are biological catalysts and all enzymes are proteins. They increase the rate of chemical reactions taking place within living cells, without themselves suffering any overall change or damage. The reactants of enzyme-catalyzed reactions are termed substrates. Each enzyme is quite specific in character, acting on a particular substrate or substrates to produce a particular product or products (Palmer & Bonner, 2007).

Enzyme kinetics is the field of biochemistry concerned with the quantitative measurement of the rates of enzyme-catalyzed reactions and the systematic study of factors that affect these rates. Kinetic analyses permit scientists to reconstruct the order and number of the individual steps by which enzymes transform substrates into products (Rodwell & Kennelly, 2003).

4.2 Enzyme kinetics: K_m determination

In an enzyme-catalyzed reaction the initial velocity (V_i) can be seen as the rate of the forward reaction. As the concentration of an enzyme substrate [S] is increased, while all other conditions are kept constant, the V_i of an enzymatic reaction increases to a maximum value (V_{max}). At this point the enzyme is saturated and a further increase in substrate concentration does not increase V_i. The Michaelis-Menten equation (Equation 4.1) can be used to illustrate the relationship between V_i and the concentration of a substrate in a hyperbolic curve (Figure 4.1).

The substrate concentration [S] that produces half-maximal velocity ($V_{max}/2$) is termed the K_m value or Michaelis constant (Rodwell & Kennelly, 2003). If the concentration of a substrate is less than K_m, the V_i is directly proportional to the concentration of the substrate. But, when the substrate concentration is much greater than K_m, the initial velocity is maximal (V_{max}) and stays unaffected by any further increases in the concentration of the substrate (Rodwell & Kennelly, 2003).

$$V_i = \frac{\mathrm{V_{max}} \times [\mathrm{S}]}{\mathrm{K_m} + [\mathrm{S}]}$$

Equation 4.1: **The Michaelis-Menten equation describes the behaviour of an enzyme under the influence of varied substrate concentrations.**

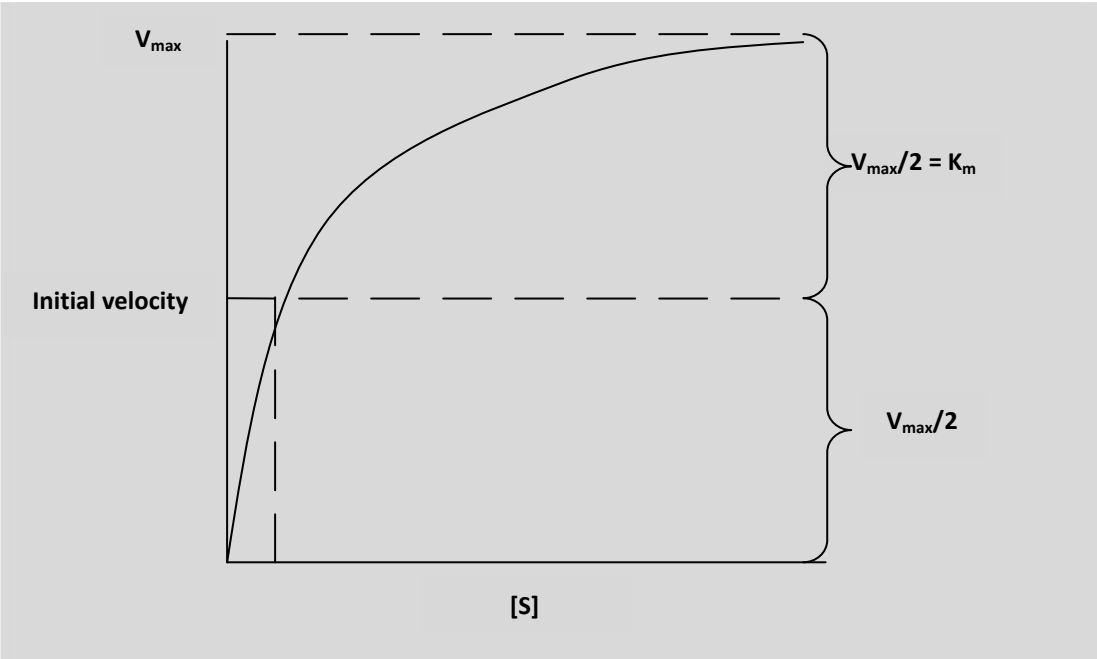

Figure 4.1: **Graphical representation of the Michealis-Menten equation (V_i vs. [S]).**

When V_i is plotted against [S], many enzymes give saturation curves that do not readily permit accurate measurement of V_{max} (and therefore K_m). In order to avoid this, the inversion of the Michaelis-Menten equation (Equation 4.2) is used to determine K_m and $V_{max.}$ This plot is called a double reciprocal plot or Lineweaver-Burke plot (Figure 4.2). By setting y ($1/V_i$) equal to zero, K_m can be calculated from the x-intercept ($-1/K_m$) (Rodwell & Kennelly, 2003).

$$\frac{1}{V_i} = \left(\frac{\mathrm{K_m}}{\mathrm{V_{max}}}\right)\frac{1}{[\mathrm{S}]} + \frac{1}{\mathrm{V_{max}}}$$

Equation 4.2: **Inversion of the Michaelis-Menten equation describes the double reciprocal plot or Lineweaver-Burke plot**

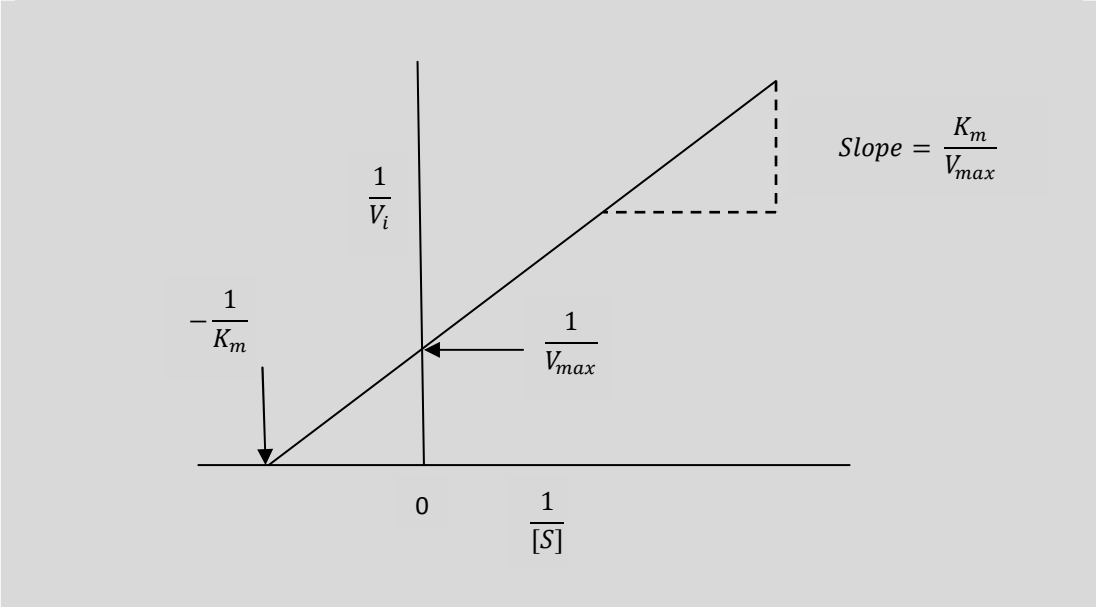

Figure 4.2: An example of the Lineweaver-Burke plot $1/V_i$ versus $1/[S]$).

When [S] is equal to K_m, V_i is responsive to the presence of inhibitors and changes in substrate concentrations. When examining the effects of inhibitors on MAO-B catalytic rate, substrate concentrations that closely bracket the reported apparent K_m value are used.

4.3 **MAO-B Inhibition studies**

4.3.1 **Introduction**

There are a variety of approaches to measure MAO-B catalytic activity. These methods are based on the disappearance of substrates (Zhou *et al.,* 1996), oxygen consumption (Meyerson *et al.,* 1978), aldehyde formation (Holt *et al.,* 1997), ammonia formation (Meyerson *et al.,* 1978; Zhou *et al.,* 1996; Holt *et al.,* 1997), hydrogen peroxide formation (Holt *et al.,* 1997) and acid formation following oxidation of the amine to the aldehyde and subsequently the acid (Meyerson *et al.,* 1978).

Some of the techniques used for measuring MAO-B activity include spectrophotometry, radiometry, fluorometry, luminometry (Zhou *et al.,* 1996), colorimetry (Meyerson *et al.,* 1978), chromatography (Vlok *et al.,* 2006) and the use of an oxygen electrode (Tipton, 1971; Weetman & Sweetman, 1971; Meyerson *et al.,* 1978). In general MAO-B activity is measured by adding a substrate to MAO-B and measuring the concentration of the product formed after a specified time (Vlok *et al.,* 2006).

The 8-(phenoxymethyl)caffeine analogues that were successfully synthesized in the previous chapter will be investigated as potential inhibitors of MAO-A and –B in this chapter. A fluorometric assay using Amplex Red will be used to determine inhibition potencies. The inhibition potencies will be expressed as the IC_{50} values for each inhibitor. The fluorometric assay is based on measuring the amount of H_2O_2 produced by the MAO catalyzed oxidation process. H_2O_2 is reacted in a horseradish peroxidase (HRP) coupled reaction with Amplex Red reagent. When Amplex Red and H_2O_2 reacts, a stable product, namely resorufin is produced (Figure 4.3). Resorufin is a fluorescent dye and since the amount of resorufin formed is directly proportional to the amount of H_2O_2 produced by MAO, the MAO catalytic rate can be measured with fluorescence spectrophotometry.

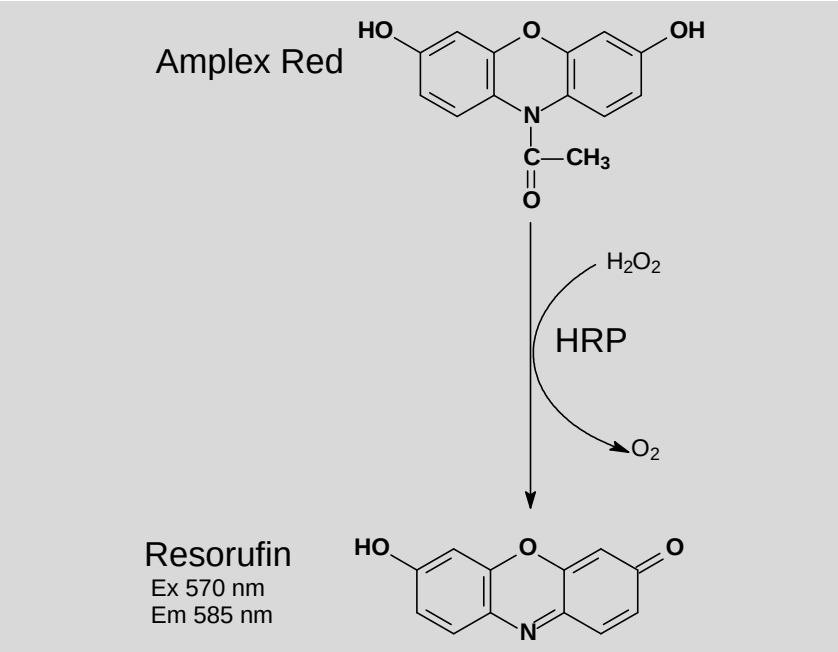

Figure 4.3: **The formation of resorufin occurs in the presence of HRP and H_2O_2**

4.3.2 **Chemicals and Instrumentation**

The following were obtained from Sigma Aldrich: Amplex Red (10-acetyl,3,7-dihydroxyphenoxazine) reagent, HRP, H_2O_2 (3%), kynuramine.2HBr and microsomes from insect cells containing recombinant MAO-A and MAO-B (5 mg/ml). A Varian Cary Eclipse fluorescence spectrophotometer was used for fluorescence spectrophotometry.

4.3.3 **Method**

The following method (Figure 4.4) was used to measure the MAO-A and -B inhibition potencies of the test compounds. Recombinant human MAO-A and –B (5 mg/ml), obtained from Sigma Aldrich, were pre-aliquoted and stored at -70 ºC. Potassium phosphate buffer

(100 mM, pH 7.4) was used to prepare all enzymatic reactions. The reactions contained various concentrations of the test inhibitor (0-100 µM), kynuramine, Amplex Red, HRP and enzyme. The HRP/Amplex Red working solution contained HRP (5 units/ml) and Amplex Red (1 mM) in potassium phosphate buffer. The kynuramine added to the incubations resulted in final concentrations of 45 µM for MAO-A and 30 µM for MAO-B. The final volumes of the incubations were 500 µl and consisted of 50 µl kynuramine (substrate), 20 µl test inhibitor, 280 µl potassium phosphate buffer, 100 µl HRP/Amplex Red working solution and 50 µl enzyme (0.075 mg/ml). Stock solutions of the test inhibitors were prepared to give a 4% (v/v) concentration of DMSO in the final reactions. The reactions were incubated for 20 minutes at 37 ℃ and terminated with the addition of 10 µl deprenyl (5 mM) for MAO-B, and 10 µl clorgyline (5 mM) for MAO-A. Distilled water (1400 µl) was added to each incubation before it was centrifuged for 10 minutes at 16,000 *g*. The concentrations of the MAO generated resorufin in the reactions were determined by measuring the fluorescence of the supernatant at an excitation wavelength of 560 nm and an emission wavelength of 590 nm (Zhou & Panchuk-Voloshina, 1997). Quantitative estimations of resorufin were made by means of a linear calibration curve, which were constructed from different concentrations of H_2O_2 (0.05–0.65 µM). Each calibration standard was prepared to a final volume of 500 µl in potassium phosphate buffer (100 mM, pH 7.4) and contained 4% DMSO. To each standard was added 10 µl deprenyl (5 mM) for MAO-B, 10 µl clorgyline (5 mM) for MAO-A and 1400 µl distilled water. The IC_{50} values were determined by plotting the initial rate of oxidation versus the logarithm of the inhibitor concentration to obtain a sigmoidal dose–response curve. For each sigmoidal curve, 6 different inhibitor concentrations spanning at least 3 orders of magnitude were used. Graphpad prism 5 was used to fit the inhibition data to the one site competition model. The IC_{50} values were determined in triplicate and expressed as mean ± standard deviation (SD).

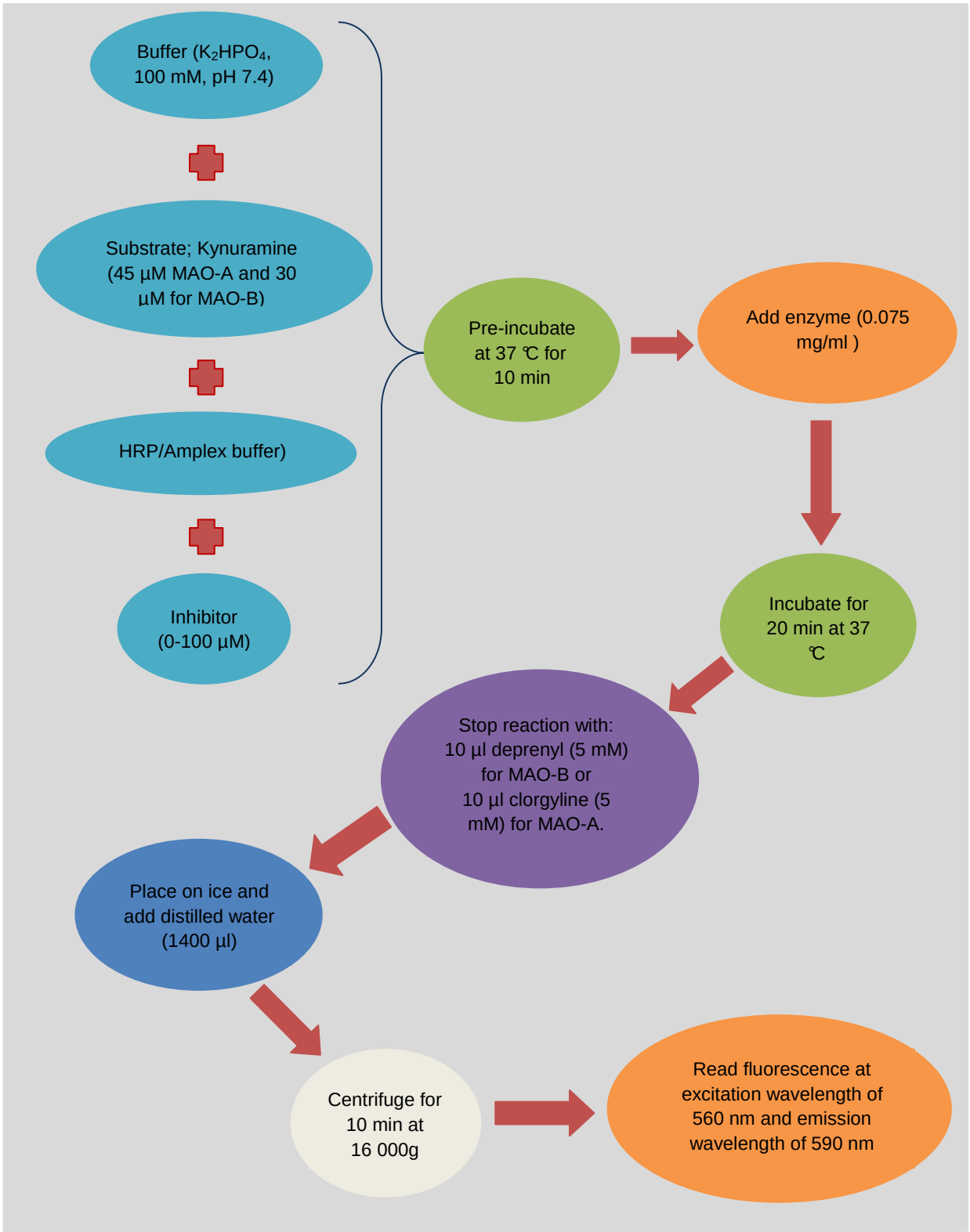

Figure 4.4: **Schematic representation of the method used to measure the MAO-A and -B inhibition potencies of the test compounds.**

4.3.4 **Results**

The IC_{50} values for the inhibition of MAO-A and MAO-B by the synthesized compounds are presented in Table 4.1. All compounds were examined as MAO-A and MAO-B inhibitors and the IC_{50} values are expressed in µM. The IC_{50} values are given as the mean ± SD of triplicate determinations. The IC_{50} of a compound signifies the concentration of an inhibitor that is needed for 50% inhibition *in vitro*. A lower IC_{50} value indicates that the compound has a higher binding affinity for the enzyme and is therefore a more potent inhibitor. The most potent inhibitor among the evaluated compounds the present is highlighted in grey in the table. Figure 4.4 depicts a typical sigmoidal dose–response curve for the measurement of an IC_{50} value. In this case, the figure depicts the most potent MAO-B inhibitor, 8-(4-iodophenoxymethyl)caffeine (**13**), which exhibits an IC_{50} of 0.46 µM.

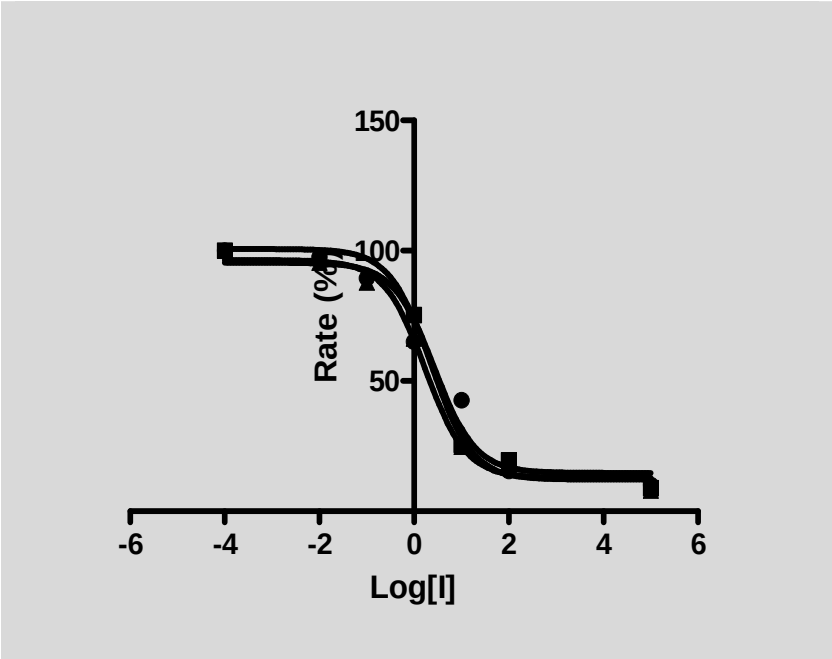

Figure 4.5: **The sigmoidal dose-response curve for the calculation of the IC_{50} value of 8-(4-iodophenoxymethyl)caffeine**

In the objectives of this study it is mentioned that one of the aims is to compare the newly synthesized 8-(phenoxymethyl)caffeine analogues to the 8-(phenoxymethyl)caffeine analogues synthesized in a previous study (Swanepoel, 2010). Table 4.1 below gives the IC_{50} values for the inhibition of recombinant human MAO-A and –B by the previously synthesized 8-(phenoxymethyl)caffeine analogues as well as the IC_{50} values of the newly synthesized compounds of series 1.

4.3.4.1 Series 1

Table 4.1: MAO inhibitory potencies of series 1, the 8-(phenoxymethyl)caffeine analogues. Also given are the IC_{50} values of the 8-(phenoxymethyl)caffeine analogues (**1**–**10**) synthesized in a previous study (Swanepoel, 2010).

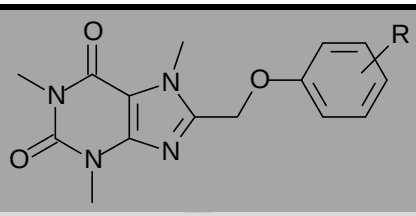

Compound:	R:	MAO-A IC_{50} (μM):	MAO-B IC_{50} (μM):
1*	H	21.1	5.78
2*	3-Cl	No Inhibition	0.334
3*	3-Br	34.0	0.148
4*	3-F	12.3	1.61
5*	3-CF_3	4.59	0.641
6*	3-CH_3	18.8	1.23
7*	3-OCH_3	No Inhibition	1.96
8*	4-Cl	20.4	0.250
9*	4-Br	10.7	0.189
10*	4-F	8.22	0.825
11	4-CH_3	32.7 ± 17.0	0.543 ± 0.083
12	4-OCH_3	No Inhibition	3.77 ± 1.291
13	4-I	No Inhibition	0.458 ± 0.215
14	3,4-diCH_3	No Inhibition	0.612 ± 0.462

***Compounds 1-10 synthesized by Swanepoel (2010).**

As shown in Table 4.1, the current study adds 4 additional homologues to those that have been synthesized previously (Swanepoel, 2010). These are the 4-CH_3 (**11**), 4-OCH_3 (**12**), 4-I (**13**) and 3,4-diCH_3 (**14**) substituted homologues. These homologues, as well as those previously synthesized belong to series 1, the 8-(phenoxymethyl)caffeine analogues. As mentioned above, the most potent MAO-B inhibitor among the newly synthesized compounds is 8-(4-iodophenoxymethyl)caffeine (**13**), which exhibits an IC_{50} of 0.46 μM. Among the newly synthesized compounds, the 4-CH_3 (**11**) and and 3,4-diCH_3 (**14**) substituted homologues also were potent MAO-B inhibitors with IC_{50} values in the submicromolar range. These analogues exhibited IC_{50} values of 0.54 μM and 0.62 μM, respectively, and may thus be classified as potent MAO-B inhibitors. In general inhibitors of MAO with IC_{50} values in the submicromolar range may be considered as potent inhibitors (Vlok *et al.,* 2006). The weakest inhibitor among the newly synthesized compounds is the 4-OCH_3 (**12**) substituted homologue. This compound exhibited an IC_{50} value of 3.77 μM,

making it a moderately potent MAO-B inhibitor. It is interesting to note that among the C4 substituted 8-(phenoxymethyl)caffeine analogues of series 1, compounds **8**–**14**, the homologues containing halogen substituents (Cl, Br and I) are more potent MAO-B inhibitors than the alkyl (CH_3 and OCH_3) containing homologues. For example, the chlorine (**8**), bromine (**9**) and iodo (**13**) containing homologues exhibited IC_{50} values of 0.189–0.458 µM while the CH_3 (**11**) and OCH_3 (**12**) exhibited IC_{50} values of 0.543–3.77 µM. The only exception to this trend is the fluorine substituted homologue **10**, which exhibited an IC_{50} value of 0.825 µM. The CH_3 substituted homologue was found to be a more potent MAO-B inhibitor than the F substituted homologue.

Another interesting observation of the current study is that the 3,4-diCH_3 (**14**) containing homologue exhibits an IC_{50} value for the inhibition of MAO-B that similar to that of the 4-CH_3 substituted homologue (**11**). These homologues possess IC_{50} values for the inhibition of MAO-B of 0.612 µM and 0.543 µM, respectively. This result shows that the addition of a second CH_3 group at C3 the the phenoxymethyl ring of series 1 does not further enhance MAO-B inhibition potency. In fact, the inhibition potency is slightly reduced (compare **11** with **14**). This observation that the addition of a 3-CH_3 does not enhance the potency of compound **11** is in accordance with the report that the 3-CH_3 substituted homologue (**6**) is only a moderately potent MAO-B inhibitor with an IC_{50} value of 1.23 µM. The 3-CH_3 group is thus not suitable for enhancing the MAO-B potencies of 8-(phenoxymethyl)caffeine analogues.

From these results we conclude that the 4 additional homologues examined in this study, compounds **11**–**14**, do not improve on the MAO-B inhibition potencies recorded for the existing 8-(phenoxymethyl)caffeine analogues, compounds **1**–**10**. For example among compounds **1**–**10**, the C3 and C4 bromine substituted homologues, compounds **3** and **9**, were highly potent MAO-B inhibitors with IC_{50} values of 0.148 µM and 0.189 µM, respectively. The most potent homologue of the current study, the iodo-substituted compound (**13**) exhibited an IC_{50} value of 0.458 µM. Compound **13** is therefore approximately 3-fold weaker as a MAO-B inhibitor than **3**. In spite of this, the most potent homologues of the current study, the 4-I (**13**), 4-CH_3 (**11**) and 3,4-diCH_3 (**14**) substituted homologues still exhibits IC_{50} values in the submicromolar range, and may therefore be viewed as potent MAO-B inhibitors.

It is useful to compare the MAO-B inhibitory potency of the most potent homologue of the newly synthesized series with a known MAO-B inhibitor. The reversible MAO-B inhibitor, lazabemide, inhibits human MAO-B with an IC_{50} value of 0.91 µM under the same conditions

(Pretorius *et al.,* 2008). Lazabemide is therefore approximately fivefold more potent than the most potent inhibitor, compound **13**, which as mentioned, exhibits an IC_{50} value of 0.458 µM.

Figure 4.6: Molecular structure of the known MAO-B inhibitor, lazabemide

Interestingly, the newly synthesized homologues are weak MAO-A inhibitors with compounds **12**–**14** exhibiting no inhibition at the maximal tested concentrations of 100 µM. Compound **11**, the 4-CH_3 substituted homologue inhibited MAO-A with an IC_{50} value of 32.7 µM. Compound **11** is therefore a 60-fold better inhibitor of human MAO-B compared to MAO-A. The MAO-B selectivity of these compounds may be considered as a desirable characteristic since the clinical use of MAO-A inhibitors have declined in recent years because of concerns of severe side effects that may arise from the indirectly-acting sympathomimetic amine, tyramine. As mentioned in the introduction, intestinal MAO-A metabolizes tyramine, which is present in certain foods, and thus reduces the amount of tyramine that enters the systemic circulation. MAO-A inhibitors may enhance tyramine blood levels and lead to a tyramine-induced release of norepinephrine from peripheral neurons (Youdim & Bakhle, 2006).

4.3.4.2 Series 2

Table 4.2: MAO inhibitory potencies of series 2, the 1,3-diethyl-7-methyl-8-(phenoxymethyl)xanthine analogues.

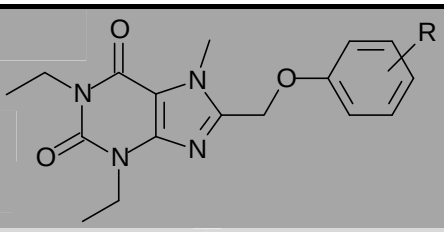

Compound:	R:	MAO-A IC_{50} (µM):	MAO-B IC_{50} (µM):
15[#]	H	No Inhibition	20.6 ± 6.47
16	4-Cl	No Inhibition	3.12 ± 1.41
17	4-Br	No Inhibition	4.07 ± 1.53
18	4-F	No Inhibition	8.05 ± 1.31
19	4-CH_3	No Inhibition	4.54 ± 1.72
20	4-OCH_3	No Inhibition	23.6 ± 5.73
21	4-I	No Inhibition	4.38 ± 0.829
22	3,4-CH_3	No Inhibition	2.23 ± 0.482

[#] **Compound 15 previously synthesized by Van Der Walt, 2012**

The results of the MAO inhibition studies with series 2 are given in Table 4.2. The results show that all the compounds are MAO-B inhibitors with IC_{50} values in the micromolar range. None of the inhibitors exhibited IC_{50} values in the submicromolar range as observed for series 1. The most potent inhibitor of series 2 is compound **22**, the 3,4-diCH_3 substituted homologue with an IC_{50} value of 2.23 µM. It is noteworthy that the 3,4-diCH_3 substituted homologue among the 8-(phenoxymethyl)caffeine analogues, compound **14** (IC_{50} = 0.612 µM) is approximately 4-fold more potent as an MAO-B inhibitor than **22**. All of the other homologues of series 2 are also consistently weaker MAO-B inhibitors than their corresponding 8-(phenoxymethyl)caffeine homologues.

As found with some of the 8-(phenoxymethyl)caffeine analogues of series 1, the 1,3-diethyl-7-methyl-8-(phenoxymethyl)xanthine analogues are not MAO-A inhibitors, with none of the compounds exhibiting inhibition at the maximal tested concentrations of 100 µM. This result suggests that the 1,3-diethyl-7-methylxanthine ring system is, in particular, not suitable for binding to MAO-A. This observation may provide a structural basis for the design of MAO-B selective inhibitors. The principal difference between the caffeine ring of series 1 and the 1,3-diethyl-7-methylxanthine ring of series 2 is the increases steric bulk provided by the 1,3-diethyl substitution (compared to the 1,3-dimethyl substitution of the caffeine ring). This steric bulk is less well tolerated in the MAO-A active site than the MAO-B active site since

those compounds containing the 1,3-diethyl-7-methylxanthine ring system (series 2) are not MAO-A inhibitors, while exhibiting moderate affinities for MAO-B. It may therefore be concluded that the addition of steric bulk to a scaffold will most likely result in a comparatively larger loss of MAO-A inhibition potency than MAO-B inhibition potency, and thus an increase in selectivity for the MAO-B isoform. This interesting observation merits further investigation.

4.3.5 **Comparison of the MAO-B inhibitory activities of series 1 and series 2**

As mentioned above, the compounds of series 2 are consistently weaker MAO-B inhibitors compared to their corresponding 8-(phenoxymethyl)caffeine homologues. This interesting behaviour merits further attention.

Table 4.3: A comparison between the MAO-B inhibition potencies of series 1 and series 2.

Series 1: 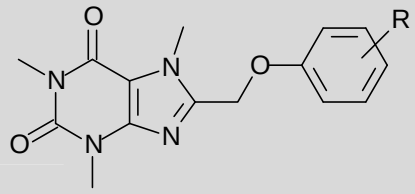			*Series 2:* 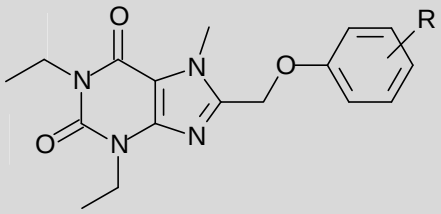		
Compound:	**Substituent:**	**MAO-B IC_{50} (µM):**	**Compound:**	**Substituent:**	**MAO-B IC_{50} (µM):**
1*	H	5.78	**15#**	H	20.60
8*	4-Cl	0.250	**16**	4-Cl	3.12
9*	4-Br	0.189	**17**	4-Br	4.07
10*	4-F	0.825	**18**	4-Fl	8.05
11	4-CH_3	0.54	**19**	4-CH_3	4.54
12	4-OCH_3	3.77	**20**	4-OCH_3	23.59
13	4-I	0.458	**21**	4-I	4.38
14	3,4-CH_3	0.62	**22**	3,4-CH_3	2.23

***Compounds 1, 8-10 synthesized by Swanepoel, 2010.**

 # Compound 15 previously synthesized by Van Der Walt, 2012

Table 4.3 shows that the 8-(phenoxymethyl)caffeine analogues (series 1) are consistently more potent MAO-B inhibitors than the corresponding 1,3-diethyl-7-methyl-8-(phenoxymethyl)xanthine homologues (series 2). This behavior is exemplified by the most potent inhibitor of series 2, compound **22** (3,4-diCH_3 substituted), which is 4-fold weaker as a MAO-B inhibitor than the corresponding 3,4-diCH_3 substituted homologue among the 8-(phenoxymethyl)caffeine analogues, compound **14**. Similarly, those homologues containing

a H, Cl, Br, F, CH_3, OCH_3 or I substituent on C4 of the phenoxy ring of 8-(phenoxymethyl)caffeine is 3.6-21.5-fold more potent as MAO-B inhibitors than the corresponding 1,3-diethyl-7-methyl-8-(phenoxymethyl)xanthine homologues. This result shows that the caffeine ring system of series 1 is more suitable for designing MAO-B inhibitors than the 1,3-diethyl-7-methylxanthine ring of series 2. Interestingly the same observation has been made for the inhibition of MAO-A. As mentioned above, none of the 1,3-diethyl-7-methyl-8-(phenoxymethyl)xanthine homologues (series 2) are MAO-A inhibitors which suggests that the 1,3-diethyl-7-methylxanthine ring system is not suitable for binding to MAO-A. Some of the 8-(phenoxymethyl)caffeine analogues (series 1) did exhibit moderate MAO-A inhibition, which shows that the caffeine ring system is also more suitable for binding to MAO-A than the 1,3-diethyl-7-methylxanthine ring system. As discussed above for MAO-A, the increased steric bulk conferred by the 1,3-diethyl substitution (compared to the 1,3-dimethyl substitution of the caffeine ring) may explain the lower MAO-B inhibition potencies of the compounds of series 2. This steric bulk is also less well tolerated in the MAO-B active site than the 1,3-dimethyl substitution pattern of series 1. It may therefore be concluded that for the design of potent MAO-B inhibitors the caffeine ring system is more suitable than the 1,3-diethyl-7-methylxanthine ring system since it has less steric bulk. Apparently the steric bulk conferred by the 1,3-diethyl substitution is better accommodated in the MAO-B active site than the MAO-A active site since the 1,3-diethyl-7-methyl-8-(phenoxymethyl)xanthines may still be considered moderately potent MAO-B inhibitors, while none of these homologues inhibited MAO-A.

4.3.6 **Comparison of the MAO-B inhibitory activities of the C3- and C4-substituted 8-(phenoxymethyl)caffeine analogues**

As mentioned above, in a previous study, a series of six 8-(phenoxymethyl)caffeine analogues containing C3 substituent were previously synthesized and evaluated as MAO inhibitors (Swanepoel, 2010). These are the 3-Cl, 3-Br, 3-F, 3-CF_3, 3-CH_3 and 3-OCH_3 substituted homologues. In the same study, a smaller series of three C4-substituted 8-(phenoxymethyl)caffeine analogues were also examined as MAO inhibitors (Swanepoel, 2010). These were the 4-Cl, 4-Br and 4-F substituted 8-(phenoxymethyl)caffeines. The present study adds 4 additional C4 substituted homologues to those that have been synthesized previously (Swanepoel, 2010). These are the 4-CH_3 (**11**), 4-OCH_3 (**12**) and 4-I (**13**) substituted homologues. With the expansion of the C4 substituted homologues, it may be useful to compare the MAO inhibitors potencies of the C3-substituted 8-(phenoxymethyl)caffeine analogues with those of the C4-substituted homologues. This analysis will be restricted to the inhibition potencies recorded for MAO-B since these

compounds were found to be only weak MAO-A inhibitors, with some compounds exhibiting no MAO-A inhibition.

Table 4.4: Comparison of the MAO-B inhibitory potencies of the C3-substituted 8-(phenoxymethyl)caffeine analogues with those of the C4-substituted homologues.

C4 Substituent:	IC_{50} Value (μM):	C3 Substituent:	IC_{50} Value (μM):
CH_3	0.543	CH_3	1.23
OCH_3	3.77	OCH_3	1.96
Cl	0.250	Cl	0.334
Br	0.189	Br	0.148
F	0.825	F	1.61

As shown in table 4.4, no clear trend is apparent, and potent MAO-B inhibitors exist among both the C3- and C4-substituted 8-(phenoxymethyl)caffeines. In some instances, C3-substitution yields more potent MAO-B inhibition, while in other instances C4-substitution is more optimal for MAO-B inhibition. For example, for the Cl, F and CH_3 substituted homologues C4-substitution yields compounds that are more potent MAO-B than the corresponding C3-substituted homologues. In contrast, the C4-substituted Br and OCH_3 8-(phenoxymethyl)caffeine homologues are weaker MAO-B inhibitors than the corresponding C3-substituted homologues. These results show that substitution of 8-(phenoxymethyl)caffeine at C3 and C4 yields potent MAO-B inhibitors, and that one position is not more optimal than the other.

Substituents which are electron withdrawing groups and relatively larger (such as Cl, Br and I) on the C4 position of 8-(phenoxymethyl)caffeine are most optimal for MAO-B inhibition. This result is in accordance with the previous data from Swanepoel (2010) which showed that electron withdrawing substituents at C3, with a high degree of lipophilicity, enhanced MAO-B inhibition potency.

4.3.7 **Conclusion**

In this chapter the 8-(phenoxymethyl)caffeine (series 1) and 1,3-diethyl-7-methyl-8-(phenoxymethyl)xanthine (series 2) analogues, which were synthesized in chapter 5, were evaluated as potential MAO-A and MAO-B inhibitors. This study adds 4 additional 8-(phenoxymethyl)caffeine to those that have been synthesized previously (Swanepoel, 2010): the 4-CH_3 (**11**), 4-OCH_3 (**12**), 4-I (**13**) and 3,4-diCH_3 (**14**) substituted homologues. In addition seven 1,3-diethyl-7-methyl-8-(phenoxymethyl)xanthine, compounds **15**–**22**, are also examined in this study. The potencies of the test compounds for the inhibition of the MAO enzymes were expressed as the IC_{50} values. For the purpose of this study, a fluorometric assay using Amplex Red was used to determine inhibition potencies. Although the compounds from both series 1 and 2 showed relatively weak or no inhibition towards MAO-A, many of the analogues were potent MAO-B inhibitors. This was especially true for series 1, the 8-(phenoxymethyl)caffeines, with the most potent MAO-B inhibitor among the newly synthesized compounds being 8-(4-iodophenoxymethyl)caffeine (**13**) with an IC_{50} of 0.458 µM. Among the 8-(phenoxymethyl)caffeine, the 4-CH_3 (**11**) and and 3,4-diCH_3 (**14**) substituted homologues also were potent MAO-B inhibitors with IC_{50} values of 0.54 µM and 0.62 µM. These inhibitors may be viewed as new potent MAO-B inhibitors. The results of the MAO inhibition studies with the 1,3-diethyl-7-methyl-8-(phenoxymethyl)xanthines (series 2), show that these compounds are are consistently weaker MAO-B inhibitors than the corresponding 8-(phenoxymethyl)caffeine analogues (series 1). These compounds did not exhibit inhibitory properties towards MAO-A. It may thus be concluded that the increased steric bulk provided by the 1,3-diethyl substitution pattern of the 1,3-diethyl-7-methylxanthine ring of series 2 is responsible for the weaker MAO-A and MAO-B inhibitory potencies of the 1,3-diethyl-7-methyl-8-(phenoxymethyl)xanthines (series 2) compared to the 8-(phenoxymethyl)caffeines (series 1). The 8-(phenoxymethyl)caffeines possess the 1,3-dimethyl substitution of the caffeine ring which is less bulky than the diethyl substitution pattern of the 1,3-diethyl-7-methylxanthine ring, and the caffeine ring is thus better tolerated in the MAO-A and MAO-B active sites. Interstingly, the addition of steric bulk via diethyl substitution result in a comparatively larger loss of MAO-A inhibition potency than MAO-B inhibition potency, and thus leads to an increase in selectivity for the MAO-B isoform.

The SARs of the inhibition of MAO-B by C4-substituted 8-(phenoxymethyl)caffeines yielded valuable insight into the structural requirements of this class of compounds to act as MAO-B inhibitors. Visual inspection of the MAO-B inhibitory data suggests that C4 substituents, which are electron withdrawing and relatively larger (such as Cl, Br and I) are most optimal for MAO-B inhibition by 8-(phenoxymethyl)caffeines.

CHAPTER 5

ADENOSINE A_{2A} RECEPTOR BINDING STUDIES

5.1 **Introduction**

Adenosine (Figure 5.1) is formed from the purine base adenine and a ribose moiety and is allied to phosphate groups to form ATP, which plays an integral part in the cellular energy system (Petzer *et al.,* 2009). As mentioned in the introduction, adenosine acts on four adenosine receptor subtypes namely A_1, A_{2A}, A_{2B} and A_3. All adenosine receptors are members of the G-protein-coupled receptor family and have 7 transmembrane domains. The adenosine A_{2A} receptor is enriched in the striatum and is currently an active area of interest for pharmaceutical research due to its potential therapeutic application in Parkinson's disease and other neurodegenerative disorders (Simola *et al.,* 2008). A_{2A} receptors are coupled mostly to GS proteins (Marala & Mustafa, 1993), thus mainly linked to adenyl cyclase activation. The ability of adenosine to stimulate adenyl cyclase, divides the A_2 receptors into two subtypes, namely A_{2A} with a high affinity for adenosine (0.1-1.0 µM), and A_{2B} receptors, with a lower affinity (> 10 µM). This sub-classification was strongly supported by the extensive characterisation of the binding properties of 1-(6-amino-9H-purin-9-yl)-1-deoxy-*N*-ethyl-*β*-D-ribofuronamide (NECA, Figure 5.1), a non-selective adenosine agonist (Bruns *et al.,* 1986). The foremost intracellular signalling pathways are through the formation of cyclic AMP, with A_1 and A_3 causing inhibition of adenyl cyclase, whereas A_{2A} and A_{2B} activate adenyl cyclase (Olah & Stiles, 2000; Fredholm *et al.,* 1999).

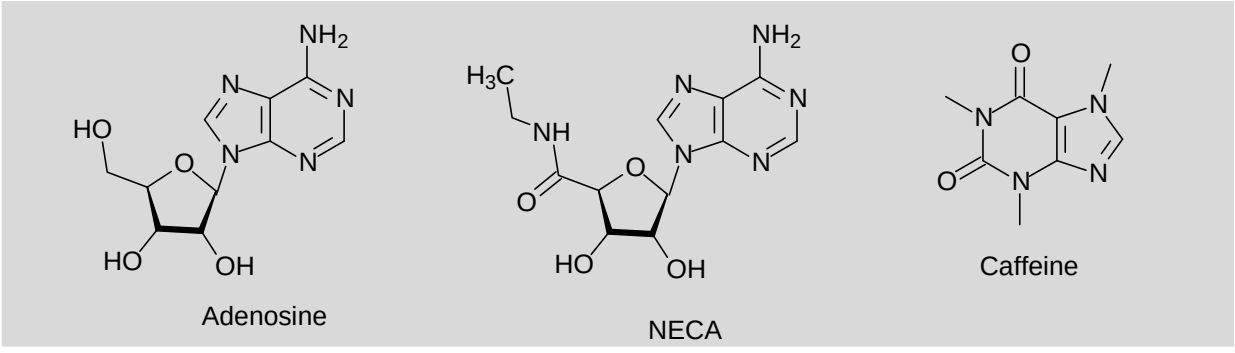

Figure 5.1: Molecular structures of adenosine, NECA and caffeine

Of the four subtypes of central adenosine receptors, the A_{2A} receptor has been linked most closely to dopaminergic neurotransmission and convincing evidence has accumulated that the A_{2A} receptor plays an important role in CNS controlled motor activity (Morelli *et al.,*

1994). This led to the identification of the A_{2A} receptor as a potential target for the development of drugs to treat motor deficits such as those encountered in PD (Ongini *et al.,* 2001). Moreover, A_{2A} binding sites are preserved in the striatum of humans diagnosed with PD (Martinez-Mir *et al.,* 1991) reaffirming the relevance of the A_{2A} receptor as a potential therapeutic target for this disease.

Activity of the adenosine A_1, A_{2A}, and A_{2B} receptor subtypes is inhibited by naturally occurring methylxanthines such as caffeine (Bruns *et al,* 1986) (Figure 5.1). Recent epidemiological studies suggest that coffee and tea consumers have a lower risk of PD (Hernan *et al.,* 2002), an effect that has been linked to the blockade of the adenosine A_{2A} receptor subtype by caffeine as the adenosine A_{2A} receptor controls locomotor behaviour and neurotransmitter release in BG (Ferrè *et al.,* 2008). In this chapter, the 8-(phenoxymethyl)caffeines (**1,8**–**14**) and 1,3-diethyl-7-methyl-8-(phenoxymethyl)xanthines (**15**–**22**) will be evaluated as potential antagonists of adenosine receptors. Since these analogues are caffeine derived structures, they may possess, similar to caffeine, affinities for A_{2A} receptors. In addition, substitution of caffeine and 1,3-diethyl-7-methylxanthine at C8 often yields structures with high potency antagonism of the A_{2A} receptor. Examples of such compounds are KW-6002 and CSC (Figure 5.2). This further suggests that the 8-(phenoxymethyl)caffeines and 1,3-diethyl-7-methyl-8-(phenoxymethyl)xanthines may bind to A_{2A} receptors.

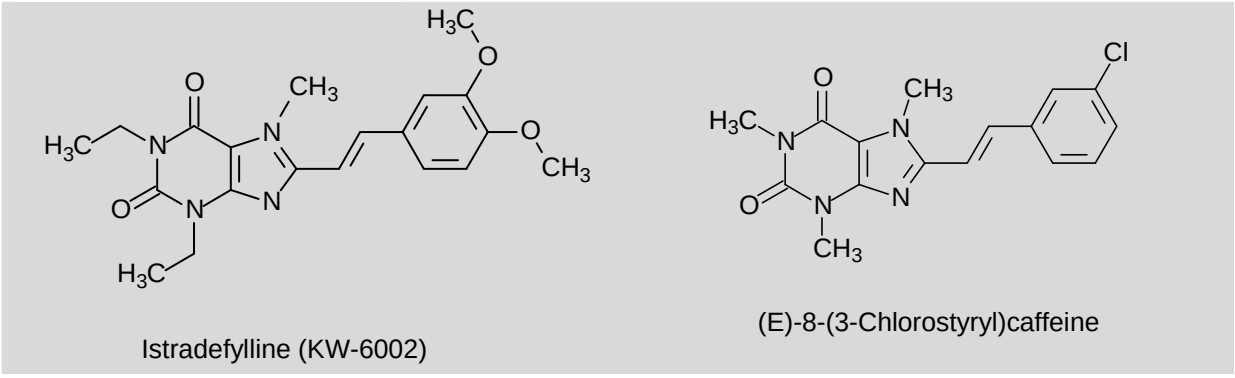

Figure 5.2: **Molecular structures of KW-6002 and CSC**

5.2 **Principles of the adenosine A_{2A} receptor binding assay**

The A_{2A} antagonistic properties of the compounds will be examined by the radioligand binding protocol described in the literature (Bruns *et al.,* 1986). Binding of the compounds to the A_{2A} receptors will be investigated by measuring the displacement of N-[^{3}H]ethyladenosine-5'-uronamide ([^{3}H]NECA) from rat striatal membranes. These studies will be carried out in the presence of N^6-cyclopentyladenosine (CPA) to minimize the binding of [^{3}H]NECA to adenosine A_1 receptors. In the study conducted by Bruns *et al.* (1986), they demonstrated that CPA can be utilized to selectively eliminate the A_1 component of [^{3}H]NECA binding to rat striatal membranes, without the use of covalent protein-modifying reagents. [^{3}H]NECA binding in the presence of 50 nM CPA has the characteristic of a selective A_{2A} adenosine receptor agonist with high affinity (Bruns *et al.,* 1986). A concentration of 50 nM CPA was therefore selected to eliminate A_1 binding. According to Bruns *et al.* (1986), a concentration of 50 nM CPA will occupy 98% of A_1 receptors while sparing 93% of A_2 receptors (Bruns *et al.,* 1986). In addition to 50 nM CPA, the standard A_{2A} binding assay contained 10 mM $MgCl_2$. This concentration of $MgCl_2$ increases A_{2A} binding and also decreases nonspecific binding (Bruns *et al.,* 1986).

5.3 **Experimental Procedure**

The structures of the 8-(phenoxymethyl)caffeine analogues and 1,3-diethyl-7-methyl-8-(phenoxymethyl)xanthine analogues that will be investigated as potential A_{2A} receptor antagonists are given in Table 5.1. In order to facilitate comparison of the the potencies of A_{2A} antagonism of the 8-(phenoxymethyl)caffeine analogues with the 1,3-diethyl-7-methyl-8-(phenoxymethyl)xanthine analogues, the compounds that were selected for this study contained identical substituents and substitution patterns on the phenoxy phenyl ring. The compounds in both series of 8-(phenoxymethyl)caffeine analogues and 1,3-diethyl-7-methyl-8-(phenoxymethyl)xanthine analogues contained H, Cl, Br, F, OCH_3, CH_3 at C4 of the phenyl ring or a 3,4-di-CH_3 on the phenoxy phenyl ring.

As positive controls the following known A_{2A} antagonists were included in this study:

- KW-6002
- CSC
- ZM 241385

Table 5.1: Compounds that were evaluated as potential A_{2A} receptor antagonists in this study.

SERIES 1:			SERIES 2:		
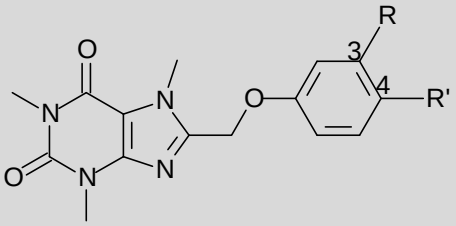			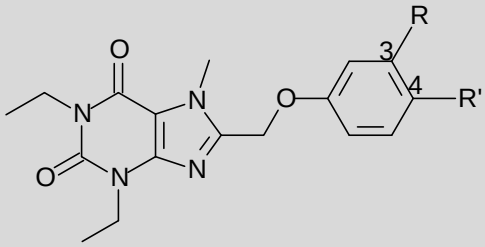		
Compound:	**R:**	**R':**	**Compound:**	**R:**	**R':**
1*	H	H	**15#**	H	H
8*	H	Cl	**16**	H	Cl
9*	H	Br	**17**	H	Br
10*	H	F	**18**	H	F
11	H	CH_3	**19**	H	CH_3
12	H	OCH_3	**20**	H	OCH_3
13	H	I	**21**	H	I
14	CH_3	CH_3	**22**	CH_3	CH_3

***Compounds 1, 8-10 were previously synthesized by Swanepoel, 2010**

#Compound 15 previously synthesized by Van Der Walt, 2012

5.3.1 **Materials and Instrumentation**

The following reagents were obtained from Sigma-Aldrich: anhydrous magnesium chloride ($MgCl_2$), silicone solution (Sigma-cote), adenosine deaminase, CPA and [^{3}H]NECA. Tris hydrochloride, Tris base, DMSO, scintillation vials, filtercount scintillation fluid and Whatman GF/B filters (25 mm diameter) were provided by Merck.

5.3.2 **Tissue Preparations**

The evaluation of the test compounds as potential A_{2A} receptor antagonists was carried out according to Bruns *et al.* (1986). Approval for the collection of rat brain striata was obtained from the North-West University's Research Ethics Committee (**NWU-0035-10-A5**). Male Sprague Dawley rats (obtained from the Animal Research Centre of the North West University, Potchefstroom Campus) weighing between 200 and 500 g were dissected to obtain the striata. After dissection, the striata were immediately frozen with a mixture of acetone and dry ice and stored at –70 ℃. Ten volumes of cold 50 mM Tris buffer (pH 7.7, 25 ℃) was added to the striata, and the resulting mixture was disrupted for 30 seconds with a Polytron PT-10 homogeniser (Brinkman). The suspension was centrifuged at 50 000 g for 10 minutes. Afterwards, the supernatant was discarded and the remaining pellet was again resuspended in 10 volumes of cold Tris buffer and the resulting mixture was disrupted for 30

seconds. The suspension was centrifuged for 10 minutes at 50 000 g. Cold Tris buffer was added to resuspend the pellet at 1 g/5 ml of the original striatal weight. Finally the suspension was placed in vials and stored at –70 ℃. When needed the tissue was thawed at room temperature, and kept on ice until use.

5.3.3 **Preparation of stock solutions and buffers**

A sufficient quantity of Tris buffer was prepared the day before the assay was carried out. The Tris buffer solution was obtained by adding the Tris hydrochloride solution (1000 ml of a 50 mM solution) to the Tris base solution (250 ml of a 50 mM solution). This yielded a buffer with pH 7.7.

CPA was also prepared beforehand in dimethylsulfoxide (DMSO) to yield a 10 mM solution. This solution was stored at –20 ºC. When needed the solution was left to thaw at room temperature.

The test compounds were dissolved the day before the assay in 1 ml of DMSO to yield a 10 mM solution.

The [^{3}H]NECA stock solution was prepared to a concentration of 40 nM solution in Tris buffer. The [^{3}H]NECA solution was prepared on the day of the experiment and stored on ice until needed.

All reaction tubes and pipette tips were coated with sigma-cote beforehand to prevent the test antagonists and radioligand from adhering to the sides of the tubes and tips.

5.3.4 **Binding affinity assay**

On the day of the assay, the inhibitor (10 mM) and CPA (10 mM) stock solutions were thawed and vortexed. CPA was diluted to a concentration of 500 nM with Tris buffer. The Tris buffer and final CPA solution were kept on ice throughout the experiment. For the preparation of the membrane working mixture, 40 ml of Tris buffer was deposited into a conical tube and $MgCl_2$ (48.21 mg) was added to yield a final concentration of 12.66 mM $MgCl_2$. Adenosine deaminase and 1.27 ml of the prepared striatal membrane was also added to yield concentrations of adenosine deaminase of 0.1 unit/0.79 ml and striatal membranes of 10 mg/0.79 ml. The membrane working mixture was kept on ice until needed. Incubations were carried in duplicate. The test compound (10 µl) was added first, followed by 790 µl of the membrane working mixture, 100 µl of the 500 nM CPA solution and 100 µl

of the 40 nM [^{3}H]NECA solution (Figure 5.3, **a**). When the membrane working mixture and CPA are added to the test antagonist, the antagonist binds to the A_{2A} receptor and the CPA binds to the A_1 receptor **(b)**, respectively. As already mentioned, CPA is used in the assay to eliminate A_1 receptor binding. When the [^{3}H]NECA is added **(c)** one of two scenarios may occur: either the test compound has a low affinity (weak antagonist) towards the A_{2A} receptor and the [^{3}H]NECA will displace it from the receptor **(d)**, or the test compound will have a high affinity (potent antagonist) towards the A_{2A} receptor and the [^{3}H]NECA will not be able to displace the test antagonist to a large degree **(e)**. To determine the degree of non-specific binding of [^{3}H]NECA to other membrane constituents, incubations were carried out in triplicate, and contained 10 µl of the 10 mM CPA solution, 790 µl membrane working mixture, 100 µl of the 500 nM CPA solution and 100 µl of the 40 nM [^{3}H]NECA solution.

After all the additions were done the incubations were vortexed and incubated for 60 minutes at 25 ℃ in a shaking water bath. After 30 minutes of incubation, the incubations were vortexed again.

The compounds were filtrated through Whatman GF/B filters (25 mm diameter) under vacuum. Each tube was filtered as follow: the filters were soaked in the Tris buffer and then fitted onto a Hoffeler vacuum system. The contents of each tube were poured onto the filter and the reaction tube was rinsed twice with 4 ml of Tris buffer. The filter was finally washed with 4 ml of Tris buffer. The damp filters were put into scintillation vials and 4 ml of scintillation fluid were added and the vials were incubated overnight. The radioactivity retained on the filters was counted with a Packard Tri-CARB 2100 TR scintillation counter.

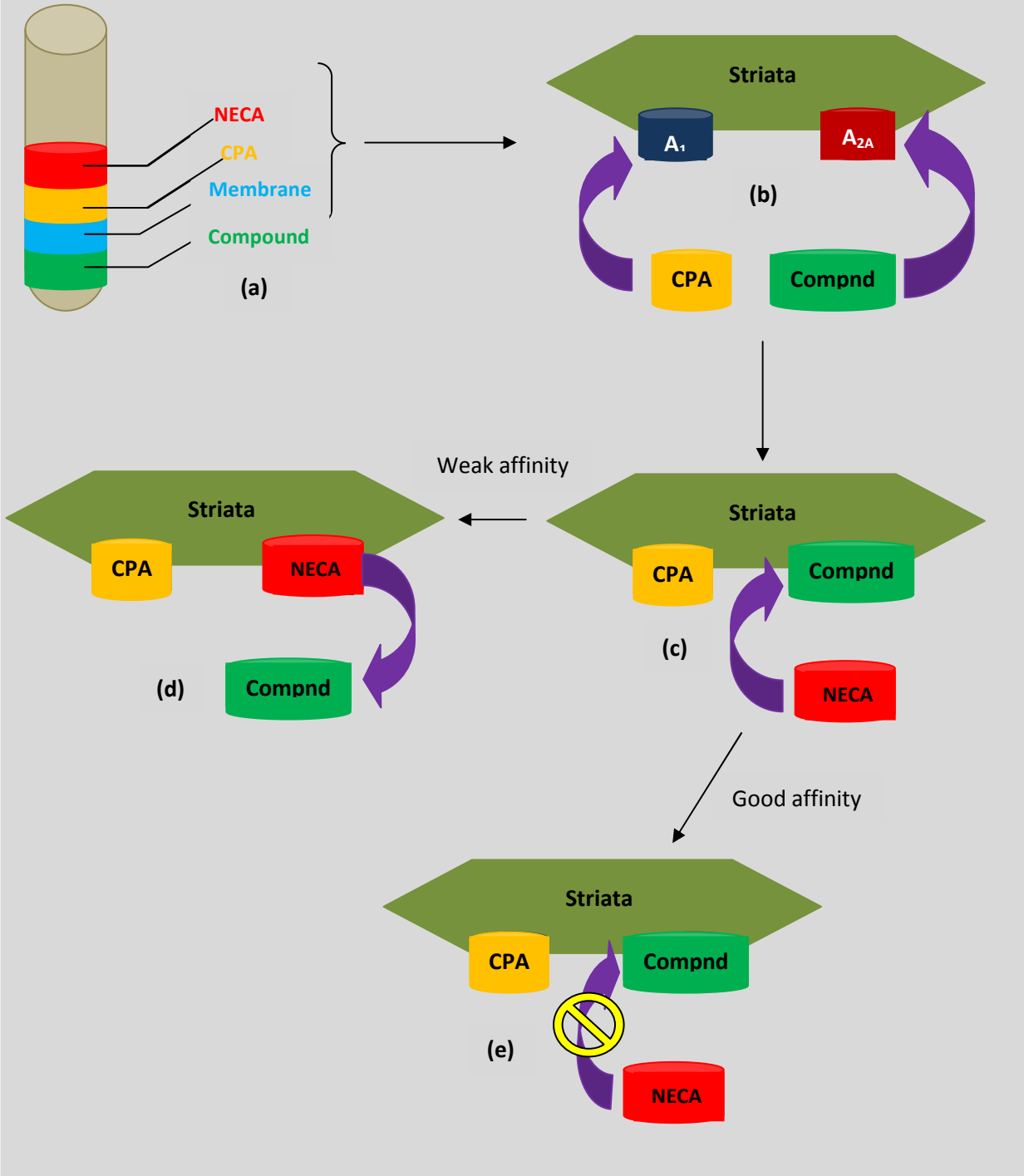

Figure 5.3: **Graphical representation of the A_{2A} receptor binding assay**

5.3.5 IC_{50} and K_i Determinations

The IC_{50} values were determined by plotting the count values versus the logarithm of the inhibitor concentration to obtain a sigmoidal dose-response curve. These kinetic data were fitted to the one site competition model incorporated into the Prism software package (GraphPad Software Inc.) to obtain IC_{50} values (Equation 5.1). Using the Cheng and Prusoff

equation (Cheng & Prusoff, 1973), the K_i values for the competitive inhibition of [^{3}H]NECA (K_d = 8.5 nM, Müller *et al.,* 1993) binding by the test compounds were calculated from the IC_{50} values. All incubations were carried out in duplicate and the IC_{50} values and K_i values were expressed as mean ± standard error of the mean (SEM). An estimate of the nonspecific binding was obtained from binding studies in the presence of an excess of CPA (1 mM).

$$Y = Bottom \times \frac{Top - Bottom}{1 + 10^{x - log IC_{50}}}$$

Equation 5.1: **On a sigmoid curve the X-axis is equal to the logarithm of the concentration of the test antagonist, and the Y-axis is equal to the count values. The count values were adjusted by contribution of non-specific binding of [^{3}H]NECA to adenosine A_1 receptors. "Top" represents the top part of the sigmoid curve and "Bottom" the bottom part of the sigmoid curve.**

The IC_{50} values can be converted to K_i values, the antagonist-receptor dissociation constant, by using the known dissociation constant (K_D) value of [^{3}H]NECA, the known concentration of the radio labelled ligand in the incubations and applying the Cheng-Prusoff equation with (Equation 5.2).

$$K_i = \frac{IC_{50}}{1 + \frac{[radioligand]}{K_D}}$$

Equation 5.2: **Cheng-Prusoff equation (Cheng, 2001) to calculate the K_i from the IC_{50} value**

5.3.6 **Results**

One of the objectives of the current study was to identify compounds that can act as both potential A_{2A} receptor antagonists and MAO-B inhibitors. Such compounds may serve as potential leads for the treatment of PD. The compounds that were successfully synthesized in Chapter 3 as well as compounds synthesized in previous studies (Swanepoel, 2010; Van der Walt, 2012) were examined for potential A_{2A} receptor antagonists (Table 5.2). As positive controls the known A_{2A} antagonists, KW-6002, CSC and ZM 241385, were included in this study. As shown in Table 5.2, KW-6002, CSC and ZM 241385 displayed K_i values for the affinity of A_{2A} receptors of 7.94 nM, 26.2 nM and 2.31 nM, respectively. These values correspond well with the literature values of 2.2 nM (Shimada *et al.,* 1997), 36–54 nM (Jacobson *et al.,* 1993; Müller *et al.,* 1997) and 2 nM (Muller & Ferre, 2007) for these antagonists, respectively.

The results document that the 8-(phenoxymethyl)caffeine analogues and 1,3-diethyl-7-methyl-8-(phenoxymethyl)xanthine analogues have affinity for the A_{2A} receptor with K_i values ranging from 0.923 to 7.544 µM. These potencies are significantly lower than those recorded for the reference A_{2A} antagonists, KW-6002, CSC and ZM 241385. The most potent potential A_{2A} anatagonist among the test compounds is compound **16** with a K_i value of 0.923 µM. Shown in Figure 5.4 is the sigmoidal dose-response curve from which the K_i value of this compound was calculated. This compound has a 34.7–400-fold weaker affinity for the A_{2A} receptor than KW-6002, CSC and ZM 241385. Based on this, it may thus be concluded that the 8-(phenoxymethyl)caffeine analogues and 1,3-diethyl-7-methyl-8-(phenoxymethyl)xanthine analogues are not potential potent A_{2A} antagonists. Since the highly potent reference A_{2A} antagonists, CSC and KW-6002 contain the caffeine and 1,3-diethyl-7-methylxanthine ring systems, respectively, which are also present in the 8-(phenoxymethyl)caffeine analogues and 1,3-diethyl-7-methyl-8-(phenoxymethyl)xanthine analogues, it may be concluded that the phenoxymethyl side chain of the test compounds is not optimal for A_{2A} antagonism. In contrast, the styryl moiety, as found in CSC and KW-6002, is a suitable C8 side chain for designing highly potent caffeine derived A_{2A} antagonists.

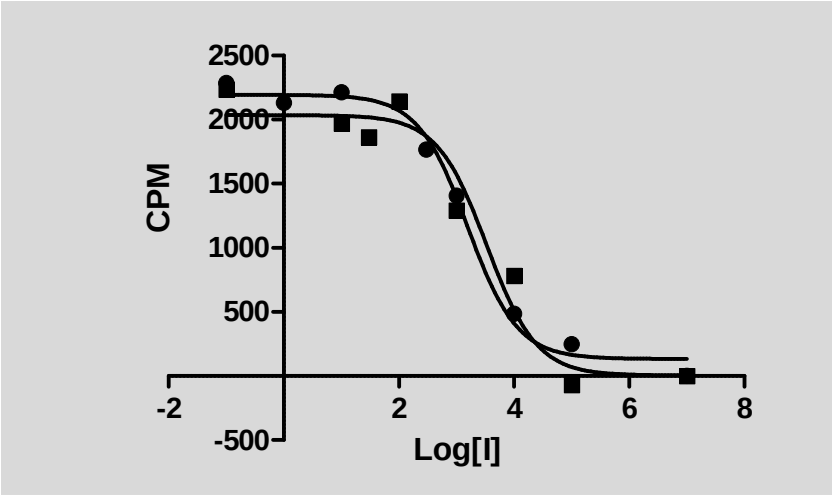

Figure 5.4: **Competitive binding of compound 16 and the radio labelled ligand to adenosine A_{2A} receptors. The sigmoidal dose-response curve represents the antagonism of [^{3}H]NECA binding to rat striatal A_{2A} receptors by antagonist 16 (expressed in µM). The IC_{50} value was determined by fitting the data, using nonlinear least-squares regression analysis, to the one site competition model incorporated into the Prism software package (GraphPad Software Inc.). The K_i value of 0.923 µM for the competitive inhibition with [^{3}H]NECA (K_D= 8.5 nM) (Müller *et al.,* 1993) binding was calculated with the Cheng-Prusoff equation (Cheng & Prusoff, 1973).**

Even though the 8-(phenoxymethyl)caffeines and 1,3-diethyl-7-methyl-8-(phenoxymethyl)xanthines have relatively weak affinities for the A_{2A} receptor, the results shown in Table 5.2 may still be of interest. With the exception of the 4-Br and 4-CH_3 substituted homologues, the 1,3-diethyl-7-methyl-8-(phenoxymethyl)xanthines proved to

have consistently more potent A_{2A} affinity than the 8-(phenoxymethyl)caffeines. For example the Cl, Br, OCH_3 and di-CH_3 substituted homologues of series 2 had a 1.3-4-fold more potent A_{2A} affinity than the corresponding homologues in series 1. The iodine substituted 1,3-diethyl-7-methyl-8-(phenoxymethyl)xanthenes antagonized A_{2A} receptors with a K_i value of 1.928 µM, while the iodine substituted 8-(phenoxymethyl)caffeine does not have affinity for A_{2A} receptors, even at a maximal tested concentration of 100 µM. It may therefore be concluded that 1,3-diethyl-7-methyl-8-(phenoxymethyl)xanthines have a more potent A_{2A} affinity than 8-(phenoxymethyl)caffeines, and that the 1,3-diethyl-7-methylxanthine ring system is more appropriate for A_{2A} affinity than the caffeine ring system.

The order of the potencies of A_{2A} affinity among the 8-(phenoxymethyl)caffeines is di-CH_3 > F > CH_3 > Cl > Br > OCH_3 > I. The order of the potencies of A_{2A} affinity among the 1,3-diethyl-7-methyl-8-(phenoxymethyl)xanthines is Cl > F > di-CH_3 > OCH_3 > I > CH_3 > Br. This analysis shows that the Cl, F and di-CH_3 substituents are the most optimal for A_{2A} antagonism among both the 8-(phenoxymethyl)caffeines and 1,3-diethyl-7-methyl-8-(phenoxymethyl)xanthines.

Interestingly, the unsubstituted homologues among both the 8-(phenoxymethyl)caffeines and 1,3-diethyl-7-methyl-8-(phenoxymethyl)xanthines did not have affinity for the A_{2A} receptors, even up to a maximal tested concentration of 100 µM. This result shows that substituents of the phenoxy ring of series 1 and series 2 are required for A_{2A} affinity. It should, however, be noted that not all substituents are suitable for enhancing the potencies of A_{2A} receptor affinity of 8-(phenoxymethyl)caffeines and 1,3-diethyl-7-methyl-8-(phenoxymethyl)xanthines. As outlined above, the Cl, F and di-CH_3 substituents are the most optimal for A_{2A} affinity.

Table 5.2: The K_i values for the competitive inhibition of [^{3}H]NECA binding to rat striatal adenosine A_{2A} receptors by 8-(phenoxymethyl)caffeines and 1,3-diethyl-7-methyl-8-(phenoxymethyl)xanthines.

Series 1: 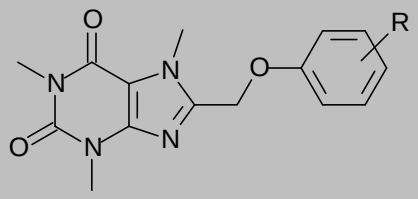			***Series 2:*** 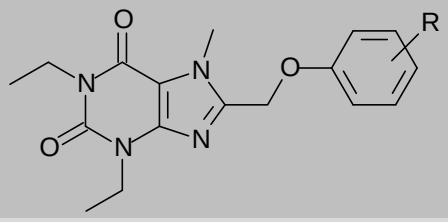			
	R:	**K_i value (µM):**		**R:**	**K_i value (µM):**	**Ratio[d]:**
1*	H	-	**15#**	H	-	-
8*	4-Cl	2.517 ± 2.101	**16**	4-Cl	0.923 ± 0.253	2.727
9*	4-Br	3.442 ± 1.402	**17**	4-Br	5.569 ± 4.450	0.618
10*	4-F	2.339 ± 1.164	**18**	4-F	1.679 ± 0.865	1.393
11	4-CH_3	2.457 ± 1.841	**19**	4-CH_3	4.579 ± 2.308	0.537
12	4-OCH_3	7.544 ± 0.199	**20**	4-OCH_3	1.807 ± 0.713	4.175
13	4-I	-	**21**	4-I	1.928 ± 2.071	-
14	3,4-CH_3	2.252 ± 0.024	**22**	3,4-CH_3	1.710 ± 1.879	1.317

KW-6002:	**CSC:**	**ZM 241385:**
K_i value (nM): 7.94 ± 1.13 (2.2[a])	K_i value (nM): 26.2 ± 5.40 (36-54[b])	K_i value (nM): 2.31 ± 0.80 (2[c])

***Compounds 1, 8-10 synthesized by Swanepoel, 2010**

 # Compound 15 synthesized by Van der Walt, 2012

-Compound has no affinity

[a] Value obtained from Shimada *et al.,* 1997; [b] Müller *et al.,* 1997; [c] Müller and Ferre, 2006

[d] Ratio: [K_i(series1)/K_i(series 2)]

5.3.7 **Conclusion**

The 8-(phenoxymethyl)caffeines and 1,3-diethyl-7-methyl-8-(phenoxymethyl)xanthines synthesized in chapter 3 were evaluated as potential adenosine A_{2A} antagonists by using a radioligand binding assay with [^{3}H]NECA as radioligand. In addition, the potencies of A_{2A} antagonism by three reference A_{2A} antagonists, KW-6002, CSC and ZM 241385, were also recorded. The results showed that, compared to the reference compounds, the potencies of A_{2A} affinity of the test compounds are significantly lower. For example the compound with the most potent A_{2A} affinity among the test compounds, Compound **16** (K_i = 0.923 µM) is 34.7-400-fold weaker than KW-6002, CSC and ZM 241385 A_{2A} affinities. In spite of the relatively

low A_{2A} affinity of the 8-(phenoxymethyl)caffeines and 1,3-diethyl-7-methyl-8-(phenoxymethyl)xanthines interesting SARs were apparent:

- The phenoxymethyl side chain of the test compounds is not optimal for A_{2A} affinity. In contrast, the styryl moiety, as found in CSC and KW-6002, is a more suitable C8 side chain for designing highly potent caffeine derived compounds with A_{2A} affinity.
- In general, 1,3-diethyl-7-methyl-8-(phenoxymethyl)xanthines have a more potent A_{2A} affinity than 8-(phenoxymethyl)caffeines. The 1,3-diethyl-7-methylxanthine ring system is therefore more appropriate for A_{2A} affinity than the caffeine ring system.
- Cl, F, CH_3 and di-CH_3 substituents on the phenoxy ring are the most optimal for affinity on the A_{2A} receptor for both the 8-(phenoxymethyl)caffeines and 1,3-diethyl-7-methyl-8-(phenoxymethyl)xanthines.

CHAPTER 6:

SUMMARY

In this study eleven 8-(phenoxymethyl)caffeine and 1,3-diethyl-7-methyl-8 (phenoxymethyl)xanthine analogues were successfully synthesized and evaluated as inhibitors of MAO and antagonists of the adenosine A_{2A} receptor. MAO-A is responsible for the oxidation of 5-HT and NA, while MAO-B is the major DA metabolizing enzyme in the brain. MAO-A inhibitors are frequently used to treat depressive illness and inhibitors of the MAO-B enzyme are used in the treatment of neurodegenerative diseases such as PD. MAO-B inhibitors also possess neuroprotective properties in PD by reducing the formation of neurotoxic by-products such as hydrogen peroxide, ammonia, and aldehydes that are associated with the oxidation of DA (Vindis *et al.,* 2000). Adenosine is a neuromodulator that coordinates responses to DA and other neurotransmitters in areas of the brain and is a promising target in the pharmaceutical industry because of its potential to treat PD and other neurodegenerative disorders (Muller *et al.,* 1998). Evidence has suggested that A_{2A} antagonists may also slow the course of PD by protecting against the underlying neurodegenerative processes (Chen *et al.,* 2001).

This study attempted to identify dual-target directed compounds that simultaneously inhibit MAO-B and antagonise the A_{2A} receptor. For this purpose 8-(4-phenoxymethyl)caffeine was used as lead. Caffeine (Figure 6.1) and the consumption of caffeinated coffee have been shown to reduce the risk of developing PD in men (Ross *et al.,* 2000) and women who have not taken postmenopausal estrogens (Ascherio *et al.,* 2003). Caffeine is, however, a weak inhibitor of MAO-B (Chen *et al.,* 2001) and a moderately potent adenosine A_{2A} antagonist (Müller *et al.,* 1997). With substitution on the C8 position of the caffeine ring caffeine's affinity for A_{2A} receptors and MAO-B greatly increases (Petzer *et al.,* 2003). An example of this behaviour is found with CSC (Figure 6.1), a well known A_{2A} antagonist and also a potent reversible MAO-B inhibitor.

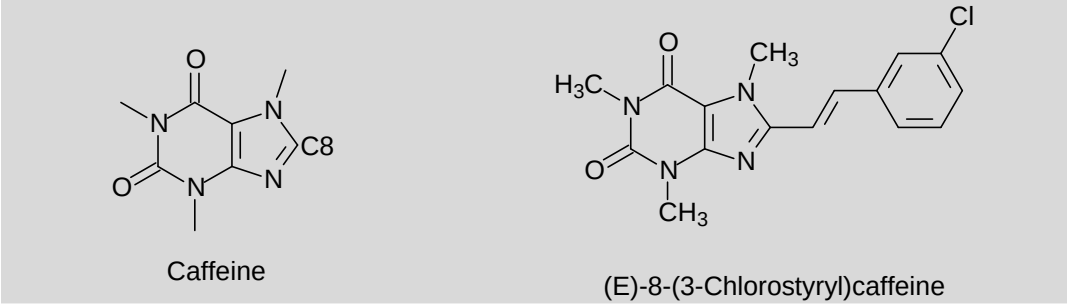

Figure 6.1: **Molecular structures of caffeine and CSC**

In PD, a dual mechanism compound that inhibits MAO-B and antagonizes adenosine A_{2A} receptors may offer a novel therapeutic approach to prevent neuronal cell death as well as provide symptomatic relief (Figure 6.2) (Youdim, 2010). The 8-(phenoxymethyl)caffeine and 1,3-diethyl-7-methyl-8-(phenoxymethyl)xanthine analogues examined in this study may act as such compounds and may thus offer symptomatic relief and also slow the progression of PD.

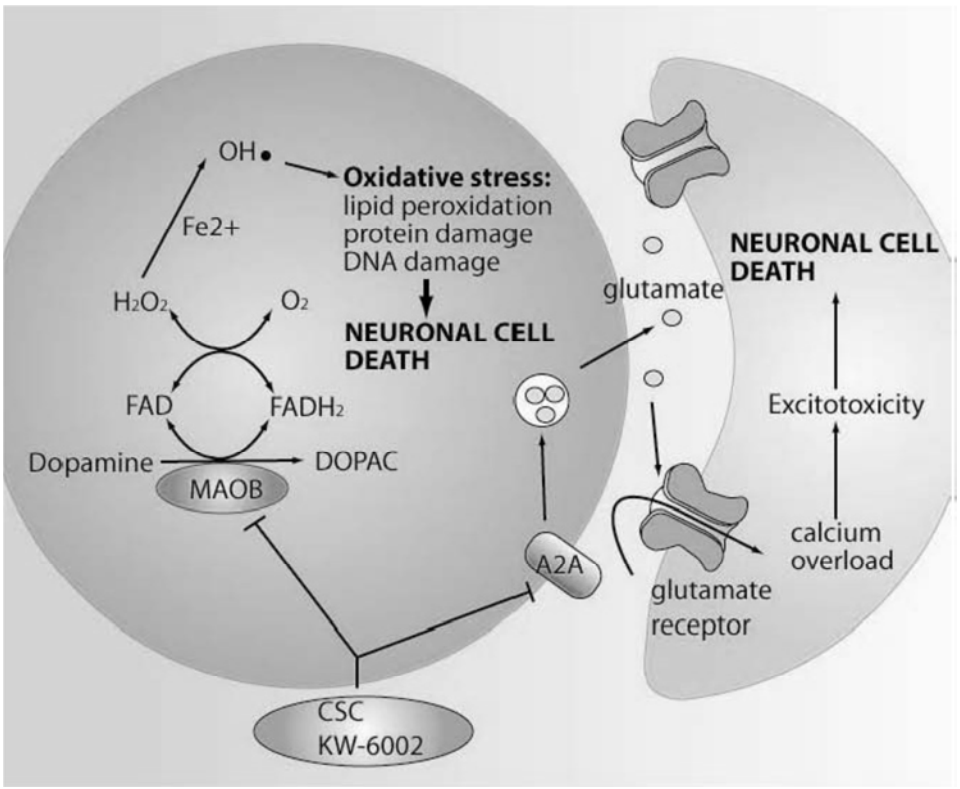

Figure 6.2: **Mechanism of dual targeted MAO-B/A_{2A} compounds such as CSC and KW-6002 (Youdim, 2010)**

Literature reports that substitution on C8 of the caffeine ring with a variety of groups yields compounds with more potent MAO-B inhibition activities than caffeine (Petzer *et al.,* 2009). In particular, a styryl side-chain in the *trans* geometry at C8 enhances MAO-B inhibition activity and A_{2A} antagonism (Shiozaki *et al.,* 1999). Saturation of this bond has a negative effect on MAO-B inhibition activity (Petzer *et al.,* 2003). Ethyl substitution on position 1 and 3 of the xanthine ring also reduces MAO-B inhibition potency compared to methyl substitution at these positions (Pretorius *et al.,* 2008). Unfortunately the requirement of 1,3-dimethyl substitution for MAO-B inhibition limits the design for a dual target directed drugs because 1,3-diethyl substitution leads to increased A_{2A} antagonism (Pretorius *et al.,* 2008; Müller *et al.,* 1997). An example of this behaviour is found with the potent A_{2A} antagonist KW-6002, which is a relative weak MAO-B inhibitor (Petzer *et al.,* 2003). Methylation on N7 of the xanthine ring enhances both MAO-B inhibition and A_{2A} antagonism (Petzer *et al.,* 2009).

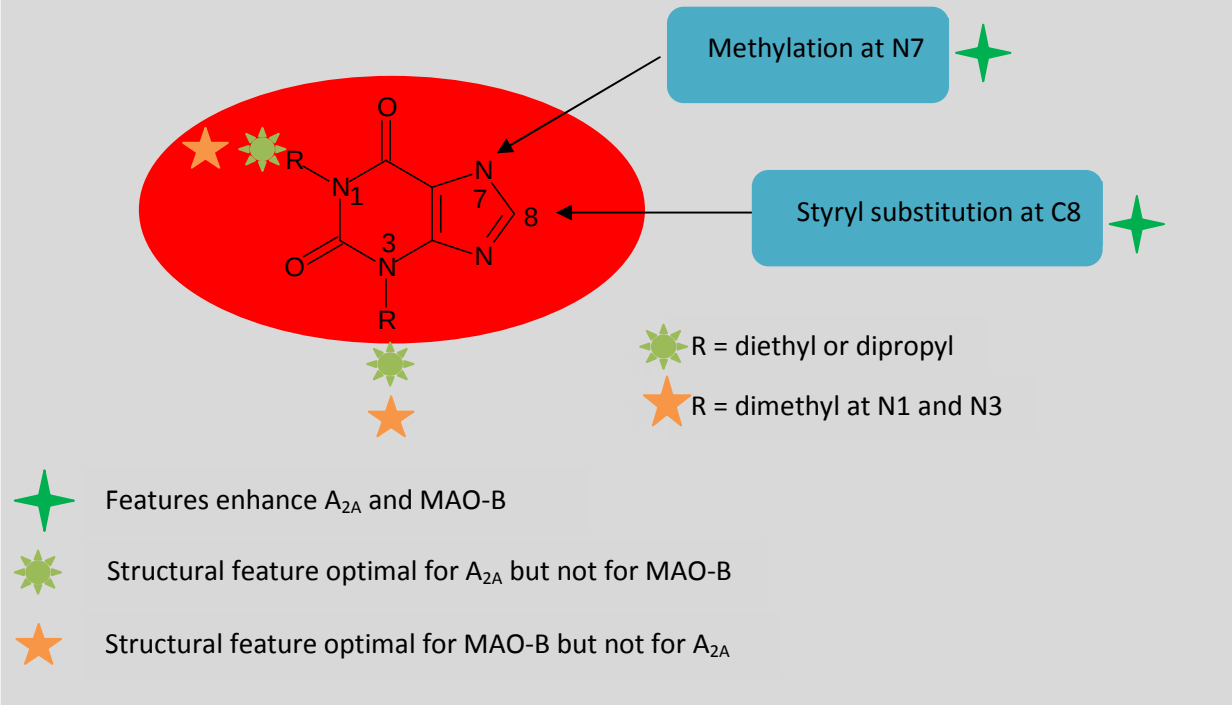

Figure 6.3: **Structural requirements for antagonizing A_{2A} receptors and inhibiting MAO-B. Ethyl groups at N1 and N3 are optimal for A_{2A} antagonism while methyl groups at positions N1 and N3 are optimal for MAO-B inhibition (adapted from Azam *et al.*, 2012).**

Chemistry: The synthesis of the target compounds was achieved by reacting 1,3-dimethyl- or 1,3-diethyl-5,6-diaminouracil with an appropriate substituted phenoxyacetic acid in the presence of EDAC. Those phenoxyacetic acids which were not commercially available were successfully prepared from the corresponding phenols. The structures of the target inhibitors

were verified by NMR and MS analysis. Both the ^{1}H-NMR and ^{13}C-NMR spectra corresponded with the proposed structures and the expected exact masses were also recorded for each compound. HPLC analysis revealed a single predominant peak for all the compounds analyzed, which indicates a high degree of purity for each compound.

MAO Inhibitory properties: The *in vitro* measurement of the MAO inhibitory properties of the caffeine analogues was done using a fluorometric assay with Amplex Red. This technique measures the amount of hydrogen peroxide that is formed in the catalytic cycle of MAO-A and MAO-B (Zhou & Panchuk-Voloshina, 1997). The reversibility of MAO inhibition by the test compounds was not evaluated as, in a previous study (Swanepoel, 2010) with the 8-(phenoxymethyl)caffeine analogues, it was found that this class of compounds are indeed reversible inhibitors of MAO-B. Since the compounds examined in this study are structurally related to the compounds of the previous study, it may be assumed that the 8-(4-phenoxymethyl)caffeine analogues of this study are also reversible inhibitors of MAO-B.

Adenosine A_{2A} affinities: The A_{2A} affinities of the caffeine analogues were measured by a radioactive ligand binding assay (Bruns *et al.,* 1986).

Table 6.1 provides the IC_{50} values for the inhibition of MAO-B and K_i values for the affinity of A_{2A} receptors of the 8-(phenoxymethyl)caffeine and 1,3-diethyl-7-methyl-8-(phenoxymethyl)xanthine analogues examined in this study. Also given for comparison are the corresponding values for CSC.

Table 6.1: IC_{50} values for the inhibition of MAO-B and K_i values for the antagonism of A_{2A} receptors of the 8-(phenoxymethyl)caffeine and 1,3-diethyl-7-methyl-8-(phenoxymethyl)xanthene analogues.

Series 1:

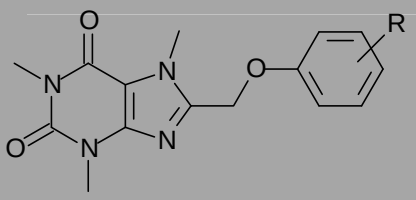

Series 2:

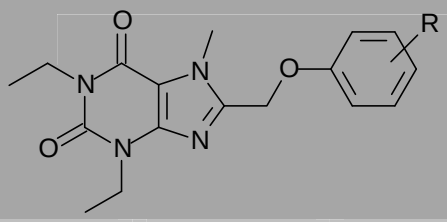

No	R	MAO-B IC_{50} value (µM):	A_{2A} K_i value (µM):	No	R	MAO-B IC_{50} value (µM):	A_{2A} K_i value (µM):
1*	H	5.78	None	15#	H	20.60	None
8*	4-Cl	0.250	2.517	16	4-Cl	3.12	0.923
9*	4-Br	0.189	3.442	17	4-Br	4.07	5.569
10*	4-F	0.825	2.339	18	4-F	8.05	1.679
11	4-CH_3	0.54	2.457	19	4-CH_3	4.54	4.579
12	4-OCH_3	3.77	7.544	20	4-OCH_3	23.59	1.807
13	4-I	0.458	None	21	4-I	4.28	1.928
14	3,4-diCH_3	0.62	2.252	22	3,4-diCH_3	2.23	1.710

CSC:

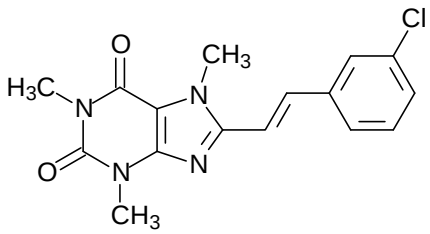

(E)-8-(3-Chlorostyryl)caffeine

A_{2A} K_i value (µM): 0.030

MAO-B IC_{50} value (µM): 0.146

***Compounds 1, 8, 9 and 10 synthesized by Swanepoel, 2010**

 # Compound 15 synthesized by Van der Walt, 2012

The values highlighted in green indicate the most potent MAO-B inhibitor and potential A_{2A} antagonist in series 1, the 8-(phenoxymethyl)caffeines. The values highlighted in yellow indicate the most potent MAO-B inhibitor and potential A_{2A} antagonist in series 2, the 1,3-diethyl-7-methyl-8-(phenoxymethyl)xanthines.

As shown in the table, compound **9**, 8-[4-bromophenoxymethyl]caffeine, is the most potent MAO-B inhibitor with an IC_{50} of 0.189 µM. This compound exhibits a K_i of 3.442 µM for A_{2A} receptor affinity. Compared to CSC, which has values of 0.146 µM for the inhibition of MAO-B and 0.030 µM for A_{2A} receptor affinity, the MAO-B inhibition potency of **9** is almost equipotent to that of CSC, but CSC has 115-fold higher affinity for A_{2A} receptors. The loss of

affinity of **9** towards the A_{2A} receptor can be attributed to the lack of a styryl functional group at C8 of the caffeine ring as well as lack of 1,3-dimethyl substitution. This finding correlates with literature.

Compound **14**, 8-[3,4-dimethylphenoxymethyl]caffeine, displayed the most potent A_{2A} affinity among the compounds of series 1 with a K_i value of 2.252 µM. This compound also was a potent MAO-B inhibitor with an IC_{50} of 0.62 µM. Compared to CSC, compound **14** is 5-fold less potent as a MAO-B inhibitor, and has a 75-fold less affinity for the A_{2A} receptor. As with all the compounds of series 1, the loss of affinity towards the A_{2A} receptor can be attributed to the lack of a styryl moiety at C8 of the caffeine ring as well as lack of 1,3-dimethyl substitution.

In Series 2, compound **16**, 1,3-diethyl-7-methyl-8-(4-chlorophenoxymethyl)xanthine, proved to have the most potent A_{2A} affinity of the compounds examined with a K_i value of 0.923 µM. This compound was a moderately potent MAO-B inhibitor with an IC_{50} of 3.12 µM. Comparing these values to those of CSC, compound **16** has an A_{2A} affinity that is 31-fold less potent and 21-fold less potent as a MAO-B inhibitor. Loss in MAO-B inhibition can be attributed to the 1,3-diethyl substitution pattern. The improvement of A_{2A} affinity may, at least in part, be attributed to the 1,3-diethyl substitution pattern, which is reported to be beneficial for A_{2A} antagonism.

Compound **22**, 1,3-diethyl-7-methyl-8-(3,4-dimethylphenoxymethyl)xanthine, was found to be the most potent MAO-B inhibitor of series 2 with an IC_{50} of 2.23 µM. Compound **22** is therefore 16-fold less potent than CSC (IC_{50} = 0.146 µM) as a MAO-B inhibitor. Compound **22** exhibits a K_i value of 1.710 µM for A_{2A} receptor affinity. Compound **22** is therefore 57-fold less potent than CSC (K_i = 0.030 µM). The relatively low A_{2A} receptor affinity can be attributed to the phenoxymethyl substitution at C8 (instead of styryl substitution) and the relatively weak MAO-B inhibitory potency may be due to 1,3-diethyl substitution on N1 and N3.

Final conclusion: From the above comparisons it may be concluded that none of the structures examined in this study are highly potent dual target directed compounds that inhibit MAO-B and have affinity for the A_{2A} receptors. This is for the most part due to the finding that the 8-(phenoxymethyl)caffeine and 1,3-diethyl-7-methyl-8-(phenoxymethyl)xanthine analogues examined in this study doesn't possess high affinity for the A_{2A} receptor. Some compounds, particularly from series 1, are, however potent MAO-B inhibitors. These compounds therefore still have application in the treatment of PD since MAO-B inhibitors are considered as both symptomatic and neuroprotective treatment of PD.

BIBLIOGRAPHY:

Abbracchio, M. P., Fogliatto, G., Paoletti, A. M., Rovati, G. E., Cattabeni, F. 1992. Prolonged in vitro exposure of rat brain slices to adenosine analogues: selective desensitization of adenosine A1 but not A2 receptors. *European journal of pharmacology,* 227:317– 324.

Agnati, L. F., Ferré, S., Lluis, C., Franco, R., Fuxe, K. 2003. Molecular mechanisms and therapeutical implications of intramembrane receptor/receptor interactions among heptahelical receptors with examples from the striatopallidal GABA neurons. *Pharmacological reviews,* 55:509-50.

Alam, Z.I., Jenner, A., Daniel, S. E., Lees, A.J., Cairns, N., Marsden, C. D., Jenner, P., Halliwell, B. 1997. Oxidative DNA damage in the parkinsonian brain: an apparent selective increase in 8-hydroxyguanine levels in substantia nigra. *Journal of neurochemistry,* 69:1196–1203.

Allain, H., Bentue-Ferrer, D., Akwa. Y. 2008. Disease-modifying drugs and Parkinson's disease. *Programmed neurobiology,* 84: 25-*39.*

Aoyama, S., Koga, K., Mori, A., Miyaji, H., Sekine, S., Kase, H., Uchimura, T., Kobayashi, H., Kuwana, Y. 2002. Distribution of adenosine A_{2A} receptor antagonist KW-6002 and its effects on gene expression in the rat brain. *Brain research,* 953:119-25.

Ascherio, A., Zhang, S. M., Hernan, M. A., Kawachi, I., Colditz, G. A., Speizer, F. E., Willett, W. C. 2001. Prospective study of caffeine consumption and risk of Parkinson's disease in men and women. *Annual neurology,* 50:56–63.

Ascherio, A., Chen, H., Schwarzschild, M. A., Zhang, S. M., Colditz, G. A., Speizer, F. E. 2003. Caffeine, postmenopausal estrogen, and risk of Parkinson's disease. *Neurology,* 60*:* 790-795.

Azam, F., Madi, A. M., Ali, H. I. 2012. Molecular docking and prediction of pharmacokinetic properties of dual mechanism drugs that block MAO-B and adenosine A_{2A} receptors for the treatment of PD. *Journal of young pharmacists,* 4:184-192.

Bara-Jimenez, W., Sherzai, A., Dimitrova, T., Favit, A., Bibbiani, F., Gillespie, M., Morris, M.J., Mouradian, M.M., Chase, T.N. 2003. Adenosine A_{2A} receptor antagonist treatment of Parkinson's disease*. Neurology,* 6:293–296.

Barnham, K. J., Masters, C. L., Bush, A. I. 2004. Neurodegenerative diseases and oxidative stress. *Nature reviews,* 3: 205.

Bibbiani, F., Oh, J.D., Petzer, J.P., Castagnoli, N., Chen, J.F., Schwarzschild, M.A., Chase, T.N. 2003. A_{2A} antagonist prevents DA agonist induced motor complications in animal models of Parkinson's disease. *Experimental neurology,* 184: 285–294.

Binda, C., Newton-Vinson, P., Hubalek, F., Edmondson, D. E., Mattevi, A. 2002. Structure of human monoamine oxidase B, a drug target for the treatment of neurological disorders. *Nature structural biology,* 9:22–26.

Binda, C., Wang, J., Pisani, L., Caccia, C., Carotti, A., Salvatti, P. 2007. Structures of human monoamine oxidase B complexes with selective noncovalent inhibitors: safinamide and coumarin analogues. *Journal of medicinal chemistry,* 50:5848-5852.

Birkmayer, W., Riederer, P, Youdim, M. B. H. Linauer, W. 1975. The potentiation of anti-akinetic effect after L-dopa treatment by an inhibitor of MAO-B, deprenyl. *Journal of neural transmission,* 36:303–326.

Blum, D., Hourez, R., Galas, M. C., Popoli, P., Schiffmann, S. N. 2003. Adenosine receptors and Huntington's disease: implications for pathogenesis and therapeutics. *Lancet neurology, 2:*366-74.

Bonnet, U. 2003. Moclobemide: therapeutic use and clinical studies. *CNS drug reviews,* 9: 97–140.

Bortolato, M., Chen, K., Shih, J. C. 2008. Monoamine oxidase inactivation: From pathophysiology to therapeutics. *Advanced drug delivery reviews, 60:*1527-1533.

Bovè, J., Prou, D., Perier, C., Przedborski, S. 2005. Toxin-induced models of Parkinson's disease. *NeuroRx. The journal of the American society for experimental neuro therapeutics,* 2:484-494.

Bower, J. H., Maraganore, D. M., McDonnel, S. D. K., Rocca, W. A. 1999. Incedence and distribution of parkinsonism in Olsmed County, Minnesota, 1976-1990. *Neurology,* 52: 1214-1220.

Brown, C. S., Kent, T. A., Bryant, S. G., Gevedon, R. M., Campbell, J. L., Felthous, A. R., Barratt, E. S., Rose, R. M. 1989. Blood platelet uptake of serotonin in episodic aggression. *Psychiatry research,* 27:5–12.

Bruns, R. F., Lu, G. H., Pugsley, T. A. 1986. Characterization of the A_{2A} adenosine receptor labeled by ^{3}[H]NECA in rat striatal membranes. *Molecular pharmacology,* 29:331-346.

Cantuti-Castelvetri, I., Lin, M. T., Zheng, K., Keller-McGandy, C. E., Betensky, R. A., Johns, D. R., Beal, M. F., Standaert, D. G., Simon, D. K. 2005. Somatic mitochondrial DNA mutations in single neurons and glia. *Neurobiology and aging,* 26:1343–1355.

Chen, J. F., Moratalla, R., Impagnatiello, F., Grandy, D. K., Cuellar, B., Rubinstein, M., Beilstein, M. A., Hackett, E., Fink, J. S., Low, M. J., Ongni, E., Schwarzschild, M. A. 2001. The role of the D_2 DA receptor (D_2R) in A_{2A} adenosine receptor ($A_{2A}R$)-mediated behavioral and cellular responses as revealed by A_{2A} and D_2 receptor knockout mice. *Proceedings of the national academy of sciences of the United States of America,* 98:1970–1975.

Chen, J.-F., Steyn, S., Staal, R., Petzer, J. P., Xu, K., Van der Schyf, C. J., Castagnoli, K., Sonsalla, P. K., Castagnoli Jr., N., Schwarzschild, M. A. 2002. 8-(3-Chlorostyryl)caffeine may attenuate MPTP neurotoxicity through dual actions of monoamine oxidase inhibition and A_{2A} receptor antagonism. *Journal of biological chemistry,* 277:36040–36044.

Chen, J. J., Swope, D. M. 2005. Clinical pharmacology of rasagiline: a novel, second-generation propargylamine for the treatment of Parkinson disease. *Journal of clinical pharmacology,* 45:878–94.

Cheng, Y., Prusoff, W. 1973. Relationship between the inhibition constant (K_i) and the concentration of inhibitor which causes 50 per cent inhibition IC_{50} of an enzymatic reaction. *Biochemical pharmacology,* 22:3099-3108.

Cheng, H. C. 2001 The power issue: determination of K_b or K_i from IC_{50} A closer look at the Cheng-Prusoff equation, the Schild plot and other related power equations. *Journal of pharmacological and toxicological methods,* 46:61-71.

Chiba, K., Trevor, A. J., Castagnoli, Jr. N. 1984. Metabolism of the neurotoxic tertiary amine, MPTP, by brain monoamine oxidase. *Biochemical and biophysical research communications,* 120:574-578.

Ciruela, F., Casado, V., Rodrigues, R. J., Lujan, R., Burgueno, J., Canals, M., Borycz, J., Rebola, N., Goldberg, S. R., Mallol, J., Cortes, A., Canela, E. I., Lopez-Gimenez, J. F., Milligan, G., Lluis, C., Cunha, R. A., Ferre, S., Franco, R. 2006. Presynaptic control of striatal glutamatergic neurotransmission by adenosine A_1–A_{2A} receptor heteromers. *Journal of neuroscience,* 26:2080–2087.

Cohen, G. 2000. Oxidative stress, mitochondrial respiration and Parkinson's disease. *Annals of the New York academy of sciences,* 8999:112-120.

Cohen, G., Farooqui, R., Kesler, N. 1997. Parkinson's disease: a new link between monoamine oxidase and mitochondrial electron flow. *Proceedings of the national academy of sciences of the United States of America,* 94: 4890– 4894.

Cohen, G., Spina, M. B. 1989. Deprenyl suppresses the oxidant stress associated with increased dopamine turnover. *Annals of neurology,* 26:689–90.

Collins, G.G.S., Sandler, M., Williams, E.D., Youdim, M.B.H. 1970. Multiple forms of human brain mitochondrial monoamine oxidase. *Nature,* 225:817-820.

Cortès, X., Soriano, J. B., Sanchez-Ramos, J. L., Azofra, J., Almar, E., Ramos, J. 1998. European study of asthma. Prevalence of atopy in young adults of 5 years in Spain. Spanish Group of European Asthma Study. *Medicina clinica,* 111: 573-577.

Cunha, R. A., Johansson, B., van der Ploeg, I., Sebastiao, A. M., Ribeiro, J. A., Fredholm, B. B. 1994. Evidence for functionally important adenosine A_{2A} receptors in the rat hippocampus. *Brain research,* 649:208– 216.

Daly, J. W., Butts-Lamb, P., Padgett, W. 1983. Subclasses of adenosine receptors in the central nervous system: interaction with caffeine and related methylxanthines. *Cellular and molecular neurobiology*, 3:69– 80.

Dauer, W., Przedborski, S. 2003. Parkinson's Disease: Mechanisms and Models. *Neuron,* 39: 889-909.

Day, M., Wang, Z., Ding, J., An, X., Ingham, C. A., Shering, A. F. Wokosin, D., Ilijic, E., Sun, Z., Sampson, A. R., Mugnaini, E., Deutch, A. Y., Sesack, S. R., Arbuthnoff, G. W., Surwmeier, D. J. 2006. Selective elimination of glutaminergic synapses on striatopallidal neurons in Parkinson's disease models. *Nature neuroscience,* 9*:*251-259.

De Colibus, L., Li, M., Binda, C., Edmonson, D. E., Mattevi, A. 2005. Three dimensional structure of human monoamine oxidase A (MAO-A): relation to the structures of rat MAO-A and human MAO-B. *Proceedings of the national academy of sciences of the United States of America,* 102:12684-12689.

Dexter, D. T., Sian, J., Rose, S., Hindmarsh, J. G., Mann, V. M., Cooper, J.M., Wells, F. R., Daniel, S. E., Lees, A. J., Schapira, A. H., *et al.,* 1994. Indices of oxidative stress and mitochondrial function in individuals with incidental Lewy body disease. *Annals of neurolology,* 35:38–44.

Dexter, D. T., Wells, F. R., Lees, A. J., Agid, F., Agid, Y., Jenner, P., Marsden, C. D. 1989. Increased nigral iron content and alterations in other metal ions occurring in brain in Parkinson's disease. *Journal of neurochemistry,* 52:1830–1836.

Dick, F. D., De Palma, G., Ahmadi, A. Scott, N. W., Prescott, G. J., Bennett, J., Semple, S., Dick, S., Counsell, C., Mozzoni, P., Haites, N., Wettinger, S. B., Mutti, A., Otelea, M., Seaton, A., Söderkvist, P., Felice, A. 2007. Environmental risk factors for Parkinson's disease and parkinsonism: the Geoparkinson study. *Occupational and environmental medicine,* 64: 666–72.

Dunwiddie, T. V., Masino, S. A. 2001. The role and regulation of adenosine in the central nervous system. *Annual review of neuroscience,* 24:31–55.

Edmonson, D. E., Binda, C., Mattevi, A. 2007. Structural insights into the mechanism of amine oxidation by monoamine oxidases A and B. *Archives of biochemistry and biophysics,* 464:269-276.

Erickson, R. H., Hiner, R. N., Feeney, S. W. Blake, P. R., Rzeszotarski, W. J., Hicks, R. P., Costello, D. G., Abreu, M. E. 1991. 1,3,8-Trisubstituted xanthines. Effects of substitution pattern upon adenosine receptor A_1/A_2 affinity. *Journal of medicinal chemistry,* 34:1431-35.

Fearnley, J., Lees, A. 1994. Pathology of Parkinson's disease. In *Neurodegenerative Diseases.* (Calne, D. B., ed.) Saunders, Philadelphia. Treatment of central nervous system degenerative disorders. Chapter 20. Goodman & Gilman's The Pharmacological Basis of Therapeutics. Brunton, Lazo, Parker. 2010. McGraw-Hill pp.545-554.

Feigin, A. 2003. NonDArgic symptomatic therapies for Parkinson's disease: turn on or turn off? *Neurology,* 61: 286–287.

Ferrè, S., Baler, R., Bouvier, M., Caron, M. G., Devi, L. A., Durroux, T., Fuxe, K., George, S. R., Javitch J. A., Lohse, M. J. Mackie, K., Milligan, G., Pfleger, K. D. G., Pin, J. P., Volkow, N. D., Waldhoer, M., Woods, A. S., Franco, R. 2009. Building a new conceptual framework for receptor heteromers. *Nature chemical biology,* 5:131-134.

Ferrè, S., Fredholm, B. B., Morelli, M., Popoli, P., Fuxe, K. 1997. Adenosine-dopamine receptor–receptor interactions as an integrative mechanism in the basal ganglia. *Trends in neuroscience,* 20:482–487.

Ferrè, S., Fuxe, K. 1992. Dopamine denervation leads to an increase in the intramembrane interaction between adenosine A_2 and dopamine D_2 receptors in the neostriatum. *Brain research,* 594:124–130.

Ferrè, S., O'Connor, W. T., Fuxe, K., Ungerstedt, U. 1993. The striopallidal neuron: a main locus for adenosine–DA interactions in the brain. *Journal of neuroscience,* 13:5402–5406.

Ferrè, S., von Euler, G., Johansson, B., Fredholm, B. B., Fuxe, K. 1991. Stimulation of high-affinity adenosine A_2 receptors decreases the affinity of DA D_2 receptors in rat striatal membranes. *Proceedings of the national academy of sciences of the United States of America,* 88:7238– 7241.

Ferrè S., Quiroz, C., Woods, A. S., Cunha, R., Popoli, P., Ciruela, F., Lluis, C., Franco, R., Azdad, K., Schiffmann, S. N. 2008. An update on adenosine A_{2A}–DA D_2 receptor interactions: implications for the function of G protein-coupled receptors. *Current pharmaceutical design,* 14:1468-1474.

Finberg, J. P., Wang, J., Bankiewicz, K., Harvey-White, J., Kopin, I. J., Goldsteen, D. S. 1998. Increased striatal dopamine production from L-dopa following selective inhibition of monoamine oxidase B by R(+)-*N*-propargyl-1-aminoindan (rasagiline) in the monkey. *Journal of neural transmission,* 52:279-285.

Fink, J.S., Weaver, D.R., Rivkees, S.A., Peterfreund, R.A., Pollack, A., Adler, E.M., Reppert, S.M. 1992. Molecular cloning of the rat A_2 adenosine receptor: selective co-expression with D_2 dopamine receptors in rat striatum. *Molecular brain research,* 14: 186–195.

Forno, L. S. 1996. Neuropathology of Parkinson's disease. *Journal of neuropathology experimental neurology,* 55:259-272.

Fowler, J. S., Logan, J., Wang, G.-J., Volkow, N. D. 2003. Monoamine oxidase and cigarette smoking. *Neurotoxicology,* 24: 75– 82.

Fredholm, B.B., Battig, K., Holmen, J., Nehlig, A., Zvartau, E.E. 1999. Actions of caffeine in the brain with special reference to factors that contribute to its widespread use. *Pharmacological reviews,* 51:83–133.

Fredholm, B. B., Ap, I. J., Jacobson, K. A., Klotz, K. N., Linden, J. 2001. International Union of Pharmacology XXV. Nomenclature and classification of adenosine receptors. *Pharmacological reviews*, 53: 527-552.

Fuxe, K., Ferrè S., Genedani, S., Franco, R., Agnati, L. F. 2007. Adenosine receptor–dopamine receptor interactions in the basal ganglia and their relevance for brain function. *Physiology & behaviour,* 92:210-217.

Gerfen, C. R. 2004. Basal Ganglia. (*In:* Paxinos G Ed., The Rat Nervous System. Amsterdam: *Elsevier Academic Press* p.445-508).

Giasson, B. I., Duda, J. E., Murray, I. V., Chen, Q., Souza, J. M., Hurtig, H. I., Ischiropoulos, H., Trojanowski, J. Q., Lee, V. M. 2000. Oxidative damage linked to neuroprotection by selective α-synuclein nitration in synucleinopathy lesions. *Science,* 290*:* 985-989.

Gibb. W. R. Neuropathology of Parkinson's disease and related syndromes. 1992. *Neurologic clinics,* 10:361-376.

Goggi, J., Theofilopoulos, S., Riaz, S. S., Jauniaux, E., Stern, G. M., Bradford, H. F. 2000. The neuronal survival effects of rasagiline and deprenyl on fetal human and rat ventral mesencephalic neurons in culture. *Neuro report,* 11:3937–41.

Graybiel, A. M., Aosaki, T., Flaherty, A. W., Kimura, M. 1994. The basal ganglia and adaptive motor control. *Science,* 265:1826–1831.

Hastings, T. G., Lewis, D. A., Zigmond, M. J. 1996. Reactive dopamine metabolites and neurotoxicity: implications for Parkinson's disease. *Advances in experimental medicine and biology,* 387:97–106.

Hauptmann, N., Grimsby, J., Shih, J. C., Cadenas, E. 1996. The metabolism of tyramine by monoamine oxidase A/B causes oxidative damage to mitochondrial DNA. *Archives of biochemistry and biophysics,* 335: 295–304.

Healy, D. G., Falchi, M., O-Sullivan, S. S., Bonifati, V., Durr, A., Bressman, S., Brice, A., Aasly, J., Zabetian, C. P., Goldwurm, S., Ferreire, J. J., Tolosa, E., Kay, D. M., Klein, C., Williams, D. R., Marras, C., Lanaq, A. E., Wszolek, Z. K., Berciano, J., Schapira, A. H., Lynch, T., Bhatia, K. P., Gasser, T., Lees, A. J., Wood, N. W., International Consortium. 2008. Phenotype, genotype, and worldwide genetic penetrance of LRRK2-associated Parkinson's disease: a case-control study. *Lancet neurology,* 7:583–90.

Hernán, M. A., Takkouche, B., Caamaño-Isorna, F., Gestal-Otero, J. J. 2002. A meta-analysis of coffee drinking, cigarette smoking, and the risk of Parkinson's disease. *Annals of neurology,* 52: 276-284.

Herraiz, T., Chaparro, C. 2005. Human monoamine oxidase enzyme inhibition by coffee and β-carbolines norharman and harman isolated from coffee. *Life sciences,* 78:795-802.

Hillion, J., Canals, M., Torvinen, M., Casado, V., Scott, R., Terasmaa, A., Hansson, A, Watson, S., Olah, M. E., Canela, E. I., Zoli, M., Agnati, L. F., Ibanez, C. F., Lluis, C., Franco, R., Ferre, S., Fuxe, K. 2002. Coaggregation, cointernalization, and codesensitization of adenosine A_{2A} receptors and dopamine D_2 receptors. *Journal of biological chemistry,* 277:18091-97.

Holt, A, Sharman, D., Baker, G., Palcic, M. 1997. A continuous spectophotometric assay for monoamine oxidase and related enzymes in tissue homogenates. *Analytical biochemistry,* 244:384-392.

Hornykiewcz, O., Kish, S. J. 1987. Biochemical patophysiology of Parkinson's disease. (*In:* Parkinson's Disease, Yahr, M., Bergmann, *eds.* New York: Raven Press. pp. 19-34).

Hubalek, F., Binda, C., Khalil, A., Li, M., Mattevi, A., Castagnoli, N., Edmondson, D.E. 2005. Demonstration of isoleucine 199 as a structural determinant for the selective inhibition of human monoamine oxidase B by specific reversible inhibitors. *Journal of biological chemistry,* 16:15761-15766.

Ikeda, K., Kurokawa, M., Aoyama, S., Kuwana, Y. 2002. Neuroprotection by adenosine A_{2A} receptor blockade in experimental models of Parkinson's disease. *Journal of neurochemistry,* 80:262–270.

Jaakola, V. P., Griffith, M. T., Hanson, M. A., Cherezov, V., Chien, E. Y., Lane, J. R., Ijzerman, A. P., Stevens, R. C. 2008. The 2.6 angstrom crystal structure of a human A_{2A} adenosine receptor bound to an antagonist. *Science,* 322: 1211-1217.

Jacobson, K. A., Gallo-Rodriguez, C., Melman, N. Fischer, B., Maillard, M., van Bergen, A., van Gralen, P. J., Karton, Y. 1993. Structureactivity relationships of 8-styrylxanthines as A_2-selective adenosine antagonists. *Journal of medicinal chemistry,* 36:1333-42.

Jahung, J. W., Houpt, T. A., Wessel, T. C., Chen, K., Shih, J. C. 1997. Localization of monoamine oxidase A and B mRNA in the rat brain by in situ hybridization. S*ynapse,* 25:30–36.

Jalkanen, S., Salmi, M. 2001. Cell surface monoamine oxidases: enzymes in search of function. *The EMBO journal,* 20:3893-3901.

Jenner, P. 2003. A_{2A} antagonists as novel non-dopaminergic therapy for motor dysfunction in PD. *Neurology,* 61: S32–S38.

Jenner, P., Mori, A., Hauser, R., Morelli, M., Fredholm, B. B., Chen, J. F. 2009. Adenosine, adenosine A_{2A} atagonists, and Parkinson's disease. *Parkinsonism and related disorders* 15:406-413.

Kalgutkar, A. S., Dalvie, D. K., Castagnoli Jr., N., Taylor, T. J. 2001. Interactions of nitrogen-containing xenobiotics with monoamine oxidase (MAO) isozymes A and B: SAR studies on MAO substrates and inhibitors. *Chemical research in toxicology,* 14:1139– 1162.

Kamiya, T., Saitoh, O., Yoshioka, K., Nakata, H. 2003. Oligomerization of adenosine A_{2A} and dopamine D_2 receptors in living cells. *Biochemical and biophysical research communications,* 306:544– 549.

Kase, H., Mori, A., Jenner, P. 2004. Progress in the persuit of therapeutic A_{2A} antagonists *Drug discovery today,* 1:51.

Katzenschlager, R., Cardozo, A., AvilaCobo, M. R., Tolosa, E., Lees, A. J. 2003. Unclassifiable parkinsonism in two European tertiary referral centres of movement disorders. *Movement disorders,* 18: 1123-1131.

Katzenschlager, R., Head, J., Schraq, A., Ben-Shlomo, Y., Evans, A., Lees, A. J. 2008. Comparing three initial treatments in Parkinson's disease. *Neurology,* 71: 474-480.

Kearney, E. B., Salach, J. I., Walker, W. H., Seng, R. L., Kenney, W., Zeszotek, E., and Singer, T. P. 1971. The covalently bound flavin of hepativ monoamine oxidase. 1. Isolation and sequence of flavin peptide and evidence for binding at the 8alpha position. *European journal of biochemistry,* 24:321–327.

Klaase, K. C., Ijzerman, A. P., Grip, W. J., Beukers, M. 2008. Internalization and desensitization of adenosine receptors *Purinergic signaling,* 4:21-28.

Klinman, J .P. and Mu, D. 1994. Quinoenzymes in biology. *Annual review of biochemistry,* 63: 299-344.

Knoll, J. 2000. (−)Deprenyl (selegiline): past, present and future. *Neurobiology,* 8:179–199.

Kumar, M. J., Nicholls, D. G., Andersen, J. K. 2003. Oxidative alpha-ketoglutarate dehydrogenase inhibition via subtle elevations in monoamine oxidase B levels results in loss of spare respiratory capacity: implications for Parinson's disease. *Journal of biological chemistry,* 278: 46432–46439.

Kurokawa, M., Koga, K., Kase, H., Nakamura, J., Kuwana, Y. 1996. Adenosine A_{2A} receptor-mediated modulation of striatal acetylcholine release in vivo. *Journal of neurochemistry,* 66:1882-1888.

Kupsch, A., Sautter, J., Gotz, M. E., Breithaupt, W., Schwarz, J., Youdim, M. B. H., Riederer, P., Gerlach, M., Oertel, W. H. 2001. Monoamine oxidase inhibition and MPTP-induced neurotoxicity in the non-human primate: comparison of rasagiline (TVP1012) with selegiline. *Journal of Neural Transmission* 108:985–1009.

Lachowicz, J., Zhai, Y., Kwee, L. 2006. Pharmacological profile of SCH 412348 and SCH 420814, selective A_{2A} adenosine receptor antagonists. Targeting Adenosine A_{2A} Receptors in Parkinson's Disease and Other CNS Disorders. Boston, USA.

Langston, J. W., Irwin, I., Langston, E. B., Forno, L. S. 1984. 1-Methyl-4- phenyl-pyridinium ion (MPP+): identification of metabolite of MPTP, a toxin selective to the substantia nigra. *Neuroscience letters,* 48: 87– 92.

Lees, A.J., Hardy, J. and Revesz, T. 2009. Parkinson's disease. *Lancet,* 373:2055-2066.

LeWitt , P. A., Segel, S. A., Mistura, K. L., Schork, M. A. 1993. Symptomatic anti-parkinsonian effects of monoamine oxidase-B inhibition: comparison of selegiline and lazabemide. *Clinical neuropharmacology,* 16:332–337.

LeWitt, P. A., Taylor, D. C. 2008. Protection against Parkinson's Disease Progression: Clinical Experience. *Neurotherapeutics*, 5: 210-225.

Liou, H. H., Tsai, M. C., Chen, C. J., Jeng, J. S., Chang, Y. C., Chen, S. Y. 1997. Environmental risk factors in Parkinson's disease: a case-control study in Taiwan. *Neurology,* 48: 1583-1588.

Lundblad, M., Vaudano, E., Cenci, M. A. 2003. Cellular and behavioural effects of the adenosine A_{2A} receptor antagonist KW-6002 in a rat model of l-DOPA-induced dyskinesia. *Journal of neurochemistry,* 6: 1398-1410.

Lyles, G. A. 1996. Mammalian plasma and tissue-bound semicarbazide sensitive amine oxidases: biochemical, pharmacological and toxicological aspects*. International journal of biochemistry: cellular biology,* 28: 259-274.

Marala, R. B., Mustafa, S. J. 1993. Direct evidence for the coupling of A2-adenosine receptor to stimulatory guanine nucleotide-binding-protein in bovine brain striatum. *The journal of pharmacology and experimental pharmaceutics,* 266:29-300.

Martinez-Mir, M. I., Probst, A., Palacios, J. M. 1991. Adenosine A_2 receptors selective localization in the human basal ganglia and alterations with disease. *Neuroscience,* 42: 697-706.

Maruyama, W., Yamamoto, T., Kitani, K., Carrillo, M. C., Youdim, M. B. H., Naoi, M. 2000. Mechanism underlying anti-apoptotic activity of a (-)deprenyl related propargylamine, rasagiline. *Mechanisms of ageing,* 116:181–91.

Matsubayashi, K. Fukuyama, H., Akiquchi, I., Kameyama, M., Imai, H., Maeda, T. 1986. Localization of monoamine oxidase (MAO) in the rat peripheral nervous system — existence of MAO-containing unmyelinated axons. *Brain research,* 368:30–35.

Meyerson, L., McMurtrey, K., Davis, V. 1978. A rapid and sensitive potentiometric assay for monoamine oxidase using a ammonia-selective electrode. *Analytical biochemistry,* 86*:* 287-297.

Monopoli, A., Lozza, G., Forlani, A., Mattavelli, A., Ongini, E. 1998. Blockade of adenosine A_{2A} receptors by SCH 58261 results in neuroprotective effects in cerebral ischaemia in rats. *Neuro report,* 9:3955–3959.

Morelli, M., Fenu, S., Pinna, A., Di Chiara, G. 1994. Adenosine A_2 receptors interact negatively with dopamine D_1 and D_2 receptors in unilaterally 6-hydroxydopamine-lesioned rats. *European journal of pharmacology* 251:21–25.

Morelli, M., Di Paolo, T., Wardas, J., Calon, F., Xiao, D., Schwarzschild, M. A. 2007. Role of adenosine A_{2A} receptors in parkinsonian motor impairment and L-dopa-induced motor complications. *Progress in neurobiology* 83:293-309.

Müller, C. E., Ferrè, S. 2006. Blocking Striatal Adenosine A_{2A} receptors: a new strategy for basal ganglia disorders. *Recent patents on CNS drug discovery,* 2:1-21.

Müller, C. E., Schobert, U., Hipp, J., Geis, U., Frobenius, W., Pawlowski, M. 1997. Configurationally stable analogs of 8-styrylxanthines as A_{2A}-adenosine receptor antagonists. *European journal of medicinal chemistry,* 32:709-19.

Müller, C. E. Geis, U., Hipp, J., Schobert, U., Frobenius, W., Pawlowski, M., Suzuki, F., Sandoval-Ramirez, J. 1998. Synthesis and structure-activity relationships of 3,7-dimethyl-1-propargylxanthine derivatives, A_{2A}-selective adenosine receptor antagonists. *Journal of medicinal chemistry,* 40: 4396-4405.

Müller, C. E. Shi, D., Manning, M., Daly, J. W. 1993. Synthesis of Paraxanthine Analogs (1,7-disubstituted xanthines) and other xanthines unsubstituted at the 3-position: Structure-activity relationships at adenosine receptors. *Journal of medicinal chemistry,* 36:3341-3349.

Nagatsu, T. 2004. Progress in monoamine oxidase (MAO) research in relation to genetic engineering. *Neurotoxicology,* 25:11-20.

Nagatsu, T., Sawada, M. 2005. Inflammatory process in Pakrinson's disease: role for cytokines. *Current pharmaceutical design,* 11:999-1016.

Nicotra, A., Pierucci, F., Parvez, H., Senatori, O. 2004. Monoamine oxidase expression during development and aging. *Neurotoxicology,* 25:155-165.

Obeso, J.A., Rodriguez-Oroz, M.C., Rodriguez, M., Lanciego, J.L., Artieda, J., Gonzalo, N., Olanow, C.W. 2000. Pathophysiology of the basal ganglia in Parkinson's disease. *Trends in neuroscience,* 23: (Suppl. 10), S8–S19.

O'Carroll, A. M., Fowler, C. J., Phillips, J. P., Tobbia, I., Tipton, K. F. 1983. The deamination of dopamine by human brain monoamine oxidase. Specificity for the two enzyme forms in seven brain regions. *Naunyn Schmiedeberg's archives of pharmacol*ogy, 322:198–202.

O'Kane, E. M., Stone, T. W. 1998. Interaction between adenosine A1 and A2 receptor-mediated responses in the rat hippocampus in vitro. *European journal of pharmacology.* 362:17– 25.

Olah, M., Stiles, G. L. 2000. The role of receptor structure in determining adenosine receptor activity. *Pharmacology & therapeutics,* 85:55-75.

Olanow, C. W. 1993. MAO-B inhibitors in Parkinson's disease. *Advances in neurology,* 60:666-671.

Olanow, C.W., Jenner, P., Brooks, D. 1998. Dopamine agonist and neuroprotection in Parkinson's disease. *Annals of neurology,* 44:S167-S174.

Olanow, C. W., McNaught, K. S. 2006. Ubiquitin-proteasome system and Parkinson's disease. *Movement disorders,* 21: 1806–23.

Ongini, E., Monopoli, A., Cacciari, B., Baraldi, P. G. 2001. Selective adenosine A_{2A} receptor antagonists. *Farmaco,* 56: 87-90.

Palmer, T., Bonner, P. Principles of Biochemistry with a human focus. 1st Ed. Toronto, Canada: Brooks/Cole Thomson Learning, pp. 62-70.

Parkinson Study Group. 1993. Effects of tocopherol and deprenyl on progression of disability in early Parkinson's disease. *New England journal of medicine,* 328:176–83.

Petzer, J. P., Steyn, S., Castagnoli, K. P., Chen, J., Schwarschild, M. A., van der Schyf, C. J., Castagnoli, N. 2003. Inhibition of monoamine oxidase B by selective adenosine A_{2A} receptor antagonists. *Bioorganic and medicinal chemistry,* 11:1299-310.

Petzer, J. P., Casatagnoli, N., Schwarzschild, M. A., Chen, J. F., Van der Schyf, C. J. 2009. Dual-target-directed drugs that block MAO-B and adenosine A_{2A} receptors for PD. *Neurotherapeutics,* 6:141-151.

Pinna, A., Fenu, S., Morelli, M. 2001. Motor stimulant effect of the adenosine A_{2A} receptor antagonist SCH 58261 do not develop tolerance after repeated treatment in 6-hydroxyDA-lesioned rats. *Synapse,* 39:233–238.

Pinna, A., Volpini, R., Cristalli, G., Morelli, M. 2005. New adenosine A_{2A} receptor antagonists: actions on Parkinson's disease models. *European journal of pharmacology,* 512:157-64.

Popoli, P., Minghetti, L., Tebano, M. T., Pintor, A., Rosaria, D., Massatti, M. 2004. Adenosine A_{2A} receptor antagonism and neuroprotection: mechanisms, lights, and shadows. *Critical reviews in neurobiology,* 16:99-106.

Pretorius, J., Malan, S. F., Castagnoli, N., Bergh, J. J., Petzer, J. P. 2008. Dual inhibition of monoamine oxidase B and antagonism of the adenosine A_{2A} receptor by (E,E)-8-(4-phenylbutadien-1-yl)caffeine analogues. *Bioorganic and medicinal chemistry,* 16:8676–8684.

Przedborski, S., Kostic, V., Jaskson-Lewis, V., Naini, A.B., Simonetti,S., Fahn, S., Carlson, E., Epstein, C.J., & Cadet, J.L. 1992. Transgenic mice with increased Cu/Zn-superoxide dismutase activity are resistant to N-methyl-4-phenyl-1,2,3,6-tetrahydropyridine-induced neurotoxicity. *Journal of neuroscience,* 12:1658-1667.

Quarta, D., Borycz, J., Solinas, M., Patkar, K., Hockemeyer, J., Ciruela, F., Lluis, C., Franco, R., Woods, A. S., Goldberg, S. R., Ferre´, S. 2004. Adenosine receptor-mediated modulation of DA release in the nucleus accumbens depends on glutamate neurotransmission and Nmethyl- D-aspartate receptor stimulation. *Journal of neurochemistry,* 91:873–880.

Ramsay, R. R, Krueger, M. J., Youngster, S. K., Gluck, M. R., Casida, J. E., Singer, T. P. 1991. Interaction of 1-methyl-4-phenylpyridinium ion (MPP+) and its analogs with the rotenoneipiericidin binding site of NADH dehydrogenase. *Journal of neurochemistry,* 56: 1184-1190.

Ravina, B. M., Fagan, S. C., Hart, R. G., Hovinga, C. A., Murphy, D. D., Dawson, T. M., Marler, J. R. 2003. Neuroprotective agents for clinical trials in Parkinson's disease: a systematic assessment. *Neurology,* 60:1234–1240.

Rebrin, I., Geha, R. M., Chen, K., Shih, J. C. 2001. Effects of carboxyl-terminal truncations on the activity and solubility of human monoamine oxidase B. *Journal of biomolecular chemistry,* 276:29499–29506.

Riederer, P., Sofic, E., Rausch, W. D., Schmidt, B., Reynolds, G. P., Jellinger, K., Youdim, M. B. 1989. Transition metals, ferritin, glutathione, and ascorbic acid in parkinsonian brains. *Journal of neurochemistry,* 52:515–520.

Riederer, P., Youdim, M. B. H., Rausch, W. D., Birkmayer, W., Jellinger, K., Seemann, D. 1987. On the mode of action of *L*-deprenyl in the human central nervous system. *Journal of neural transmission,* 43:217–26.

Rodwell, V. W., Kennely, P. J. Harper's Illustrated Biochemistry. 28th Ed. America: Rockefeller Centre. McGraw-Hill Medical, pp.162-174.

Rosin, D. L., Hettinger, B. D., Lee, A., Linden, J. 2003. Anatomy of adenosine A_{2A} receptors in brain: morphological substrates for integration of striatal function*. Neurology,* 61:*(*11 (Suppl. 6), S12–S18.

Ross, G. W., Abbott, R. D., Petrovitch, H., Morens, D. M., Grandinetti, A., Tung, K. H., Tanner, C. M., Masaki, K. H., Blanchette, P. L., Curb, J. D., Popper, J. S., White, L. R. 2000. Association of coffee and caffeine intake with the risk of Parkinson disease. *Journal of the American medical association,* 283:2674–2679.

Sagi, Y., Drigues, N., Youdim, M. B. H. 2005. The neurochemical and behavioral effectsof the novel cholinesterase-monoamine oxidase inhibitor, ladostigil, in response to L-dopa and L-tryptophan, in rats. *British journal of pharmacology,* 146: 553–560.

Samii, A., Nutt, J. G., Ransom, B. R. 2004. Parkinson's disease. *Lancet,* 363:1783–93.

Saura, J., Richards, J. G., Mahy, N. 1994. Age-related changes in MAO in Bl/C57 mouse tissues: a quantitative radioautography study. *Journal of neural transmission,* 41:89–94.

Schiffmann, S. N., Fisone, G., Moresco, R., Cunha, R. A., Ferrè, S. 2007. Adenosine A_{2A} receptors and basal ganglia physiology. *Progress in neurobiology,* 83:277-292.

Schiffmann, S. N., Jacobs, O., Van der Haeghen, J. J. 1991. Striatal restricted adenosine A_2 receptor (RDC8) is expressed by enkephalin but not by substance P neurons: an in situ hybridization histochemistry study. *Journal of neurochemistry,* 57:1062–1067.

Schwarzschild, M. A., Agnati, L., Fuxe, K., Chen, J., Morelli, M. 2006. Targeting adenosine A_{2A} receptors in Parkinson's disease. *Trends in Neuroscience. 29:*674-654.
Seiler, N. 1990. Polyamine metabolism. *Digestion,* 46:319-330.

Shamim, M. T., Ukena, D., Padgett, W. L., Daly, J. W. 1989. Effects of 8- phenyl and 8-cycloalkyl substituents on the activity of mono-, di- , and trisubstituted alkylxanthines with substitution at the 1-, 3-, and 7-positions. *Journal of medicinal chemistry,* 32:1231-37.

Sherman, M. Y., Goldberg, A. L. 2001. Cellular defenses against unfolded proteins: a cell biologist thinks about neurodegenerative disease. *Neuron, 29:*15-32.
Shih, J. C. 1979. Monoamine oxidase in aging human brain, In: Singer, T. P., van Korff, R. W., Murphy, D. L., editors. Monoamine oxidase: structure, function, and altered functions. *New York: Academic Press*, pp. 413–21.

Shih, J. C., Chen, K., Ridd, M. J. 1999. Monoamine oxidase: from genes to behavior. *Annual review of neuroscience, 22:* 197-217.

Shimada, J., Suzuki, F., Nonaka, H., Ishii, A. 1992. 8-Polycycloalkyl-1,3-dipropylxanthines as potent and selective antagonists for adenosine receptors. *Journal of medicinal chemistry,* 35*:*924-930.

Shimada, J., Koike, N., Nonaka, H., Shiozaki, S., Yanagawa, K., Kanada, T., Kobayashi, H., Fumio, S. 1997. Adenosine A_{2A} antagonists with potent anti-cataleptic activity. *Bioorganic and medicinal chemistry letters,* 7: 2349-2352.

Shiozaki, S., Ichikawa, S., Nakamura, J., Kitamura, S., Yamada, K., Kuwana, Y. 1999. Actions of adenosine A_{2A} receptor antagonist KW-6002 on drug induced catalepsy and hypokinesia caused by reserpine or MPTP. *Psychopharmacology,* 147*:*90-95.

Silverman, R. B. 1995. Radical ideas about monoamine oxidase. *Accounts of chemical research,* 28:335–342.

Simola, N., Fenu, S., Baraldi, P. G., Tabrizi, M. A., Morelli, M. 2004. Blockade of adenosine A_{2A} receptors antagonizes parkinsonian tremor in the rat tacrine model by an action on specific striatal regions. *Experimental neurology,* 189:182–188.

Simola, N., Morelli, M., Pinna, A. 2008. Adenosine A_{2A} receptor antagonists and Parkinson's disease: state of the art and future directions. *Current pharmaceutical design,* 14:1475.

Speer, J.H., Raymond, A.L. 1953. Some alkyl homologues of theophyline. *Journal of the American chemical society,* 75:114-115.

Spillantini, M. G., Crowther, R. A., Jakes, R., Hasegawa, M., and Goedert, M. 1998. α-synuclein in filamentous inclusions of Lewy bodies from Parkinson's disease and dementia with Lewy bodies. *Proceedings of the national academy of sciences of the United States of America, 95:*6469-6473.

Standaert, D. G., Young, A. B. 2006. Treatment of central nervous system degenerative disorders: Parkinson's disease. (*In:* Brunton, L. L., Lazo, J. S., and Parker, K. L. (eds). *Goodman & Gilman's: The pharmacological basics of therapeutics 10th edition:* New York. McGraw-Hill, pp. 529-533).

St. Clair, R. N., Rodriguez, W. E., Joshua, I. 2005. The basal ganglia and the serial order of communicative signs. *Intercultural communication studies,* 16: 1-11.

Suzuki, F., Shimada, J., Shiozaki, S., Ichikawa, S., Ishii, A., Nakamura, J., Nonaka, H., Kobayashi, H., Fuse, E. 1993. Adenosine A_1 antagonists. 3 Structure-activity relationships on amelioration against scopolamine- or N^6-(R-phenylisopropyl)adenosine-induced cognitive disturbance. *Journal of medicinal chemistry,* 36: 2508-2518.

Svennigsson, P., Le Moine, C., Aubert, I., Burbaud, P., Fredholm, B. B., Bloch, B. 1998. Cellular distribution of adenosine A_{2A} receptor mRNA in the primate striatum. *Journal of comparative neurology,* 399*:*229-240.

Swanepoel, A. B. 2010. The synthesis and evaluation of phenoxymethylcaffeine analogues as inhibitors of monoamine oxidase. Potchefstroom: NWU. (Dissertation – M.Sc).

Talpade, D. J., Greene, J. G., Higgins, D. S. Jr., Greenamyre, J. T. 2000. In vivo labelling of mitochondrial complex I (NADH:ubiquinone oxidoreductase) in rat brain using [(3)H]-dihydrorotenone. *Journal of neurochemistry,* 75: 2611-2621.

Taylor, K. S., Counsell, C. E., Gordon, J. C., Harris, C. E. 2005. Screening for undiagnosed parkinsonism among older people in general practice. *Age and ageing,* 34: 501–04.

Tugwell, C. 2008**.** Parkinson's disease in focus. 1st Ed.London, UK: Pharmaceutical Press. pp. 60-153.

Van der Walt, M. M. 2012. Syntheses of sulfanylphthalimide and xanthine analogues and their evaluation as inhibitors of monoamine oxidase and as antagonists of adenosine receptors. Potchefstroom: NWU. (Dissertation – PhD).

Vindis, C., Se´gue´las, M.-H., Bianchi, P., Parini, A., Cambon, C. 2000. Monoamine oxidase B induces ERK-dependent cell mitogenesis by hydrogen peroxide generation. *Biochemical and biophysical research communications,* 271: 181–185.

Vlok, N., Malan, S. F., Castagnoli, N. Jr, Bergh, J. J., Petzer, J. P. 2006. Inhibition of monoamine oxidase B by analogues of the adenosine A_{2A} receptor antagonist (*E*)-8-3-chlorostyryl)caffeine CSC). *Bioorganic and medicinal chemistry,* 14:3512-21.

Wardas, J., Konieczny, J., Lorenc-Koci, E., 2001. SCH 58261, an A_{2A} adenosine receptor antagonist, counteracts the parkinsonian-like muscle rigidity in rats. *Synapse,* 41:160–171.

Wu, D. C., Teismann, P., Tieu, K., villa, M., Jackson-Lewis, V., Ischiropoulos, H., Przedborski, S. 2003. NADPH oxidase mediates oxidative stress in the MPTP model of Parkinson's disease. *Proceedings of the national academy of sciences of the United States of America,* 100:6145-6150.

Xu, K., Bastia, E., Schwarzschild, M., 2005. Therapeutic potential of adenosine A_{2A} receptor antagonists in Parkinson's disease. *Pharmacology and therapeutics,* 105:267–310.

Yacoubain, T. A., Standaert, D. G. 2009. Targets for neuroprotection in Parkinson's disease. *Biochimica et biophysica acta: molecular basis of disease,* 1792:676-687.

Youdim, M. B. H. 2010. Why do we need multifunctional neuroprotective and neurorestorative drugs for Parkinson's and Alzheimer's diseases as disease modifying agents? *Experimental neurobiology,* 29:121-135.

Youdim, M. B. H., Finberg, J. P. M., Tipton, K. F. 1988. Monoamine oxidase. In: Advances in Experimental Pharmacology. Catecholamine. II. ed. Trendelenburg, U. & Weiner, U., Berlin: Springer-Verlag. pp. 119–192.

Youdim, M. B. H., Buccafusco, J. J. 2005. Multi-functional drugs for various CNS targets in the treatment of neurodegenerative disorders. *Trends in pharmacological sciences,* 26:1-9.

Youdim, M. B. H., Bakhle, Y. S. 2006. Monoamine oxidase: isoforms and inhibitors in Parkinson's disease and depressive illness. *British journal of pharmacology,* 147: 287-296.

Zesiewicz, T. A., Hauser, R. A. 2002. Depression in Parkinson's disease. *Current Psychiatry reports,* 4:69-73.

Zhou, J., Zhong, B., Silverman, R. 1996. Direct continuous fluorometric assay for monoamine oxidase. *Analytical biochemistry,* 234:9-12.

Zhou, M., Panchuk-Voloshina, N. 1997. A one-step fluorometric method for the continuous measurement of monoamine oxidase activity. *Analytical biochemistry,* 253:169-174.

APPENDIX A

LIST OF SYMBOLS AND ABBREVIATIONS

5HT	-	Serotonin
ADH	-	Aldehyde dehydrogenase
AO	-	Amine oxidase
BG	-	Basal ganglia
CNS	-	Central nervous system
COMT	-	Catechol-O-methyltransferase
CPA	-	Cyclopentyladenosine
CPu	-	caduate-putamen
CSC	-	(E)-8-(3-Chlorostyryl)caffeine
Cys-397	-	Cysteine 397
DA	-	Dopamine
DAT	-	Dopamine transporter
DMSO	-	Dimethylsulfoxide
E	-	*trans*
EDAC	-	N-(3-dimethylaminopropyl)-N'-ethylcarbodiimide hydrochloride
FAD	-	Flavin adenine dinucleotide
g	-	gravitational force of the earth (~10 $m.s^{-1}$)
GP	-	Globus pallidus
GPCR	-	G-protein coupled receptor
GPe	-	Globus pallidus externa
GPi	-	Globus pallidus interna

GPO	-	Glutathione peroxidase
Glu	-	Glutamate
GSH	-	Glutathione
^{3}[H]NECA	-	1-(6-Amino-9H-purin-9-yl)-1-deoxy-*N*-ethyl-β-D-ribofuronamide
HPLC	-	High performance liquid chromatography
HRMS	-	High resolution mass spectra
HRP	-	Horse radish peroxidase
[I]	-	Inhibitor concentration
Ile-199	-	Isoleucine 199
K_i	-	Enzyme-inhibitor dissociation constant
LB's	-	Lewy bodies
MAO	-	Monoamine oxidase
MAO A	-	Monoamine oxidase A
MAO B	-	Monoamine oxidase B
$MgCl_2$	-	Magnesium chloride
mGlu5	-	Metabotropic glutamate 5
mGlu	-	Metabotropic receptors
Mp	-	Melting point
$MPDP^+$	-	1-Methyl-4-phenyl-2,3-dihydropyridinium
MPP^+	-	1-Methyl-4-phenylpyridinium
MPPP	-	1-Methyl-4-phenyl-4-propionoxypiperidine
MPTP	-	1-Methyl-4-phenyl-1,2,3,6-tetrahydropyridine
MS	-	Mass spectra
NA	-	Nor-adrenaline

PD	-	Parkinson's Disease
pH	-	Indicates acidity
PNS	-	Peripheral nervous system
QSAR	-	Quantitative structure-activity relationship
ROS	-	Reactive oxygen species
[S]	-	Substrate concentration
SEM	-	Standard Error of the Mean
SN	-	Substantia nigra
SNpc	-	Substantia nigra pars compacta
ST	-	Serotonin toxicity
$t_{1/2}$	-	Half life
TPQ	-	Topa-quinone
Tris	-	Tris(hydroxymethyl)aminomethane
U	-	Units (enzyme activity)
V_i	-	Initial velocity
V_{max}	-	Maximal velocity

APPENDIX B

LIST OF FIGURES

CHAPTER:	FIGURE:	DESCRIPTION:	P NO:
1	1.1	Molecular structures of CSC and KW-6002	4
	1.2	Molecular structures of caffeine and 8-(phenoxymethyl)caffeine	4
	1.3	(a) 8-(Phenoxymethyl)caffeine analogues synthesized in a previous study (Swanepoel, 2010).	5
		(b) 8-(Phenoxymethyl)caffeine analogues for Series 1 of current study.	6
		(c) 8-(Phenoxymethyl)caffeine analogues with 1,3 diethyl substitution for Series 2 of the current study.	6
2	2.1	Breakdown of the BG (St. Clair *et al.,* 2005)	9
	2.2	(a) Represents the normal nigrostraital pathway (b) Represents a diseased nigrostraital pathway	10
	2.3	Immunohistochemical labeling of Lewy bodies	11
	2.4	Molecular structure of MPTP and MPPP	12
	2.5	Molecular structure of rotenone and paraquat	13
	2.6	Comparison of chemical structures of MPP^+ and paraquat (Przedborski & Ischiropoulos)	13
	2.7	DA Metabolism	15
	2.8	Metabolism of L-dopa	19
	2.9	Molecular structure of pramipexole and ropinirole	20
	2.10	Molecular structure of COMT inhibitors, tolcapone and entacapone	21
	2.11	Molecular structure of a selective MAO-B inhibitor, deprenyl	22
	2.12	Molecular structures of muscarinic receptor antagonists.	22
	2.13	Adenosine A_{2A} antagonists, istradefylline and (E)-8-(3-chlorostyryl)caffeine	24
	2.14	Classification of Amine Oxidase (Adapted from Jalkanen & Salmi, 2001)	26

	2.15	MAO-A and MAO-B affinities	27
	2.16	Ribbon diagram of MAO-B and MAO-A	28
	2.17	Aromatic cage of MOA-B (Edmonson *et al.,* 2007)	29
	2.18	The crystal structure of MAOB and effect of stereochemistry on rasagiline binding to human MAO-B (Youdim *et al.,* 2006)	30
	2.19	Comparison of the active site cavities of human MAO-A (left) and human MAO-B (right).	31
	2.20	Representation of the single electron transfer mechanism proposed for MAO catalysis	32
	2.21	Representation of the polar nucleophilic mechanism proposed for MAO catalysis (Edmonson *et al.,* 2004).	33
	2.22	The cheese reaction (Youdim *et al.,* 2006)	35
	2.23	Molecular Structure of deprenyl	36
	2.24	Molecular structure of rasagiline	36
	2.25	Molecular structure of lazabemide	37
	2.26	Molecular structure of ladostigil.	38
	2.27	Crystal structure of the A_{2A} receptor	40
	2.28	Distribution of A_{2A} receptor in the BG of different mammalian species	41
	2.29	Schematic diagram of the anatomical relationship between various BG nuclei, responsible for the motor dysfunction in PD	42
	2.30	Functional interactions between DA D_2, adenosine A_{2A} and metabotropic glutamate 5 receptors in striatopallidal neurons.	43
	2.31	A_2-D_2 receptor interaction	46
	2.32	Molecular structure of CSC	47
	2.33	Molecular structure of KW-6002	48
	2.34	Molecular structure of SCH-42081	48
	3.1	Molecular structures of caffeine, CSC and 8-phenoxymethylcaffeine	50
	3.2	Reaction scheme for the synthesis of 8-(phenoxymethyl)caffeine analogues.	52
3	3.3	Reaction scheme for the synthesis of 1,3-dimethyl-5,6-	54

		diaminouracil.	
	3.4	Reaction scheme of the synthesis of the phenoxyacetic acids	55
4	4.1	Graphical representation of the Michealis-Menten equation (V_i vs. [S]).	71
	4.2	An example of the Lineweaver-Burke plot $1/V_i$ versus 1/[S]).	72
	4.3	The formation of resorufin occurs in the presence of Amplex Red and H_2O_2	73
	4.4	Schematic representation of MAO-B assay	75
	4.5	The sigmoidal dose response curve for the calculation of the IC_{50} value of 8-(4-iodophenoxymethyl)caffeine	76
	4.6	Molecular structure of a known MAO-B inhibitor, lazabemide	79
5	5.1	Molecular structures of adenosine, NECA and caffeine	85
	5.2	Molecular structure of KW-6002 and CSC	86
	5.3	Graphical representation of the A_{2A} binding affinity assay	91
	5.4	Competitive study between compound 16 and the radio labelled ligand. The sigmoidal dose-response curve for the inhibition of [^{3}H]NECA binding to rat striatal A_{2A} receptors by antagonist 16 (expressed in µM),	93
6	6.1	Molecular structures of caffeine and CSC	98
	6.2	Mechanism of dual targeted MAO-B/A_{2A} compounds such as CSC and KW-6002 (Youdim, 2010)	98
	6.3	Structural requirements for antagonizing A_{2A} and inhibiting MAO-B (adapted from Azam *et al.,* 2012).	99

APPENDIX C

LIST OF TABLES

CHAPTER:	TABLE:	DESCRIPTION:	P NO:
1	-	-	-
2	2.1	Diagnostic criteria for PD (Katzenschlager *et al.,* 2003)	18
3	3.1	Chemical structures of the 8-(phenoxymethyl)caffeine derivates (Compounds 1,8-22)	51
	3.2	Phenoxyacetic acids needed for synthesis of target compounds	55
	3.3	Interpretation of mass spectra	73
	3.4	Interpretation of HPLC traces	74
4	4.1	MAO inhibitory potencies of series 1, the 8(phenoxymethyl)caffeine analogues. Also given are the IC_{50} values of the 8-(phenoxymethyl)caffeine analogues (**1**–**10**) synthesized in a previous study (Swanepoel, 2010) .	77
	4.2	MAO inhibitory potencies of series 2, the 1,3-diethyl-7-methyl-8-(phenoxymethyl)xanthine analogues.	80
	4.3	A comparison between the MAO-B inhibition potencies of series 1 and series 2	81
	4.4	Comparison of the MAO-B inhibitory potencies of the C3-substituted 8 (phenoxymethyl)caffeine analogues with those of the C4-substituted homologues	83
5	5.1	Compounds that were evaluated as potential A_{2A} receptor antagonists in this study.	88
	5.2	The K_i values for the competitive inhibition of [^{3}H]NECA binding to rat striatal adenosine A_{2A} receptors by 8-(phenoxymethyl)caffeines and 1,3-diethyl-7-methyl-8-(phenoxymethyl)xanthines	95
6	6.1	Comparison between the two series K_i and IC_{50} values	101

		to that of CSC's K_i and IC_{50} values.	

APPENDIX D

LIST OF EQUATIONS

CHAPTER:	EQUATIONS:	DESCRIPTION:	P NO:
1	-	-	-
2	-	-	-
3	-	-	-
4	4.1	The Michaelis-Menten equation describes the behaviour of an enzyme under the influence of varied substrate concentrations.	71
	4.2	Inversion of the Michaelis-Menten equation describes the double reciprocal plot or Lineweaver Burke plot	71
5	5.1	Non-linear regression equation	92
	5.2	Cheng-Prusoff equation (Cheng, 2001) to calculate the K_i from the IC_{50} value	92
6	-	-	-

APPENDIX E

^{1}H-NMR and ^{13}C-NMR

a) 8-(4-Methylphenoxymethyl)caffeine (**11**)
b) 8-(4-Methoxyphenoxymethyl)caffeine (**12**)
c) 8-(4-Iodophenoxymethyl)caffeine (**13**)
d) 8-(3,4-Methylphenoxymethyl)caffeine (**14**)
e) 1,3-Diethyl-7-methyl-8-(4-chlorophenoxymethyl)xanthine (**16**)
f) 1,3-Diethyl-7-methyl-8-(4-bromophenoxymethyl)xanthine (**17**)
g) 1,3-Diethyl-7-methyl-8-(4-fluorophenoxymethyl)xanthine (**18**)
h) 1,3-Diethyl-7-methyl-8-(4-methylphenoxymethyl)xanthine (**19**)
i) 1,3-Diethyl-7-methyl-8-(4-methoxyphenoxymethyl)xanthine (**20**)
j) 1,3-Diethyl-7-methyl-8-(4-iodophenoxymethyl)xanthine (**21**)
k) 1,3-Diethyl-7-methyl-8-(4-dimethylphenoxymethyl)xanthine (**22**)

^{1}H NMR and ^{13}C NMR:

8-(4-Methylphenoxymethyl)caffeine (**11**)

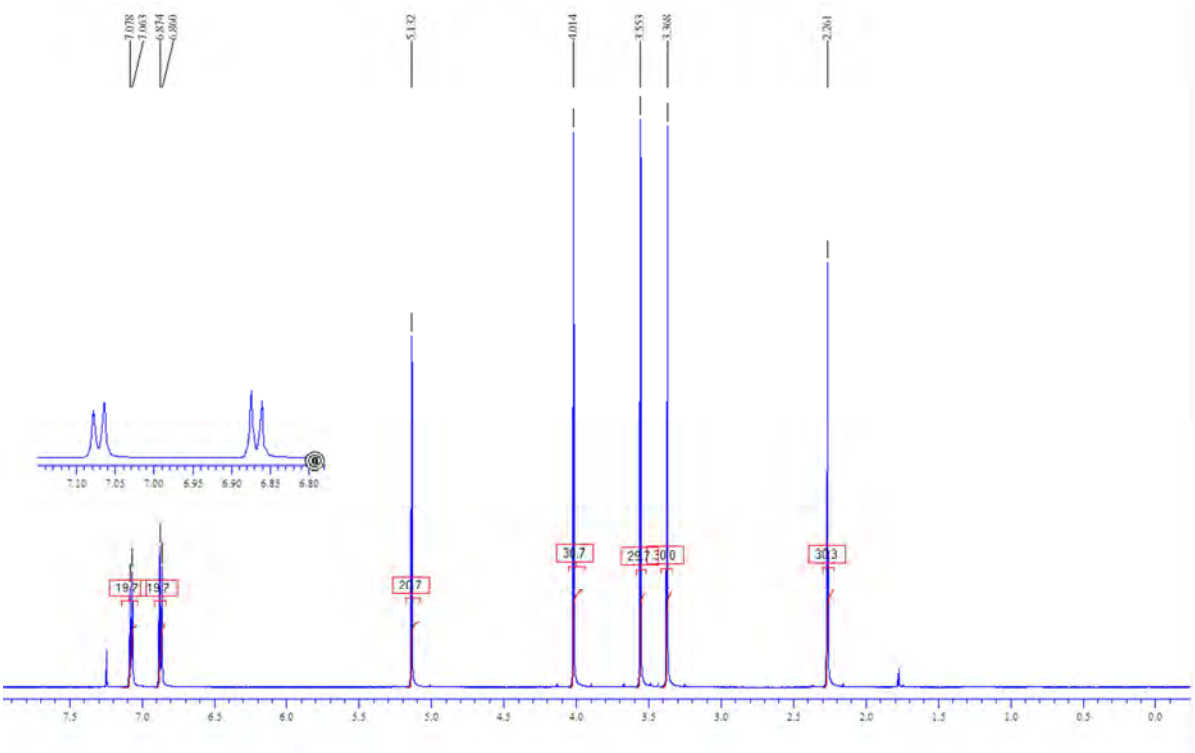

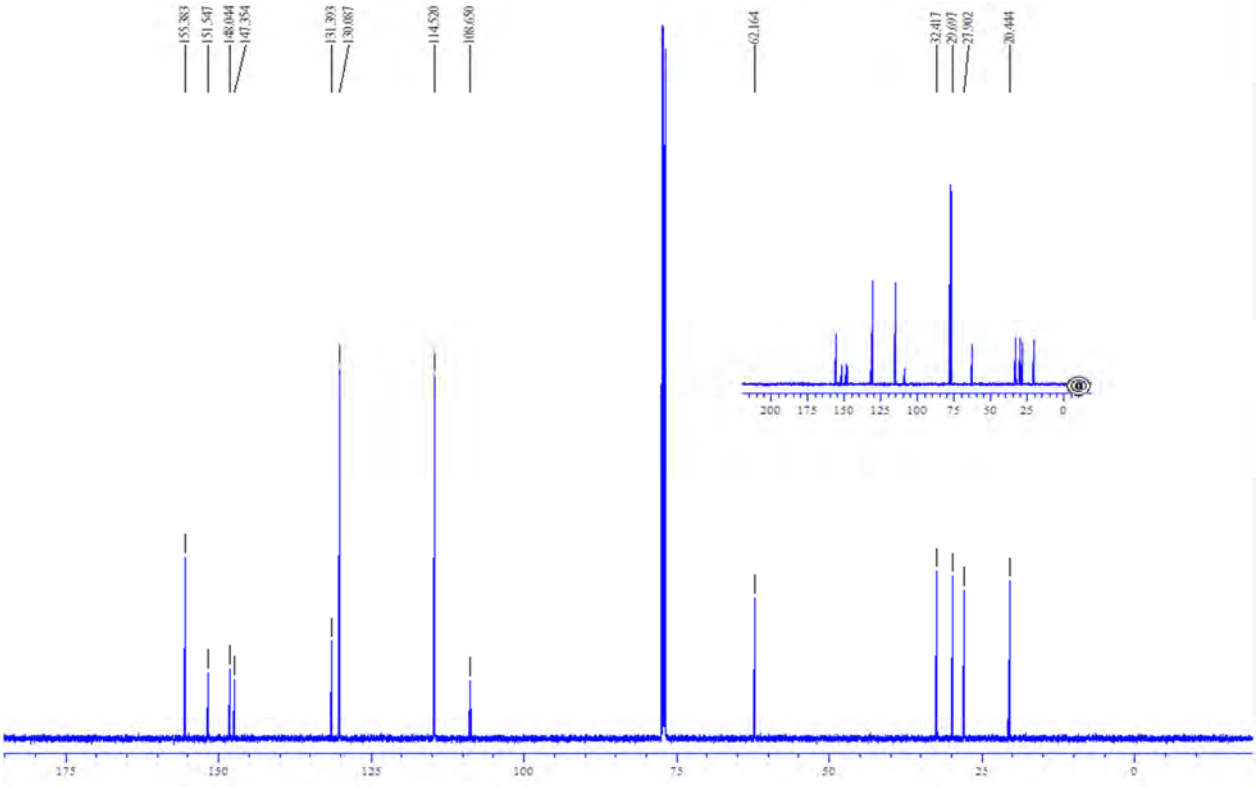

^{1}H NMR and ^{13}C NMR:

8-(4-Methoxyphenoxymethyl)caffeine (**12**)

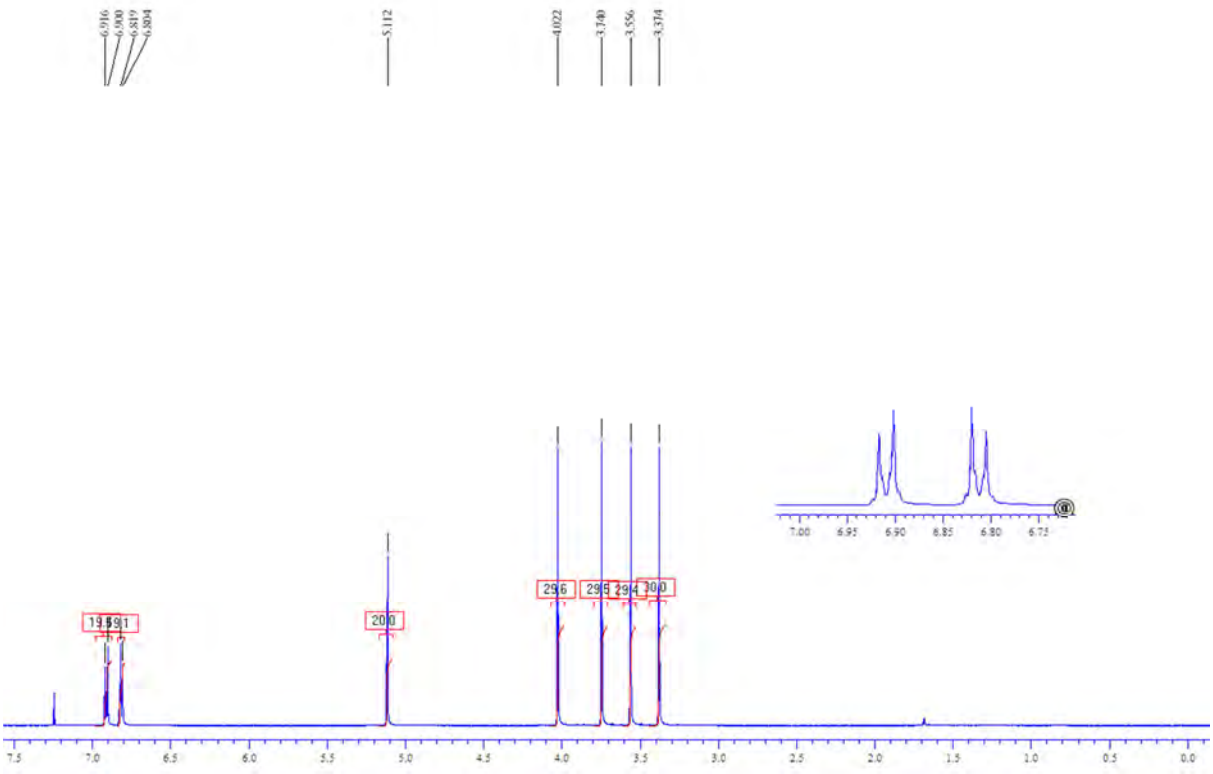

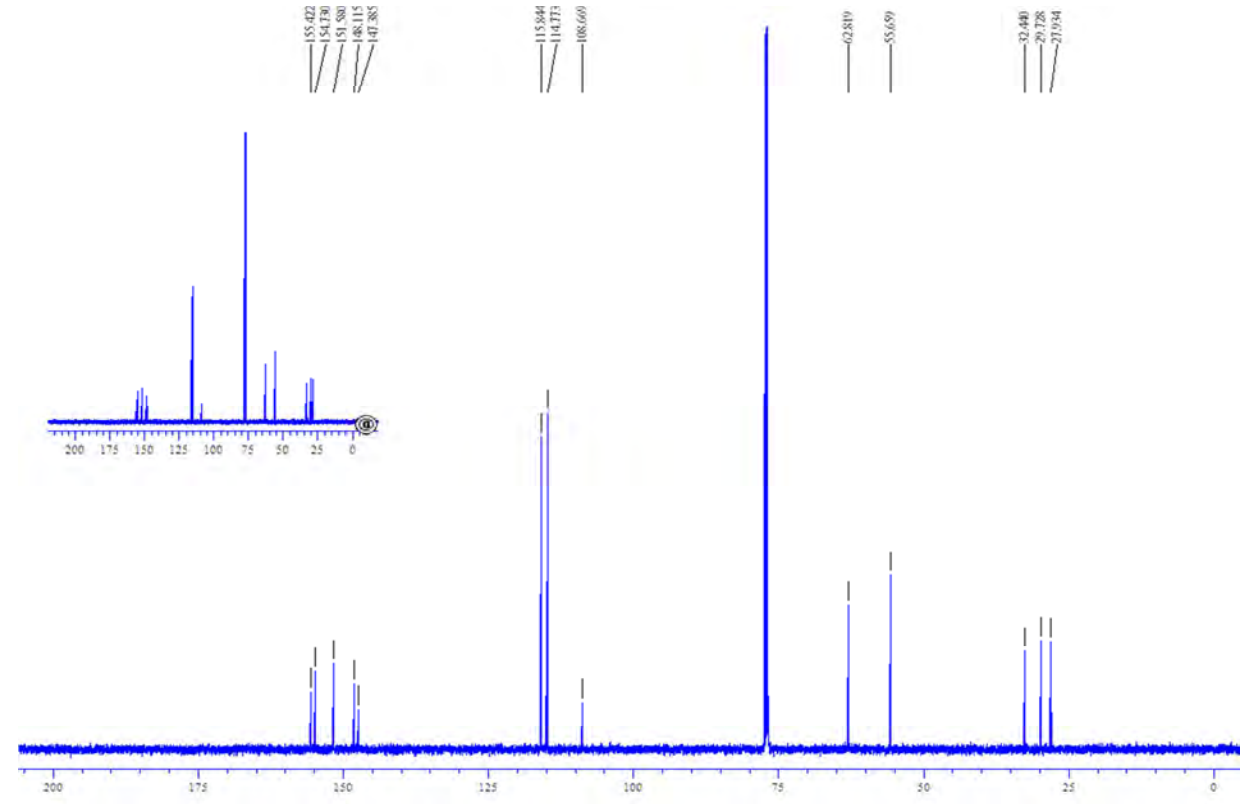

^{1}H NMR and ^{13}C NMR:

8-(4-Iodophenoxymethyl)caffeine (**13**)

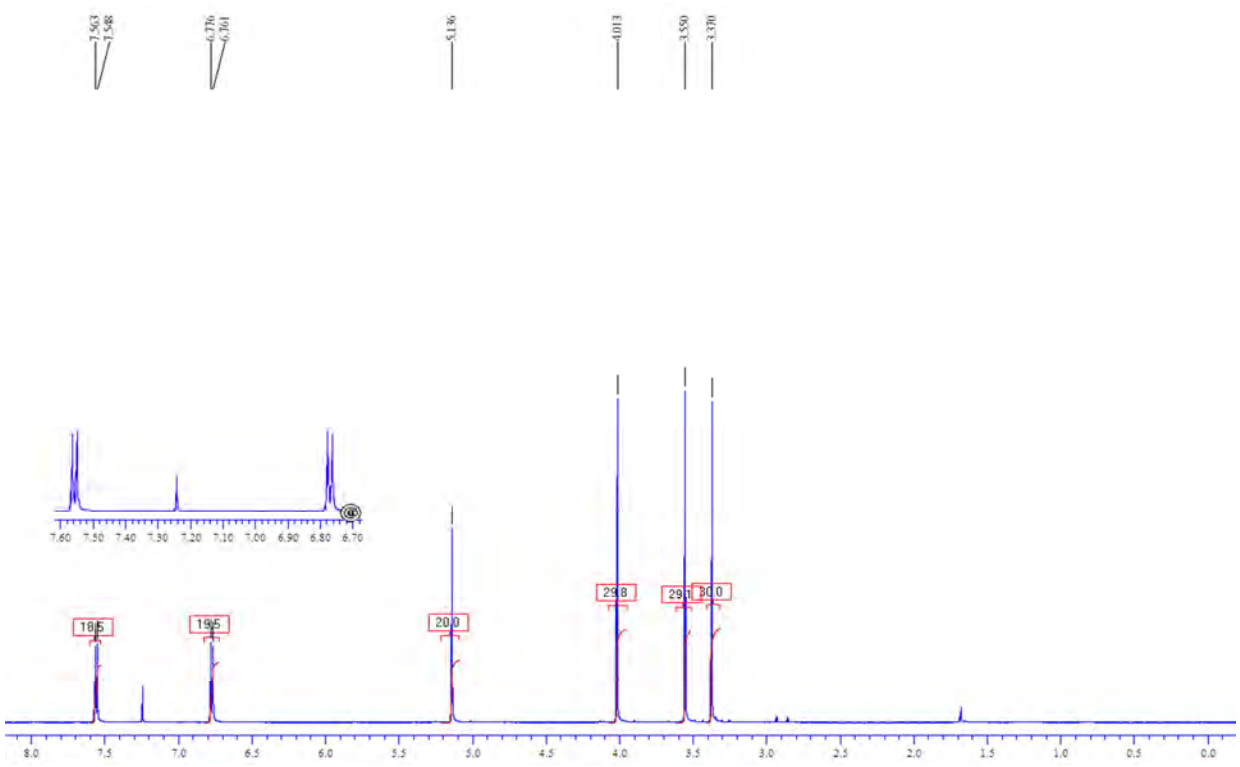

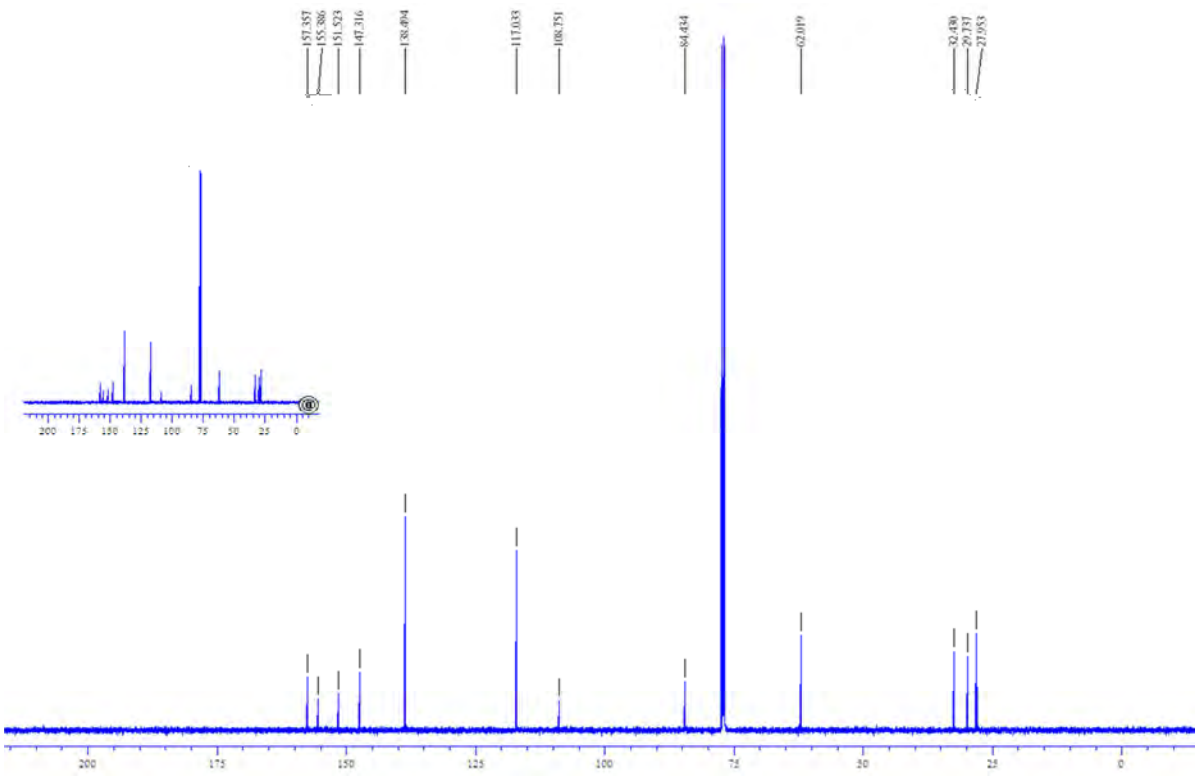

^{1}H NMR and ^{13}C NMR:

8-(3,4-Methylphenoxymethyl)caffeine (**14**)

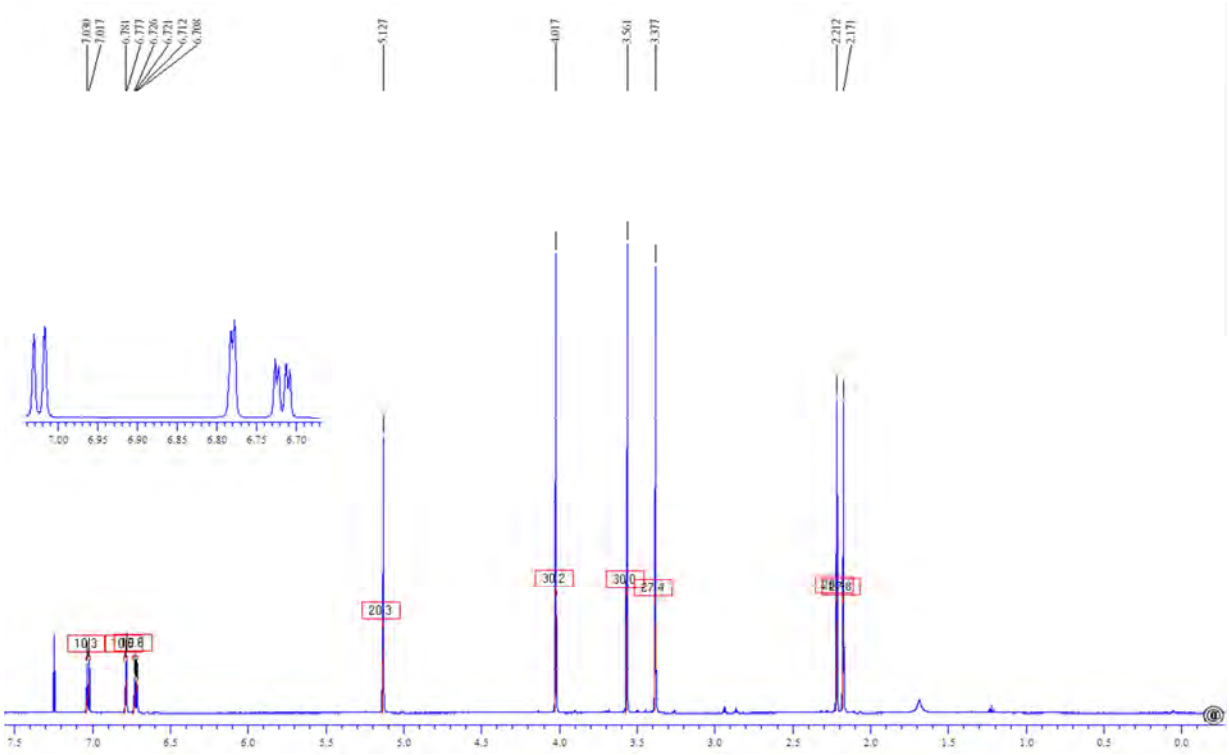

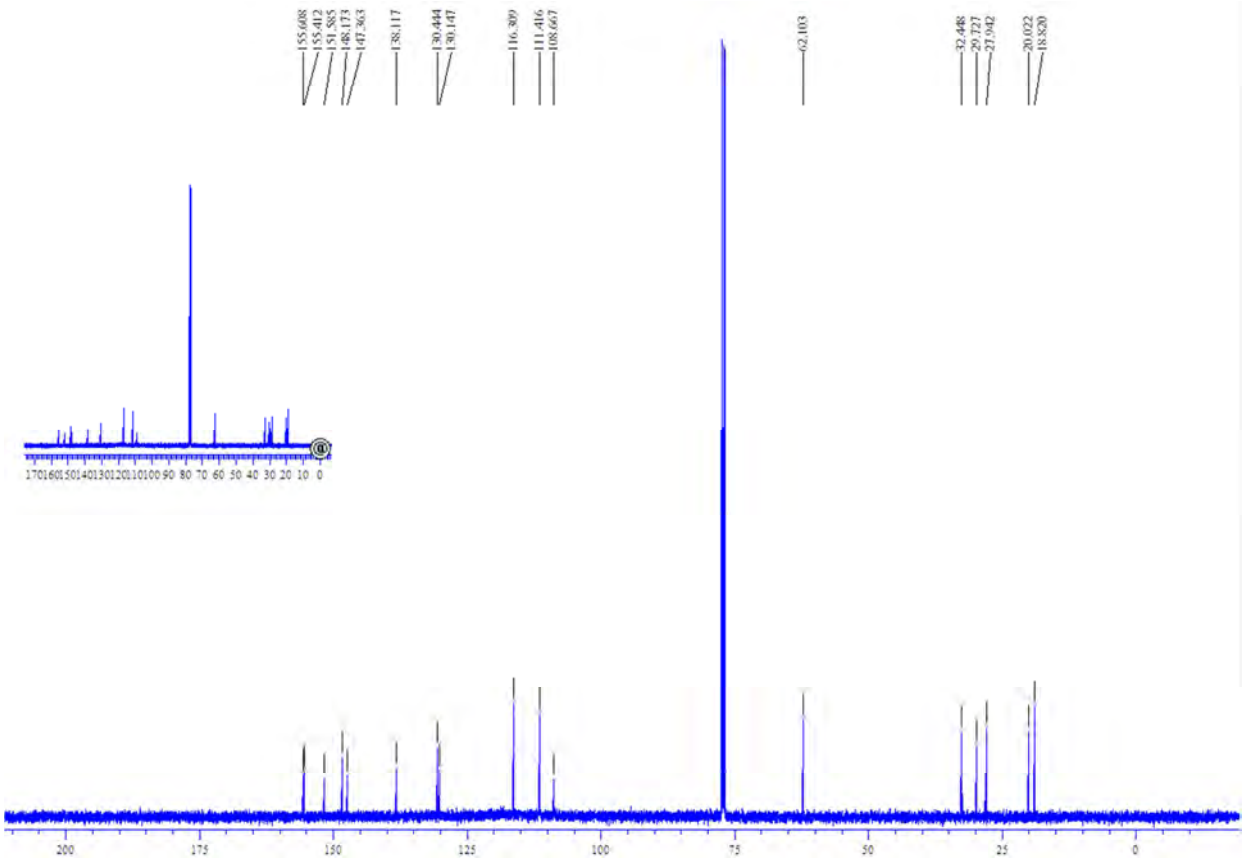

^{1}H NMR and ^{13}C NMR:

1,3-Diethyl-7-methyl-8-(4-chlorophenoxymethyl)xanthine (**16**)

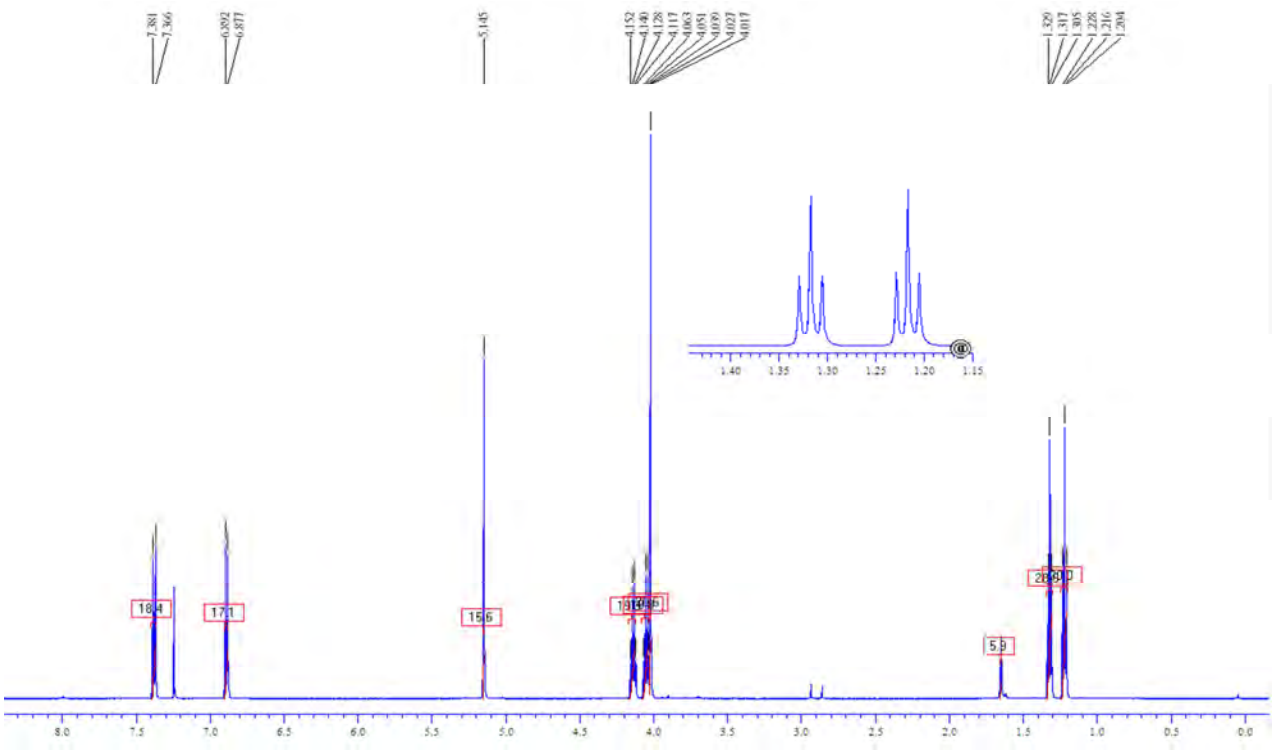

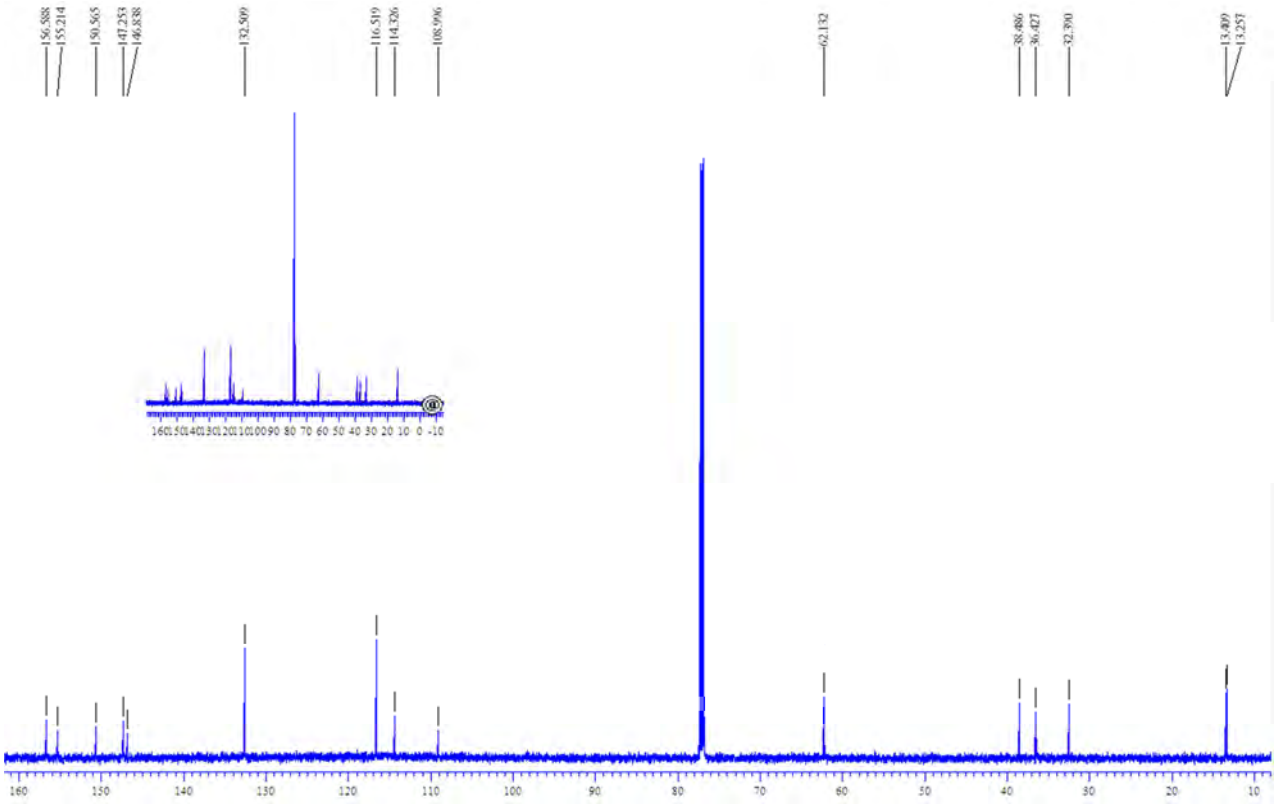

^{1}H NMR and ^{13}C NMR:

1,3-Diethyl-7-methyl-8-(4-bromophenoxymethyl)xanthine (**17**)

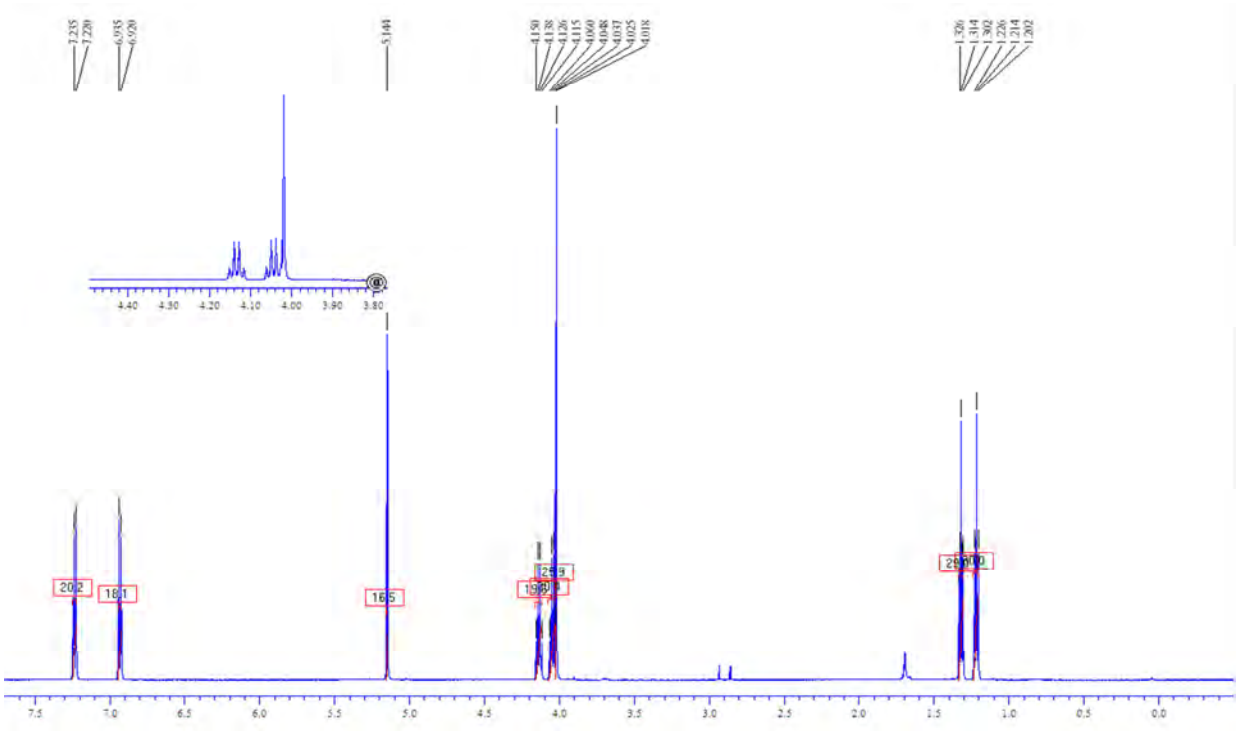

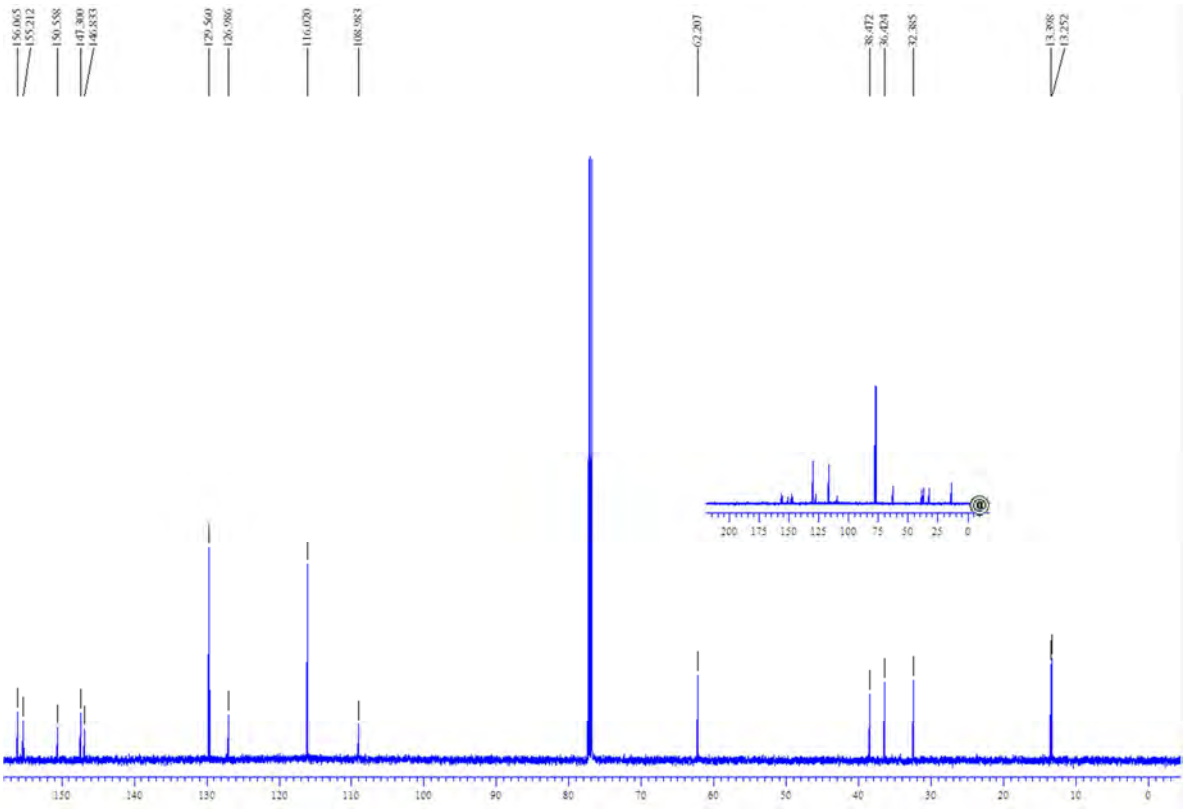

^{1}H NMR and ^{13}C NMR:

1,3-Diethyl-7-methyl-8-(4-fluorophenoxymethyl)xanthine (**18**)

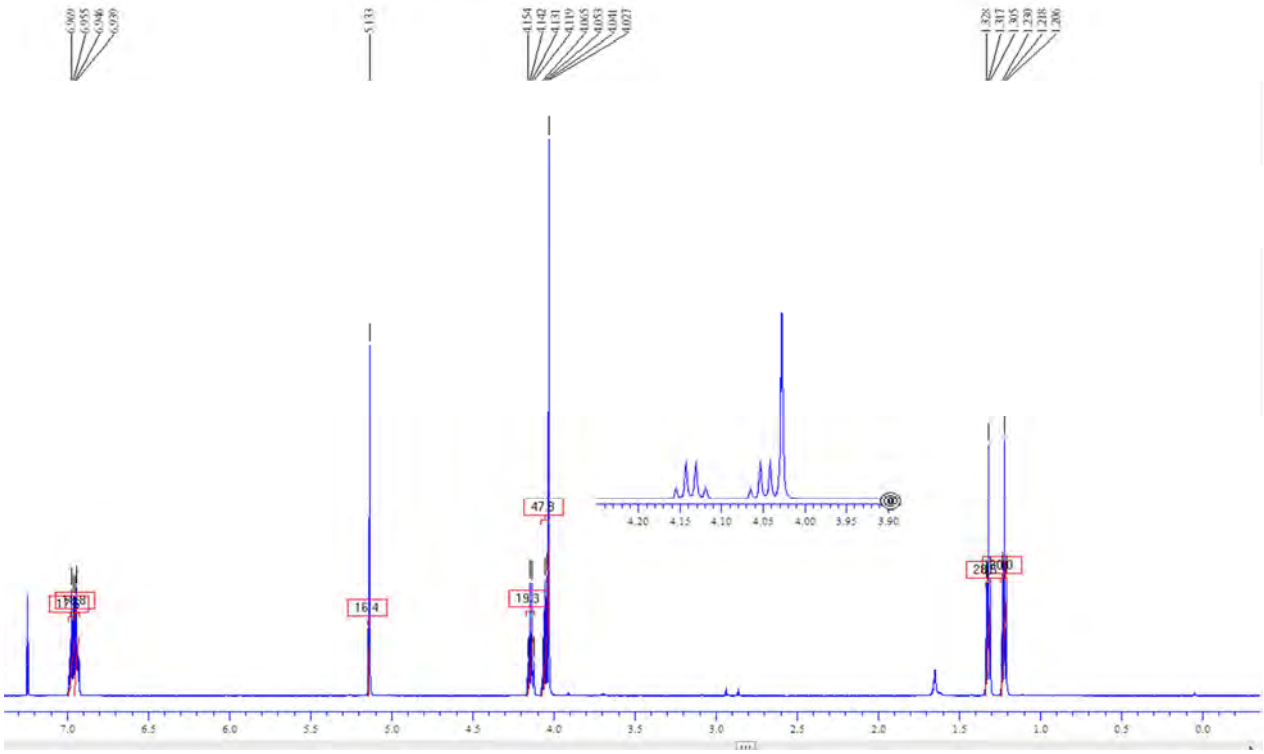

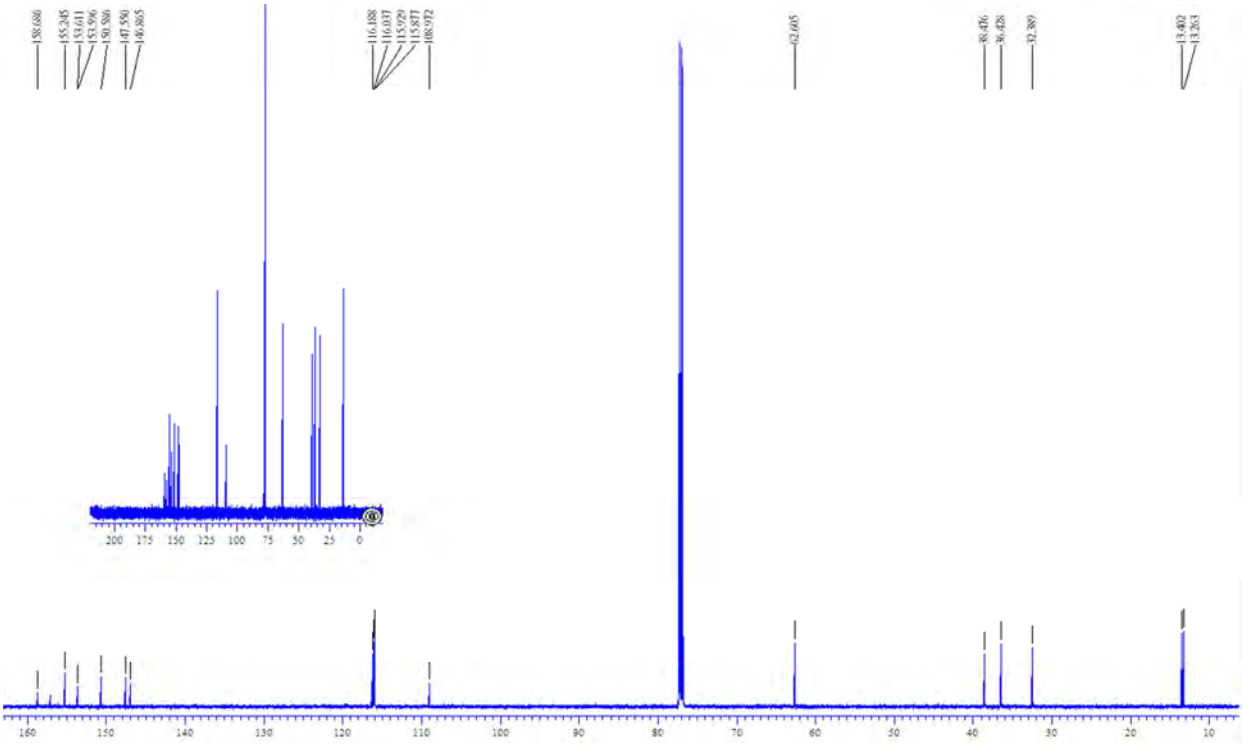

^{1}H NMR and ^{13}C NMR:

1,3-Diethyl-7-methyl-8-(4-methylphenoxymethyl)xanthine (**19**)

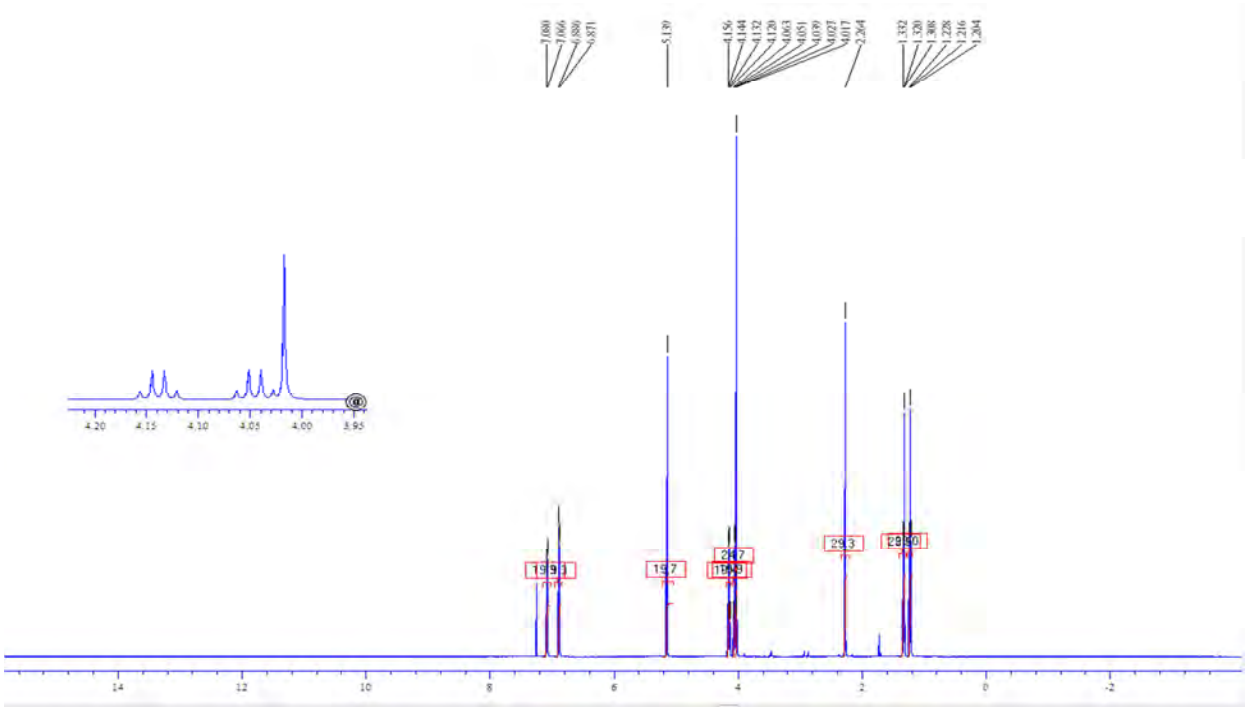

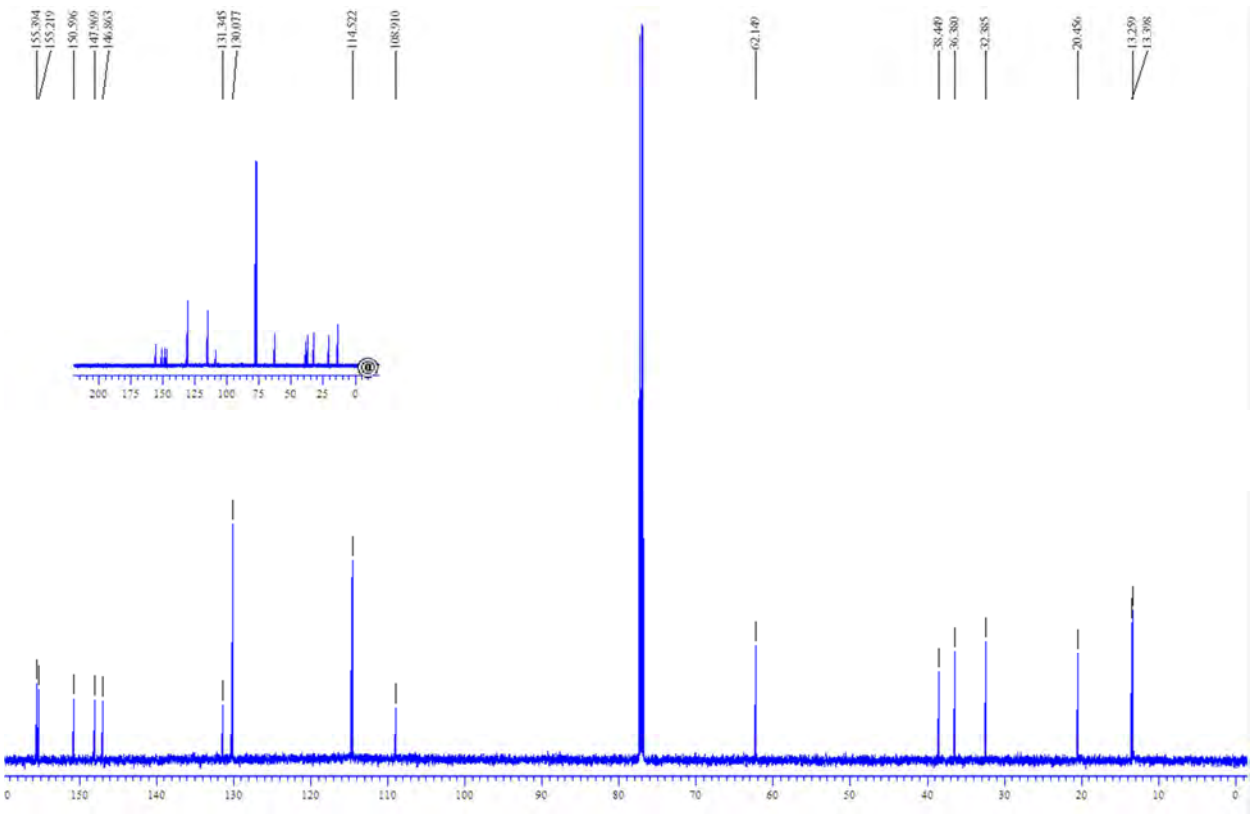

^{1}H NMR and ^{13}C NMR:

1,3-Diethyl-7-methyl-8-(4-methoxyphenoxymethyl)xanthine (**20**)

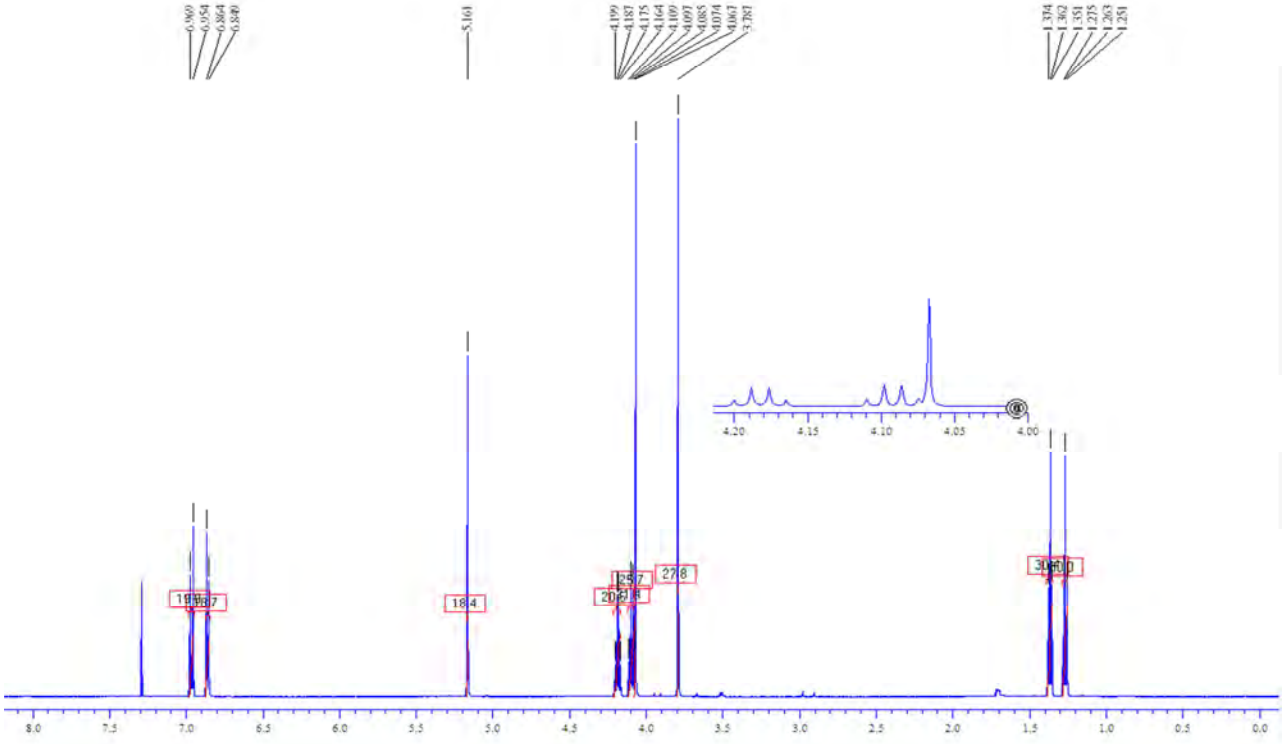

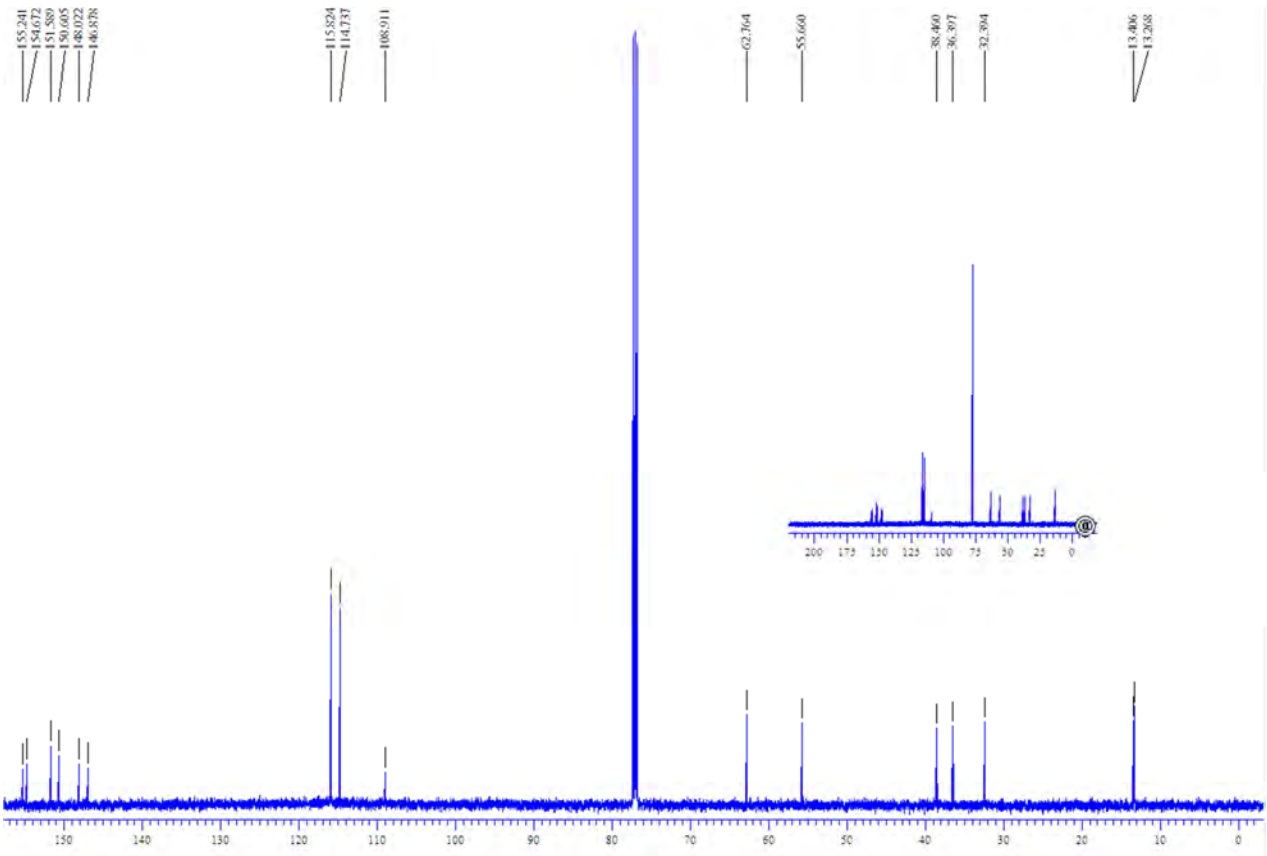

^{1}H NMR and ^{13}C NMR:

1,3-Diethyl-7-methyl-8-(4-iodophenoxymethyl)xanthine (**21**)

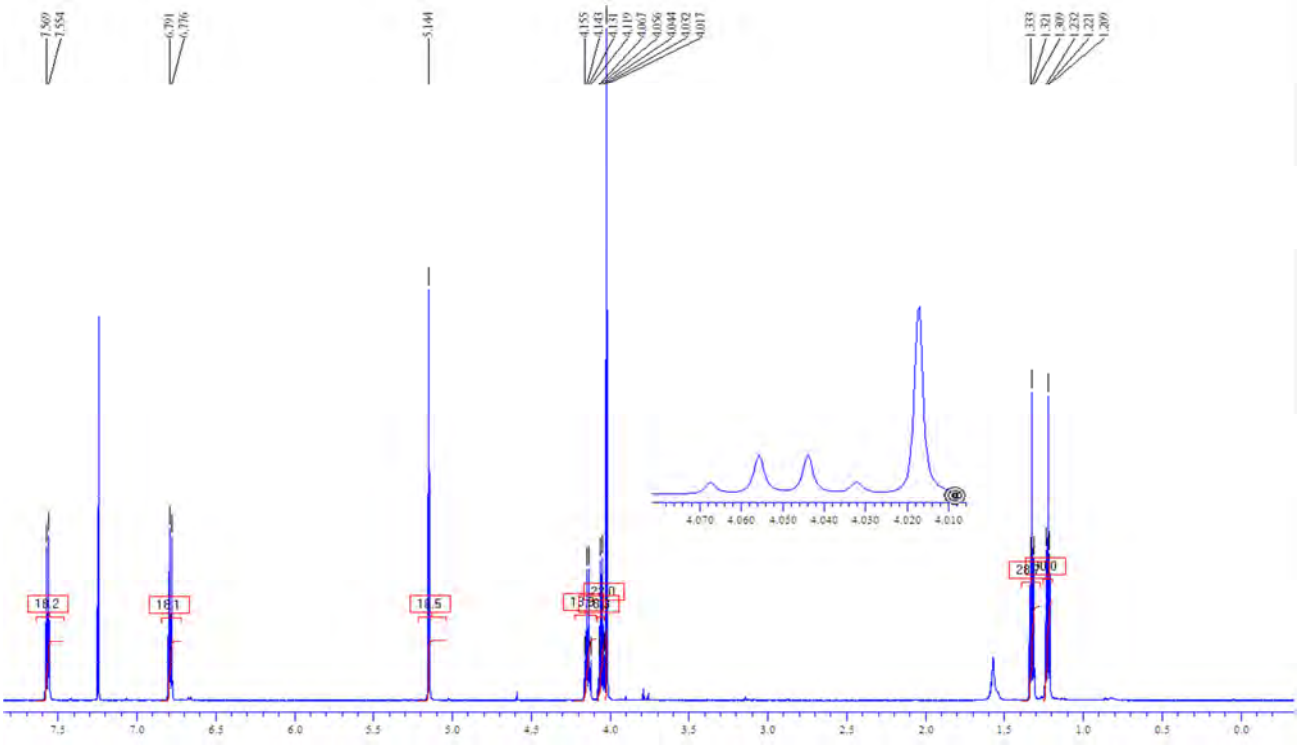

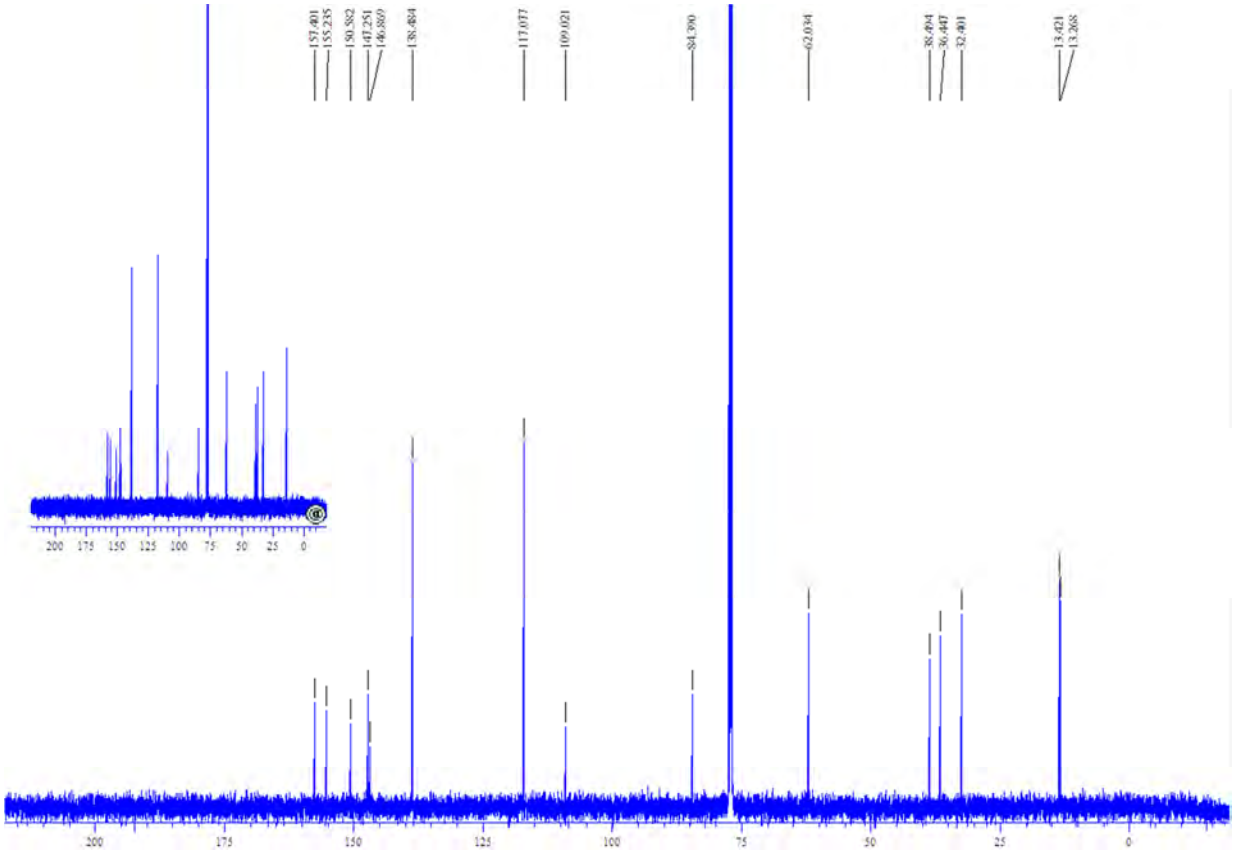

^{1}H NMR and ^{13}C NMR:

1,3-Diethyl-7-methyl-8-(3,4-dimethylphenoxymethyl)xanthine (**22**)

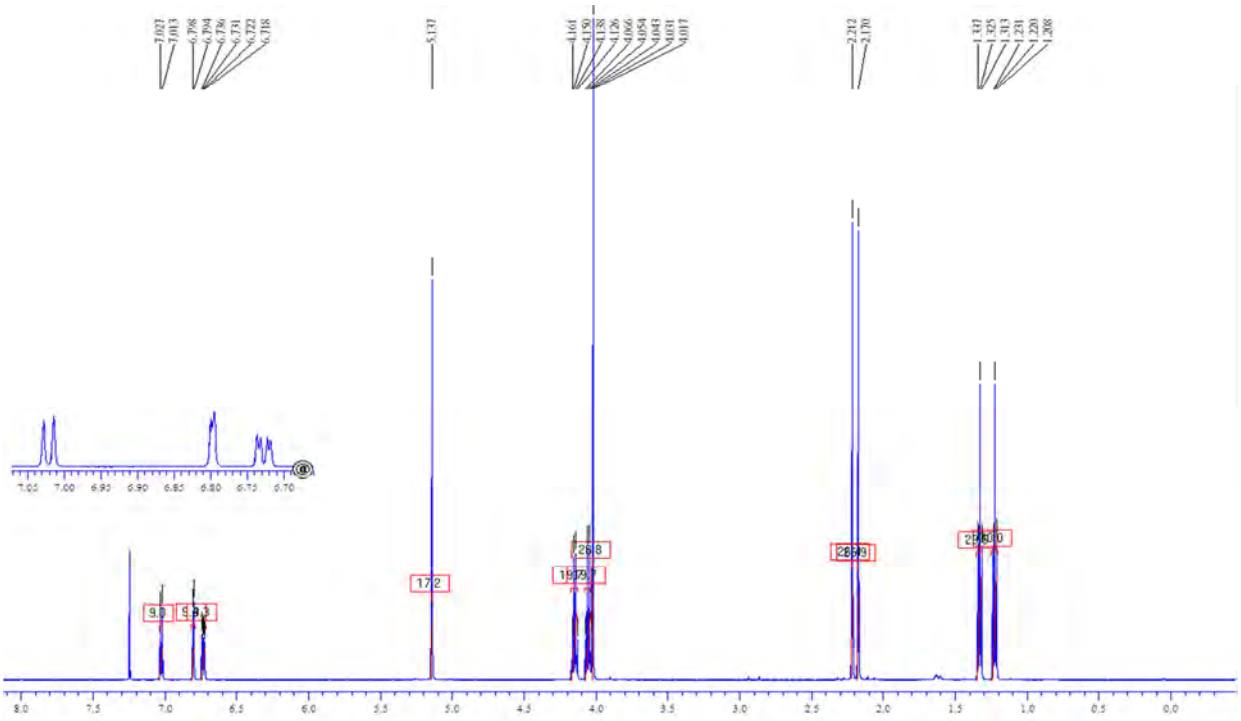

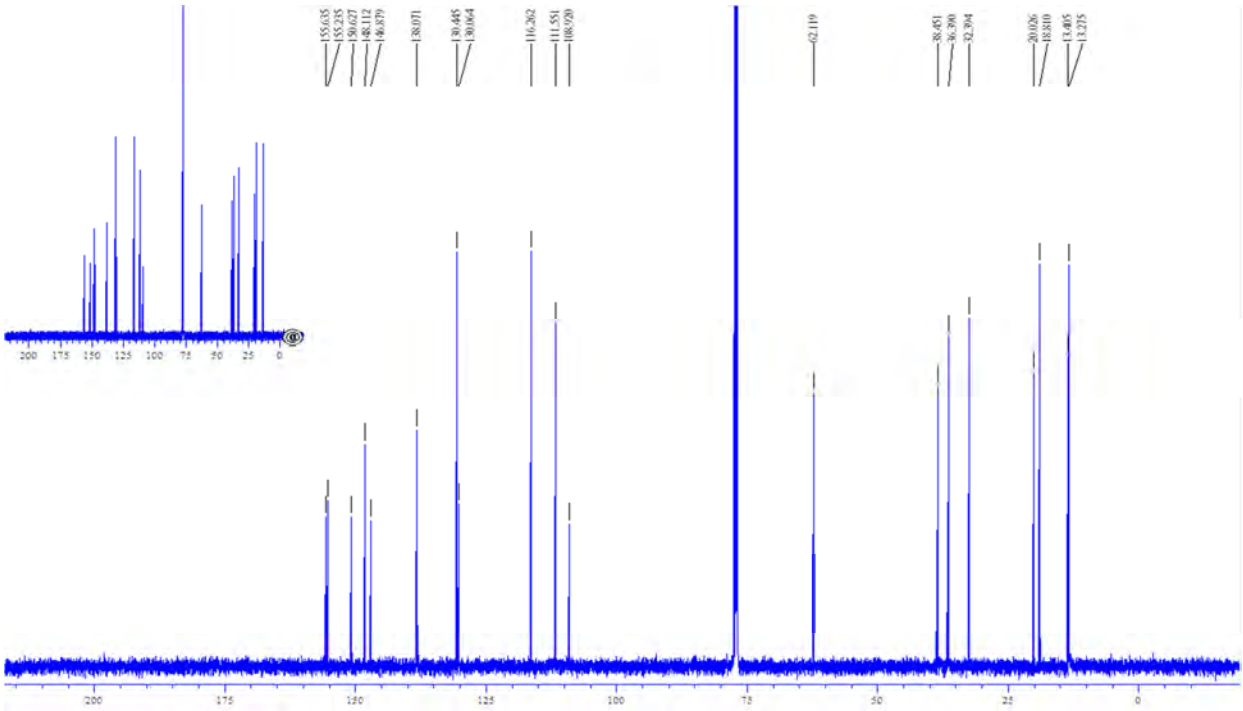

APPENDIX F

HPLC DATA

- 8-(4-Methylphenoxymethyl)caffeine (**11**)
- 8-(4-Methoxyphenoxymethyl)caffeine (**12**)
- 8-(4-Iodophenoxymethyl)caffeine (**13**)
- 8-(3,4-Methylphenoxymethyl)caffeine (**14**)
- 1,3-Diethyl-7-methyl-8-(4-chlorophenoxymethyl)xanthine (**16**)
- 1,3-Diethyl-7-methyl-8-(4-bromophenoxymethyl)xanthine (**17**)
- 1,3-Diethyl-7-methyl-8-(4-fluorophenoxymethyl)xanthine (**18**)
- 1,3-Diethyl-7-methyl-8-(4-methylphenoxymethyl)xanthine (**19**)
- 1,3-Diethyl-7-methyl-8-(4-methoxyphenoxymethyl)xanthine (**20**)
- 1,3-Diethyl-7-methyl-8-(4-iodophenoxymethyl)xanthine (**21**)
- 1,3-Diethyl-7-methyl-8-(4-dimethylphenoxymethyl)xanthine (**22**)

Method: To determine the purity of the compounds, HPLC analyses were carried out. HPLC analyses were performed with an Agilent 1100 HPLC system equipped with a quaternary pump and an Agilent 1100 series diode array detector. A Venusil XBP C18 column (4.60 $\times$ 150 mm, 5 µm) was used and the mobile phase consisted initially of 30% acetonitrile and 70% MilliQ water at a flow rate of 1 mL/min. At the start of each HPLC run a solvent gradient program was initiated by linearly increasing the composition of the acetonitrile in the mobile phase to 85% acetonitrile over a period of 5 min. Each HPLC run lasted 15 min and a time period of 5 min was allowed for equilibration between runs. A volume of 20 µL of solutions of the test compounds in acetonitrile (1 mM) was injected into the HPLC system and the eluent was monitored at wavelengths of 210, 254 and 300 nm.

Controle: Solvent

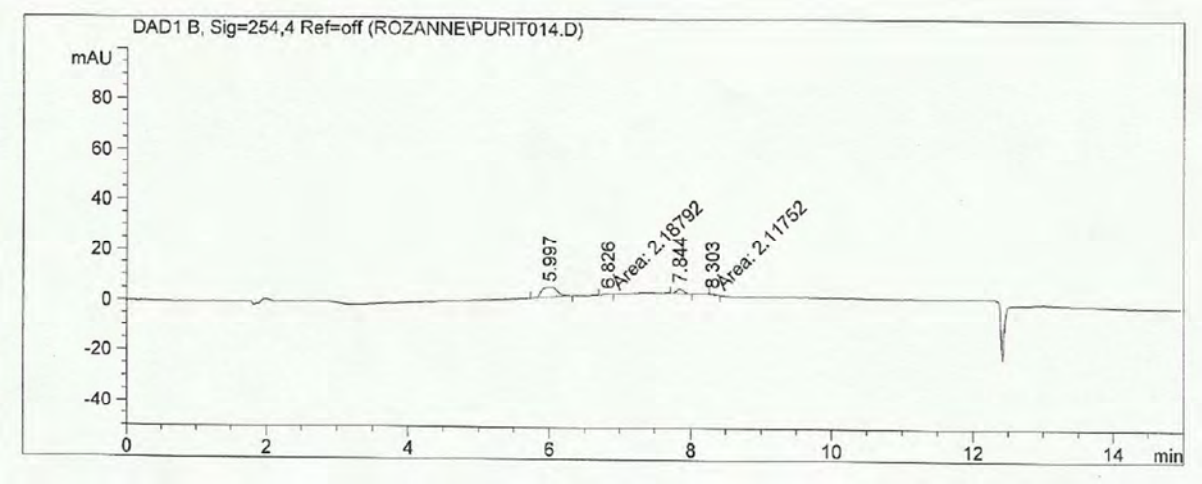

8-(4-Methylphenoxymethyl)caffeine (**11**)

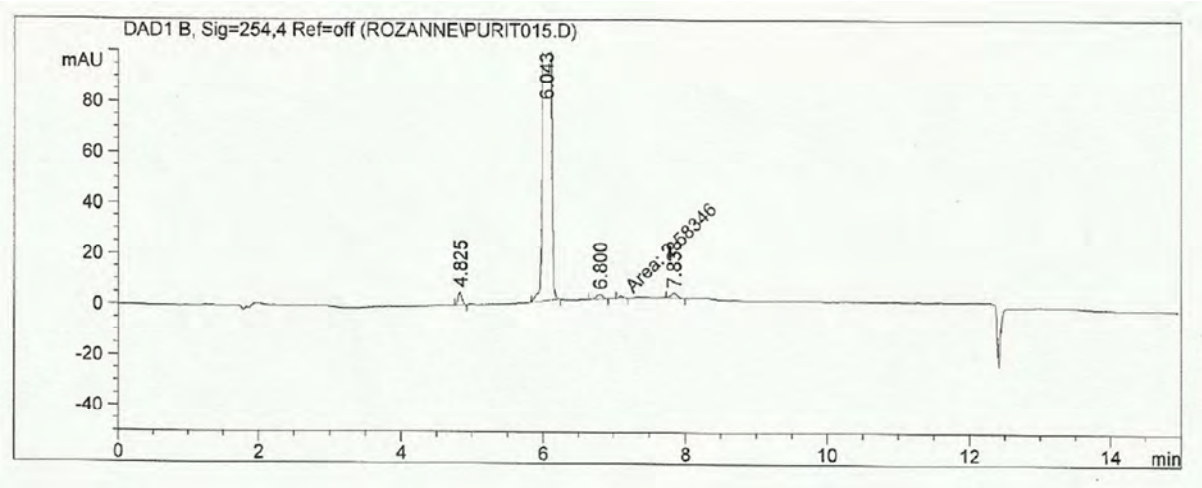

8-(4-Methoxyphenoxymethyl)caffeine (**12**)

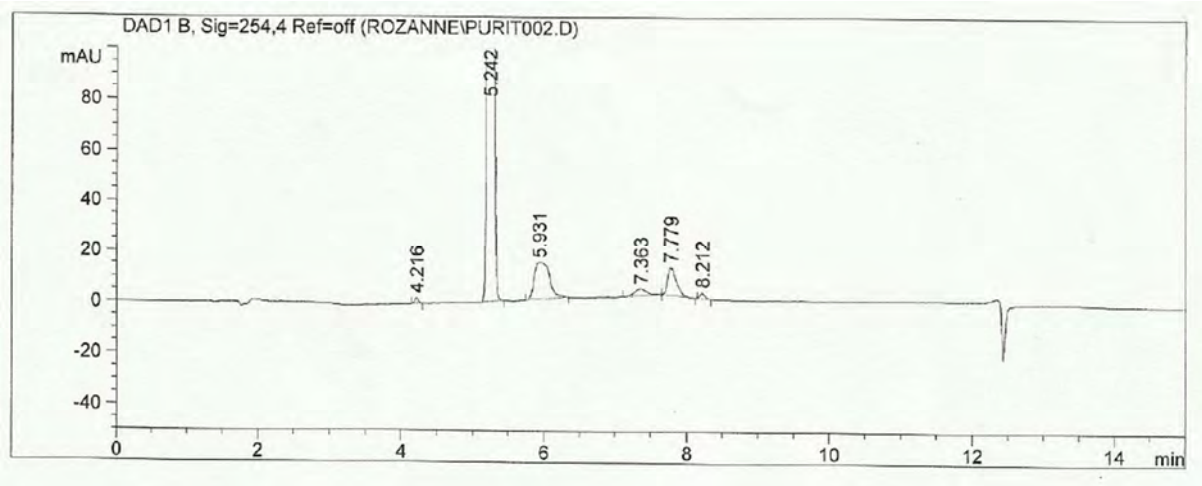

8-(4-Iodophenoxymethyl)caffeine (**13**)

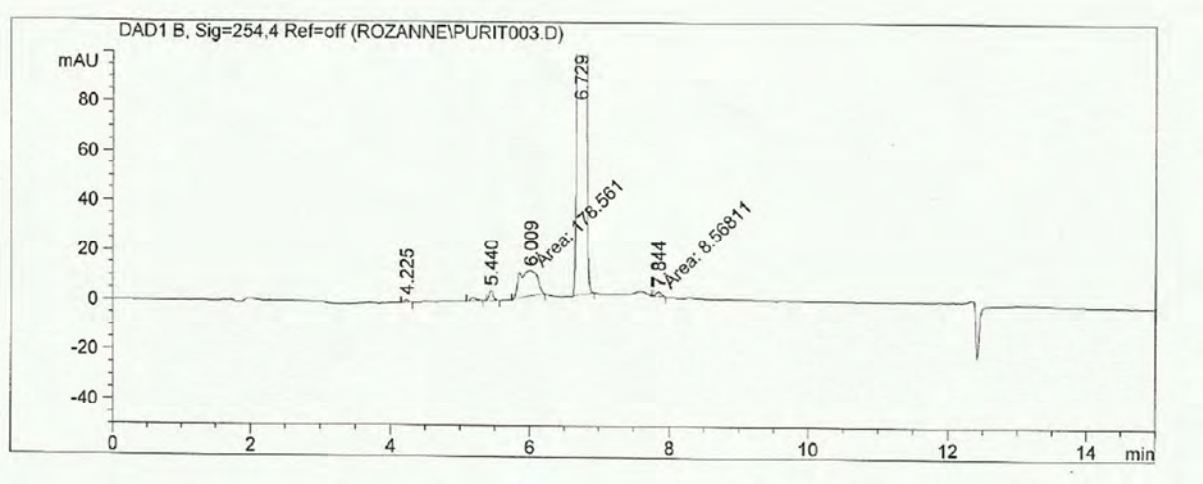

8-(3,4-Methylphenoxymethyl)caffeine (**14**)

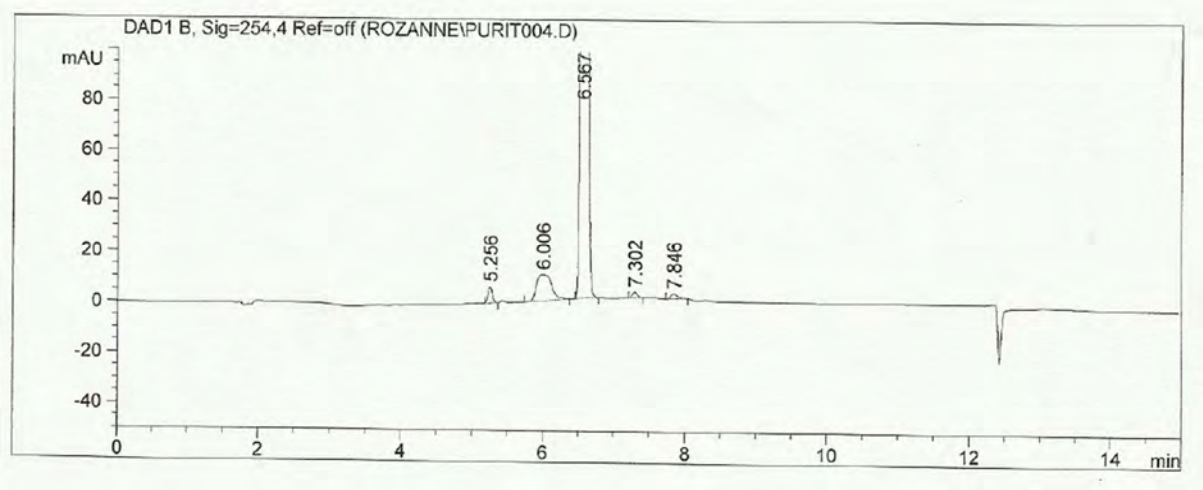

1,3-Diethyl-7-methyl-8-(4-chlorophenoxymethyl)xanthine (**16**)

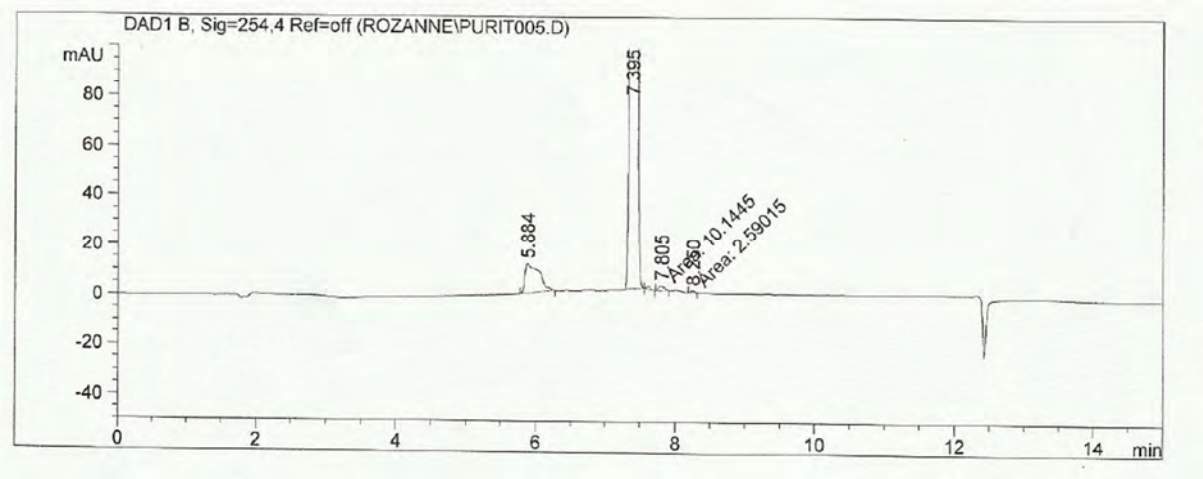

1,3-Diethyl-7-methyl-8-(4-bromophenoxymethyl)xanthine (**17**)

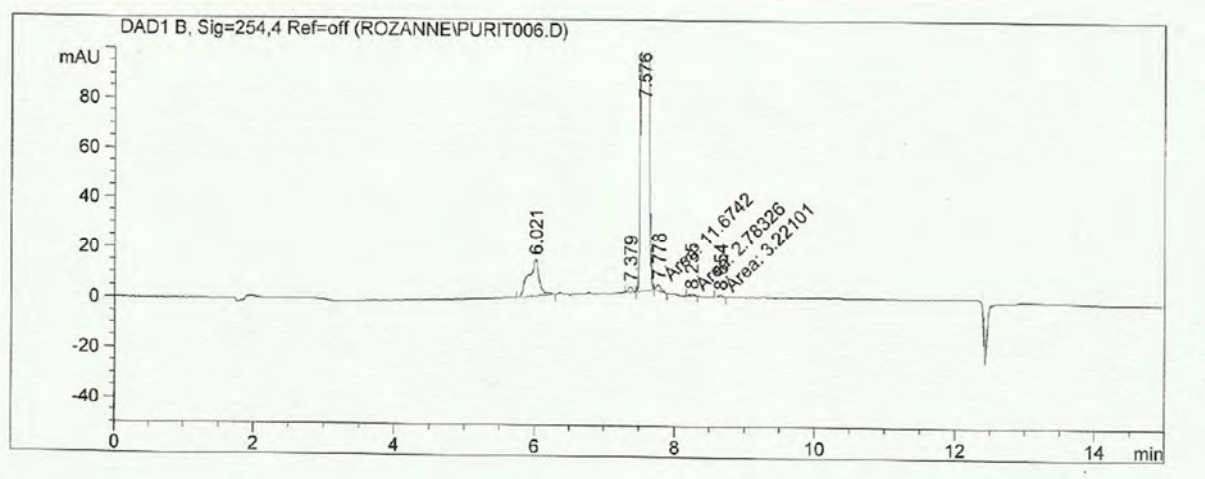

1,3-Diethyl-7-methyl-8-(4-fluorophenoxymethyl)xanthine (**18**)

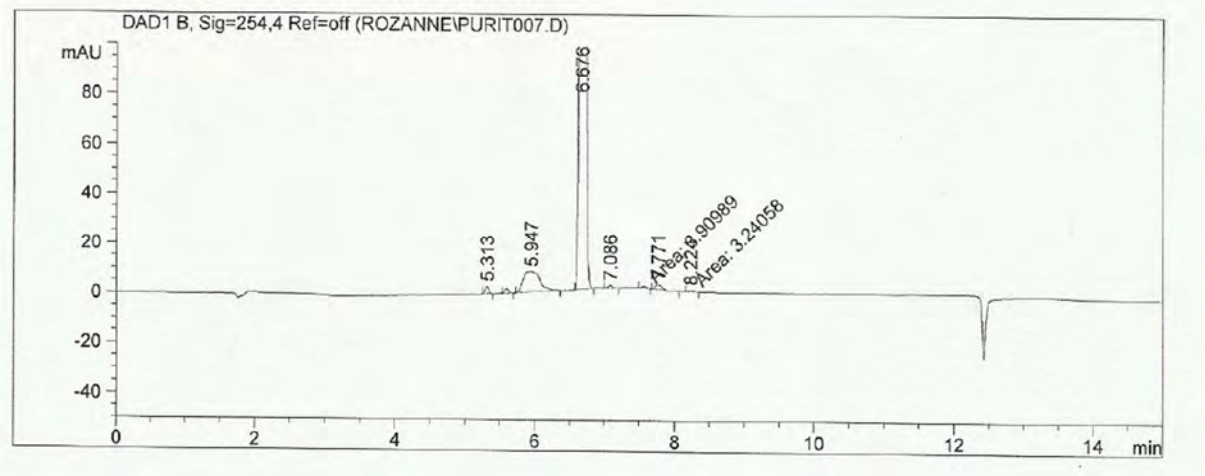

1,3-Diethyl-7-methyl-8-(4-methylphenoxymethyl)xanthine (**19**)

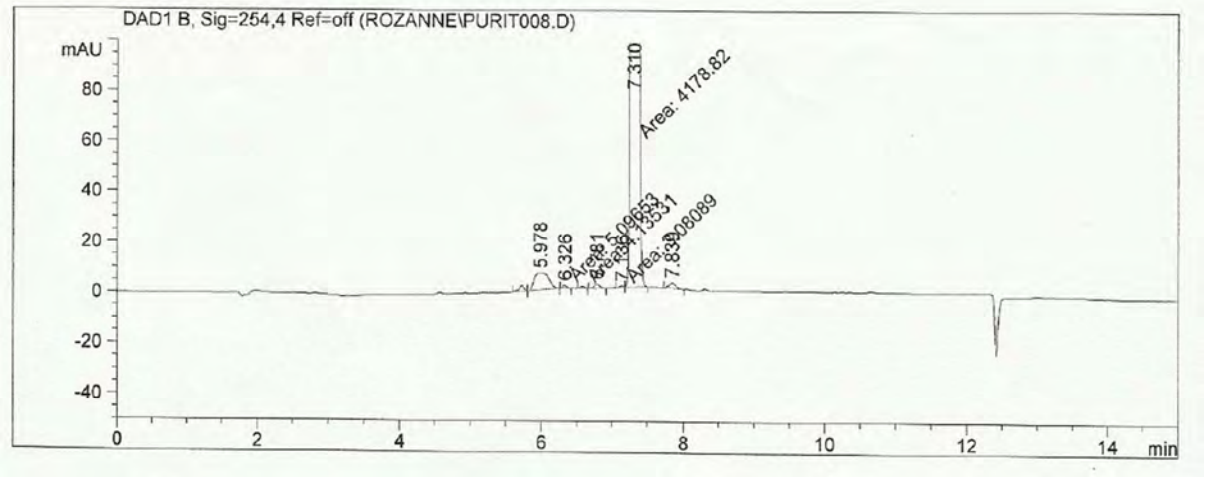

1,3-Diethyl-7-methyl-8-(4-methoxyphenoxymethyl)xanthine (**20**)

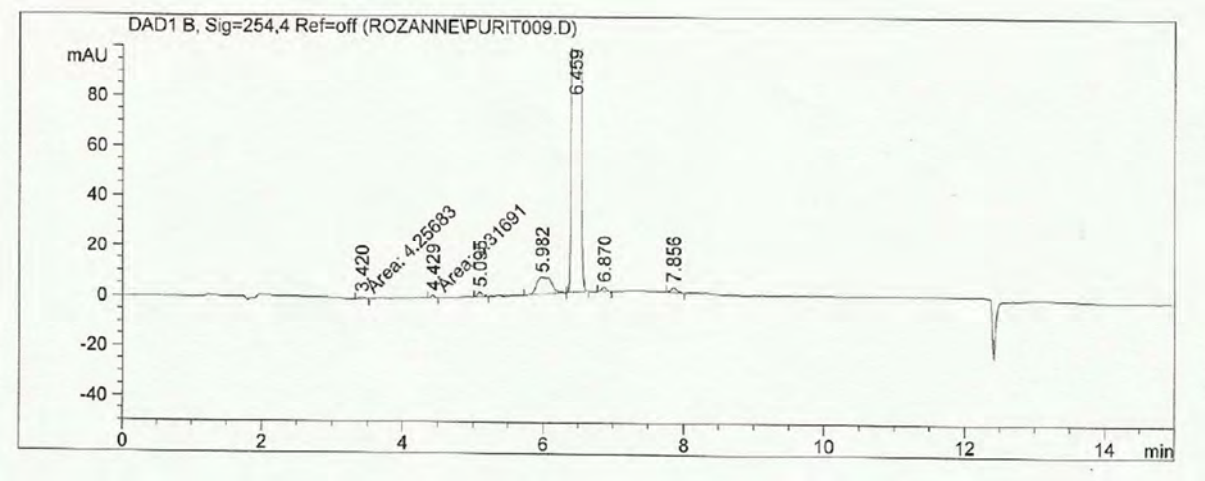

1,3-Diethyl-7-methyl-8-(4-iodophenoxymethyl)xanthine (**21**)

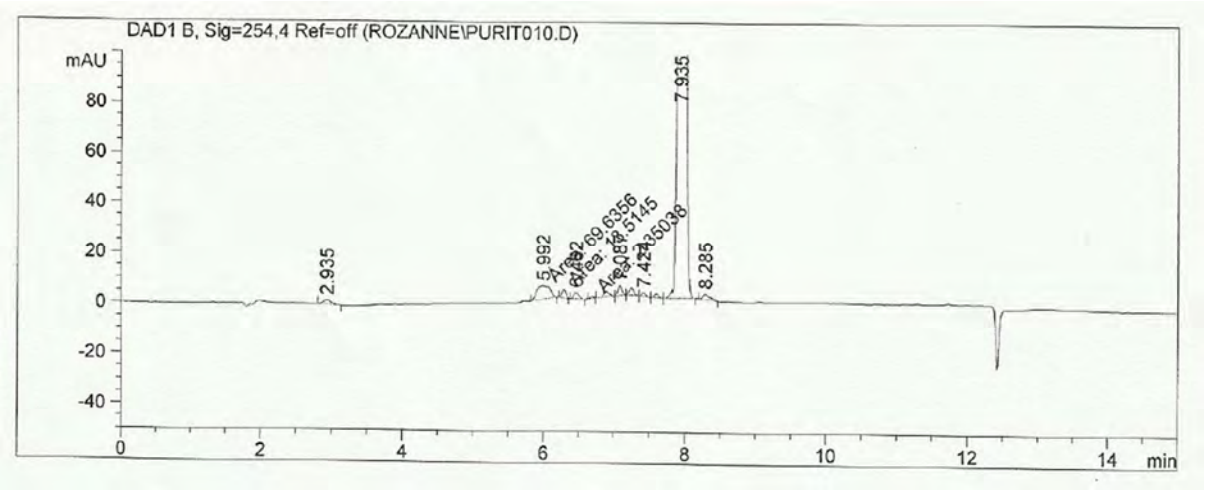

1,3-Diethyl-7-methyl-8-(3,4-dimethylphenoxymethyl)xanthine (**22**)

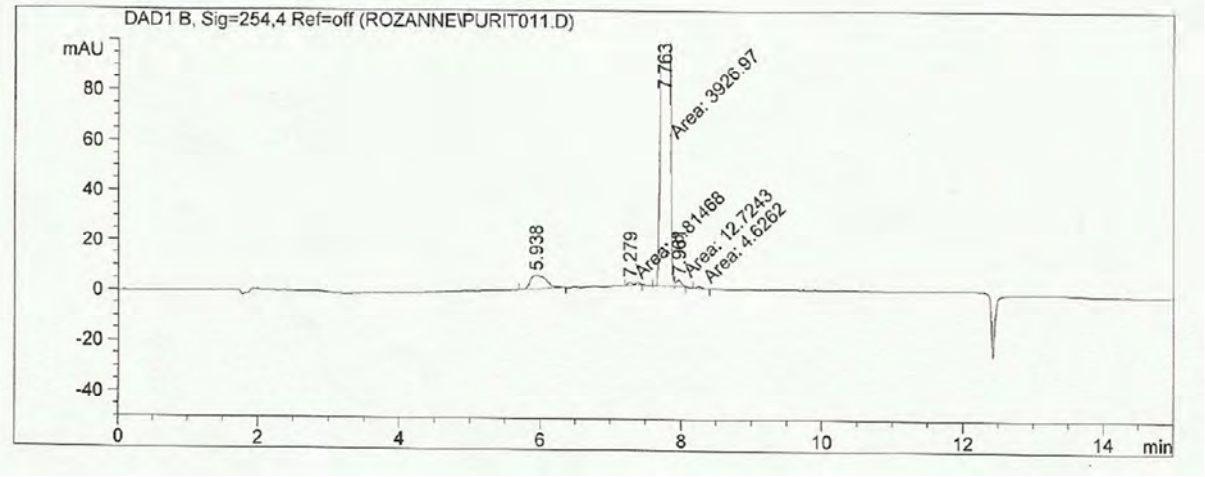

APPENDIX G

MASS SPECTRAL DATA

- 8-(4-Methylphenoxymethyl)caffeine (**11**)
- 8-(4-Methoxyphenoxymethyl)caffeine (**12**)
- 8-(4-Iodophenoxymethyl)caffeine (**13**)
- 8-(3,4-Methylphenoxymethyl)caffeine (**14**)
- 1,3-Diethyl-7-methyl-8-(4-chlorophenoxymethyl)xanthine (**16**)
- 1,3-Diethyl-7-methyl-8-(4-bromophenoxymethyl)xanthine (**17**)
- 1,3-Diethyl-7-methyl-8-(4-fluorophenoxymethyl)xanthine (**18**)
- 1,3-Diethyl-7-methyl-8-(4-methylphenoxymethyl)xanthine (**19**)
- 1,3-Diethyl-7-methyl-8-(4-methoxyphenoxymethyl)xanthine (**20**)
- 1,3-Diethyl-7-methyl-8-(4-iodophenoxymethyl)xanthine (**21**)
- 1,3-Diethyl-7-methyl-8-(4-dimethylphenoxymethyl)xanthine (**22**)

8-(4-Methylphenoxymethyl)caffeine (**11**):

Mass Spectrum SmartFormula Report

Analysis Info

Analysis Name	D:\Data\R HARMSE\RH-S11000001.d	Acquisition Date	9/26/2012 3:19:42 PM
Method	tune_low10082012.m	Operator	Dr JHL Jordaan
Sample Name	RH-S11	Instrument / Ser#	micrOTOF-Q II 10390
Comment			

Acquisition Parameter

Source Type	APCI	Ion Polarity	Positive	Set Nebulizer	1.6 Bar
Focus	Not active	Set Capillary	4500 V	Set Dry Heater	200 °C
Scan Begin	50 m/z	Set End Plate Offset	-500 V	Set Dry Gas	8.0 l/min
Scan End	1500 m/z	Set Collision Cell RF	100.0 Vpp	Set Divert Valve	Waste

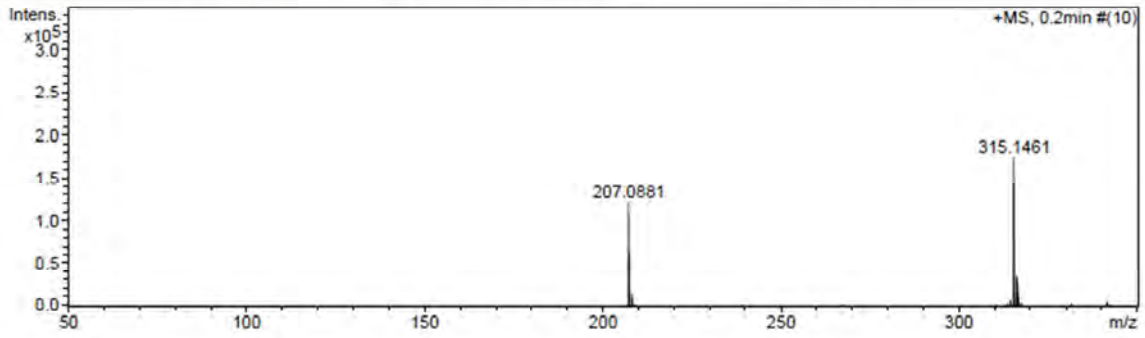

Meas. m/z	#	Formula	Score	m/z	err [mDa]	err [ppm]	mSigma	rdb	e⁻ Conf	N-Rule
315.1461	1	C 16 H 19 N 4 O 3	100.00	315.1452	-0.9	-2.8	8.9	9.5	even	ok
	2	C 21 H 19 N 2 O	14.92	315.1492	3.1	9.9	18.1	13.5	even	ok

8-(4-Methoxyphenoxymethyl)caffeine (**12**)

Mass Spectrum SmartFormula Report

Analysis Info

Analysis Name	D:\Data\R HARMSE\RH-S12000001.d	Acquisition Date	9/26/2012 3:23:20 PM
Method	tune_low10082012.m	Operator	Dr JHL Jordaan
Sample Name	RH-S12	Instrument / Ser#	micrOTOF-Q II 10390
Comment			

Acquisition Parameter

Source Type	APCI	Ion Polarity	Positive	Set Nebulizer	1.6 Bar
Focus	Not active	Set Capillary	4500 V	Set Dry Heater	200 °C
Scan Begin	50 m/z	Set End Plate Offset	-500 V	Set Dry Gas	8.0 l/min
Scan End	1500 m/z	Set Collision Cell RF	100.0 Vpp	Set Divert Valve	Waste

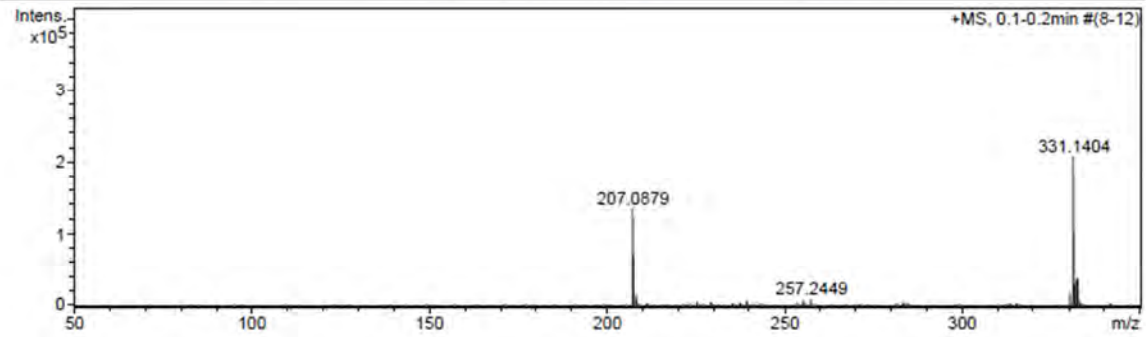

Meas. m/z	#	Formula	Score	m/z	err [mDa]	err [ppm]	mSigma	rdb	e⁻ Conf	N-Rule
331.1404	1	C 16 H 19 N 4 O 4	100.00	331.1401	-0.4	-1.1	0.9	9.5	even	ok
	2	C 17 H 15 N 8	56.25	331.1414	1.0	2.9	15.6	14.5	even	ok

8-(4-Iodophenoxymethyl)caffeine (**13**)

Mass Spectrum SmartFormula Report

Analysis Info

Analysis Name	D:\Data\R HARMSE\RH-S13000001.d	Acquisition Date	9/26/2012 3:24:36 PM
Method	tune_low10082012.m	Operator	Dr JHL Jordaan
Sample Name	RH-S13	Instrument / Ser#	micrOTOF-Q II 10390
Comment			

Acquisition Parameter

Source Type	APCI	Ion Polarity	Positive	Set Nebulizer	1.6 Bar
Focus	Not active	Set Capillary	4500 V	Set Dry Heater	200 °C
Scan Begin	50 m/z	Set End Plate Offset	-500 V	Set Dry Gas	8.0 l/min
Scan End	1500 m/z	Set Collision Cell RF	100.0 Vpp	Set Divert Valve	Waste

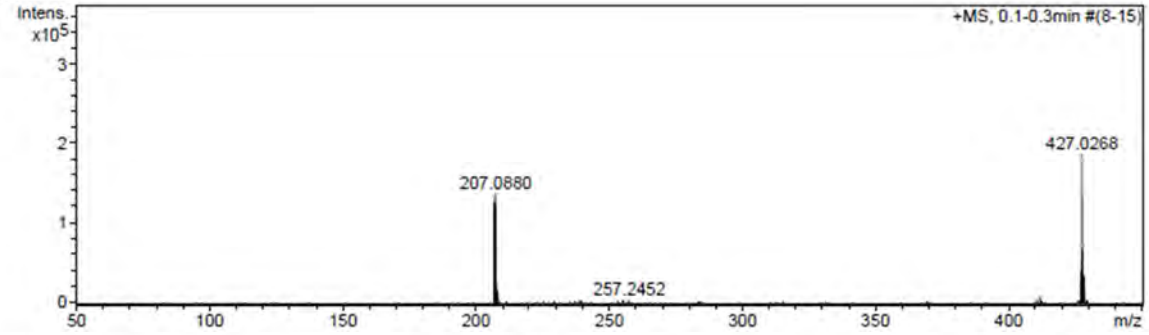

Meas. m/z	#	Formula	Score	m/z	err [mDa]	err [ppm]	mSigma	rdb	e¯ Conf	N-Rule
427.0268	1	C 15 H 16 I N 4 O 3	87.30	427.0262	-0.6	-1.5	4.8	9.5	even	ok
	2	C 16 H 7 N 6 O 9	100.00	427.0269	0.1	0.3	10.3	16.5	even	ok
	3	C 15 H 11 N 2 O 13	55.86	427.0256	-1.2	-2.9	11.2	11.5	even	ok
	4	C 17 H 3 N 10 O 5	39.04	427.0282	1.5	3.4	21.5	21.5	even	ok
	5	C 28 H 3 N 4 O 2	8.42	427.0251	-1.7	-4.1	68.0	29.5	even	ok

8-(3,4-Methylphenoxymethyl)caffeine (**14**)

Mass Spectrum SmartFormula Report

Analysis Info

Analysis Name	D:\Data\R HARMSE\RH-S14.d	Acquisition Date	9/26/2012 3:26:16 PM
Method	tune_low10082012.m	Operator	Dr JHL Jordaan
Sample Name	RH-S14	Instrument / Ser#	micrOTOF-Q II 10390
Comment			

Acquisition Parameter

Source Type	APCI	Ion Polarity	Positive	Set Nebulizer	1.6 Bar
Focus	Not active	Set Capillary	4500 V	Set Dry Heater	200 °C
Scan Begin	50 m/z	Set End Plate Offset	-500 V	Set Dry Gas	8.0 l/min
Scan End	1500 m/z	Set Collision Cell RF	100.0 Vpp	Set Divert Valve	Waste

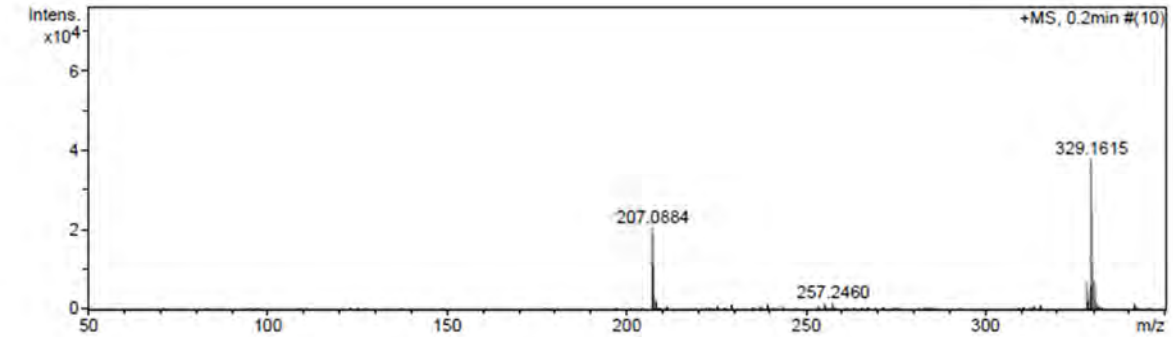

Meas. m/z	#	Formula	Score	m/z	err [mDa]	err [ppm]	mSigma	rdb	e¯ Conf	N-Rule
329.1615	1	C 17 H 21 N 4 O 3	100.00	329.1608	-0.7	-2.1	11.5	9.5	even	ok

1,3-Diethyl-7-methyl-8-(4-chlorophenoxymethyl)xanthine (**16**)

Mass Spectrum SmartFormula Report

Analysis Info

Analysis Name	D:\Data\R HARMSE\RH-S21.d	Acquisition Date	9/26/2012 3:27:25 PM
Method	tune_low10082012.m	Operator	Dr JHL Jordaan
Sample Name	RH-S21	Instrument / Ser#	micrOTOF-Q II 10390
Comment			

Acquisition Parameter

Source Type	APCI	Ion Polarity	Positive	Set Nebulizer	1.6 Bar
Focus	Not active	Set Capillary	4500 V	Set Dry Heater	200 °C
Scan Begin	50 m/z	Set End Plate Offset	-500 V	Set Dry Gas	8.0 l/min
Scan End	1500 m/z	Set Collision Cell RF	100.0 Vpp	Set Divert Valve	Waste

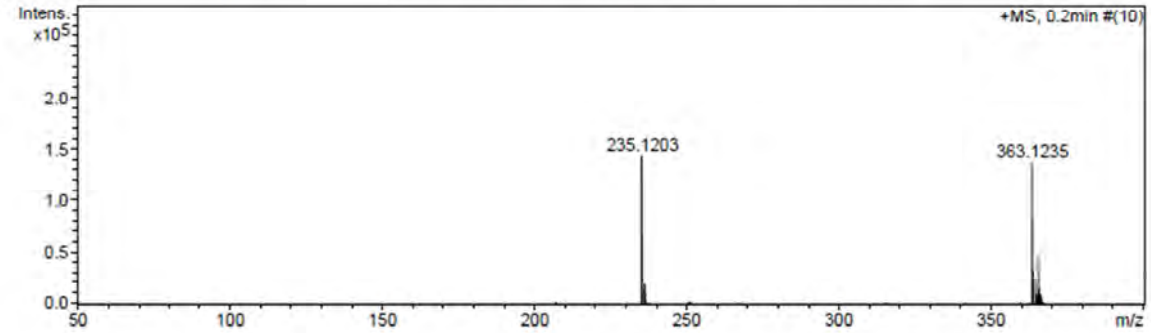

Meas. m/z	#	Formula	Score	m/z	err [mDa]	err [ppm]	mSigma	rdb	e⁻ Conf	N-Rule
363.1235	1	C 17 H 20 Cl N 4 O 3	100.00	363.1218	-1.6	-4.4	1.1	9.5	even	ok
	2	C 22 H 19 O 5	0.07	363.1227	-0.8	-2.1	177.6	13.5	even	ok
	3	C 23 H 15 N 4 O	0.05	363.1240	0.6	1.6	182.3	18.5	even	ok

1,3-Diethyl-7-methyl-8-(4-bromophenoxymethyl)xanthine (**17**)

Mass Spectrum SmartFormula Report

Analysis Info

Analysis Name	D:\Data\R HARMSE\RH-S22.d	Acquisition Date	9/26/2012 3:28:43 PM
Method	tune_low10082012.m	Operator	Dr JHL Jordaan
Sample Name	RH-S22	Instrument / Ser#	micrOTOF-Q II 10390
Comment			

Acquisition Parameter

Source Type	APCI	Ion Polarity	Positive	Set Nebulizer	1.6 Bar
Focus	Not active	Set Capillary	4500 V	Set Dry Heater	200 °C
Scan Begin	50 m/z	Set End Plate Offset	-500 V	Set Dry Gas	8.0 l/min
Scan End	1500 m/z	Set Collision Cell RF	100.0 Vpp	Set Divert Valve	Waste

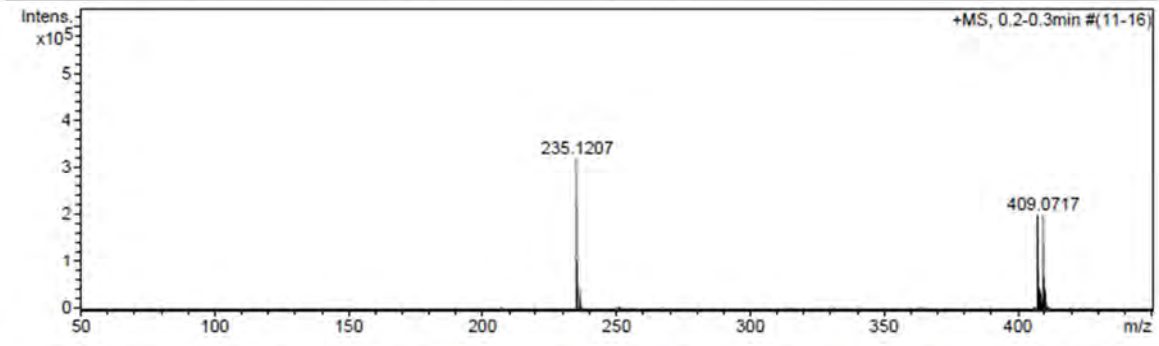

Meas. m/z	#	Formula	Score	m/z	err [mDa]	err [ppm]	mSigma	rdb	e⁻ Conf	N-Rule
407.0735	1	C 17 H 20 Br N 4 O 3	99.86	407.0713	-2.2	-5.4	8.4	9.5	even	ok
	2	C 22 H 20 Br N 2 O	100.00	407.0754	1.8	4.5	21.5	13.5	even	ok
	3	C 29 H 11 O 3	0.00	407.0703	-3.2	-8.0	485.7	24.5	even	ok
	4	C 22 H 15 O 8	0.00	407.0761	2.6	6.5	488.5	15.5	even	ok
	5	C 17 H 15 N 2 O 10	0.00	407.0721	-1.4	-3.4	490.9	11.5	even	ok
	6	C 23 H 11 N 4 O 4	0.00	407.0775	4.0	9.7	554.1	20.5	even	ok
	7	C 18 H 11 N 6 O 6	0.00	407.0735	-0.1	-0.1	557.4	16.5	even	ok
	8	C 19 H 7 N 10 O 2	0.00	407.0748	1.3	3.2	559.3	21.5	even	ok

1,3-Diethyl-7-methyl-8-(4-fluorophenoxymethyl)xanthine (**18**)

Mass Spectrum SmartFormula Report

Analysis Info

Analysis Name	D:\Data\R HARMSE\RH-S23.d	Acquisition Date	9/26/2012 3:31:30 PM
Method	tune_low10082012.m	Operator	Dr JHL Jordaan
Sample Name	RH-23	Instrument / Ser#	micrOTOF-Q II 10390
Comment			

Acquisition Parameter

Source Type	APCI	Ion Polarity	Positive	Set Nebulizer	1.6 Bar
Focus	Not active	Set Capillary	4500 V	Set Dry Heater	200 °C
Scan Begin	50 m/z	Set End Plate Offset	-500 V	Set Dry Gas	8.0 l/min
Scan End	1500 m/z	Set Collision Cell RF	100.0 Vpp	Set Divert Valve	Waste

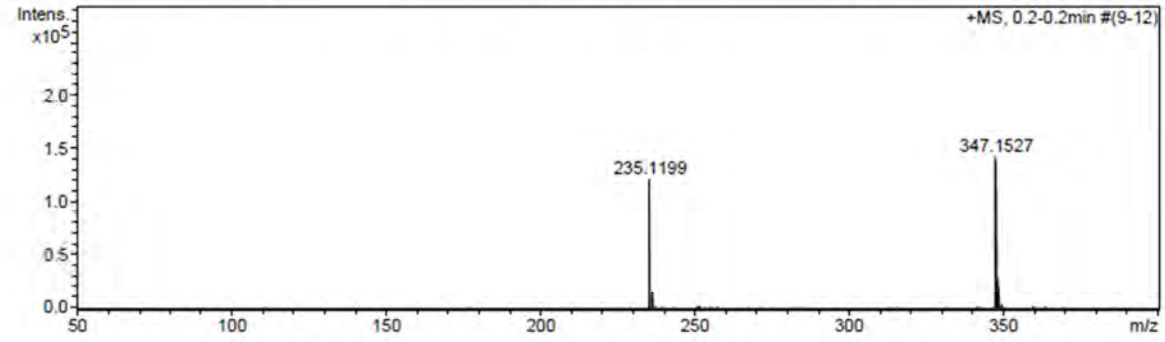

Meas. m/z	#	Formula	Score	m/z	err [mDa]	err [ppm]	mSigma	rdb	e⁻ Conf	N-Rule
347.1527	1	C 17 H 20 F N 4 O 3	100.00	347.1514	-1.3	-3.8	1.0	9.5	even	ok
	2	C 25 H 19 N 2	31.03	347.1543	1.6	4.5	45.3	17.5	even	ok

1,3-Diethyl-7-methyl-8-(4-methylphenoxymethyl)xanthine (**19**)

Mass Spectrum SmartFormula Report

Analysis Info

Analysis Name	D:\Data\R HARMSE\RH-S24.d	Acquisition Date	9/26/2012 3:36:52 PM
Method	tune_low10082012.m	Operator	Dr JHL Jordaan
Sample Name	RH-24	Instrument / Ser#	micrOTOF-Q II 10390
Comment			

Acquisition Parameter

Source Type	APCI	Ion Polarity	Positive	Set Nebulizer	1.6 Bar
Focus	Not active	Set Capillary	4500 V	Set Dry Heater	200 °C
Scan Begin	50 m/z	Set End Plate Offset	-500 V	Set Dry Gas	8.0 l/min
Scan End	1500 m/z	Set Collision Cell RF	100.0 Vpp	Set Divert Valve	Waste

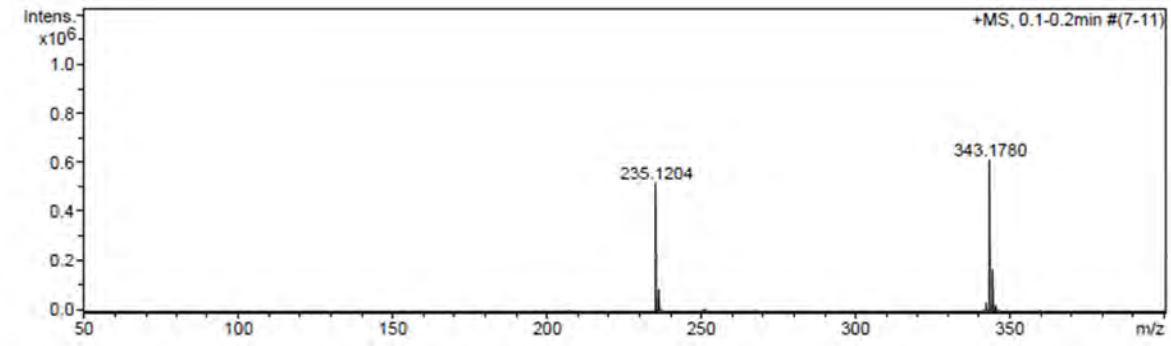

Meas. m/z	#	Formula	Score	m/z	err [mDa]	err [ppm]	mSigma	rdb	e⁻ Conf	N-Rule
343.1780	1	C 18 H 23 N 4 O 3	100.00	343.1765	-1.5	-4.4	37.1	9.5	even	ok

1,3-Diethyl-7-methyl-8-(4-methoxyphenoxymethyl)xanthine (**20**)

Mass Spectrum SmartFormula Report

Analysis Info

Analysis Name	D:\Data\R HARMSE\RH-S25.d	Acquisition Date	9/26/2012 3:39:01 PM
Method	tune_low10082012.m	Operator	Dr JHL Jordaan
Sample Name	RH-25	Instrument / Ser#	micrOTOF-Q II 10390
Comment			

Acquisition Parameter

Source Type	APCI	Ion Polarity	Positive	Set Nebulizer	1.6 Bar
Focus	Not active	Set Capillary	4500 V	Set Dry Heater	200 °C
Scan Begin	50 m/z	Set End Plate Offset	-500 V	Set Dry Gas	8.0 l/min
Scan End	1500 m/z	Set Collision Cell RF	100.0 Vpp	Set Divert Valve	Waste

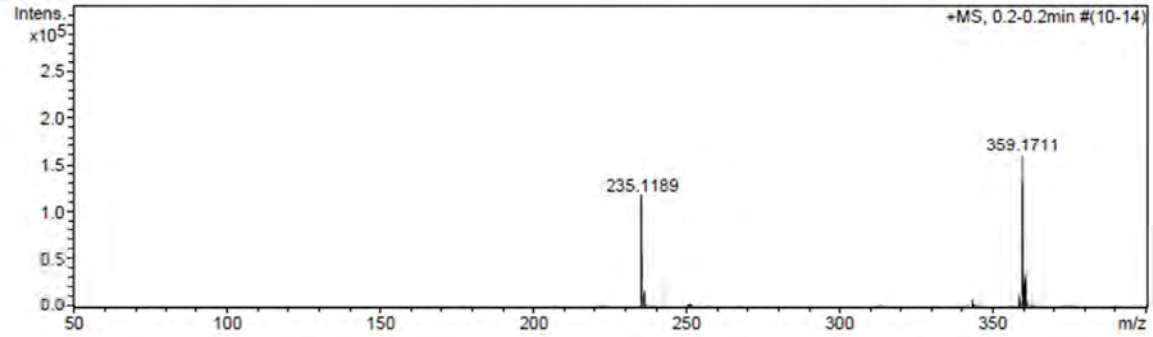

Meas. m/z	#	Formula	Score	m/z	err [mDa]	err [ppm]	mSigma	rdb	e⁻ Conf	N-Rule
359.1711	1	C 18 H 23 N 4 O 4	100.00	359.1714	0.2	0.7	2.0	9.5	even	ok
	2	C 17 H 27 O 8	53.34	359.1700	-1.1	-3.0	12.9	4.5	even	ok
	3	C 19 H 19 N 8	36.12	359.1727	1.6	4.4	16.9	14.5	even	ok

1,3-Diethyl-7-methyl-8-(4-iodophenoxymethyl)xanthine (**21**)

Mass Spectrum SmartFormula Report

Analysis Info

Analysis Name	D:\Data\R HARMSE\RH-S26.d	Acquisition Date	9/26/2012 3:40:05 PM
Method	tune_low10082012.m	Operator	Dr JHL Jordaan
Sample Name	RH-26	Instrument / Ser#	micrOTOF-Q II 10390
Comment			

Acquisition Parameter

Source Type	APCI	Ion Polarity	Positive	Set Nebulizer	1.6 Bar
Focus	Not active	Set Capillary	4500 V	Set Dry Heater	200 °C
Scan Begin	50 m/z	Set End Plate Offset	-500 V	Set Dry Gas	8.0 l/min
Scan End	1500 m/z	Set Collision Cell RF	100.0 Vpp	Set Divert Valve	Waste

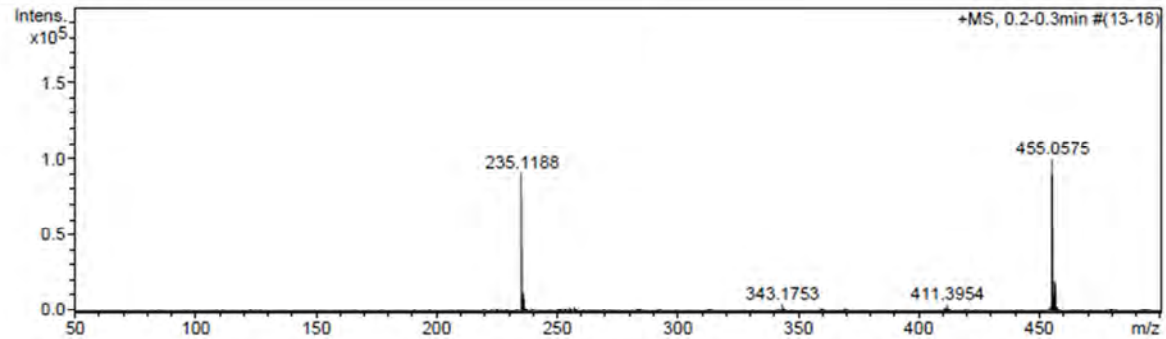

Meas. m/z	#	Formula	Score	m/z	err [mDa]	err [ppm]	mSigma	rdb	e⁻ Conf	N-Rule
455.0575	1	C 17 H 20 I N 4 O 3	100.00	455.0575	-0.0	-0.0	1.1	9.5	even	ok
	2	C 14 H 7 N 12 O 7	30.97	455.0555	-2.0	-4.3	4.8	17.5	even	ok
	3	C 17 H 15 N 2 O 13	65.08	455.0569	-0.6	-1.3	10.3	11.5	even	ok
	4	C 18 H 11 N 6 O 9	59.99	455.0582	0.7	1.6	11.4	16.5	even	ok
	5	C 15 H 3 N 16 O 3	62.54	455.0569	-0.6	-1.4	12.2	22.5	even	ok
	6	C 16 H 24 I O 7	38.27	455.0561	-1.4	-3.0	16.0	4.5	even	ok
	7	C 30 H 7 N 4 O 2	8.96	455.0564	-1.1	-2.5	71.6	29.5	even	ok

1,3-Diethyl-7-methyl-8-(3,4-dimethylphenoxymethyl)xanthine (**22**)

Mass Spectrum SmartFormula Report

Analysis Info

Analysis Name	D:\Data\R HARMSE\RH-S27.d	Acquisition Date	9/26/2012 3:41:19 PM
Method	tune_low10082012.m	Operator	Dr JHL Jordaan
Sample Name	RH-27	Instrument / Ser#	micrOTOF-Q II 10390
Comment			

Acquisition Parameter

Source Type	APCI	Ion Polarity	Positive	Set Nebulizer	1.6 Bar
Focus	Not active	Set Capillary	4500 V	Set Dry Heater	200 °C
Scan Begin	50 m/z	Set End Plate Offset	-500 V	Set Dry Gas	8.0 l/min
Scan End	1500 m/z	Set Collision Cell RF	100.0 Vpp	Set Divert Valve	Waste

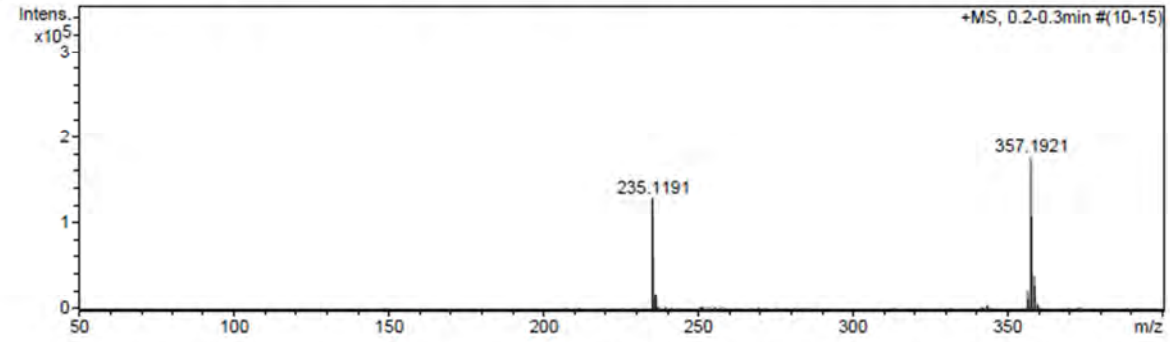

Meas. m/z	#	Formula	Score	m/z	err [mDa]	err [ppm]	mSigma	rdb	e⁻ Conf	N-Rule
357.1921	1	C 19 H 25 N 4 O 3	100.00	357.1921	0.0	0.1	1.5	9.5	even	ok
	2	C 18 H 29 O 7	41.08	357.1908	-1.3	-3.7	14.2	4.5	even	ok